TRANSPORTATION RESEARCH

# RECORD

No. 1323

*Materials and Construction*

# Asphalt Mix Materials 1991


*A peer-reviewed publication of the Transportation Research Board*

TRANSPORTATION RESEARCH BOARD
NATIONAL RESEARCH COUNCIL
WASHINGTON, D.C. 1991

**Transportation Research Record 1323**
Price: $26.00

Subscriber Category
IIIB materials and construction

TRB Publications Staff
*Director of Publications*: Nancy A. Ackerman
*Senior Editor*: Naomi C. Kassabian
*Associate Editor*: Alison G. Tobias
*Assistant Editors*: Luanne Crayton, Norman Solomon
*Graphics Coordinator*: Diane L. Snell
*Production Coordinator*: Karen S. Waugh
*Office Manager*: Phyllis D. Barber
*Production Assistant*: Betty L. Hawkins

Printed in the United States of America

**Library of Congress Cataloging-in-Publication Data**
National Research Council. Transportation Research Board.

Asphalt mix materials, 1991 : a peer-reviewed publication of the Transportation Research Board.
p. cm.—(Transportation research record ; no. 1323)
ISBN 0-309-05163-0
1. Asphalt emulsion mixtures. 2. Asphalt emulsion mixtures—Testing. I. National Research Council (U.S.). Transportation Research Board. II. Series: Transportation research record ; 1323.
TE7.H5 no. 1323
[TE275]
388 s—dc20
[625.8′5] 92-6268
CIP

**Sponsorship of Transportation Research Record 1323**

**GROUP 2—DESIGN AND CONSTRUCTION OF TRANSPORTATION FACILITIES**
*Chairman: Raymond A. Forsyth, Sacramento, California*

**Bituminous Section**
*Chairman: Leonard E. Wood, Purdue University*

Committee on Characteristics of Bituminous Materials
*Chairman: Vytautas P. Puzinauskas, Silver Spring, Maryland*
*Chris A. Bell, Bernard Brule, Joe W. Button, Brian H. Chollar, Jack N. Dybalski, Norman W. Garrick, Bobby J. Huff, John E. Huffman, Prithvi S. Kandhal, N. Paul Khosla, Robert P. Lottman, Tinh Nguyen, R. D. Pavlovich, Rowan J. Peters, J. Claine Petersen, Charles F. Potts, Peggy L. Simpson, Bernard A. Vallerga, John S. Youtcheff*

Committee on Characteristics of Nonbituminous Components of Bituminous Paving Mixtures
*Chairman: N. Paul Khosla, North Carolina State University*
*Secretary: John E. Huffman, U. S. Oil and Refining Company*
*Joe W. Button, Douglas M. Colwill, Ervin L. Dukatz, Jr., Frank Fee, Ilan Ishai, Prithvi S. Kandhal, Kang-Won Wayne Lee, Kamyar Mahboub, Roderick W. Monroe, John W. H. Oliver, Roger C. Olson, G. C. Page, J. Claine Petersen, Michael W. Rouse, Russell H. Schnormeier, Scott Shuler, H. Barry Takallou, Ronald L. Terrel*

Frederick D. Hejl, Transportation Research Board staff

Sponsorship is indicated by a footnote at the end of each paper. The organizational units, officers, and members are as of December 31, 1990.

# Transportation Research Record 1323

## Contents

# Foreword

This Record contains information on asphalt mix materials and associated tests. It should be of interest to state and local materials and construction engineers, as well as contractors and material producers.

Bishara et al. investigated the interrelationship among performance-related properties of asphalt cement and their correlation with molecular size distribution. Brannan et al. examined the adsorption of seven single model species representative of functionalities prevalent in asphalt in siliceous and calcareous aggregates. They concluded their research with a ranking of the seven model species based on their Langmuir monolayer adsorption amounts as well as their adsorption amounts on 1 or 2 g of aggregates. Branthaver et al. report on the compatibilities of eight virgin asphalts studied in Strategic Highway Research Program (SHRP). They report that relative viscosities determined by dividing asphalt viscosities by maltene viscosities appear to be good indicators of asphalt compatibilities. Bell et al. present the results of preliminary tests to evaluate laboratory aging methods for asphalt-aggregate mixtures conducted as a part of a SHRP project. Cipione et al. evaluated solvents for the extraction of residual asphalt from aggregates. They report that trichloroethylene containing 15 percent ethanol is the best solvent of the ones they tested for removing residual asphalt from aggregates. Shiau et al. present the results of a study on the use of the Corbett-Swarbrick fractionation procedure for characterization of age-hardening potentials of asphalts. The fractionation procedure was used to separate asphalts into four fractions (asphaltenes, saturates, naphthene-aromatics, and polar-aromatics) and to identify trends in the changes to the proportions of these fractions during aging.

Romine et al. report on a survey of state highway agencies and asphalt-modifier manufacturers on the performance of asphalt modifiers. They identify and evaluate modifiers with varying levels of performance and present performance ratings for the modifiers evaluated regarding their effect on fatigue cracking, low-temperature cracking, moisture susceptibility, permanent deformation, and aging. Burr et al. investigated the hardening of asphalts during extraction and recovery. They concluded that light, oxygen, and temperature all have a significant effect on this phenomenon. They also suggest that reflux methods of extraction should be avoided when the properties of the extracted material are to be investigated. Jemison et al. evaluated the thin film oven test and the rolling thin film oven test used to simulate the asphalt hardening that occurs in hot-mix plants. They found that the two oven tests closely agree with hot-mix plant hardening at standard test times, but they do not agree if the test times are extended. Al-Balbissi et al. studied the modular properties of selected plasticized sulfur mixes. They concluded that plasticized sulfur mixtures exhibit modulus properties similar to asphalt concrete and are stiffer than asphalt concrete.

Kennedy and Ping compared the wet-dry indirect tensile (Lottman) test and the boiling test for evaluating antistripping treatments in asphalt mixtures. Kim and Amirkhanian determined that fuzzy set procedures can be successfully used for selecting the best-performing antistrip additive. Al-Suhaibani and Tons investigated the effect of three sizes (coarse, medium, and fine) of fly ash on the resilient modulus, rutting potential, and water resistance of asphalt concrete mixes. Their investigation indicated that the medium-size fly ash was the best asphalt extender. Balghunaim determined that washing dust-contaminated coarse aggregates generally improves its strength characteristics and reduces the asphalt content required to attain a certain level of strength, density, and air voids.

# Interrelationship Between Performance-Related Properties of Asphalt Cement and Their Correlation with Molecular Size Distribution

S. W. BISHARA, R. L. MCREYNOLDS, AND E. R. LEWIS

Rheological parameters, Corbett analysis, colloidal instability, and molecular size distribution (MSD) were applied to investigate relationships between several physicochemical parameters. Emphasis is on the correlation between MSD and viscosity at 60°C, viscosity at 135°C, viscosity ratio at 60°C (after and before thin film oven test), penetration at 25°C, viscosity-temperature susceptibility (VTS), penetration-viscosity number (PVN) at 60°C and 135°C, colloidal instability ($I_c$), and asphaltene content. The MSD was obtained using a semipreparative column and a gravimetric finish. The 20 virgin asphalts studied cover a wide viscosity range and were supplied over 7 years by 14 refineries. Virgin asphalts were laboratory-aged; field cores for seven were extracted. For virgin asphalts, viscosity at 60°C correlates strongly with each of viscosity at 135°C and penetration at 25°C. The MSD showed a strong correlation with viscosity at 135°C, PVN at 135°C, VTS, $I_c$, and asphaltene content, and a weak correlation with viscosity ratio. The direction (sign) of association demonstrates that a high PVN and a low VTS (i.e., low temperature susceptibility), a low viscosity ratio (i.e., high resistance to aging), a low $I_c$, and a low asphaltene content are all favored by high large molecular size (LMS), low medium molecular size (MMS), and low small molecular size percentages. Asphalts with high LMS/MMS ratios demonstrated common parameters.

The current methods used routinely to specify and characterize asphalts can no longer monitor asphalt chemical composition. It is possible to have asphalts with the same viscosity grading and similar physical test results but with very different performance in a pavement (*1*, p. 17; *2*, p. 277; *3*).

Evidence indicates that chemical or compositional factors have a major impact on performance of asphalt. The use of high-performance gel permeation chromatography (HPGPC) to study other physicochemical parameters such as molecular size distribution (MSD) has been recommended (*3–9*). The technique allows differentiation among asphalts of the same grade but different composition.

Garrick and Wood (*5*), working on asphalts of varying chemical composition (e.g., resins, oils, asphaltenes) but derived from the same crude and refinery process, have found that temperature susceptibility is relatively insensitive to chemical composition. They conclude that asphalts of different chemical composition can have similar rheological properties. They report a high correlation between MSD and viscosity at 60°C, MSD and viscosity at 135°C, and MSD and penetration, but they wonder whether the relationships can be applied to asphalts from different sources. Other investigators (*4,10*) have also reported the possibility of asphalt cements with the same specifications but substantially different chemical compositions.

Price and Burati (*3*) present a quantitative HPGPC method to predict laboratory results of asphalt cement. They used samples collected monthly over a 7-month period from four suppliers; the asphalts were from different crude oil sources but belonged to the same viscosity grade, AC-20. It is not clear what type of detector was used to develop the HPGPC profiles.

The majority of investigations have used analytical, ultrastyragel columns (300 mm × 7.8 mm) in conjunction with either ultraviolet (UV) or refractive index (RI) detection to generate MSD profiles. Tetrahydrofuran (THF) seems to be the mobile phase (and solvent) of choice, even though toluene has been used (*8*). Recently, a semipreparative, phenogel column (300 mm × 22.5 mm)—as part of an HPGPC system—was used to fractionate asphalt cement samples into five fractions that were collected and weighed to give an exact measure of the amount of asphalt material eluting from a column over a given period of time (*10,11*).

In this study, 20 virgin asphalt samples (asphalt material that has not been used for paving and does not contain recycled asphalt), covering a wide viscosity range of 500 to 2,200 poises and collected over 7 years from 14 different refineries and crude sources, were analyzed for their MSD using a gravimetric finish. The virgin asphalts were laboratory-aged by a 16-hr thinfilm oven test (TFOT) and the residue treated similarly for MSD. Cores from field projects were obtained for 7 out of the 20 asphalts, and, after extraction following ASTM D1856-79, the asphalts were analyzed for MSD. The physical properties of the virgin, laboratory-aged, and field-aged asphalts were measured by the materials testing unit of the Kansas Department of Transportation.

## EXPERIMENTAL METHODS

### Apparatus

A Waters HPGPC system was used. This consisted of a solvent delivery system, a U6K injector, a Digital Equipment

Materials and Research Center, Kansas Department of Transportation, 2300 Van Buren, Topeka, Kans. 66611.

Corporation computer, a printer, and a Waters system interface module. A Phenomenex, 5 μm, 500 Å phenogel semipreparative column (300 mm × 22.5 mm) with THF as solvent was used.

### Procedure

An asphalt sample was weighed accurately (to within 0.01 mg) in the range of 2.0 to 2.5 g. About 25 mL of THF was added before sonifying for 15 min at room temperature. The sample was then transferred quantitatively to a 50-mL volumetric flask, and the flask was filled to volume with THF. The solution was then filtered through a 0.2 μm membrane.

An exact aliquot (100–200 μL) chosen to contain 6 to 7 mg of the asphalt material was then injected. A mobile phase, composed of 95 percent THF and 5 percent pyridine at a flow rate of 6.0 mL/min, was used. The phenogel column was maintained at ambient temperature. The eluting material was collected in a series of five small, glass, accurately weighed (to within 0.01 mg) petri dishes at 4.5 to 7.5, 7.5 to 8.5, 8.5 to 9.5, 9.5 to 11, and 11 to 14 min from injection. The petri dishes were then set aside to allow the solvent to evaporate.

Under exactly the same conditions, the injection was repeated using an aliquot equal to that used before. Fractions were collected in corresponding petri dishes from the previous injection. This repeated injection was done to have fraction weights compatible with the balance available at the time of study. The petri dishes were set aside until dry, then heated in an oven at 160°C for 90 min. The dishes were then cooled in a desiccator until constant weight was attained. For more details, see Bishara and McReynolds (*11*).

## DISCUSSION OF RESULTS

### Rheological Parameters

Asphalts with high temperature susceptibility may contribute to rutting at high temperatures and cracking at low temperatures. Temperature susceptibility can be evaluated by penetration ratio, penetration index, penetration-viscosity number (PVN) based on viscosity at 60°C or at 135°C, and viscosity-temperature susceptibility (VTS). However, it has recently been reported (*12*) that penetration of some asphalts can be significantly affected by routine handling, for example storage and reheating. It is therefore believed that PVN and VTS would provide a better measure of temperature susceptibility. A high PVN and a low VTS indicate minimum susceptibility.

The rheological properties of 20 virgin asphalts are given in Table 1. The VTS was calculated using the formula reported by Glover et al. (*6*). Resistance to aging may be expressed by viscosity ratio (viscosity at 60°C after and before TFOT).

Asphalt performance is thought to be primarily related to temperature susceptibility and resistance to aging; the two characteristics are indirectly specified in ASTM D3381 and AASHTO M226. Figures 1 and 2 plot the two characteristics expressed as PVN (at 135°C, Figure 1, and at 60°C, Figure 2) versus viscosity ratio. The best-performing asphalts are those with low temperature susceptibility (high PVN) and high resistance to aging (low viscosity ratio). Therefore, points at the upper left corner of Figures 1 and 2 represent asphalts with desirable properties (*9*). It is shown that the majority (about 75 percent) of the 20 asphalts fall in the upper left corners of the two figures.

Table 1 reveals that PVN at 135°C, changes over a relatively wide range (−0.07 to −1.18) compared with that (−1.05 to −1.30) reported by Garrick and Wood (*5*), who used asphalts from the same source and refinery. Corbett and Schweyer (*13*) report a perfectly linear relationship between $\log_{10}$ of absolute viscosity and $\log_{10}$ of kinematic viscosity and between $\log_{10}$ of absolute viscosity and $\log_{10}$ of penetration for asphalt cements of varying consistency level but the same source. Garrick and Wood (*5*) report similar observations. Plotting $\log_{10}$ of absolute viscosity versus $\log_{10}$ of kinematic viscosity for the 20 asphalts used in this study (and obtained from different crude sources and refineries) revealed a correlation coefficient ($r$) of 0.67 (Figure 3). Because $r$ is not resistant (*14*) (i.e., one entry can greatly change the value of $r$), the correlation coefficient was recalculated after excluding data corresponding to two asphalt cements obtained from one refinery (Diamond Shamrock). The value of $r$ for the remaining 18 samples amounted to 0.87. Excluding the two points corresponding to Shamrock asphalts may be justified as follows: In 1988, Glover et al. (*6*) compared asphalts from six suppliers and reported that five of the six HPGPC profiles were quite similar; the profile of Shamrock asphalt demonstrated that it is composed, on average, of larger molecular size material. This was found to be also true for the two asphalts studied, and it will be discussed later under HPGPC analysis. Glover et al. further noted that Shamrock asphalt is different in other characteristics as well, which makes it a unique and interesting asphalt for further study. The present work confirms this observation.

A plot of $\log_{10}$ absolute viscosity versus $\log_{10}$ penetration at 25°C for the 20 asphalts under investigation (Figure 4) has a correlation coefficient of −0.81. Contrary to Figure 3, excluding the two Shamrock asphalts produced a small and adverse effect on $r$, causing it to drop to −0.79, that is, farther from the perfect correlation of −1.0 (*14*). It is therefore evident that the absolute viscosity-penetration plot could not detect the two unique asphalts that were shown to be different from the rest by the absolute viscosity-kinematic viscosity plot (as well as HPGPC analysis discussed later). The distinctly higher proportion of large molecular size components of the 2 unique asphalts, as opposed to the other 18, may have caused kinematic viscosity to be relatively higher than would be expected, thus forcing the two data points away from the linear relationship (Figure 3). The predominance of large molecular size components, however, does not appear to have a parallel effect on absolute viscosity or penetration. It may be that prior existence of a high percentage of large molecules, being predominantly polar, enhances the tendency toward formation of even larger viscosity-building molecules that contribute positively to the viscosity value when measured at high temperature (135°C).

Data in Table 1 reveal that the two Shamrock asphalts (88-2570 and 88-2787) are characterized by the lowest VTS and the highest PVN at 135°C (i.e., low temperature susceptibility), as well as a low viscosity ratio (i.e., high resistance to aging). Because their absolute viscosities and penetration at

TABLE 1 PHYSICAL PROPERTIES OF 20 VIRGIN ASPHALTS

| * Sample | Pen 25°C, mm | Vis. 60°C, poises | Vis.60°C (after TFOT) poises | Vis. Ratio | Vis. 135°C, cst | VTS | ** PVN 60°C | *** PVN 135°C |
|---|---|---|---|---|---|---|---|---|
| 82-1214 | 93 | 1678 | 3966 | 2.36 | 416 | 3.454 | -0.33 | -0.25 |
| 1332 | 79 | 1141 | 3056 | 2.68 | 271 | 3.659 | -0.99 | -1.06 |
| 1522 | 85 | 1727 | 5051 | 2.93 | 398 | 3.500 | -0.45 | -0.42 |
| 2746 | 87 | 1204 | 2765 | 2.29 | 305 | 3.579 | -0.79 | -0.81 |
| 83-3203 | 65 | 2149 | 6335 | 2.95 | 395 | 3.591 | -0.64 | -0.71 |
| 3284 | 99 | 1464 | 3530 | 2.41 | 369 | 3.500 | -0.37 | -0.36 |
| 85-1230 | 85 | 1311 | 3253 | 2.48 | 359 | 3.454 | -0.74 | -0.57 |
| 3695 | 94 | 1408 | 3693 | 2.62 | 352 | 3.522 | -0.50 | -0.49 |
| 3890 | 94 | 858 | 1822 | 2.12 | 248 | 3.614 | -1.03 | -1.02 |
| 4116 | 96 | 1368 | 3844 | 2.81 | 321 | 3.591 | -0.50 | -0.60 |
| 86-3063 | 93 | 1353 | 3960 | 2.93 | 360 | 3.489 | -0.56 | -0.47 |
| 3113 | 96 | 1265 | 5127 | 4.05 | 326 | 3.545 | -0.58 | -0.58 |
| 87-2040 | 94 | 881 | 2361 | 2.68 | 223 | 3.727 | -1.00 | -1.18 |
| 88-2381 | 85 | 1275 | 1435 | 1.12 | 307 | 3.591 | -0.77 | -0.78 |
| 2192 | 162 | 501 | 1248 | 2.49 | 233 | 3.432 | -0.74 | -0.51 |
| 2483 | 119 | 979 | 3214 | 3.28 | 301 | 3.492 | -0.51 | -0.46 |
| 2570 | 130 | 707 | 1386 | 1.96 | 360 | 3.204 | -0.72 | -0.07 |
| 2787 | 93 | 1123 | 2483 | 2.21 | 450 | 3.216 | -0.76 | -0.13 |
| 3680 | 105 | 1090 | 2295 | 2.10 | 343 | 3.432 | -0.60 | -0.40 |
| 3719 | 103 | 994 | 2589 | 2.60 | 283 | 3.557 | -0.73 | -0.72 |

*The first two digits refer to the year sample was received.

**PVN, 60°C = $\frac{-1.5(6.489 - 1.59 \log_{10} \text{Pen } 25^{\circ}\text{C} - \log_{10} \eta\ 60^{\circ}\text{C})}{1.05 - 0.2234 \log_{10} \text{Pen } 25^{\circ}\text{C}}$ Ref.(21)

***PVN, 135°C = $\frac{-1.5(4.258 - 0.79674 \log_{10} \text{Pen } 25^{\circ}\text{C} - \log_{10} \eta\ 135^{\circ}\text{C})}{0.795 - 0.1858 \log_{10} \text{Pen } 25^{\circ}\text{C}}$ Ref.(5)

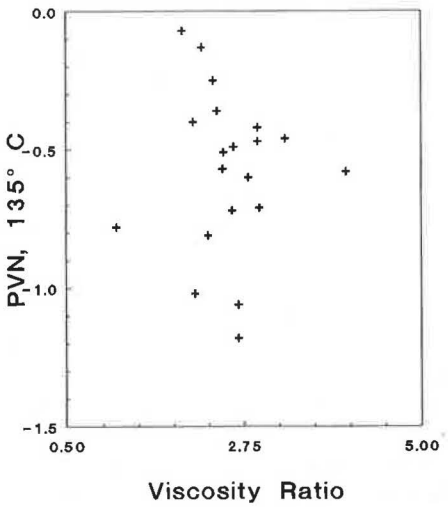


**FIGURE 1 PVN at 135°C versus viscosity ratio.**

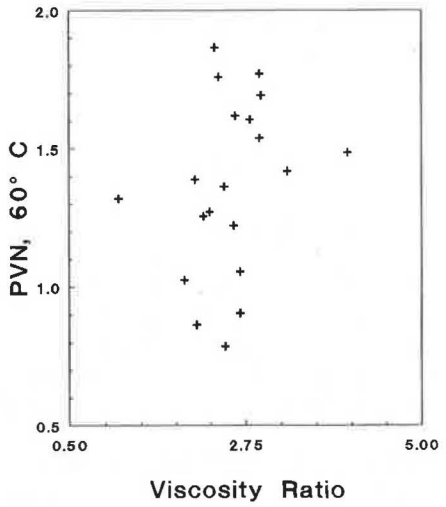


**FIGURE 2 PVN at 60°C versus viscosity ratio.**

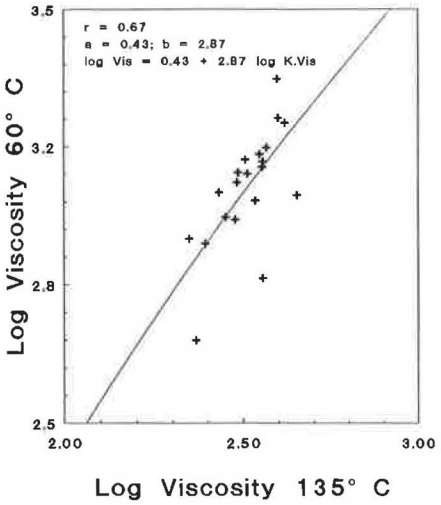


**FIGURE 3 Absolute viscosity versus kinematic viscosity.**

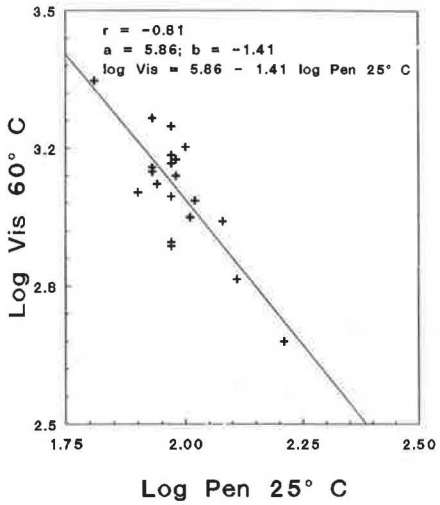


**FIGURE 4 Absolute viscosity versus penetration at 25°C.**

25°C are more or less concordant with those of the rest, their PVNs at 60°C are well within the range of variation of the whole set.

### Effect of Aging on Rheological Properties

Table 2 presents the physical properties of the 20 asphalts after a 16-hr TFOT. Comparing Tables 1 and 2 reveals that laboratory aging causes penetration to decrease and causes absolute viscosity, kinematic viscosity, VTS, PVN at 60°C, and PVN at 135°C to increase. The only exception was one of the two Shamrock asphalts (88-2787), whose PVN at 135°C decreased; the other Shamrock sample showed practically no change.

Cores from seven field projects were treated according to ASTM D1856-79. The physical properties of extracted asphalts are given in Table 3. Generally, penetration decreased, whereas absolute viscosity, kinematic viscosity, VTS, PVN at 60°C, and PVN at 135°C increased. Only one field sample (82-1332) had a lower PVN at 135°C as compared with that of corresponding virgin asphalt.

Data in Tables 2 and 3 confirm previous findings (*4,9*) that characteristics of asphalt after laboratory aging (short term, high temperature) may not necessarily reflect aging characteristics of asphalt in pavement (long term, low temperature). Exposing asphalt to a high temperature (as with a 16-hr TFOT) destroys steric hardening (*15*).

TABLE 2 PHYSICAL PROPERTIES OF VIRGIN ASPHALTS AFTER 16-hr TFOT

| Sample | Pen 25°C, mm | Vis. 60°C, poises | Vis. 135°C, cst | VIS | PVN 60°C | PVN 135°C |
|---|---|---|---|---|---|---|
| 82-1214 | 41 | 19456 | 1190 | 3.568 | 0.79 | 0.31 |
| 1332 | 22 | 11656 | 704 | 3.773 | -0.58 | -0.94 |
| 1522 | 30 | 56352 | 1270 | 3.875 | 1.27 | 0.66 |
| 2746 | 20 | 20456 | 910 | 3.773 | -0.22 | -0.71 |
| 83-3203 | 24 | 39750 | 1269 | 3.761 | 0.62 | -0.15 |
| 3284 | 30 | 25203 | 1256 | 3.614 | 0.54 | 0.05 |
| 85-1230 | 23 | 12747 | 930 | 3.602 | -0.44 | -0.58 |
| 3695 | 30 | 22308 | 1035 | 3.716 | 0.43 | -0.19 |
| 3890 | 24 | 11395 | 641 | 3.841 | -0.48 | -0.98 |
| 4116 | 27 | 35449 | 1180 | 3.773 | 0.69 | -0.13 |
| 86-3063 | 38 | 47083 | 1230 | 3.841 | 1.50 | 0.27 |
| 3113 | 24 | 93751 | 1442 | 3.943 | 1.37 | 0.00 |
| 87-2040 | 30 | 17172 | 696 | 3.920 | 0.20 | -0.68 |
| 88-2381 | 22 | 16711 | 889 | 3.727 | -0.26 | -0.66 |
| 2192 | 50 | 20657 | 798 | 3.875 | 1.18 | -0.01 |
| 2483 | 30 | 70334 | 1593 | 3.784 | 1.47 | 0.35 |
| 2570 | 42 | 8251 | 879 | 3.489 | 0.02 | -0.06 |
| 2787 | 35 | 10632 | 827 | 3.625 | -0.02 | -0.33 |
| 3680 | 40 | 12425 | 1024 | 3.523 | 0.33 | 0.08 |
| 3719 | 30 | 17600 | 914 | 3.727 | 0.22 | -0.34 |

TABLE 3 PHYSICAL PROPERTIES OF ASPHALTS EXTRACTED FROM FIELD CORES

| Sample* | Pen 25°C, mm | Vis. 60°C, poises | Vis. 135°C, cst | VIS | PVN 60°C | PVN 135°C |
|---|---|---|---|---|---|---|
| 82-1332 | 34 | 3581 | 422 | 3.739 | -1.06 | -1.21 |
| 82-1522 | 37 | 21342 | 1029 | 3.704 | 0.72 | 0.01 |
| 85-4116 | 26 | 17518 | 979 | 3.670 | 0.01 | -0.39 |
| 86-3063 | 44 | 8114 | 644 | 3.716 | 0.07 | -0.43 |
| 87-2040 | 59 | 3018 | 441 | 3.636 | -0.44 | -1.04 |
| 88-2483 | 46 | 6719 | 613 | 3.682 | -0.04 | -0.07 |
| 88-3680 | 93 | 2416 | 432 | 3.568 | 0.06 | -0.19 |

*The first two digits refer to the year sample was received.

## HPGPC Analysis

Evidence is growing about the potentialities of HPGPC as a tool to provide insight into a unique physicochemical parameter of asphalt—the MSD. HPGPC can distinguish between asphalts that belong to the same viscosity grade (*3,6*) and that have identical rheological properties (absolute viscosity, kinematic viscosity, and penetration) and temperature susceptibility (expressed by PVN). Garrick and Wood (*5*) report two AC-10 samples with a difference of less than 2 percent between their absolute viscosities, kinematic viscosities, PVN, and a difference of about 5 percent between their penetrations at 25°C. Comparison between MSD parameters revealed detectable differences between the two otherwise similar asphalts. In the present work, two samples provided from the same supplier yielded the results in Table 4. Rheological properties are not much different, but fraction percentages exhibit detectable differences, especially for the two major parts—large molecular size (LMS) and medium molecular size (MMS)—as well as the LMS/MMS ratio.

An advantage of using gravimetry to determine fraction proportion is the nonexistence of sources of error associated with UV and RI detectors. RI detectors are neither highly reproducible (*16*) nor sensitive, and RI varies with molecular weight. UV detectors suffer from undetectability of saturated oils as well as continuous variation of the molar absorptivity "constant" throughout the duration of analysis (*10,11,16*). Gravimetric analyses are known to be highly accurate and reproducible. The cutoff points were selected so that each of the five fractions contained approximately the same proportion of asphalt material. As mentioned before (*11*), the sample elutes over the period of 5 to 14 min after injection. Therefore, where appropriate, reference will be made to LMS, MMS, and small molecular size (SMS) to designate $F_1 + F_2$ (5.0 to 8.5 min), $F_3 + F_4$ (8.5 to 11.0 min), and $F_5$ (11.0 to 14.0 min), respectively. Table 5 shows the MSD of the 20 virgin asphalts. For the following correlations, the MSD data ($F_1$, %, $F_2$, %, . . .) are considered the independent variables, and the physical property investigated as the dependent variable.

TABLE 4 COMPARISON OF TWO SAMPLES PROVIDED BY SAME REFINERY

| | | | | |
|---|---|---|---|---|
| Pen. 25°C | 99 | | 94 | |
| Vis. 60°C, poises | 1464 | | 1408 | |
| Vis. 135°C, cst | 369 | | 352 | |
| Tests on TFOT Residue | | | | |
| Loss on heat, % | 0.09 | | 0.22 | |
| Pen. 25°C | 63 | | 64 | |
| Vis. 60°C, poises | 3530 | | 3693 | |
| Duct. 25°C | 100+ | | 100+ | |
| VIS | 3.500 | | 3.522 | |
| HPGPC Analysis* | | | | |
| $F_1$,% (LMS) | 18.3 | 41.2 | 15.4 | 37.9 |
| $F_2$,% (LMS) | 22.9 | | 22.5 | |
| $F_3$,% (MMS) | 35.6 | 51.8 | 38.3 | 54.3 |
| $F_4$,% (MMS) | 16.2 | | 16.0 | |
| $F_5$,% –SMS | 7.1 | | 7.8 | |
| LMS/MMS | 0.795 | | 0.698 | |

* $F_1$ denotes the largest molecular size components, $F_5$ the smallest.

TABLE 5 GPC DATA FOR 20 VIRGIN ASPHALTS USING GRAVIMETRIC FINISH

| Sample | $F_1$,% | $F_2$,% | $F_3$,% | $F_4$,% | $F_5$,% |
|---|---|---|---|---|---|
| 82-1214 | 14.1 | 27.3 | 40.7 | 12.9 | 4.9 |
| 82-1332 | 11.0 | 22.9 | 42.3 | 18.3 | 5.5 |
| 82-1522 | 16.2 | 26.7 | 39.4 | 11.7 | 6.0 |
| 82-2746 | 14.5 | 28.1 | 36.5 | 12.9 | 4.9 |
| 83-3203 | 13.7 | 22.6 | 38.6 | 15.7 | 9.4 |
| 83-3284 | 18.3 | 22.9 | 35.6 | 16.2 | 7.1 |
| 85-1230 | 17.1 | 28.9 | 34.6 | 13.7 | 5.6 |
| 85-3695 | 15.4 | 22.5 | 38.3 | 16.0 | 7.8 |
| 85-3890 | 7.8 | 25.3 | 45.5 | 18.0 | 3.4 |
| 85-4116 | 15.9 | 23.6 | 37.1 | 18.6 | 4.8 |
| 86-3063 | 16.4 | 27.4 | 42.0 | 11.2 | 3.0 |
| 86-3113 | 13.8 | 25.0 | 40.7 | 13.7 | 6.8 |
| 87-2040 | 12.3 | 24.2 | 41.6 | 15.7 | 6.2 |
| 88-2381 | 12.6 | 25.5 | 36.3 | 14.6 | 11.0 |
| 88-2192 | 15.2 | 25.4 | 43.4 | 10.5 | 5.4 |
| 88-2483 | 14.3 | 24.8 | 39.2 | 15.4 | 6.4 |
| 88-2570 | 23.4 | 36.1 | 25.7 | 9.6 | 5.3 |
| 88-2787 | 26.3 | 35.3 | 25.1 | 8.2 | 5.2 |
| 88-3680 | 12.4 | 34.1 | 37.4 | 10.4 | 5.7 |
| 88-3719 | 12.6 | 21.2 | 39.5 | 17.8 | 8.9 |

### *Correlation Between MSD Data and PVN*

No correlation exists between PVN at 60°C and the percentage of any of the separate fractions ($F_1, F_2, \ldots$); for the composite LMS fraction, $r$ amounted to only $-0.01$.

On the other hand, PVN at 135°C correlates with each of the five fractions. The correlation is stronger if the collective fractions LMS and MMS are used (Table 6). Because good performance is to be expected from asphalts with low temperature susceptibility (high PVN), and because PVN is associated positively with LMS percentage, it follows that a high LMS proportion is desirable. This agrees with Enustun et al. (*9*), who recommend that the LMS percentage and its amount of change after a TFOT be included in the Iowa trial specification. The negative association of MMS and PVN at 135°C suggests a low MMS content for better performance; the same applies for SMS content. However, the fact that the SMS percentage for any of the 20 asphalts never exceeded 11 percent limits the significance of this fraction.

The MSDs of seven asphalts extracted from field cores are given in Table 7. A correlation exists between fraction percentage and PVN at 135°C (Table 8). The correlation has the same direction (sign) but differs in strength from that calculated for virgin asphalts (Table 6).

TABLE 6 CORRELATION COEFFICIENT ($r$) FOR MSD DATA AND SOME PHYSICAL PROPERTIES FOR 20 VIRGIN ASPHALTS

| Fraction | PVN 135°C | Kinematic Viscosity, 135°C | Viscosity ratio | Abs. Vis. 60°C | VTS | pen. 25°C |
|---|---|---|---|---|---|---|
| $F_1$ | 0.59 | 0.64 | -0.09 | -0.02 | -0.84 | 0.21 |
| LMS* | 0.76** | 0.59 | -0.26 | -0.16 | -0.91 | 0.24 |
| $F_2$ | 0.65 | 0.43 | -0.36 | -0.26 | -0.80 | 0.22 |
| $F_3$ | -0.49 | -0.58 | 0.34 | 0.03 | 0.75 | -0.04 |
| MMS* | -0.73*** | -0.61 | 0.32 | 0.09 | 0.87 | -0.18 |
| $F_4$ | -0.25 | -0.46 | 0.17 | 0.15 | 0.78 | -0.36 |
| $F_5$ or SMS | -0.19 | -0.02 | -0.19 | 0.29 | 0.27 | -0.26 |

* LMS = $F_1 + F_2$; MMS = $F_3 + F_4$

** The correlation coefficient, r, for LMS and PVN, 135°C,...etc.

*** The correlation coefficient, r, for MMS and PVN, 135°C,...etc.

TABLE 7 MSD DATA FOR ASPHALTS EXTRACTED FROM FIELD CORES

| | 82-1332 | 82-1522 | 85-4116 | 86-3063 | 87-2040 | 88-2483 | 88-3680 |
|---|---|---|---|---|---|---|---|
| LMS | 35.8 | 46.0 | 41.3 | 43.2 | 41.2 | 42.4 | 45.5 |
| MMS | 54.6 | 50.1 | 53.2 | 50.9 | 53.8 | 55.8 | 47.1 |
| SMS | 9.6 | 3.8 | 5.4 | 5.8 | 5.0 | 1.8 | 7.4 |

TABLE 8 CORRELATION COEFFICIENTS ($r$) FOR MSD DATA AND SOME PHYSICAL PROPERTIES FOR SEVEN FIELD-AGED ASPHALTS

| Fraction | PVN 135°C | Kinematic Viscosity, 135°C | Abs. Vis., 60°C | VTS | pen., 25°C |
|---|---|---|---|---|---|
| LMS ($F_1$+$F_2$) | 0.84 | 0.04 | 0.37 | -0.49 | 0.44 |
| MMS ($F_3$+$F_4$) | -0.43 | -0.08 | -0.10 | 0.53 | -0.61 |
| SMS ($F_5$) | -0.64 | -0.46 | -0.40 | 0.02 | 0.15 |

*Correlation Between MSD Data and Viscosity Ratio*

For virgin asphalts, the viscosity ratio at 60°C showed a weak correlation with MSD (Table 6). Excluding SMS because of its small content and hence limited effect, the direction of association between the two variables was opposite of that reported for PVN at 135°C. Because good field performance is believed to accompany a low viscosity ratio, it then follows that a high LMS percentage and a low MMS percentage are desirable features in an asphalt.

The weak correlation between MSD and viscosity ratio may be attributable to shortcomings of the TFOT method (*15*).

*Correlation Between MSD Data and Kinematic Viscosity*

For virgin asphalts, $r$ has the same direction and nearly the same strength as that calculated for correlation between MSD and PVN at 135°C (Table 6). Field-aged samples showed a weaker correlation between the two variables, but the direction of association was maintained (Table 8).

*Correlation Between MSD Data and Absolute Viscosity*

A weak correlation exists between the two variables for virgin asphalts (Table 6). This agrees with Glover et al. (*6*), who studied the same relationship for 18 virgin asphalts from different Texas refineries. That conclusion does not contradict that of Garrick and Wood (*5*), who report an excellent correlation between MSD and absolute viscosity, because they used blended asphalts obtained from the same source and refinery process. In the present investigation, comparing MSD for pairs of samples (83-3203 and 88-3719, 86-3063 and 88-2192, 88-2570 and 88-2787), received from the same refinery but showing a different viscosity grade, confirms the conclusion of Garrick and Wood (*5*).

Field-aged asphalts showed $r$ values that have the same direction and practically the same strength as those reported for correlation between MSD and kinematic viscosity (Table 8). This similarity is probably attributable to the fact that field-aged asphalts, having been subjected to hot mixing conditions during paving, have already undergone molecular interactions to the point where heating to 60°C or 135°C does not create any net effect, and $r$ is maintained at essentially the same level. Virgin asphalts, on the other hand, showed a marked difference in the value of $r$ to the point of having opposite directions of association between MSD and each of the two types of viscosity (Table 6).

*Correlation Between MSD and VTS*

A strong to excellent correlation exists between the MSD and VTS variables (Table 6). From the direction of association, a low VTS (low temperature susceptibility) is expected for asphalts with a high percentage of LMS components and a low percentage of MMS components. The correlation between SMS and VTS is weak (0.27) and does not allow a definite conclusion to be reached; the positive association, however, favors a low SMS percentage.

That the MSD of virgin asphalts correlates strongly with VTS has also been noted by Glover et al. (*6*); they, too, report weaker correlation for asphalts extracted from field cores. The findings of this paper (Tables 6 and 8) favor the same conclusion.

*Correlation Between MSD Data and Penetration at 25°C*

In agreement with previous research, virgin asphalts demonstrated weak correlation between MSD and penetration (Table 6). For field-aged samples, correlation is stronger for the two major parts: LMS and MMS (Table 8).

The above correlations share the following: (a) a linear fit is assumed; other forms of curve fit—for example, logarithmic, exponential, or power—did not improve correlation; (b) because the virgin asphalts studied were randomly selected ("random" here refers to asphalts covering a wide range of viscosity and a large number of sources and being received over a long period of time) it then follows that the correlation coefficient ($r$) calculated herein is an unbiased estimate of the correlation coefficient ($\mu$) for population of asphalt cements (*17*).

The high value of $r$, and consequently the high value of the coefficient of determination ($r^2$) for correlation of MSD and PVN at 135°C, MSD and kinematic viscosity, and MSD and VTS suggests the possibility of using MSD data to predict these physical parameters.

## Chemical Analysis

Eleven of the 20 virgin asphalts were randomly selected and analyzed into four fractions according to ASTM D4124, Method B. The results—together with the colloidal instability index ($I_c$), as suggested by Gaestel et al. (*18*)—are given in Table 9. The higher the value of $I_c$, the lower the colloidal stability and the more an asphalt will be of the gel type (*4*). It is shown that four out of the five samples with a high colloidal stability ($I_c < 0.35$) appear in the upper left corner of Figure 1.

The colloidal instability index correlates fairly well with MSD (Table 10). The direction of association suggests that a high colloidal stability is satisfied by a high LMS proportion, together with low MMS and SMS proportions. Glover et al. (*6*) and Hattingh (*19*) reported that a high LMS content is a feature of nontender asphalts.

TABLE 9 CHEMICAL ANALYSIS OF VIRGIN ASPHALTS INTO FOUR FRACTIONS ACCORDING TO ASTM D4124, METHOD B

| Sample | Asphaltenes | Saturates | Naphthene Aromatics | Polar Aromatics | $I_C$* |
|---|---|---|---|---|---|
| 82-1332 | 13.19 | 9.98 | 46.84 | 29.04 | 0.305 |
| 82-1522 | 15.48 | 16.32 | 38.18 | 28.97 | 0.474 |
| 83-3284 | 20.54 | 10.79 | 38.42 | 28.82 | 0.466 |
| 85-3695 | 17.92 | 10.77 | 41.66 | 28.06 | 0.411 |
| 85-3890 | 10.27 | 10.33 | 42.57 | 34.95 | 0.266 |
| 86-3063 | 15.60 | 17.11 | 36.87 | 29.36 | 0.494 |
| 87-2040 | 14.31 | 15.91 | 38.89 | 29.90 | 0.439 |
| 88-2483 | 17.75 | 17.02 | 36.62 | 27.04 | 0.546 |
| 88-2570 | 6.19 | 13.09 | 43.58 | 35.78 | 0.243 |
| 88-2787 | 5.21 | 8.63 | 43.78 | 41.17 | 0.163 |
| 88-3680 | 11.27 | 13.61 | 39.50 | 34.74 | 0.335 |

$$*I_C = \frac{\text{Asphaltenes + Saturates}}{\text{Naphthene Aromatics + Polar Aromatics}}$$

TABLE 10 CORRELATION COEFFICIENTS FOR FRACTION CONTENT AND EACH OF THE COLLOIDAL INSTABILITY INDEX AND ASPHALTENE CONTENT

| Fraction | $I_C$ | % Asphaltene |
|---|---|---|
| LMS | -0.51 | -0.66 |
| MMS | 0.47 | 0.60 |
| SMS | 0.28 | 0.45 |

Table 10 also reveals that MSD correlates well with asphaltene content; $r$ has same direction and a higher strength compared with that reported for $I_c$. This is not surprising, because asphaltene content is directly proportional to $I_c$ (*18*). Brulé (*20*) using HPGPC, reports that—contrary to general belief—asphaltenes are not composed of only large molecules but that practically the whole range of molecular sizes present in asphalt is found in asphaltenes.

## Relationship Between MSD and Physicochemical Parameters

To sum up the foregoing strong correlations: a high PVN at 135°C and a low VTS (low temperature susceptibility), a low viscosity ratio (high resistance to aging), a high colloidal stability, and a low asphaltene content would all be favored by a high LMS, together with a low MMS percentage. The SMS fraction demonstrated a weak correlation with most variables and constituted less than 11 percent of any of the virgin samples. Direction of associations, nevertheless, favors a low SMS percentage.

## LMS Versus MMS

In Figure 5, MMS is plotted versus LMS for the 20 virgin asphalts, and it has a correlation coefficient of −0.97. The two Shamrock asphalts are far from the others and appear in the extreme lower right corner. Figure 6 represents the same relationship after the two unique asphalts are excluded. The seven samples appearing in the lower right corner of Figure 6 are arranged according to the LMS/MMS ratio in Table 11.

It is interesting to note that all seven asphalts (35 percent of the whole set) with high LMS/MMS ratios appear in—or at the periphery of—the upper left corner of Figure 1, which includes other samples as well (75 percent of the whole set). Using MSD, it is thus possible to further screen asphalts with potential for good field performance. This set of seven asphalts has common characteristics: absolute viscosity of 1,100 to 1,700 poises, kinematic viscosity of 300 to 400 cst, a viscosity ratio of 2.1 to 2.9, a VTS of 3.43 to 3.58, a PVN at 60°C of −0.3 to −0.8, and a PVN at 135°C of −0.3 to −0.8.

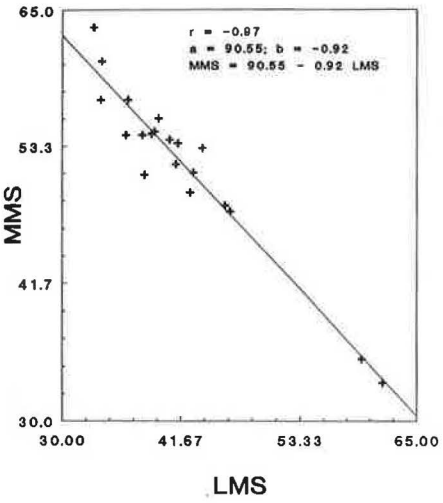


**FIGURE 5 MMS versus LMS for 20 virgin asphalts.**

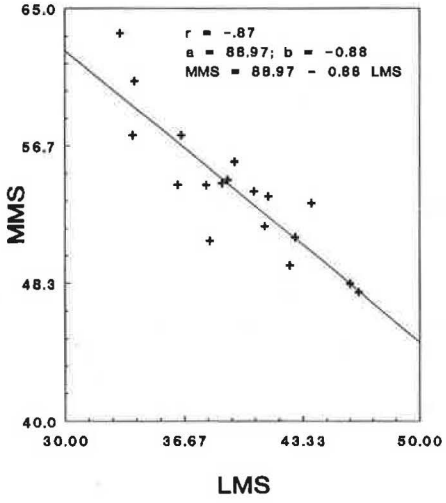


**FIGURE 6 MMS versus LMS for 18 of the asphalts shown in Figure 5.**

TABLE 11 ASPHALTS WITH HIGH LMS AND LOW MMS FRACTIONS

| Sample | LMS, % / MMS, % |
|---|---|
| 88-3680 | 0.97 |
| 85-1230 | 0.95 |
| 82-2746 | 0.86 |
| 82-1522 | 0.84 |
| 86-3063 | 0.82 |
| 83-3284 | 0.80 |
| 82-1214 | 0.77 |

### Laboratory Aging Versus Field Aging

To compare the effects of the two types of aging, the change in MSD for some asphalts was calculated (Table 12). In agreement with other investigators' findings, both types of aging caused the LMS proportion to increase and the MMS proportion to decrease. The only exceptions were three field-aged samples, none of which had more than 3 years of service. The odd change (LMS decreased, and MMS increased) was within the accuracy of data ($\pm 1$ percent of the original) (*11*). The SMS proportion showed mixed response; however, the small percentage of SMS ($< 6.5$ percent) limits the role of this fraction.

## CONCLUSIONS

First, 2 asphalts supplied by Diamond Shamrock demonstrated unique characteristics as opposed to the other 18: They have high penetration at 25°C, low absolute viscosity, low viscosity of residue after TFOT, highest kinematic viscosity, lowest viscosity ratio, lowest VTS, highest PVN at 135°C, highest LMS, lowest MMS, lowest asphaltene content, and highest colloidal stability.

Second, $\log_{10}$ of absolute viscosity correlates strongly with each of $\log_{10}$ kinematic viscosity ($r = 0.87$, excluding the two Shamrock asphalts), and just as strongly ($r = -0.81$) with $\log_{10}$ penetration at 25°C for the 20 virgin asphalts.

Third, a 16-hr TFOT causes penetration and MMS components to decrease but absolute viscosity, kinematic viscosity, VTS, PVN at 60°C, PVN at 135°C, and LMS components to increase. Field aging (up to 7 years) caused changes that are similar in direction but less drastic in magnitude.

Fourth, MSD correlates strongly with PVN at 135°C, viscosity at 135°C, VTS, colloidal instability, and asphaltene content but less strongly with viscosity ratio at 60°C. For all

TABLE 12 COMPARISION BETWEEN LABORATORY AGING AND FIELD AGING AS REVEALED BY HPGPC ANALYSIS

| Sample # | 82-1332 | 82-1522 | 85-4116 | 86-3063 | 87-2040 | 88-2483 | 88-3680 |
|---|---|---|---|---|---|---|---|
| Years of Service | 7 | 7 | 4 | 3 | 2 | 1 | 1 |
| δLMS | +1.9 | +3.1 | +1.8 | -0.6 | +4.7 | +3.3 | -1.0 |
| δLMS' | +3.0 | +1.7 | +4.5 | +4.1 | +3.3 | +5.0 | +3.9 |
| δMMS | -6.0 | -1.0 | -2.5 | -2.3 | -3.5 | +1.2 | -0.7 |
| δMMS' | -5.2 | -3.7 | -4.2 | -2.9 | -2.6 | -5.2 | -1.4 |
| δSMS | +4.1 | -2.2 | +0.6 | +2.8 | -1.2 | -4.6 | +1.7 |
| δSMS' | +2.1 | +1.9 | -0.4 | -1.1 | -0.7 | 0.0 | -2.6 |

δLMS = LMS% of field aged sample - LMS,% of original.

δLMS' = LMS% after TFOT - LMS,% of original.

correlations, direction of associations points out that high PVN at 135°C and low VTS (low temperature susceptibility), low viscosity ratio (high resistance to aging), high colloidal stability, and low asphaltene content are all favored by high LMS and low MMS proportions. The SMS fraction correlates weakly with most variables investigated and constitutes less than about 10 percent of any of the asphalts under consideration. Direction of associations, however, favors a low SMS proportion.

Fifth, among those studied, virgin asphalts with high LMS/MMS ratio (> 0.75) are characterized by low temperature susceptibility and high resistance to aging.

Sixth, because asphalts with low temperature susceptibility and high resistance to aging are expected to exhibit good field performance, and because the LMS/MMS ratio provides a further screening characteristic, it is recommended that HPGPC be used to determine the MSD of a given asphalt. However, further work to tie the optimum MSD to actual field performance is needed.

Finally, from the 20 virgin asphalts tested, those with the highest LMS/MMS ratio have common features: viscosity at 60°C between 1,100 and 1,700 poises, viscosity at 135°C between 300 and 400 cst, viscosity ratio from 2.1 to 2.9, VTS from 3.43 to 3.58, PVN at 60°C between −0.3 and −0.8, and PVN at 135°C between −0.3 and −0.8.

## ACKNOWLEDGMENTS

This work was accomplished in cooperation with FHWA and its Kansas division. Thanks are due to Hope Alban and Condie Erwin for entering text on the word processors.

## REFERENCES

1. J. L. Goodrich and L. H. Dimpfi. Performance and Supply Factors to Consider in Paving Asphalt Specifications. *Proc., Association of Asphalt Paving Technologists*, Vol. 55, 1986.
2. F. S. Rostler and R. M. White. *Influence of Chemical Composition of Asphalts on Performance, Particularly Durability*. ASTM STP, 1959.
3. R. P. Price and J. L. Burati, Jr. A Quantitative Method Using HP-GPC to Predict Laboratory Results of Asphalt Cement Tests. *Proc., Association of Asphalt Paving Technologists*, Vol. 58, 1989, pp. 182–219.
4. B. Brulé, G. Ramond, and C. Such. Relationships Between Composition, Structure, and Properties of Road Asphalts: State of Research at the French Public Works Central Laboratory. In *Transportation Research Record 1096*, TRB, National Research Council, Washington, D.C., 1986, pp. 22–34.
5. N. W. Garrick and L. E. Wood. Relationship Between High-Pressure Gel Permeation Chromatography Data and the Rheological Properties of Asphalts. In *Transportation Research Record 1096*, TRB, National Research Council, Washington, D.C., 1986, pp. 35–41.
6. C. J. Glover, R. R. Davison, J. A. Bullin, J. W. Button, and G. R. Donaldson. Chemical Characterization of Asphalt Cement and Performance-Related Properties. In *Transportation Research Record 1171*, TRB, National Research Council, Washington, D.C., 1988, pp. 71–81.
7. P. W. Jennings, J. A. S. Pribanic, J. Smith, and T. M. Mendes. Predicting the Performance of Montana Test Sections by Physical and Chemical Testing. In *Transportation Research Record 1171*, TRB, National Research Council, Washington, D.C., 1988, pp. 59–65.
8. G. R. Donaldson, M. W. Hlavinka, J. A. Bullin, C. J. Glover, and R. R. Davison. The Use of Toluene as a Carrier Solvent for Gel Permeation Chromatography Analysis of Asphalt. *Journal of Liquid Chromatography*, Vol. 11, 1988, pp. 749–765.
9. B. V. Enustun, S. S. Kim, and D. Y. Lee. *Correlation of Locally-based Performance of Asphalts with their Physicochemical Parameters*. Final Report on Project HR-298. Iowa Department of Transportation, Des Moines, March 1990, pp. 1–107.
10. S. W. Bishara and R. L. McReynolds. Use of HPGPC with UV Detection for Determination of Molecular Size Distribution of Asphalt Cement After Quantitative Corrections for Molar Absorptivity Variation and Saturated Oils. In *Transportation Research Record 1269*, TRB, National Research Council, Washington, D.C., 1990, pp. 40–47.
11. S. W. Bishara and R. L. McReynolds. The Use of HPGPC for Determination of MSD of Asphalt Cement: A Spectrophotometric vs. Gravimetric Finish. *Proc., 200th National Meeting*, American Chemical Society, Vol. 35, No. 3, 1990, pp. 396–406.
12. *Recovery of Asphalt from Methylene Chloride and Trichloroethylene by the Abson Method*. Publication FHWA-RD-89-207. FHWA, U.S. Department of Transportation, Nov. 1989.
13. L. W. Corbett and H. E. Schweyer. Viscosity Characterization of Asphalt Cement. In *Viscosity Testing of Asphalt and Experience with Viscosity Graded Specifications*, ASTM STP 532, 1973, pp. 40–49.
14. D. S. Moore and G. P. McCabe. *Introduction to the Practice of Statistics*. W. H. Freeman and Company, New York, N.Y., 1989, pp. 197–212.
15. Asphalt Binder Specification "Hypothesis" Developed. *Focus*, Strategic Highway Research Program, National Research Council, Washington, D.C., Sept. 1989.
16. B. Brulé. Contribution of Gel Permeation Chromatography (GPC) to the Characterization of Asphalts. In *Liquid Chromatography of Polymers and Related Materials II* (J. Cazes and X. Delamare, eds.), Marcel Decker, Inc., New York, N.Y., 1980, pp. 215–248.
17. R. L. Anderson. *Practical Statistics for Analytical Chemists*. Van Nostrand Reinhold Company, New York, N.Y., 1987, pp. 118–120.
18. C. Gaestel, R. Smadja, and K. A. Lamminan. Contribution à la Connaissance des Propriétés des Bitumes Routiers. *Revue Générale des Routes et Aérodromes*, Vol. 466, 1971, pp. 85–94.
19. M. M. Hattingh. The Fractionation of Asphalt. Presented at the Annual Meeting of Association of Asphalt Paving Technologists, Scottsdale, Ariz., 1984.
20. B. Brulé. Characterization of Bituminous Compounds by Gel Permeation Chromatography (GPC). *Journal of Liquid Chromatography*, Vol. 2, 1979, pp. 165–192.
21. D. W. Christensen and D. A. Anderson. Effect of Amine Additive on the Properties of Asphalt Cement. *Journal, Association of Asphalt Paving Technologists*, Vol. 54, 1985, pp. 593–615.

*Publication of this paper sponsored by Committee on Characteristics of Bituminous Materials.*

# Adsorption Behavior of Asphalt Models and Asphalts on Siliceous and Calcareous Aggregates

C. J. BRANNAN, Y. W. JEON, L. M. PERRY, AND C. W. CURTIS

The adsorption of seven single model species representative of functionalities prevalent in asphalt on siliceous and calcareous aggregates was examined. The seven model species were ranked based on their Langmuir monolayer adsorption amounts as well as their adsorption amounts on one or two grams of aggregates. The aggregates used were gravels, limestones, and greywacke. Benzoic acid showed the greatest affinity for the aggregates tested. In addition, the adsorption and desorption behavior of three asphalts with substantially different chemical compositions was determined on a single siliceous aggregate. Differences observed in their behaviors may be attributed to differences in their chemical compositions. The adsorption and water desorption behavior of an AR-4000 asphalt was also determined on three different aggregates: limestone, gravel, and greywacke. Substantial differences in the amount adsorbed and desorbed as well as the shapes of their adsorption curves were observed. Limestone adsorbed the most asphalt and retained the largest amount of asphalt after desorption by water. Limestone desorbed the most asphalt in the presence of water, and greywacke desorbed the least. The precoating of antistripping agent on greywacke resulted in less asphalt desorption by water in comparison with coadsorbing antistripping agent with asphalt or with no antistripping agent being present in the system.

A number of factors affect the interaction of asphalt with aggregate in a road pavement. These factors include the chemistry and composition of the asphalt and aggregate, the surface area and chemistry of the aggregate surface, the specific bonding interactions between the asphalt and aggregate, and the resistivity to moisture of a particular asphalt-aggregate combination. Other factors that influence the interaction involve pavement construction practices, the roughness of the aggregate surface, the propensity of a particular combination toward oxidation of the asphalt as well as the environment of the pavement, both in a localized context at the asphalt-aggregate interface and in a more global sense of heat, cold, and traffic. Although many factors influence the interaction between asphalt and aggregate, the effect of the chemistry and composition of asphalt and aggregate on the affinity of asphalt for adsorbing on a particular aggregate and resistivity of the particular combination to moisture is the focus of this paper.

Previous researchers (*1*,*2*) have found that the more polar constituents of asphalt appear to be concentrated at the surface of the aggregate and more sensitive to moisture. Scott (*3*, p. 19) has stated that oxygen-containing groups present in the asphaltenes of asphalts were preferentially adsorbed onto the aggregate surfaces. Fritschy and Papirer (*4*) have shown that asphaltenes, the concentrated polar fraction of the asphalts, adsorbed more onto aggregates than the whole asphalt. Curtis et al. (*5*,*6*) have shown that asphaltenes behave similarly to whole asphalt on both sandstone and limestone. The chemistry of the aggregate, particularly the surface chemistry, affects the interaction between asphalt and aggregate. The affinity of a given asphalt for different aggregates may vary considerably depending on the composition and surface activity of the aggregate. The adsorption behavior of asphalts on aggregates is related to the stripping phenomenon only when water is present in the system.

The overall objective was to elucidate chemical interactions that occur at the asphalt-aggregate interface. Three approaches were taken: relative adsorption affinities of model asphalt compounds were determined on aggregates; the adsorption and desorption behavior of asphalt on different aggregates was determined; and the effect of an antistripping (AS) agent on the adsorption and desorption behavior of asphalt was evaluated. Seven compounds representing key functionalities present in asphalt cements were used as models for evaluating physical parameters, for example, monolayer surface coverage, Gibb's free energy of adsorption ($\Delta G^\circ$), and the equilibrium constant ($K$), relating to the adsorptive interactions. The relative adsorption affinities of each of the seven model compounds were determined on five aggregates. This information served as a means of characterizing the chemical reactivity of each aggregate and provided possible explanations for the observed adsorption and desorption behavior of different asphalt-aggregate pairs. The adsorption and desorption behavior of asphalts on both siliceous and calcareous aggregates were determined and compared. The amount of asphalt remaining on each of the aggregates was determined. The effect of an AS agent on the adsorptive and desorptive behavior of an asphalt-aggregate system was also evaluated. Precoating of aggregate surface with AS agent before adsorption investigations as well as coadsorption of AS agent with asphalt onto aggregate surface were examined. The amounts adsorbed by both methods were compared with respect to water sensitivity.

## EXPERIMENT

### Single Component Adsorption

Benzoic acid, indole, phenanthridine, naphthalene, 1-naphthol (all at least 99 percent pure), phenylsulfoxide (97 percent),

Department of Chemical Engineering, Auburn University, Ala. 36849-5127.

9-fluorenone (98 percent), and cyclohexane (at least 99 percent spectrophotometric grade) were supplied by Aldrich Chemical Company. Cyclohexane was dried before being used with activated 4Å molecular sieves. All other compounds were used as received. Aggregates—RC-limestone, RD-limestone, RH-greywacke, RJ-gravel, and RL-gravel—used in the single adsorption study were obtained from the Strategic Highway Research Program (SHRP) Material Reference Library (MRL) at the University of Texas, Austin. Chemical and physical properties of the aggregates were determined by Southwestern Laboratories, Inc., Houston, Texas, and lithologies were provided by the Center for Applied Energy Research, University of Kentucky, Lexington. Aggregates were sized to −40 +80 mesh, washed thoroughly with distilled water, dried at 150°C for 1 week, and stored in a brown bottle. Aggregates were dried for an additional 24 hr before use.

### *Procedures*

For single component adsorption experiments, standard stock solutions of 100 mg/L of each model compound were prepared in cyclohexane. Exactly 20 mL of the stock solution were pipetted into serum bottles (30 mL capacity) containing varying amounts (1, 2, 3, 4, 6, 8, 10 g) of aggregate. The serum bottles were placed in the controlled temperature (25°C) environment of an orbital shaker (Labline, Fisher Scientific), agitated for 1 hr, and allowed to settle for an additional hour. Powdered aggregate that remained suspended in the solution was removed by filtration through a 0.22 micron MSI teflon membrane (Fisher Scientific). The filtrate was monitored by ultraviolet (UV) spectroscopy, at the wavelength of maximum absorbance of the model compound, to determine the concentration of the model not adsorbed by the aggregate. All experiments were performed at least in duplicate.

### *Calculations*

Langmuir plots of adsorption data were used for the determination of equilibrium constants, monolayer surface coverages, and Gibb's free energies of adsorption. The Langmuir equation can be stated as follows (*7*):

$$C/q = C/q_m + 1/bq_m \tag{1}$$

where

$C$ = equilibrium solution concentration (mg/L),
$q$ = equilibrium amount adsorbed (mg/g),
$q_m$ = saturated monolayer amount (mg/g), and
$b$ = constant related to strength of adsorption (unitless).

Parfitt and Rochester derived the Langmuir equation to describe adsorption data obtained from dilute solutions, which is given as follows (*8*):

$$c/x = c/x_m + 1/(K - 1)x_m \tag{2}$$

where

$c$ = mole fraction of solute concentration (unitless),
$x$ = moles of solute adsorbed per unit mass of adsorbent (moles/g),
$x_m$ = molar monolayer of adsorbed solute per unit weight of adsorbent (moles/g), and
$K$ = equilibrium constant for the interaction of asphalt model $M$ in cyclohexane with aggregate surface $A$ to yield the product $MA$.

$$M + A \rightarrow M \cdot A$$

$$K = (MA)/(M)(A) \tag{3}$$

For strongly adsorbing solutes, $K > 1$, the Langmuir equation is simplified to the following:

$$c/x = c/x_m + 1/Kx_m. \tag{4}$$

$K$ and $x_m$ can be determined from the slope and intercept of a linear plot of $c/x$ versus $c$. Determination of the equilibrium constant ($K$) allows calculation of the Gibb's free energy of adsorption ($\Delta G°$ in joules) from the following relation:

$$\Delta G° = -nRT\,(\ln K) \tag{5}$$

where

$n$ = number of moles of solute adsorbed (mole),
$R$ = universal gas constant 8.314 J/$K$ mole, and
$T$ = absolute temperature in $K$.

The amount of model compound adsorbed onto aggregate surface is determined from a calibration curve composed of adsorbate solutions with known concentrations for each asphalt model compound at its maximum absorbance wavelength. Beer's law was employed for the determination of solution concentrations before and after the adsorption experiments. Beer's law, $A = abc$, is valid for dilute solutions where $A$ is the absorbance at a given wavelength (unitless), $a$ the absorptivity (L/mole cm), $b$ the path length of cell (cm), and $c$ the concentration (moles/L). The absorbance values obtained in the adsorption experiments were converted to concentrations and the amount of compound adsorbed isothermally onto aggregate was determined from the following:

$$q_i = (C_o - C_i)V/M \tag{6}$$

where

$q_i$ = amount adsorbed (mg/g aggregate),
$C_o$ and $C_i$ = concentrations of adsorbate before contact and after contact with aggregate (mg/L),
$V$ = volume of adsorbate solution introduced into the system (L), and
$M$ = mass of aggregate used (g).

## Adsorption and Desorption of Asphalt

The asphalts, AAD-1 (AR-4000), AAM-1 (AC-20), and AAK-1 (AC-30), and aggregates, RC-limestone, RH-greywacke, and RL-gravel, used in this study were obtained from the SHRP MRL. Aggregates were sized to −40 +80 mesh, washed with distilled water, dried at 150°C for 1 week and stored in a brown bottle before use. Chemical and physical properties of the aggregates and asphalts are given in Tables 1 and 2, respectively.

TABLE 1 PHYSICAL AND CHEMICAL PROPERTIES OF AGGREGATES

| Property[a,b] | Aggregates | | | | |
|---|---|---|---|---|---|
| | RC-limestone | RD-limestone | RH-greywacke | RJ-gravel | RL-gravel |
| **POROSITY** | | | | | |
| Avg. Pore Diam. (μm) | 0.0611 | 0.0111 | NA* | 0.0151 | 0.0138 |
| Total Pore Area ($m^2/g$) | 2.548 | 1.465 | NA | 1.888 | 3.027 |
| **WATER ABSORPTION** | | | | | |
| % Absorption | 0.37 | 0.3 | NA | 0.7 | 0.9 |
| **BULK SPECIFIC GRAVITY** | 2.536 | 2.704 | NA | 2.625 | 2.568 |
| **ACID INSOLUBLES** | | | | | |
| Insoluble Residue % | 4.8 | 18.1 | NA | 99.2 | 88.2 |
| **WATER INSOLUBLES** | | | | | |
| Water solubles % | 2.4 | 1.9 | NA | 4.1 | 1.8 |
| pH | 9.47 | 9.12 | NA | 9.12 | 9.18 |
| **SURFACE AREA ($m^2/g$)[c]** | 1.79 | 0.43 | 3.12 | 0.37 | 0.93 |
| **MAJOR OXIDES** | | | | | |
| $SiO_2$, % | 6.49 | 16.4 | 66.0 | 76.5 | 63.1 |
| $Al_2O_3$, % | 1.23 | 2.28 | 10.4 | 12.2 | 4.66 |
| $Fe_2O_3$, % | 0.78 | 0.08 | 12.9 | 1.09 | 1.67 |
| MgO, % | 2.52 | 5.29 | 2.44 | 0.27 | 0.32 |
| CaO, % | 48.9 | 39.1 | 2.35 | 1.45 | 14.5 |
| $Na_2O$, % | 0.24 | 0.16 | 2.57 | 2.91 | 0.92 |
| $K_2O$, % | 0.22 | 1.16 | 0.99 | 4.31 | 1.72 |
| Other, % | < 0.2 | < 0.2 | < 0.8 | < 0.2 | < 0.2 |
| Loss of Volatiles, % | 40.3 | 35.0 | 0.96 | 0.59 | 11.2 |
| **LITHOLOGY** | 100% Limestone | 53.3% Shaly Limestone<br>26.8% Limestone<br>19.7% Arcenaceous Limestone | 71.3% Micaceous Sandstone<br>11.2% Miscellaneous<br>10.9% Granite<br>6.6% Chert | 47.4% Sandstone<br>28.4% Granite<br>23.7% Miscellaneous<br>0.4% Basalt | 59.1% Chert<br>18.2% Arcenaceous Limestone<br>11% Granite<br>5.8% Miscellaneous |

*NA = Not Available

[a] Porosity, water absorption, bulk specific gravity, acid insolubles and water insoluble data were obtained from SHRP A-001.
[b] Surface areas and major oxides were obtained from Western Research Institute in SHRP A-003B.
[c] Surface area measurements were obtained by $N_2$ BET by WRI.

Toluene and methylene chloride, Fisher spectranalyzed, were dried with 4Å molecular sieves before use, and polyamine AS agent (M-AS-005-001) obtained from SHRP MRL was used as received. Distilled, deionized water was used in desorption studies.

Adsorption of asphalt from toluene solution onto aggregate was performed using a recirculating system that consisted of a thermojacketed column containing aggregate through which a solution of toluene and asphalt was circulated repeatedly through a bed of aggregate. The column temperature was maintained at 25°C. Concentration changes of asphalt in solution were monitored after adsorption equilibrium of 7 hr by visible absorbance spectroscopy at 410 nm. Six independent columns that run in parallel, each containing an asphalt solution of specific concentration, were pumped by a microprocessor pump drive. The asphalt concentration of the initial solutions used to develop the isotherm ranged from 0.10 to 0.66 g/L. Desorption of asphalt from aggregate was achieved by introducing ~280 mmolar water after adsorption equilibrium was achieved. The amount of asphalt desorbed was monitored at 410 nm after 2 hr.

The concentration of the asphalt in solution after both adsorption and desorption was obtained using Beer's law. The equations used for calculating these amounts are

$$C/C_o = \text{Abs}/\text{Abs}_o$$

$$AW = V(C_o - C)$$

$$A = VC_o(\text{Abs}_o - \text{Abs})/W\text{Abs}_o$$

$$D_wW = -V_w(C - C_w)$$

$$D_w = -V_wC(\text{Abs} - \text{Abs}_w)/W\text{Abs} \quad (7)$$

where

$C_o$ and $C$ = initial and equilibrated asphalt solution concentrations (g/L),
$\text{Abs}_o$ and Abs = absorbances of initial and equilibrated solutions,
$A$ = amount of asphalt adsorbed per gram of aggregate (g/g),
$W$ = mass of aggregate used (g),
$V$ and $V_w$ = initial and final solution volumes used for desorption (L),
$D_w$ = amount of asphalt desorbed per gram of aggregate (g/g),
$C_w$ = asphalt solution concentration after desorption (g/L), and
$\text{Abs}_w$ = absorbance of the extracted solution.

TABLE 2 PHYSICAL AND CHEMICAL PROPERTIES OF ASPHALTS

| PROPERTY | Asphalt Properties | | |
|---|---|---|---|
| | AAD-1 | AAM-1 | AAK-1 |
| | AR4000 | AC-20 | AC-30 |
| 140°F, Viscosity Poise | 1055 | 1992 | 3256 |
| 275°F, cst | 309 | 569 | 562 |
| **Component Analysis** | | | |
| Asphaltenes, % | 23.0 | 3.9 | 21.1 |
| Polar Aromatics, % | 41.3 | 50.3 | 41.8 |
| Naphthene Aromatics, % | 25.1 | 41.9 | 30.0 |
| Saturates, % | 8.6 | 1.9 | 5.1 |
| **Elemental Analysis** | | | |
| Carbon, % | 81.6 | 86.8 | 80.7 |
| Hydrogen, % | 10.8 | 11.2 | 10.2 |
| Oxygen, % | 0.9 | 0.5 | 0.8 |
| Nitrogen, % | 0.9 | 0.5 | 0.8 |
| Sulfur, % | 8.6 | 2.4 | 6.6 |
| Vanadium, ppm | 293 | 60 | 1427 |
| Nickel, ppm | 145 | 29 | 128 |
| $C_{aromatic}$, % | 23.7 | 24.7 | 31.9 |
| $H_{aromatic}$, % | 6.8 | 6.5 | 6.8 |
| **Absorptivity (liters/ gm cm)** | | | |
| 410 nm | 3.79 | 5.74 | 7.40 |
| 375 nm | 4.90 | 8.11 | 6.57 |
| **Functional Groups** | | | |
| Carboxylic Acids | 0.011 | 0.013 | 0.000 |
| Acid Salts | 0.000 | 0.000 | 0.000 |
| Acid Anhydrides | 0.000 | 0.000 | 0.000 |
| Quinolones | 0.024 | 0.012 | 0.012 |
| Ketones | trace | trace | trace |
| Phenols | 0.124 | 0.027 | 0.070 |
| Sulfoxides | trace | trace | trace |
| Pyrroles | 0.168 | 0.110 | 0.157 |

### Asphalt and Antistripping Agent Systems

Two different asphalt adsorption experiments using AAD-1 asphalt were performed with AS agent: (a) asphalt from toluene solution was adsorbed onto RH-greywacke precoated with AS agent and (b) asphalt and AS agent were coadsorbed from a 3:1 with toluene/methylene chloride solution onto RH-greywacke. Methylene chloride was required to prevent precipitation of the AS agent. For comparison, AAD-1 asphalt was adsorbed and subsequently desorbed from both toluene and toluene-methylene chloride solution onto uncoated RH-greywacke. Asphalt remaining on the aggregate surface was determined by subtracting the amount of asphalt desorbed from that originally absorbed.

For the first set of experiments, RH-greywacke was precoated with AS agent from methylene chloride in a batch system that was temperature controlled at 25°C and orbitally agitated at 250 rpm for 1 hr. Initial concentrations of AS agent in methylene chloride of 0.2–5.0 g/L were used to determine the adsorption isotherm; a saturation concentration of 4.3 g/L of AS agent in methylene chloride was selected for precoating the aggregate at a coating level of 7.8 weight per-

cent. RH-greywacke precoated with this AS agent was used for asphalt adsorption experiments from toluene followed by desorption with ~280 mmolar water.

Coadsorption of asphalt and AS agent from the 3:1 toluene to methylene chloride solution was conducted at two different concentrations of AS agent: 4.05 g/L (corresponding with the chosen AS concentration for the precoated aggregate) and 0.1025 g/L (corresponding with that used in actual practice). Asphalt, at 0.66 g/L, was added to each of these solutions containing AS agents. As the concentrations of these initial solutions were diluted to perform the adsorption isotherms, the ratio of AS agent to asphalt remained constant.

Although the absorbance spectra of asphalt and AS agent were similar, a significant difference in their molar absorptivities was observed. The ratio of the absorptivity of asphalt to the absorptivity of the AS agent was ~30 at 410 nm. Therefore, quantitative determination of adsorbed asphalt was based on a weight ratio of asphalt and AS agent. To determine the amount of asphalt adsorbed and desorbed during the coadsorption experiments, a calibration curve of the ratio of the amount of asphalt adsorbed to the amount of AS agent adsorbed versus the ratio of the initial concentration of AS agent (AS) to asphalt (ASP) was developed. This calibration curve resulted from a series of experimental observations and calculations using Beer's law. For a given solution with an initial concentration ratio of $(AS)_o/(ASP)_o$, the total absorbance of both asphalt and AS agent was measured. The absorptivity of the solution was determined by measuring the visible absorbance at 410 nm at different ratios of $(AS)_o$ to $(ASP)_o$. To determine the amount of asphalt adsorbed onto aggregate introduced into the system, the following relationship was used:

$$AMT_{ASP} = AMT_{Tot}\left(\frac{a_{ASP}}{a_{Tot}}\right) \quad (8)$$

where

$AMT_{ASP}$ = amount of asphalt adsorbed onto the aggregate,
$AMT_{Tot}$ = total amount of asphalt and AS agent adsorbed that was obtained experimentally,
$a_{ASP}$ = absorptivity of asphalt at 410 nm obtained experimentally, and
$a_{Tot}$ = absorptivity of the asphalt and AS agent combined at 410 nm and measured as described above.

The amount of AS agent adsorbed ($AMT_{AS}$) was obtained from the difference $AMT_{Tot} - AMT_{ASP}$. The quantities for the ratio of the $AMT_{ASP}$ to $AMT_{AS}$ were then calculated. Experimental points were generated at varying ratios of $(AS)_o/(ASP)_o$ and used to produce a curve, Figure 1, of the ratio of amount adsorbed ($AMT_{ASP}/AMT_{AS}$) versus the ratio of concentration of AS agent to concentration of asphalt $[(AS)_o/(ASP)_o]$ that followed the equation

$$y = 16.6x^{-0.581} \quad (9)$$

where $y$ is the ratio $AMT_{ASP}/AMT_{AS}$ and $x$ is the initial concentration ratio $(AS)_o/(ASP)_o$. When a coadsorption experiment was performed, $(AS)_o/(ASP)_o$ was known and the ratio of $AMT_{ASP}/AMT_{AS}$ was determined from Equation 9. Because the total amount of adsorption was known, the amount of asphalt and AS agent could be determined individually.

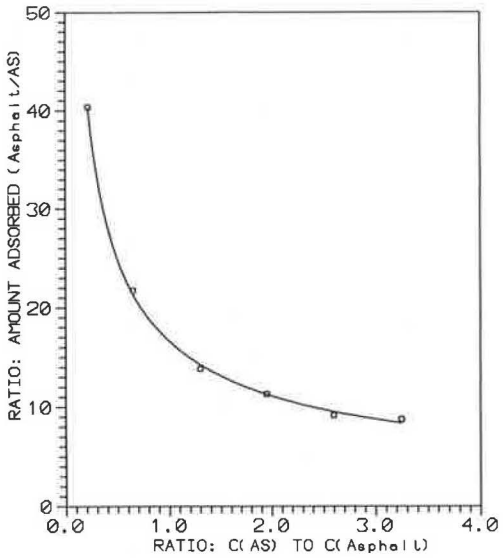


**FIGURE 1 Adsorption ratio determination from solution concentration ratio.**

## RESULTS AND DISCUSSION

### Adsorption of Model Asphalt Compounds onto MRL Aggregates

The adsorption properties of seven model compounds were investigated on five MRL aggregates: RC-limestone, RD-limestone, RH-greywacke, RJ-gravel, and RL-gravel. Each model compound was chosen to represent key asphaltic components that have been reported to be present at the asphalt-aggregate interface (*1,2*). Benzoic acid was chosen as the model compound to represent carboxylic acids; phenylsulfoxide, to represent sulfoxides; 1-naphthol, phenols; phenanthridine, pyridinics; indole, pyrrolics; 9-fluorenone, ketones; and naphthalene, aromatic species. All model compounds, because of their respective functionalities, exhibited absorbance characteristics in the same spectral region as asphalt.

Mineralogical characterization of the MRL aggregates used in these studies shows three compositionally different aggregate types (*9,10*), as shown in Table 1. RJ-gravel and RL-gravel are both mixtures of siliceous gravels consisting of igneous, metamorphic, and sedimentary rocks. RL-gravel contains a small percentage of limestone, thus distinguishing it from RJ-gravel. RC-limestone consists mainly of three major limestone groups: fine-grained crushed limestone, dolomitic limestone, and a significant amount of clay seams. RD-limestone consists of calcareous rocks rich in shale and quartz with small amounts of iron pyrite. The RH-greywacke is a sedimentary rock consisting of a mixture of clay, silt, sand, and rock fragments. These aggregates with different mineralogical, compositional, and acid-base behavior were chosen for testing with the model compounds. The surface areas of

the aggregates ranged in order of magnitude. RH-greywacke had the largest surface area, 3.12 $m^2/g$, and RJ-gravel and RD-limestone possessed the least surface areas, 0.37 and 0.43 $m^2/g$, respectively. The variety in the aggregate characteristics for the selected aggregates can be observed by comparing the differences in the percentage of water solubles, the percentage of acid insoluble residue, the percentage of volatiles loss, and the percentage of different oxide-containing compounds attributed to the different aggregates. Although the percentage of water solubles was similar (< 5 percent) for all the aggregates—except RH-greywacke, for which these particular physical constants were not determined—the percentage of acid insoluble residue for RL-gravel was more than 15 times greater than for RC-limestone and almost 5 times greater than RD-limestone. The solubility of limestone aggregates in acidic media indicated a strong preference for limestone for interactions with acidic asphalt models. The relatively high percentage of acid insoluble residue given for RL-gravel and RJ-gravel, 88.2 and 99.2 percent, respectively, indicated a lack of preference for acidic asphalt models.

The Langmuir adsorption model was applied to the adsorption data to describe the adsorption behavior of each functionality on each aggregate. Monolayer surface coverages, equilibrium constants, and Gibb's free energies of adsorption for each model compound-aggregate pair were obtained from Langmuir treatment of the adsorption data and are summarized in Table 3. RD-limestone exhibited poor adherence to the Langmuir model for almost all asphalt models with the exception of benzoic acid. RJ-gravel also responded unfavorably to Langmuir treatment for three asphalt models—benzoic acid, indole, and 9-fluorenone—as did RL-gravel with indole. Perhaps this behavior can be attributed to the heterogeneity of these particular aggregates surfaces that might have more than one type of bonding interaction site for these models. Although adsorption occurred for these compounds, and the Langmuir model was applied, not all Langmuir physical constants could be determined for these compounds.

Langmuir monolayer surface coverages ($\mu$mole/g and $\mu$mole/$m^2$) for each asphalt model compound on each aggregate are presented in Table 3. Most model compound-

TABLE 3 COMPARISON OF PHYSICAL CONSTANTS DETERMINED FROM LANGMUIR EQUATION FOR SPECIFIC ASPHALT MODELS ADSORBED ON MRL AGGREGATES

| Model/Aggregate | Monolayer Amount | | Equilibrium Constant (K) $x10^{-5}$ | Gibb's Free Energy ($\Delta G^o$) (KJ/mole) | Correlation Coefficient |
|---|---|---|---|---|---|
| | $\mu$mole/g | $\mu$mole/$m^2$ | | | |
| Benzoic Acid | | | | | |
| RC-limestone | 4.65 | 2.61 | 3.87 | -31.9 | 0.99 |
| RD-limestone | 1.97 | 4.59 | 4.09 | -32.0 | 0.99 |
| RH-greywacke | 7.38 | 2.39 | 1.51 | -29.5 | 0.99 |
| RJ-gravel | 2.23 | 6.02 | — | — | 0.99 |
| RL-gravel | 9.15 | 9.84 | 5.92 | -32.9 | 0.99 |
| Phenylsulfoxide | | | | | |
| RC-limestone | 3.96 | 2.23 | 5.51 | -32.8 | 1.00 |
| RD-limestone | 0.667 | 1.55 | — | — | 0.89 |
| RH-greywacke | 6.35 | 2.04 | 6.91 | -33.3 | 1.00 |
| RJ-gravel | 8.62 | 23.27 | 2.16 | -30.4 | 0.94 |
| RL-gravel | 6.33 | 6.81 | 2.05 | -30.3 | 0.96 |
| 1-Naphthol | | | | | |
| RC-limestone | 3.59 | 2.02 | 3.50 | -31.6 | 1.00 |
| RD-limestone | 0.636 | 1.48 | — | — | 0.99 |
| RH-greywacke | 4.94 | 1.58 | 2.78 | -31.1 | 1.00 |
| RJ-gravel | 1.46 | 3.93 | 4.44 | -32.2 | 0.99 |
| RL-gravel | 3.40 | 3.65 | 2.78 | -31.1 | 1.00 |
| Phenanthridine | | | | | |
| RC-limestone | 2.86 | 1.61 | 6.10 | -33.0 | 1.00 |
| RD-limestone | 0.562 | 1.31 | — | — | 0.77 |
| RH-greywacke | 4.80 | 1.54 | 2.07 | -30.3 | 1.00 |
| RJ-gravel | 2.53 | 6.83 | 1.18 | -28.9 | 0.96 |
| RL-gravel | 4.55 | 4.89 | 2.86 | -31.1 | 0.99 |
| Indole | | | | | |
| RC-limestone | 2.94 | 1.65 | 1.61 | -29.7 | 0.93 |
| RD-limestone | 0.464 | 1.08 | — | — | 0.68 |
| RH-greywacke | 4.36 | 1.40 | 1.65 | -29.8 | 0.99 |
| RJ-gravel | 0.095 | 0.256 | — | — | 0.72 |
| RL-gravel | 2.02 | 2.17 | — | — | 0.93 |
| 9-Fluorenone | | | | | |
| RC-limestone | 1.70 | 0.957 | 17.5 | -35.6 | 0.99 |
| RD-limestone | 0.323 | 0.751 | — | — | 0.83 |
| RH-greywacke | 3.06 | 0.980 | 1.84 | -30.0 | 1.00 |
| RJ-gravel | 0.619 | 1.67 | — | — | 0.87 |
| RL-gravel | 3.63 | 3.90 | 6.21 | -33.0 | 1.00 |

— Adsorption isotherm did not conform to Langmuir Equation, yielding a negative intercept that prevented calculation of K and $\Delta G^o$.

aggregate combinations were in good agreement with the Langmuir model as determined by the correlation coefficients. Correlation coefficients ranging between .68 and 1.00 were considered to be acceptable for the determination of Langmuir surface amounts considering the heterogeneous chemical compositions of actual aggregates that might allow for numerous and varied interactions. The adsorption behavior of indole on RD-limestone was the only asphalt model-aggregate combination that did not adhere to Langmuir monolayer analysis.

For any given aggregate tested with the seven asphalt model compounds (see Table 3), benzoic acid consistently produced the highest relative monolayer coverage (μmole/g), with the exception of phenylsulfoxide and phenanthridine on RJ-gravel, which showed larger monolayer amounts. For the five aggregates tested, benzoic acid monolayer surface coverages ranged from 1.97 to 9.15 μmole/g on RD-limestone and RL-gravel, respectively. In general, the lowest monolayer surface coverages (μmole/g) were produced by indole and 9-fluorenone adsorption on all aggregates. Correction of the Langmuir asphalt model surface amounts for aggregate areas, μmole/$m^2$, produced slightly different results for the relative amounts of asphalt models adsorbed to aggregate surface. Very large surface amounts were observed for benzoic acid on RJ-gravel and RL-gravel at 6.02 and 9.84 μmole/$m^2$, respectively. The largest of all monolayer surface coverages corrected for aggregate surface area was produced by phenylsulfoxide on RJ-gravel, 23.27 μmole/$m^2$. Low, less than 1 μmole/$m^2$, adsorption surface amounts were observed for 9-fluorenone on RC-limestone, RD-limestone, and RH-greywacke in addition to that observed for indole on RJ-gravel. The adsorption of indole on RD-limestone did not fit the Langmuir model; thus, the Langmuir monolayer surface amount was not determined. In general, indole and 9-fluorenone showed the lowest Langmuir monolayer surface coverages, μmole/$m^2$, for all aggregates tested. RJ-gravel and RL-gravel showed high Langmuir surface amounts, μmole/$m^2$, for all the asphalt models tested with the exception of indole. Although naphthalene, representing aromatic functionality, was tested as an asphalt model on all aggregates, adsorption was observed only on RJ-gravel yielding the smallest amount of surface coverage for any asphalt model-aggregate combination, 0.011 μmole/$m^2$.

The strength of the interfacial bond between the model functionalities and the aggregate surfaces is represented by the Gibb's free energy values as listed in Table 3. Although all of the Gibb's free energy of adsorption values are similar, the most negative values and, hence, the strongest interfacial bonds were observed for 9-fluorenone on RC-limestone and RL-gravel, phenylsulfoxide on RH-greywacke, and phenanthridine on RC-limestone at −35.6, −33.0, −33.3, and −33.0 KJ/mole, respectively. The strengths of interaction between 9-fluorenone and RC-limestone, RL-gravel, and RH-greywacke were relatively strong compared with other model compound-aggregate combinations. Langmuir treatment of benzoic acid on RH-greywacke, indole on RC-limestone and RH-greywacke, and phenanthridine on RJ-gravel produced the least free energy values at less than 30 KJ/mole. The differences in the free energy values of benzoic acid, phenanthridine, and 9-fluorenone on all aggregates may be indicative of variation in bonding sites or heterogeneity of the aggregates.

The equilibrium constants shown on Table 3 can be correlated to the extent of interaction between the model compound and the active sites on the aggregate surface. The equilibrium constant for benzoic acid on RL-gravel of $5.92 \times 10^5$ as compared to $1.51 \times 10^5$ for the same functionality on RH-greywacke indicates that benzoic acid interacted more with RL-gravel than RH-greywacke. Thus, for this investigation, each model-aggregate pair that interacted the most, as determined by the magnitude of the equilibrium constants, was as follows: benzoic acid and RL-gravel, phenylsulfoxide and RH-greywacke, 1-naphthol and RJ-gravel, phenanthridine and RC-limestone, indole and RC-limestone or RH-greywacke, and 9-fluorenone and RC-limestone. The largest equilibrium constant, $17.5 \times 10^5$, was observed for 9-fluorenone and RC-limestone. The smallest, $1.18 \times 10^5$, was observed for phenanthridine and RJ-gravel.

Because some of the adsorption data on the model compound–aggregate pairs showed poor adherence to Langmuir treatment, the relative affinities of the model compounds for each of the aggregates were determined by duplicate adsorption experiments, employing 1 and 2 g of aggregate, for each model compound–aggregate pair. The relative rankings of surface coverage, that is, relative affinities of model compounds for aggregates, are normalized and summarized in Table 4. Benzoic acid showed the greatest affinity for all aggregates (μmole/$m^2$), with the exception of RJ-gravel, and naphthalene showed the least. Phenylsulfoxide was a good adsorber on all the aggregates. Indole usually was a poor adsorber. This method of affinity rankings (Table 4) shows good agreement with similar rankings achieved by Langmuir data (μmole/$m^2$) with the exceptions presented by RD-limestone whereby Langmuir treatment shows 1-naphthol, phenylsulfoxide, and phenanthridine with different relative affinity rankings than those obtained by the empirical method devised for four sample measurements. A reversal in the rankings of benzoic acid and phenanthridine on RJ-gravel is also noted. These anomalies can be attributed to the heterogeneous nature of the aggregate.

### Adsorption and Desorption Behavior of Asphalts on RH-Greywacke

The adsorption and desorption behavior of three different asphalts—AAD-1, AAM-1, and AAK-1—from toluene solution onto RH-greywacke should indicate the effect of their different chemical properties on the interaction and affinity of the asphalt with a given aggregate. The viscosities of the asphalts (Table 2) corresponded to AC-10, AC-20, and AC-30 for AAD-1, AAM-1, and AAK-1, respectively. AAD-1 and AAK-1 contained asphaltene contents of 23.0 and 21.1 percent, respectively, and AAM-1 possessed a lower asphaltene content of 3.9 percent. AAM-1 contained higher amounts of polar and naphthene aromatics and a lower amount of saturates than did either AAD-1 or AAK-1.

AAD-1 and AAK-1 showed a substantial amount of self-assembly, which is an attraction of asphalt molecules to one another. Although AAM-1 did not show obvious self-assembly, it contained large molecular weight components (*11*, Pribanic 1990, personal communication). Some of the differences observed among the asphalts were small. The ar-

TABLE 4 RELATIVE AFFINITY RANKINGS OF SURFACE COVERAGE OF MRL AGGREGATES BY MODEL ASPHALT MODELS (μmole/g = μmole/m², mg/g = mg/m²)

| Asphalt Model (Functionalities) | RC-limestone | | | RL-gravel | | | RH-greywacke | | | RJ-gravel | | | RD-limestone | | |
|---|---|---|---|---|---|---|---|---|---|---|---|---|---|---|---|
| | mg/m² | μmole/m² | | mg/m² | μmole/m² | | mg/m² | μmole/m² | | mg/m² | μmole/m² | | mg/m² | μmole/m² | |
| | | * | ** | | * | ** | | * | ** | | * | ** | | * | ** |
| Benzoic Acid (Carboxylic Acids) | 2 | 1 | 1 | 1 | 1 | 1 | 2 | 1 | 1 | 3 | 2 | 3 | 1 | 1 | 1 |
| Indole (Pyrrolics) | 5 | 4 | 4 | 6 | 6 | 6 | 6 | 5 | 5 | 7 | 7 | 6 | 6 | 5 | 5 |
| 9-Fluorenone (Ketones) | 6 | 6 | 6 | 4 | 4 | 4 | 5 | 6 | 6 | 5 | 5 | 5 | 5 | 6 | 6 |
| 1-Naphthol (Phenolics) | 4 | 3 | 3 | 5 | 5 | 5 | 4 | 3 | 3 | 4 | 4 | 4 | 4 | 4 | 3 |
| Phenanthridine (Pyrindinics) | 3 | 5 | 5 | 3 | 3 | 3 | 3 | 4 | 4 | 2 | 3 | 2 | 3 | 2 | 4 |
| Phenylsulfoxide (Sulfoxides) | 1 | 2 | 2 | 2 | 2 | 2 | 1 | 2 | 2 | 1 | 1 | 1 | 2 | 3 | 2 |
| Naphthalene (Aromatics) | — | — | | — | — | | — | — | | 6 | 6 | 7 | — | — | |

— No adsorption occurred
* Mass basis, average of 4 adsorption experiments using a maximum 2 g of aggregate.
** Ranking determined from Langmuir treatment.

omatic hydrogen content determined by proton nuclear magnetic resonance (NMR) using the calculation of $H_{aromatic}/(H_{aromatic} + H_{aliphatic})$ yielded aromatic hydrogen contents between 6.5 to ~6.8 percent for the three asphalts (Jennings 1990, personal communication). The aromatic carbon content measured by $^{13}C$ NMR and calculated by the equation of $C_{aromatic}/(C_{aromatic} + C_{aliphatic})$ showed larger differences and ranked AAD-1 at ~23.7 percent, AAM-1 at ~24.7 percent and AAK-1 at 31.9 percent. A substitution index, defined as the ratio of aromatic carbon to aromatic hydrogen, provides an indication of the number of aromatic carbons linked to hydrogens compared with those linked to other types of carbons. The lower the number obtained, the greater the correspondence between the numbers of aromatic carbons and aromatic hydrogens present, and the lesser the substitution. The higher the number obtained, the greater the substitution. AAD-1 showed the least substitution at a ratio value of 2.2; AAM-1 yielded 2.7; the most substituted was AAK-1 at 3.1 (Jennings 1990, personal communication).

The sulfur content of AAD-1 at 8.6 percent was nearly four times that of AAM-1, although the vanadium content of AAK-1 at 1,427 ppm was four times greater than AAD-1 and 20 times greater than AAM-1 (Table 3). When the amount of heteroatoms (O, S, N) present was calculated as the ratio of heteroatoms per asphalt molecule, AAK-1 gave 3.1; AAD-1, 2.65; and AAM-1, 1.8 (Jennings 1990, personal communication).

The chemical composition and characteristics of the asphalts used in this study varied considerably. Experiments were performed adsorbing each of the asphalts from toluene solution onto RH-greywacke to evaluate the effect of their chemistry on adsorption and desorption behavior. After asphalt adsorption onto aggregate, water was added to the system. After adsorption and desorption were completed, the amount of asphalt present in solution was determined and the amount of asphalt on the aggregate was calculated.

The adsorption and desorption behavior of the three asphalts presented in terms of the amount of asphalt adsorbed per gram of RH-greywacke as a function of the equilibrium concentration of the solution is shown in Figure 2. The points shown are the data points obtained for the different asphalt-aggregate pairs. The solid line represents the best-fit curve obtained by fitting the data points with a polynomial. The shape of the adsorption isotherms was different with AAD-1 showing more adsorption at lower equilibrium concentration

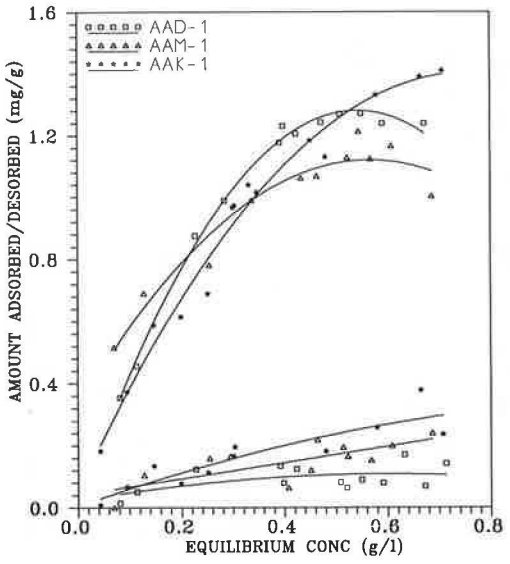


**FIGURE 2 Adsorption and desorption of asphalts onto RH-greywacke.**

but achieving a lower saturation amount than did AAK-1. AAM-1 showed the least adsorption at all equilibrium concentration levels. AAD-1 and AAM-1 asphalts displayed a maximum in adsorption behavior between 0.5 and 0.7 g/L equilibrium concentration; AAK-1 adsorption appeared to be still rising. At 0.6 g/L equilibrium concentration, the adsorption of the asphalts ranked at AAK-1 > AAD-1 > AAM-1.

Desorption of the adsorbed asphalt with water resulted in the behavior given in the desorption isotherms presented in Figure 2. Water, introduced at ~280 mmolar, was immiscible with toluene. The scatter in the points obtained from the desorption data was larger than that observed from the adsorption data, which was partially caused by the presence of a two-phase system after desorption. AAD-1 lost the least asphalt from the RH-greywacke surface, followed by AAM-1 and then AAK-1. The asphalt was reduced by 9 percent for AAD-1, 20 percent for AAK-1, and 17 percent for AAM-1. The amount of asphalt retained on the aggregate was determined by subtracting the amount desorbed from the amount adsorbed. AAD-1 and AAK-1—with the higher heteroatom contents, metals content, and asphaltenes—retained more asphalt after desorption than did AAM-1, the most hydrocarbonaceous and least polar of the asphalts; however, the differences were not large on RH-greywacke. Other aggregates must be tested to determine the sensitivity of asphalt adsorption behavior to chemical composition.

### Adsorption and Desorption Behavior of AAD-1 on Three Aggregates

The adsorption behavior of AAD-1 asphalt on three aggregates—RH-greywacke, RC-limestone, and RL-gravel—was determined (Figure 3). The surface areas of these three aggregates as measured by $N_2$ BET are quite different: RH-greywacke had 3.12 $m^2/g$; RC-limestone, 1.78 $m^2/g$; and RL-gravel, 0.93 $m^2/g$. Because of these rather substantial differences, the adsorption and desorption behavior is plotted on a basis of mass of asphalt adsorbed per unit surface area of the aggregate ($mg/m^2$) rather than per gram. Placing the adsorption on a surface area basis assumes that the BET surface area represents active sites of an aggregate that participate most actively in the adsorption of asphalt. Although this assumption may not be exactly correct, it is likely that the presence of a larger surface area results in a greater number of active sites. This basis changes the ranking of asphalt adsorption when plotted on a mass basis because of the differences in the surface areas among the aggregates.

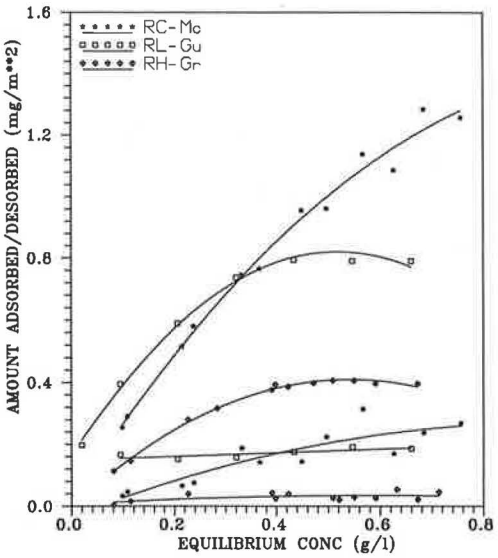


**FIGURE 3 Adsorption and desorption of AAD-1 asphalt onto aggregates.**

The shape of the isotherms as well as the amount of asphalt adsorbed was substantially different for the three aggregates (Figure 3). Both RH-greywacke and RL-gravel leveled off and showed definite plateaus at the higher equilibrium concentrations tested. The asphalt adsorption for RL-gravel rose more steeply than that for either RH-greywacke or RC-limestone. When the aggregates are compared on an equivalent surface area or active site basis, AAD-1 had much lower affinity for RH-greywacke than it did for either RC-limestone or RL-gravel. At high-equilibrium concentrations, AAD-1 showed a much higher affinity for RC-limestone than RL-gravel. Because the primary goal was to observe differences among the adsorption behavior of the different asphalt-aggregates, the high concentration levels required to achieve the saturation amount on RC-limestone were not employed.

The desorption of AAD-1 asphalt by water from the three aggregates, also given in Figure 3, showed the different water sensitivities of each asphalt-aggregate combination. AAD-1 desorbed the most from RC-limestone and the least from RH-greywacke; RL-gravel was intermediate. The desorption behavior of AAD-1 varied considerably, depending on the aggregate type. The ranking of the amount of asphalt remaining on the aggregate surfaces after water desorption was the same as that for the initial adsorption; however, the total amount remaining was less. A decrease in the asphalt amount adsorbed was 20 percent for RC-limestone, 22 percent for RL-gravel, and 9 percent for RH-greywacke. Thus, the RL-gravel and RC-limestone showed more than twice the water sensitivity of RH-greywacke.

### Effect of AS Agent on AAD-1 Adsorption

The effect of AS agent on the adsorption of AAD-1 asphalt on RH-greywacke was examined in two ways: (a) adsorption and desorption experiments with AAD-1 and RH-greywacke precoated with AS-agent, and (b) coadsorption of asphalt and AS agent from solution on RH greywacke. Two different concentrations of AS agent were used, one low and the other high. Toluene was used as the solvent for the first method and a 3:1 toluene–to–methylene-chloride solution was used for the second.

The adsorption behavior of the AAD-1 asphalt in three experiments involving AS agent plus that of AAD-1 asphalt on RH-greywacke, in the absence of AS agent and in toluene, is presented in Figure 4. The amount of AAD-1 adsorbed ranked according to the conditions of no AS agent present, coadsorption with a low concentration of AS agent, adsorption onto precoated RH-greywacke, and coadsorption with a high concentration of AS agent. The amount of AS agent used for adsorbing from solution in the precoated experiment

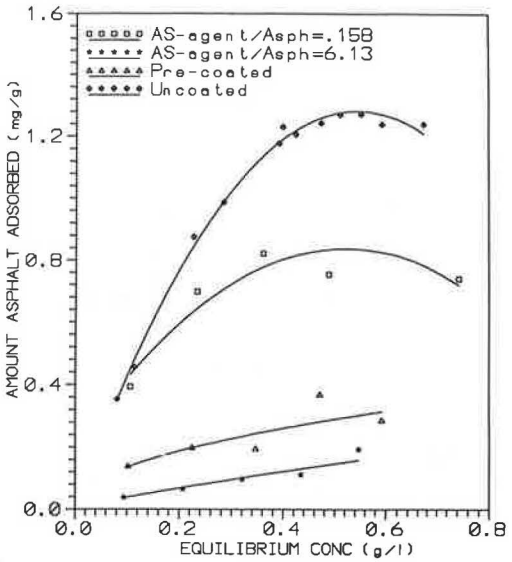


**FIGURE 4 Adsorption of AAD-1 asphalt onto RH-greywacke using AS agent.**

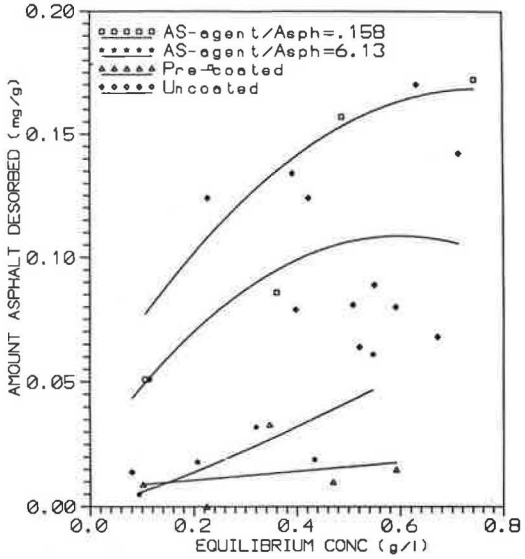


**FIGURE 5 Desorption of AAD-1 asphalt from RH-greywacke using AS agent.**

and in the coadsorption experiment with a high AS agent concentration was equivalent. In all cases in which AS agent was present in the system, the amount of asphalt adsorption decreased. The precoated aggregate was not as detrimental to asphalt adsorption as was the coadsorption with the high concentration of AS agent present. A substantial difference was observed between the AAD-1 adsorption low and high levels of AS agent. Table 5 compares the amount of AAD-1 and AS agent adsorbed at specific equilibrium concentrations of asphalt. AS agent appeared to compete for active sites on the aggregate surface in the coadsorption experiments, thereby limiting the amount of AAD-1 asphalt that was adsorbed.

Precoated RH-greywacke and the high concentration of AS in the coadsorption experiment showed the least amount of asphalt desorbed by water (Figure 5). The asphalt adsorbed individually and the asphalt coadsorbed with a low concentration of AS agent were more readily desorbed by water. AS agent from the high-concentration AS agent coadsorption was removed from the aggregate surface by water more readily than that from the low-concentration AS agent coadsorption. A comparison of the desorption data at six different equilibrium concentrations of asphalt, presented in Table 5, shows a significant solvent effect on asphalt desorption. Approximately 10 percent more asphalt was desorbed by water when methylene chloride was combined with toluene than when toluene was the sole solvent.

The AS agent in the asphalt-aggregate system, regardless of whether it was precoated or coadsorbed, affected the amount of asphalt adsorption on the aggregate. The more AS agent present, the greater the effect. If the total amount of asphalt adsorbed is the most important factor in bonding asphalt to aggregate, then AS agent interferes with that phenomenon. If the AS agent promotes stronger bonding through a lesser quantity of asphalt, then the AS agent may be beneficial to the longevity and water resistivity of the system. The ranking of the amount of asphalt remaining on RH-greywacke after water desorption was the same as it was for the initial adsorption. The effectiveness of the AS agent for retaining asphalt in the presence of water ranked according to the following order: precoated aggregate at 6.5 percent desorption > low concentration of AS agent at ~20 percent desorption > high concentration of AS agent at ~30 percent.

## SUMMARY AND CONCLUSIONS

The adsorption and desorption behavior of asphalts varied according to their chemical compositions as evidenced by their different isotherm shapes and adsorption amounts on RH-greywacke. Different chemical functional groups representative of heteroatomic-containing groups in asphalt showed different affinities and adsorption amounts. Benzoic acid and phenylsulfoxide had the highest adsorption affinity, followed by such species as phenanthridine, fluorenone, and naphthol. Low affinity was shown by the least polar species, indole and naphthalene. Different aggregates showed varied adsorption amounts for the same asphalt, indicating that aggregate-asphalt pairs have unique interactions between the active sites on the surface of the aggregate and the composition of the asphalt. A similar behavior was observed between the asphaltic models and five aggregates. Some aggregates adsorbed considerably more material than others, whereas some aggregates had more affinity for particular polar functional groups than others. Introduction of AS agent into the system reduced the amount of asphalt adsorbed. Precoating of the aggregate surface by AS agent decreased both the adsorption and desorption of asphalt.

## RECOMMENDATIONS

Characterization of the aggregates by evaluating the adsorption behavior of models that represent specific functionalities provides a good measure of the reactivity of different aggregate surfaces. This reactivity measure may be applicable to asphalt systems and provide a predictive means for matching

TABLE 5 ASPHALT AND AS AGENT ADSORPTION AND DESORPTION BEHAVIOR ON RH-GREYWACKE

| | Concentration of Asphalt (g/L) | | | | | |
|---|---|---|---|---|---|---|
| | 0.1 | 0.2 | 0.3 | 0.4 | 0.5 | 0.6 |
| **Adsorption (mg/g) Asphalt** | | | | | | |
| No AS (Toluene) | 0.426 | 0.769 | 1.024 | 1.192 | 1.273 | 1.266 |
| No AS ($MeCl_2$ + Tol) | 0.418 | 0.714 | 0.940 | 1.095 | 1.180 | 1.195 |
| Low AS | 0.420 | 0.595 | 0.723 | 0.804 | 0.837 | 0.823 |
| High AS | 0.038 | 0.068 | 0.096 | 0.122 | 0.148 | 0.172 |
| Precoated | 0.129 | 0.173 | 0.205 | 0.232 | 0.255 | 0.275 |
| **AS Agent** | | | | | | |
| Low AS | 0.007 | 0.010 | 0.012 | 0.013 | 0.013 | 0.013 |
| High AS | 0.006 | 0.012 | 0.016 | 0.021 | 0.025 | 0.029 |
| **Desorption (mg/g) Asphalt** | | | | | | |
| No AS (Toluene) | 0.048 | 0.070 | 0.087 | 0.102 | 0.106 | 0.109 |
| No AS ($MeCl_2$ + Tol) | 0.027 | 0.084 | 0.135 | 0.180 | 0.220 | 0.254 |
| Low AS | 0.075 | 0.102 | 0.124 | 0.141 | 0.154 | 0.163 |
| High AS | 0.005 | 0.015 | 0.025 | 0.035 | 0.045 | 0.055 |
| Precoated | 0.009 | 0.011 | 0.013 | 0.014 | 0.016 | 0.018 |
| **AS Agent** | | | | | | |
| Low AS | 0.002 | 0.001 | 0.002 | 0.003 | 0.003 | 0.003 |
| High AS | 0.001 | 0.002 | 0.004 | 0.006 | 0.007 | 0.009 |
| **Remainder (mg/g) Asphalt** | | | | | | |
| No AS (Toluene) | 0.378 | 0.699 | 0.937 | 1.090 | 1.167 | 1.157 |
| No AS ($MeCl_2$ + Tol) | 0.391 | 0.630 | 0.805 | 0.915 | 0.960 | 0.941 |
| Low AS | 0.345 | 0.493 | 0.599 | 0.663 | 0.683 | 0.660 |
| High AS | 0.033 | 0.053 | 0.071 | 0.087 | 0.103 | 0.117 |
| Precoated | 0.120 | 0.162 | 0.192 | 0.218 | 0.239 | 0.257 |
| **AS Agent** | | | | | | |
| Low AS | 0.005 | 0.009 | 0.010 | 0.010 | 0.010 | 0.010 |
| High AS | 0.005 | 0.010 | 0.012 | 0.015 | 0.018 | 0.020 |
| **% Desorbed Asphalt** | | | | | | |
| No AS (Toluene) | 11.3 | 9.1 | 8.5 | 8.6 | 8.3 | 8.6 |
| No AS ($MeCl_2$ + Tol) | 6.5 | 11.8 | 14.4 | 16.4 | 18.6 | 21.3 |
| Low AS | 17.9 | 17.1 | 17.2 | 17.5 | 18.4 | 19.8 |
| High AS | 13.2 | 22.1 | 26.0 | 28.7 | 30.4 | 32.0 |
| Precoated | 7.0 | 6.4 | 6.3 | 6.0 | 6.3 | 6.5 |
| **AS Agent** | | | | | | |
| Low AS | 28.6 | 10.0 | 16.7 | 23.1 | 23.1 | 23.1 |
| High AS | 16.7 | 16.7 | 25.0 | 28.6 | 28.0 | 31.0 |

asphalt with aggregate. Determining the adsorption and desorption behavior of asphalt on aggregate provides a direct means of evaluating the interaction between the asphalt-aggregate pairs. These methods lay the groundwork for a simple laboratory test evaluating specific asphalt-aggregate interactions. More experiments are under way to evaluate the applicability of these tests to a wide variety of asphalt-aggregate systems.

## ACKNOWLEDGMENTS

The support of this research by SHRP is gratefully acknowledged. The technical assistance of G. Li, S. Roberts, J. Sheih, M. H. Liu, B. Whidbee, L. Slater, and W. Slaten in the single component adsorption study is also gratefully acknowledged.

## REFERENCES

1. H. Plancher, S. M. Dorrence, and J. C. Petersen. *Proc., Association of Asphalt Paving Technologists*, Vol. 46, pp. 151–175. Viking Press, Eden Prairie, Minn., 1977.
2. J. C. Petersen, H. Plancher, E. K. Ensley, R. L. Venable, and G. Miyake. Chemistry of Asphalt-Aggregate Interaction: Relationship with Pavement Moisture-Damage Prediction Test. In *Transportation Research Record 843*, TRB, National Research Council, Washington, D.C., 1982, pp. 95–104.
3. J. A. N. Scott. *Proc., Association of Asphalt Paving Technologists*, Vol. 47, Viking Press, Eden Prairie, Minn., 1978.
4. G. Fritschy and E. Papier. *Fuel*, 57: pp. 701–704. IPC Science and Technology Press, Guildford, England, 1978.
5. C. W. Curtis, Y. W. Jeon, and D. J. Clapp. *Fuel Science and Technology International*, Vol. 7, No. 9, Marcel Dekkar, Inc. Woodbridge, Conn., 1989.
6. C. W. Curtis, Y. W. Jeon, D. J. Clapp, and B. M. Kiggundu. Adsorption of Asphalt Functionalities, AC-20, and Oxidized Asphalts on Aggregate Surfaces. In *Transportation Research Record 1228*, TRB, National Research Council, Washington, D.C., 1989.
7. G. M. Barrow. *Physical Chemistry*, 4th ed. McGraw-Hill Book Company, New York, N.Y., 1979, pp. 742–748.
8. G. D. Parfitt and C. H. Rochester. *Adsorption from Solution at the Solid/Liquid Interface*. Academic Press, San Diego, Calif., 1983.
9. A. C. McLean and C. D. Gribble. *Geology for Civil Engineers*. Allen & Unwin, Boston, Mass., 1979.
10. Southwestern Laboratories, SWL Report 913661. Southwestern Laboratories, Houston, Tex., 1990.
11. J. Pribanic. *Proc., Petersen Asphalt Conference*, 1990.

*Publication of this paper sponsored by Committee on Characteristics of Bituminous Materials.*

# Compatibilities of Strategic Highway Research Program Asphalts

J. F. BRANTHAVER, J. C. PETERSEN, J. J. DUVALL, AND P. M. HARNSBERGER

The so-called colloidal model of asphalt structure views asphalts as dispersions of relatively aromatic, polar, associating molecules in a less aromatic, less polar solvent phase. The extent to which solvent phases disperse associating species, therefore, should determine many fundamental properties of asphalts, and measurements of states of dispersion should allow for prediction of important properties. States of dispersion, or compatibility, of eight virgin asphalts studied in the Strategic Highway Research Program were measured by several methods. These methods were the Heithaus titration method, measurements of asphaltene yields by precipitation with n-heptane followed by iso-octane, measurements of relative viscosities (viscosity of asphalt divided by viscosity of maltenes) at different temperatures, and determination of sulfur content. All these methods served to identify two asphalts as being fundamentally much more compatible than the other six. Among the other six less well dispersed, less compatible asphalts, the methods did not serve to differentiate one from another in the same way. For the eight asphalts studied, determining the sulfur content or measuring n-heptane asphaltene yields appeared to be equally good as indicators of compatibility as the more complicated methods. Absolute viscosities of asphalts do not correlate with asphalt compatibilities, as is well known. However, relative viscosities determined by dividing asphalt viscosities by maltene viscosities (the maltenes are considered to be the solvent phase) appear to be good indicators of asphalt compatibilities.

One of the primary objectives of the Strategic Highway Research Program (SHRP) is to develop performance-related tests that are based on fundamental properties. According to one widely accepted model (the so-called colloidal model), asphalts are associations of polar, aromatic molecules that are dispersed in a nonpolar solvent phase. This model predicts that the effectiveness of the solvent phase in dispersing the associated phase should strongly influence many of the physical properties of asphalts. The state of dispersion, or compatibility, of an asphalt therefore should be an important fundamental property (*1*).

A method that is commonly used to determine the compatibility of asphalts is the Heithaus titration method (*2,3*). This method involves dissolving a specified amount of asphalt in varying amounts of toluene and measuring the amounts of n-heptane required to cause flocculation in each of the solutions. From these data, parameters are calculated that estimate the state of peptization of an asphalt ($P$), the peptizability of its asphaltenes ($P_a$), and the peptizing power of its maltenes ($P_o$). Most asphalts contain substantial amounts of asphaltenes, which are solids that precipitate when asphalts are mixed with several volumes of alkanes with low molecular weight. The residual materials remaining after separation of asphaltenes and solvent removal are referred to as maltenes. In the Heithaus method, asphaltenes are identified as the equivalent of the asphalt-dispersed phase, and maltenes are identified as the equivalent of the solvent phase.

Asphaltene yields resulting from mixing asphalts with large volumes of alkanes are a function of the structure of the precipitating solvent (*4*). For example, with n-heptane, asphaltene yields are lower than for n-pentane. The heptane asphaltenes also are more aromatic and contain more of the heteroatoms N, O, and S than the pentane asphaltenes. This is because the solubility parameter ($\delta$) of n-pentane ($\delta = 7.18$) is somewhat less than that of n-heptane ($\delta = 7.46$). The branched hydrocarbon iso-octane (2,2,4 trimethylpentane) has a solubility parameter of 6.90, which is substantially lower than that of n-pentane. When this solvent is used to precipitate asphaltenes from an asphalt, yields are high and the asphaltenes are relatively aliphatic and contain smaller concentrations of heteroatoms.

The asphaltene fraction, however prepared, is known to have a large influence on the viscosity of an asphalt. Deasphaltened asphalts (maltenes) are much less viscous than their parent asphalts measured under identical conditions. However, correlations between viscosity and asphaltene concentrations of different asphalts are not good (*5*). Two asphalts having nearly identical viscosities can have significantly different asphaltene concentrations.

The lack of a good correlation between asphaltene concentrations and viscosities for different asphalts is probably due to compositional differences among asphalts, which may be reflected in differences in compatibilities of asphalt components. A particular asphalt might consist of highly viscous maltenes but have a relatively small amount of polar molecules comprising its dispersed asphaltenes. Another asphalt might consist of much less viscous maltenes but contain more polar materials in its dispersed asphaltenes. These two asphalts might have similar viscosities (although other rheological properties would differ) but would be expected to have quite different asphaltene contents if n-heptane or n-pentane were used as precipitating solvent (*6*). The first asphalt would be designated as a well-dispersed system, and the second would be designated as a poorly dispersed system.

When asphaltenes are precipitated by n-heptane, polar molecules are partitioned between the insoluble asphaltenes and soluble maltenes. Most of these polar molecules are assumed

Western Research Institute, Box 3395, University Station, Laramie, Wyo. 82071.

to be viscosity builders. Their solubility in n-heptane is governed by the types of functional groups they contain, by their molecular weights, and to a lesser degree by subtle differences in their molecular structures. Most, if not all, the asphaltenes precipitated by n-heptane presumably form part of the asphalt-dispersed phase. Molecules precipitated by n-heptane are highly polar molecules of high and low molecular weight, and less polar molecules of higher molecular weight. Some relatively polar molecules will remain in the maltene fraction when asphaltenes are precipitated from an asphalt by n-heptane. Because petroleum consists of compound types that often exist as homologous series that range over many carbon numbers, some components of asphaltenes may resemble those in maltenes fairly closely. Individual compounds may be found in both asphaltenes and maltenes in different concentrations if the compounds have measurable solubilities in n-heptane. Therefore, this solvent will not remove all polar molecules from asphalts.

The branched hydrocarbon iso-octane is a much poorer solvent for polar molecules than n-heptane. When heptane maltenes are mixed with iso-octane, more asphaltenes precipitate. Almost all polar viscosity-building molecules not precipitated by n-heptane should be precipitated in the iso-octane asphaltenes. This precipitate should include the remainder of the asphalt-dispersed phase and some of the "resins" that are critical factors in effecting compatibility of the asphalt-dispersed phase with the asphalt-solvent phase. The iso-octane maltenes should show some similarity to the asphalt-solvent phase if the colloidal model of asphalt structure is valid.

Relative amounts of n-heptane and iso-octane asphaltenes should vary from one asphalt to another. Some asphalts contain large amounts of highly polar molecules. Others are characterized by relatively aromatic solvent phases, which retain polar molecules in solution even when treated with large volumes of n-heptane. Asphalts with large amounts of highly polar molecules and aliphatic solvent phases may be considered to be poorly dispersed systems, or relatively incompatible systems. Such asphalts should be characterized by large yields of asphaltenes when treated with n-heptane, and the heptane maltenes should not yield comparatively large amounts of asphaltenes when treated with iso-octane. Asphalts with small amounts of polar molecules engaging in associations, and which have aromatic solvent phases, should be characterized by small yields of n-heptane asphaltenes. Their n-heptane maltenes should yield relatively large amounts of asphaltenes when treated with iso-octane. These asphalts are well dispersed, or compatible. Thus, the yield of asphaltenes obtained by mixing an asphalt with several volumes of n-heptane should be an indicator of the compatibility of a system. The relative amounts of the two types of asphaltenes should be a better indicator of compatibility than yields of n-heptane alone. If this is so, relative yields of both kinds of asphaltenes for an asphalt should correspond to some degree with results derived from Heithaus titrations.

Relative viscosities also should be measures of compatibilities of asphalt systems. In order to calculate relative viscosities, it is arbitrarily assumed that n-heptane maltenes resemble asphalt-solvent phases fairly closely (although not as closely as iso-octane maltenes). Thus, relative viscosities discussed later are quotients of the asphalt absolute viscosities divided by maltene absolute viscosities measured under identical conditions. High relative viscosity values should be characteristic of poorly dispersed systems, and low relative viscosity values should be characteristic of well-dispersed systems. When relative viscosities are plotted versus temperature, curves that have relatively flat slopes should be observed for well-dispersed systems (assuming temperature is the abscissa). Poorly dispersed systems should exhibit steep relative-viscosity–temperature curves. This is because heat improves the compatibility of an incompatible system more than a compatible one.

Elemental composition of an asphalt is not necessarily an indicator of compatibility. Asphalts with differing elemental concentrations of elements may have similar compatibilities. However, those asphalts having large heteroatom (N, O, S) contents usually are observed to have large yields of asphaltenes, and asphalts relatively deficient in heteroatoms usually are characterized by low asphaltene yields.

## EXPERIMENTAL METHODS

The asphalts studied were the eight core asphalts selected by SHRP for intensive study. Asphalt AAA-1 is 150/200 penetration grade and is a distillation residue. Asphalt AAB-1 is AC-10 grade and is a distillation residue. Asphalt AAC-1 is AC-8 grade and is a distillation residue. Asphalts AAD-1 and AAG-1 are AR-4000 grade and are distillation residua. Asphalts AAF-1 and AAM-1 are AC-20 grade and are solvent deasphaltened asphalts. Asphalt AAK-1 is AC-30 grade and is a distillation residue.

Asphaltenes were prepared by mixing 40 volumes n-heptane (EM Sciences, Omni-Solv, glass distilled) for each gram of asphalt in Erlenmeyer flasks of appropriate sizes. After standing 16 hr with occasional swirling, the contents of the flasks were poured onto sintered glass funnels (M porosity) resting on suction flasks. Asphaltenes were washed several times with n-heptane, and washings were combined with the filtrate. The filtrate then was transferred to a round-bottom flask, and the solvent was removed on a rotary evaporator using heat and reduced pressure. The residual n-heptane maltenes were checked for solvent levels of below 0.1 percent by gas chromatographic-simulated distillation. Asphaltenes adhering to the Erlenmeyer flask were removed and combined with the filter cake. The asphaltenes were pulverized, dried, and weighed. They were stored under an inert gas atmosphere for future study.

Portions of the n-heptane maltenes were mixed with 40 volumes of iso-octane (J. T. Baker, high-performance liquid chromatography-grade) in Erlenmeyer flasks of appropriate sizes. After 16 hr, during which the flasks were occasionally swirled, the contents of the flasks were filtered and processed as for the n-heptane–treated asphalt samples above. Iso-octane maltenes and asphaltenes are the products of this treatment. The precipitated iso-octane asphaltenes are black, friable solids, as are the n-heptane asphaltenes.

Asphaltene compatibility indexes (ACIs) were obtained by dividing the weight percent of iso-octane asphaltenes (based on amount of total asphalt) by the sum of the weight percents of n-heptane and iso-octane (based on amount of total asphalt) asphaltenes and multiplying the quotient by 10. Thus, for AAA-1 the calculation is $[3.4/(15.8 + 3.4)] \times 10 = 1.77$. Actual yields of iso-octane yields from n-heptane maltenes

are corrected to yields based on total asphalt by multiplication by n-heptane maltene weight fractions. Thus the actual yield of iso-octane asphaltenes from n-heptane maltenes of asphalt AAA-1 was 4.04 weight percent. This number was multiplied by (100 − 15.8)/100 = 0.842, which is the weight fraction of n-heptane maltenes in AAA-1, to obtain the iso-octane asphaltene yield of 3.4 weight percent based on total asphalt.

Heithaus titrations were performed using a method developed by Heithaus (*2*) and modified by Kiggundu et al. (*7*) and in our laboratories. In this improved procedure, four 1.0 g samples of the test asphalt were weighed into 125 mL Erlenmeyer flasks. To the four flasks were added amounts of 1.0, 2.0, 4.0, or 6.0 mL toluene (Burdick and Jackson, redistilled prior to use). Dissolution of the asphalt in toluene may take several hours at ambient temperatures. Use of heat is not advised due to potential loss of solvent. After dissolution was complete, a stirring bar was added to each flask, and the flasks were immersed in a water bath maintained at 25°C (77°F) for 30 min. The flasks then were titrated with 1.0 mL aliquots of n-heptane (Phillips Petroleum Company, 99 percent, redistilled over calcium hydride before use). After each addition of n-heptane, the contents of the flask were stirred 5 min on a magnetic stirrer. Flocculation was determined by transferring a drop of the solution to a filter paper with a glass rod. The development of two rings on the filter paper is indicative of flocculation. Otherwise, only one ring is observed. For replicate determinations of an asphalt, all but 1 mL of the amount of n-heptane required for flocculation may be added at once, followed by addition of 0.1 mL increments. For some asphalts, flocculation points could not be determined for the samples mixed with 1.0 mL toluene. In these cases, 1.0 g asphalt was dissolved in 8.0 mL toluene, so that the four flasks contained 2.0, 4.0, 6.0, and 8.0 mL toluene, respectively.

If and when asphaltene flocculation was observed, Heithaus parameters were calculated as follows:

$$\text{Flocculation Ratio: FR} = \frac{V_T}{V_T + V_H}$$

$$\text{Dilution Ratio: } X = \frac{V_T + V_H}{W_A}$$

where

$V_T$ = volume of toluene in flask,
$V_H$ = volume of n-heptane required for flocculation, and
$W_A$ = weight of asphalt in flask (1.00 ± 0.05 g).

These calculations resulted in four values of FR and four values of $X$. A graph in which FR is plotted versus $1/X$ was prepared. A straight line was drawn through the data points and extrapolated to both axes. The intercept with the ordinate is $FR_{max}$. The intercept with the abscissa is $1/X_{min}$, from which $X_{min}$ is calculated. These two values were used to calculate $P_a$, $P_o$, and $P$ as follows:

Peptizability of asphaltenes, $P_a = 1 - FR_{max}$
Peptizing power of maltenes, $P_o = FR_{max}(X_{min} + 1)$
State of peptization of asphalt, $P = P_o/1 - P_a) = X_{min} + 1$

Viscosity measurements were performed on a Rheometrics mechanical spectrometer. Asphalts and maltenes measured were flooded with argon and placed in an oven at 110°C (230°F) for 1 hr and 10 min. After the samples were removed from the oven, rheological measurements were made within 40 to 60 hr. If this "annealing" step is not performed, viscosity determinations will be erratic. Relative viscosities were calculated by dividing absolute viscosities of asphalts by absolute viscosities of their n-heptane maltenes determined at the same temperature and rate of shear.

Molecular weight determinations were performed by vapor phase osmometry in toluene or pyridine at 60°C (140°F).

Elemental analyses were performed by the analytical services division of Western Research Institute using standard methods.

## RESULTS

SHRP has designated eight asphalts for intensive study, and these asphalts are referred to as "core asphalts." Code designations for these core asphalts and some of their chemical and physical properties are reported in Table 1. The relative aromaticities of the eight asphalts are not greatly different, as indicated by their H/C ratios, but heteroatom contents vary considerably. Sulfur concentrations range from 1.2 percent for AAM-1 to 6.9 percent for AAD-1. The high nitrogen content of AAG-1 is noteworthy. Number-average molecular weight (MW) values are similar for seven of the asphalts, but the MW of AAM-1 is significantly larger.

Seven of the core asphalts were titrated by the method of Heithaus (*2*) to obtain the parameters $P$, $P_a$, and $P_o$. The parameter $P$ is a measure of the state of dispersion of the asphalt as a whole. A large $P$ value indicates a well-dispersed or highly peptized system. The parameter $P_a$ measures peptizability of asphaltenes. As $P_a$ increases, asphaltenes should be more readily solvated. The parameter $P_o$ measures the solvent power of maltenes, here identified with the dispersing phase. A large $P_o$ value indicates that the dispersing phase is a good solvent. The values of each of these three parameters for each of seven core asphalts obtained in duplicate measurements are reported in Table 2. Reproducible data could not be obtained for AAC-1, probably because of the waxy nature of this asphalt.

Asphalts AAM-1 and AAG-1 stand out from the other five for at least two of the three Heithaus parameters. Their average values of $P$ indicate that they are much better peptized, or well-dispersed, systems than the other five asphalts. The asphaltenes of AAG-1 and AAM-1 are also more readily dispersed, as shown by high average $P_a$ values. The values for $P_o$ exhibit substantial variances for most of the asphalts, so firm conclusions about maltene solvent powers are not readily drawn. The average $P_o$ values range from 1.13 (Asphalt AAA-1) to 1.33 (Asphalt AAD-1) and thus indicate that AAD-1 maltenes have the best solvation powers of all the asphalts tested. Yet, from the $P$ value for AAD-1, it would appear that AAD-1 is not a well-dispersed system. This may be due to the high asphaltene content and low asphaltene peptizability ($P_a$) of AAD-1, discussed later. The Heithaus parameters $P_a$ and $P_o$ measure inherent properties of asphaltenes and maltenes and do not take into account relative quantities of these materials in an asphalt.

TABLE 1 ELEMENTAL ANALYSES AND MOLECULAR WEIGHTS OF EIGHT CORE ASPHALTS

| Asphalt and Asphalt Grade | Element, wt% | | | | | H/C | MW (Toluene) |
|---|---|---|---|---|---|---|---|
| | C | H | N | O | S | | |
| AAA-1, 150/200 pen | 84.2 | 10.5 | 0.50 | 0.60 | 5.50 | 1.48 | 790 |
| AAB-1, AC-10 | 82.3 | 10.6 | 0.60 | 0.80 | 4.70 | 1.54 | 840 |
| AAC-1, AC-8 | 86.5 | 11.3 | 0.70 | 0.90 | 1.90 | 1.56 | 870 |
| AAD-1, AR-4000 | 81.4 | 10.8 | 0.80 | 0.90 | 6.90 | 1.58 | 700 |
| AAF-1[1], AC-20 | 84.5 | 10.4 | 0.50 | 1.10 | 3.50 | 1.47 | 840 |
| AAG-1, AR-4000 | 85.6 | 10.5 | 1.10 | 1.10 | 1.30 | 1.46 | 710 |
| AAK-1, AC-30 | 80.7 | 10.2 | 0.70 | 0.80 | 6.40 | 1.51 | 860 |
| AAM-1[1], AC-20 | 86.7 | 11.4 | 0.60 | 0.50 | 1.20 | 1.57 | 1300 |

[1]Asphalts AAF-1 and AAM-1 were obtained by solvent deasphaltening. The other six asphalts are distillation residua.

TABLE 2 HEITHAUS PARAMETERS FOR SEVEN ASPHALTS

| Asphalt | Run Number | P | $P_a$ | $P_o$ | Asphalt | Run Number | P | $P_a$ | $P_o$ |
|---|---|---|---|---|---|---|---|---|---|
| AAA-1 | 1 | 3.29 | 0.69 | 1.02 | AAG-1 | 1 | 5.30 | 0.80 | 1.06 |
| | 2 | 3.50 | 0.68 | 1.12 | | 2 | 5.80 | 0.80 | 1.16 |
| | 3 | 3.56 | 0.68 | 1.14 | | 3 | 5.50 | 0.80 | 1.10 |
| | 4 | 3.26 | 0.65 | 1.14 | | 4 | 4.65 | 0.74 | 1.21 |
| | 5 | 3.42 | 0.64 | 1.23 | | 5 | 4.96 | 0.74 | 1.29 |
| | Avg. | 3.41 | 0.67 | 1.13 | | Avg. | 5.24 | 0.76 | 1.16 |
| AAB-1 | 1 | 3.30 | 0.67 | 1.09 | AAK-1 | 1 | 3.73 | 0.67 | 1.23 |
| | 2 | 3.65 | 0.66 | 1.24 | | 2 | 3.79 | 0.67 | 1.24 |
| | 3 | 3.62 | 0.63 | 1.34 | | 3 | 3.56 | 0.68 | 1.14 |
| | 4 | 3.49 | 0.63 | 1.29 | | 4 | 3.60 | 0.65 | 1.26 |
| | Avg. | 3.51 | 0.65 | 1.24 | | 5 | 3.66 | 0.65 | 1.28 |
| AAD-1 | 1 | 3.42 | 0.62 | 1.30 | | Avg. | 3.67 | 0.66 | 1.25 |
| | 2 | 3.50 | 0.62 | 1.33 | AAM-1 | 1 | 15.87 | 0.92 | 1.27 |
| | 3 | 3.47 | 0.62 | 1.32 | | 2 | 14.87 | 0.92 | 1.19 |
| | 4 | 3.40 | 0.60 | 1.36 | | 3 | 14.62 | 0.92 | 1.17 |
| | 5 | 3.38 | 0.60 | 1.35 | | 4 | 10.50 | 0.86 | 1.47 |
| | Avg. | 3.43 | 0.61 | 1.33 | | 5 | 10.57 | 0.86 | 1.48 |
| AAF-1 | 1 | 3.55 | 0.62 | 1.35 | | 6 | 9.58 | 0.88 | 1.15 |
| | 2 | 3.39 | 0.62 | 1.29 | | 7 | 9.33 | 0.88 | 1.12 |
| | 3 | 3.53 | 0.62 | 1.34 | | Avg. | 12.19 | 0.89 | 1.26 |
| | 4 | 3.27 | 0.63 | 1.21 | | | | | |
| | 5 | 3.17 | 0.64 | 1.14 | | | | | |
| | Avg. | 3.38 | 0.63 | 1.27 | | | | | |

Asphaltenes were prepared from all eight core asphalts by precipitation with n-heptane. After solvent was removed from each of the maltene fractions, iso-octane was mixed with the maltenes to precipitate more asphaltenes. Elemental analyses and MWs of the two types of asphaltenes are reported in Table 3 for one series of runs for each of the core asphalts.

For each of the core asphalts, the n-heptane asphaltenes are more aromatic and of higher MW than the iso-octane asphaltenes, as would be expected. Asphaltene aromaticities and MWs vary considerably among asphalts. Asphaltene MWs do not appear to relate to compatibility as measured by Heithaus parameters *P*, because the asphaltenes from AAM-1

TABLE 3 ELEMENTAL ANALYSES AND MOLECULAR WEIGHT DETERMINATIONS FOR ASPHALTENES OF CORE ASPHALTS

| Asphalt | Asphaltene Type | Element, wt% | | | | | | Molecular Weight | |
|---|---|---|---|---|---|---|---|---|---|
| | | C | H | N | O | S | H/C | Toluene | Pyridine |
| AAA-1 | heptane | 80.6 | 7.8 | 1.2 | 1.5 | 8.5 | 1.15 | 8,000 | 5,800 |
| | iso-octane | 80.8 | 8.3 | 0.9 | 1.8 | 8.2 | 1.22 | 4,500 | 3.700 |
| AAB-1 | heptane | 84.9 | 7.4 | 1.4 | 1.2 | 5.2 | 1.04 | 6,500 | 4,600 |
| | iso-octane | 83.9 | 7.7 | 1.1 | 1.5 | 5.9 | 1.09 | 4,500 | 3,400 |
| AAC-1 | heptane | 86.4 | 7.6 | 1.4 | 1.1 | 3.4 | 1.05 | 5,000 | 4,400 |
| | iso-octane | 86.6 | 8.1 | 1.2 | 1.2 | 3.1 | 1.11 | 2,800 | 2,800 |
| AAD-1 | heptane | 79.9 | 8.1 | 1.8 | 1.9 | 8.8 | 1.21 | 7,400 | 4,600 |
| | iso-octane | 79.8 | 8.8 | 1.4 | 2.0 | 8.1 | 1.31 | 3,500 | 2,600 |
| AAF-1 | heptane | 84.1 | 7.1 | 1.0 | 1.6 | 6.4 | 1.01 | 4,500 | 3,600 |
| | iso-octane | 84.9 | 8.0 | 0.8 | 1.6 | 5.4 | 1.12 | 2,600 | 2,300 |
| AAG-1 | heptane | 82.7 | 7.8 | 2.2 | 2.9 | 1.5 | 1.12 | 5,500 | 3,100 |
| | iso-octane | 84.4 | 8.2 | 2.2 | 2.4 | 1.2 | 1.16 | 3,000 | 2,100 |
| AAK-1 | heptane | 80.9 | 7.9 | 1.7 | 1.5 | 6.7 | 1.16 | 7,900 | Insol |
| | iso-octane | 81.0 | 8.4 | 1.3 | 1.6 | 7.6 | 1.24 | 4,500 | 3,900 |
| AAM-1 | heptane | 83.9 | 7.7 | 1.1 | 1.4 | 2.4 | 1.13 | 10,000 | Insol |
| | iso-octane | 86.9 | 8.6 | 1.0 | 1.1 | 1.9 | 1.18 | 7,200 | insol |

are of high MW and those of AAG-1 are of low MW. These two asphalts supposedly are the most highly peptized systems, on the basis of the Heithaus data. For most of the asphaltenes, MW determinations in pyridine are much lower than MW determinations in toluene, particularly for the n-heptane asphaltenes. This is because pyridine has a higher solubility parameter ($\delta$ = 10.3) than toluene ($\delta$ = 8.9) and more effectively breaks up asphaltene associations. For Asphalts AAC-1 and AAF-1, iso-octane asphaltenes have nearly identical MWs determined both in pyridine and in toluene. These asphaltenes are therefore weakly associating, and the MW values of 2,300 to 2,800 probably represent monomeric or dimeric molecular species.

For some of the iso-octane asphaltenes, sulfur and oxygen concentrations are greater than in the corresponding n-heptane asphaltenes. Nitrogen concentrations in the n-heptane asphaltenes are greater than or equal to the iso-octane asphaltenes for all core asphalts.

Table 4 reports yields of duplicate runs of asphaltene precipitations by n-heptane and iso-octane for each of the eight core asphalts. With the exception of Asphalts AAG-1 and AAM-1, yields of n-heptane asphaltenes are much greater than yields of iso-octane asphaltenes. For these two asphalts, total asphaltene yields are much lower than total asphaltene yields of the other six core asphalts. The ACI data shown in Table 4 will be discussed later.

Inspection of Tables 2 and 4 shows that low yields of n-heptane asphaltenes and relatively high Heithaus *P* values distinguish Asphalts AAG-1 and AAM-1 from the other core asphalts. Assuming the Heithaus method to be a meaningful measure of asphalt compatibility, then a high *P* value should correlate with a low yield of asphaltenes when an asphalt is treated with n-heptane. For the other five asphalts for which Heithaus *P* values were obtained, that parameter does not readily distinguish one from another. Based on Heithaus *P* values, AAF-1 is the most poorly dispersed system and AAK-1 the most well dispersed of the five. The *P* values, however, do not vary greatly, ranging from 3.38 to 3.67. The n-heptane asphaltene concentrations of the five asphalts vary considerably, from 13.4 percent to 20.2 percent. Therefore, among asphalts with similar Heithaus *P* values, n-heptane asphaltene concentration may not accurately measure state of dispersion if it is assumed that the Heithaus *P* values are correct indicators of peptization. Alternatively, it is possible that the Heithaus *P* value is not a good indicator of relative compatibilities among incompatible asphalts. The other two Heithaus parameters of the five asphalts having similar *P* values cannot be used to demonstrate that any one differs from the other four in a meaningful way because either the $P_a$ values are similar or there is too much error in the $P_o$ measurement.

Table 5 reports viscosities of each of the core asphalts obtained on a mechanical spectrometer at 25°C (77°F) and 60°C (140°F), and 1.0 radian/sec rate of shear. Viscosities at 60°C (140°F) vary considerably from one asphalt to another, and viscosities at 25°C (77°F) vary greatly when measured with the mechanical spectrometer. This is to be expected, as the asphalts vary in grade from AC-8 to AC-30. Asphalts AAB-1, AAF-1, and AAG-1 have high temperature coefficients of viscosity, whereas AAK-1 has a lesser variance of viscosity with temperature. Comparison of the data in Table 5 with data in Table 2 and 4 shows that there is little correlation with viscosity at 25°C (77°F) or 60°C (140°F) with either the Heit-

TABLE 4 ASPHALTENE YIELDS AND ACIs OF CORE ASPHALTS

| Asphalt | Operator (Initials) | Heptane Asphaltenes (HA), wt% | Iso-octane Asphaltenes (IA), wt% | ACI, $\left(\frac{IA}{HA+IA}\right)_{x10}$ |
|---|---|---|---|---|
| AAA-1 | MS | 15.1 | 3.8 | |
| | MC | 16.6 | 3.0 | |
| | Average | 15.8 | 3.4 | 1.77 |
| AAB-1 | MC | 17.1 | 2.2 | |
| | MC | 17.6 | 1.8 | |
| | Average | 17.3 | 2.0 | 1.04 |
| AAC-1 | MC | 9.8 | 3.1 | 2.40 |
| AAD-1 | MC | 19.7 | 3.6 | |
| | SP | 20.8 | 3.3 | |
| | Average | 20.2 | 3.4 | 1.44 |
| AAF-1 | MC | 13.2 | 2.7 | |
| | JW | 13.7 | 3.5 | |
| | Average | 13.4 | 3.1 | 1.88 |
| AAG-1 | MS | 4.9 | 3.4 | |
| | MC | 5.1 | 3.3 | |
| | Average | 5.0 | 3.3 | 3.97 |
| AAK-1 | MS | 19.2 | 3.4 | |
| | MC | 20.9 | 2.3 | |
| | Average | 20.1 | 2.8 | 1.22 |
| AAM-1 | MC | 3.4 | 4.6 | |
| | SP | 4.1 | 6.2 | |
| | Average | 3.7 | 5.4 | 5.93 |

haus parameter *P* or n-heptane asphaltene yields. If the Heithaus parameter *P* or n-heptane asphaltene yields measure the compatibility of a system, then the absolute viscosity of an asphalt is not a direct function of compatibility. This is why correlations between asphaltene concentrations and viscosities among various asphalts have not been observed. Many years ago, Traxler (*8*) observed that the absolute viscosities of asphalts do not necessarily correlate with other rheological properties of asphalts. He noted that well-dispersed asphalt systems exhibited little non-Newtonian behavior or thixotropy but were often characterized by high absolute values of viscosity and high temperature coefficients of viscosities. Poorly dispersed systems exhibit considerable non-Newtonian behavior (or complex flow, as defined by Traxler), lesser temperature coefficients of viscosities, but they may be of high or low absolute viscosities. Parameters that measure compatibilities should correlate with complex flow and variation in viscosity with temperature, but not necessarily with absolute viscosity. Absolute viscosity would appear to be a function of asphalt preparation, because it is a made-to-order property.

Table 6 reports viscosities of n-heptane maltenes of eight asphalts at 25°C (77°F) and 60°C (140°F). The high viscosities

TABLE 5 VISCOSITIES OF EIGHT ASPHALTS AT 25°C AND 60°C, 1.0 RADIAN/SEC

| Asphalt | Temperature, °C | Viscosity, poises |
|---|---|---|
| AAA-1 | 25 | 275,400 |
| | 60 | 1,245 |
| AAB-1 | 25 | 1,125,000 |
| | 60 | 1,507 |
| AAC-1 | 25 | 945,400 |
| | 60 | 1,194 |
| AAD-1 | 25 | 405,700 |
| | 60 | 1,644 |
| AAF-1 | 25 | 3,078,000 |
| | 60 | 2,893 |
| AAG-1 | 25 | 3,540,000 |
| | 60 | 2,998 |
| AAK-1 | 25 | 1,077,000 |
| | 60 | 4,703 |
| AAM-1 | 25 | 3,180,000 |
| | 60 | 4,539 |

TABLE 6 VISCOSITIES OF MALTENE[1] FRACTIONS OF EIGHT ASPHALTS AT 25°C AND 60°C, 1.0 RADIAN/SEC

| Asphalt | Temperature, °C | Viscosity, poises |
|---|---|---|
| AAA-1 | 25 | 8,040 |
| | 60 | 77 |
| AAB-1 | 25 | 30,200 |
| | 60 | 85 |
| AAC-1 | 25 | 105,000 |
| | 60 | 248 |
| AAD-1 | 25 | 3,290 |
| | 60 | 36 |
| AAF-1 | 25 | 250,000 |
| | 60 | 334 |
| AAG-1 | 25 | 1,143,000 |
| | 60 | 1,316 |
| AAK-1 | 25 | 16,200 |
| | 60 | 123 |
| AAM-1 | 25 | 1,018,000 |
| | 60 | 1,394 |

[1] Maltenes obtained by precipitation of asphaltenes with n-heptane.

of asphalts have low asphaltene contents (AAM-1, AAG-1, and AAF-1) because of the high viscosities of their maltenes. Maltene viscosities appear to correlate with Heithaus *P* values and inversely with n-heptane asphaltene yields. The maltenes having relatively high viscosities may be part of systems so well dispersed that many viscosity-building polar components

are not precipitated by n-heptane. It may be possible that these materials are precipitated by iso-octane. Inspection of Table 4 shows that iso-octane asphaltene yields derived from n-heptane maltenes are relatively low for all eight asphalts and range from 2.0 percent to 5.4 percent. Yields of n-heptane asphaltenes are greater than 5.4 percent for all asphalts except Asphalt AAM-1, for which the n-heptane asphaltene yield is only 3.7 percent. This is the only asphalt having a greater amount of iso-octane asphaltenes than n-heptane asphaltenes. For Asphalt AAG-1, the yield of n-heptane asphaltenes is comparable to the yield of iso-octane asphaltenes from the n-heptane maltenes. These are the two asphalts whose n-heptane maltene viscosities are highest. Therefore, those asphalts having low yields of n-heptane asphaltenes may yield relatively large amounts of asphaltenes when their n-heptane maltenes are treated with iso-octane, and presumably some viscosity-building materials would be included in these iso-octane asphaltenes. Thus an asphalt having a low n-heptane asphaltene content may be higher in absolute viscosity than an asphalt having a large amount of n-heptane asphaltenes. Asphalts having relatively large amounts of iso-octane asphaltenes must be well-dispersed systems, and asphalts having relatively small amounts of iso-octane asphaltenes must be poorly dispersed systems for which n-heptane is sufficient to remove almost all polar viscosity-building materials. On the basis of these criteria, Asphalt AAM-1 is the most well dispersed of the eight asphalts, followed closely by AAG-1. Asphalt AAB-1 is the least well dispersed system, followed closely by AAK-1 (see ACI values in Table 4 and the discussion of them).

It is likely that iso-octane does not remove all viscosity-building materials from asphalts but does so to varying degrees among the asphalts. Viscosity data on iso-octane maltenes have yet to be measured. These maltenes should approximate real solvent phases of asphalts in their rheological properties more so than n-heptane maltenes. It is likely that some asphalts have solvent phases that are relatively more aromatic and more viscous than others.

A parameter designated as the ACI was calculated for each of the core asphalts (Table 4). This factor is 10 times the quotient of the average iso-octane asphaltene yield divided by the total average asphaltene yield (sum of n-heptane and iso-octane asphaltene yields). This parameter measures the relative amounts of the two asphaltene types in an asphalt. Intuitively, asphalts with high ACI values should be well-dispersed systems and asphalts with low ACI values should be poorly dispersed systems. Comparison with the Heithaus titration data (Table 2) shows that the ACI values correspond to the Heithaus parameters $P$ reasonably well. Both parameters identify Asphalts AAM-1 and AAG-1 as being fundamentally different from the other asphalts tested. Both of these asphalts are much better dispersed systems than the five other asphalts for which Heithaus parameters and ACI values were obtained. Among the five poorly dispersed asphalts, the Heithaus method indicates that AAF-1 is the most poorly dispersed system; the ACI index indicates that AAB-1 is the most poorly dispersed. The differences in Heithaus parameters $P$ among Asphalts AAA-1, AAB-1, AAD-1, AAF-1, and AAK-1 are not great. The ACI parameter provides a measure of the state of dispersion of AAC-1, for which $P$ cannot be measured reproducibly, indicating that it is intermediate between AAG-1, AAM-1, and the other five asphalts. A plot of Heithaus $P$ values versus ACI values for seven asphalts is shown in Figure 1.

Except for AAB-1 and AAD-1, ACI values correlate with n-heptane asphaltene yields in assessing asphalt dispersibilities for the eight asphalts measured. A large number of asphalts are observed to have asphaltene contents in the 18 to 22 percent range when n-hepane is used as precipitating solvent. The states of dispersion of such asphalts are not high, but they vary significantly. It is hoped that the combination of iso-octane asphaltene yields with n-heptane asphaltene yields into ACI values can provide more information about asphalt compatibility for the large number of asphalts of this type than n-heptane asphaltene yields alone. Determination of asphaltene yields by n-heptane is sufficient to identify outliers such as Asphalts AAG-1 and AAM-1, which are well-dispersed systems.

If absolute viscosities of asphalts do not correlate with indexes of compatibility but maltene viscosities do, then relative viscosity values for the asphalts may be related to compatibility. To calculate relative viscosities, n-heptane maltenes are assumed to approximate the asphalt solvent phase. The absolute viscosity of an asphalt then is divided by the absolute viscosity of its n-heptane maltenes at the same temperature and shear rate (Table 7) to obtain relative viscosities. Relative viscosities of asphalts may be compared at a given temperature, and the change in relative viscosities with temperature may be measured to provide information about asphalt compatibilities. As an illustrative example from polymer science, for solutions of polymers in good solvents (compatible systems), relative viscosity versus temperature curves are flat and nearly parallel the abscissa. Polymers dissolved in poor solvents (incompatible systems) are characterized by steep relative viscosity versus temperature curves (*9*).

Examination of Table 7 shows that the values of the relative viscosities of Asphalts AAM-1, AAG-1, AAC-1, and AAF-1 are low at 25°C (77°F) and 60°C (140°F) and are not greatly different at the two temperatures. For the other four asphalts, relative viscosity values are high at 25°C (77°F) but much lower at 60°C (140°F). In these asphalts, heating results in considerable breakup of molecular associations as a result of a great improvement in the solvent power of the dispersing

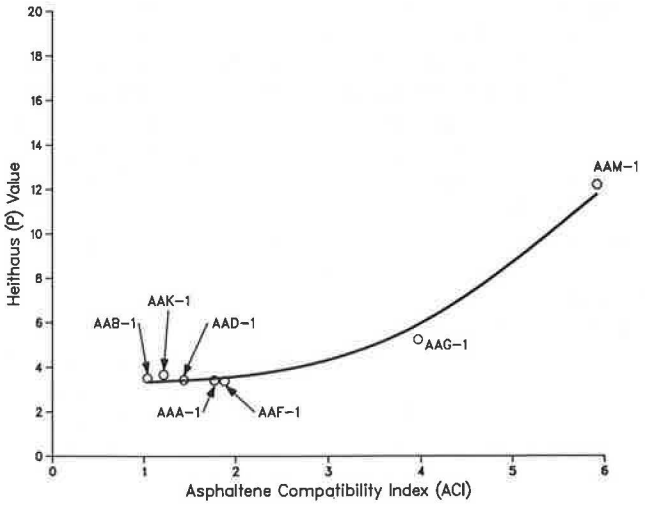


**FIGURE 1 State of peptization of core asphalts versus ACI.**

TABLE 7 RELATIVE VISCOSITIES[1] OF ASPHALTS AT TWO TEMPERATURES, 1.0 RADIAN/SEC

| | RELATIVE VISCOSITY | |
|---|---|---|
| ASPHALT | 25°C | 60°C |
| AAA-1 | 34.2 | 16.2 |
| AAB-1 | 37.3 | 17.3 |
| AAC-1 | 9.0 | 4.8 |
| AAD-1 | 123.3 | 45.7 |
| AAF-1 | 12.3 | 8.7 |
| AAG-1 | 3.1 | 2.3 |
| AAK-1 | 66.5 | 38.2 |
| AAM-1 | 3.1 | 3.3 |

1 Relative viscosities are calculated by dividing absolute viscosities of each asphalt at a given temperature by the absolute viscosity of its n-heptane maltenes.

phase. For the four incompatible, or poorly dispersed asphalts, asphalt viscosities decrease with increasing temperature relatively more than maltene viscosities. It would appear that relative viscosity measurements of asphalts provide a direct indication of compatibility. On the basis of this criterion, the asphalts may be ranked in order of relative increasing compatibility as AAD-1 < AAK-1 < AAB-1 < AAA-1 < AAF-1 < AAC-1 < AAG-1 < AAM-1. This ranking holds at either temperature of measurement (Table 7). Relative viscosities of the asphalts are plotted versus three other measures of compatibilities in Figures 2, 3, and 4. The correlation between n-heptane asphaltene content and relative viscosity (Figure 2) is better than the correlations of ACI values or sulfur contents with relative viscosity (Figures 3 and 4).

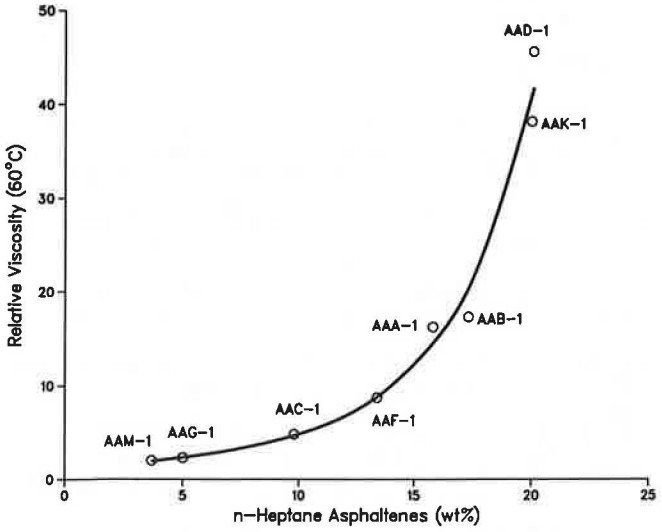


**FIGURE 2 Relative viscosity of core asphalts as related to n-heptane asphaltenes.**

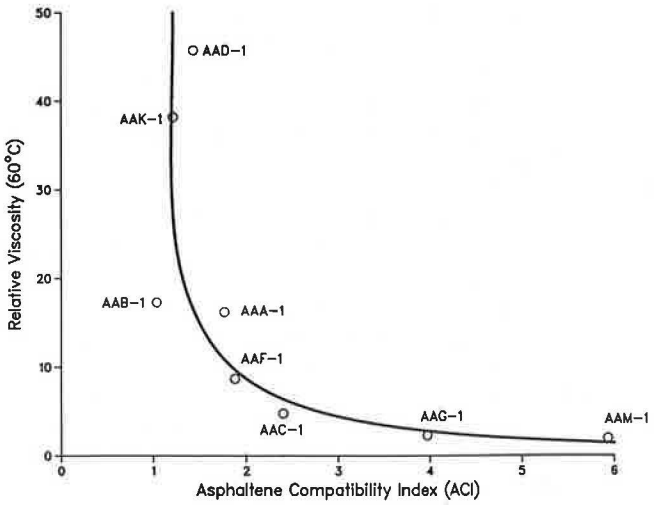


**FIGURE 3 Relative viscosity of core asphalts versus ACI.**

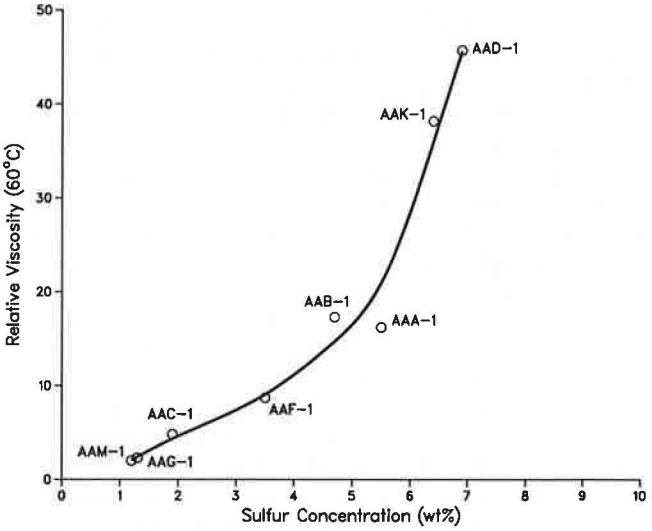


**FIGURE 4 Relative viscosity of core asphalts as related to sulfur content.**

## SUMMARY AND CONCLUSIONS

Seven asphalts were titrated by the Heithaus method to obtain parameters that are presumed to measure the compatibility, or state of dispersion, of the asphalts. By this method, two asphalts were identified as particularly well dispersed systems. Five other asphalts were identified as being relatively poorly dispersed systems and did not show significant differences among their Heithaus parameters from one asphalt to another. One asphalt that was part of this study could not be titrated by the Heithaus method because of excessive wax content.

Asphaltene contents using n-heptane as precipitating solvent were determined for the eight study asphalts. The maltenes resulting from this process were treated with iso-octane, causing additional precipitation of asphaltenes. Viscosities of the asphalts and the maltenes derived from n-heptane treatment were measured at 25°C (77°F) and 60°C (140°F). Ele-

mental analyses and molecular weights were obtained for the asphalts and both the n-heptane and iso-octane asphaltenes. Asphaltene contents of the asphalts as defined by n-heptane precipitation correlate inversely, but poorly with the Heithaus parameter ($P$). The two asphalts identified as well-dispersed systems by the Heithaus method are characterized by low n-heptane asphaltene yields. The n-heptane asphaltene yields of the other asphalts were much higher and varied more than their Heithaus parameters. For unaged asphalts, measuring n-heptane asphaltene yields may be as accurate as Heithaus titration in assessing states of dispersion.

Absolute viscosities of the eight asphalts at two temperatures did not correlate with either Heithaus parameters ($P$) or n-heptane asphaltene yields. Absolute viscosity of an asphalt therefore is not a direct function of state of dispersion, as pointed out by earlier workers. This is because the maltene fractions of some of the asphalts are highly viscous and those of others are not. If relative viscosities are calculated for each asphalt by dividing absolute viscosities of asphalts by absolute viscosities of their n-heptane maltenes measured under identical conditions, then these relative viscosities correlate with n-heptane asphaltene yields and less well with Heithaus $P$ values. Asphalts having low n-heptane asphaltene yields have maltenes with high viscosities, and vice versa.

Iso-octane precipitates additional amounts of asphaltenes from n-heptane maltenes. Yields of these iso-octane asphaltenes vary somewhat among the eight asphalts examined. For two of the asphalts, yields were comparable to those obtained by n-heptane, but they were less for the other six. The two asphalts characterized by the largest iso-octane asphaltene concentrations were the two with the highest Heithaus $P$ values. An index incorporating both yields of n-heptane and iso-octane asphaltenes was developed that measured compatibility somewhat differently than the Heithaus method or that measured n-heptane asphaltene yields alone. This index was designated as the ACI. It is similar to one developed earlier in these laboratories in which asphaltene yields were determined by mixing each of these two solvents with whole asphalts. The two asphalts with the highest Heithaus $P$ values also had the highest ACI values. Two other asphalts with moderate yields of n-heptane asphaltenes also had fairly high ACI values. Heithaus $P$ values could not be obtained for one of these. The ACI index ranks the remaining four asphalts slightly different with regard to compatibility than n-heptane asphaltene yields alone.

Iso-octane asphaltenes are lower in molecular weight than n-heptane asphaltenes from the same asphalts. They are also less aromatic, but not necessarily lower in heteroatom content.

Sulfur concentrations of asphalts correlate well with n-heptane asphaltene yields, as is well known. Sulfur concentrations of asphalts also correlate inversely with Heithaus $P$ values and with ACI values. Asphalts containing small amounts of sulfur tend to be well-dispersed systems, and asphalts containing large amounts of sulfur are poorly dispersed systems. This is to be expected, as sulfur contents of asphalts are a measure of the ages of their parent crudes. Mature crudes should contain less sulfur compounds because of degradation of reactive components over time.

When the several methods used to evaluate the states of dispersion, or compatibilities, of eight unaged asphalts were compared, all methods readily distinguish two asphalts as being much more highly dispersed than the others. Heithaus $P$ parameters do not serve to distinguish the other asphalts studied from one another very well. Yields of n-heptane asphaltenes, which may be as good a criterion as any for rapidly estimating compatibilities of unaged asphalts, correlate inversely with relative viscosities for all eight asphalts. Sulfur contents and asphaltene compatibility indexes rank the asphalts slightly different with respect to compatibility than do n-heptane asphaltene yields and relative viscosities. These last four named indicators all identify four asphalts as being poorly dispersed systems and two of the other four asphalts as being well-dispersed systems. The remaining two asphalts are of an intermediate nature. The evaluation of these methods will be extended to blends and to aged asphalts, in which sulfur concentrations can hardly be expected to serve as indicators of compatibility, and n-heptane asphaltene yields may not prove to be as useful as for virgin unblended asphalts. More accuate measurements of asphalt compatibilities may be compared with physical property data to determine which physical properties are functions of states of dispersion.

## ACKNOWLEDGMENTS

The work reported herein has been conducted as a part of a SHRP project being conducted by the Western Research Institute, Laramie, Wyoming, in cooperation with the Pennsylvania Transportation Institute, Texas Transportation Institute, and SRI International. Raymond E. Robertson is the principal investigator. The support and encouragement of Edward Harrigan and Jack Youtcheff is gratefully acknowledged. Heithaus titrations were performed by J. M. Wolf and M. V. Aldrich. Asphaltenes and maltenes were prepared by M. W. Catalfomo, S. C. Preece, and M. A. Scott. Viscosity determinations were performed by H. Plancher and F. A. Reid. Molecular weight determinations were performed by G. W. Gardner and B. W. Lowry. Elemental analyses were performed by the analytical services division of Western Research Institute. The manuscript was prepared by M. Knadler and J. Greaser. The authors are grateful to R. E. Robertson for a thoughtful review.

## REFERENCES

1. J. C. Petersen. Chemical Composition of Asphalt as Related to Asphalt Durability: State of the Art. In *Transportation Research Record 999*, TRB, National Research Council, Washington, D.C., 1984, pp. 13–30.
2. J. J. Heithaus. Measurement of Significance of Asphaltene Peptization. *Preprints, Division of Petroleum Chemistry, American Chemical Society*, Vol. 5, 1960, pp. A23–A37.
3. J. J. Heithaus. Measurement and Significance of Asphaltene Peptization. *Journal of the Institute of Petroleum*, Vol. 48, 1962, pp. 45–53.
4. R. B. Girdler. Constitutions of Asphaltenes and Related Studies. *Proc., Association of Asphalt Paving Technologists*, Vol. 34, 1965, pp. 45–79.
5. H. Plancher, E. L. Green, and J. C. Petersen. Reduction of Oxidative Hardening of Asphalts by Treatment with Hydrated Lime—A Mechanistic Study. *Proc., Association of Asphalt Paving Technologists*, Vol. 45, 1976, pp. 1–24.
6. K. H. Altgelt and O. M. Harle. The Effect of Asphaltenes on Asphalt Viscosity. *Industrial and Engineering Chemistry, Product Research and Development*, Vol. 14, 1975, pp. 240–247.

7. B. M. Kiggundu, B. Nusser-Humphrey, and D. M. Zallen. *Recycling Agent Selection and Tentative Specification.* USAF Report ESL-TR-84-47. 1984.
8. R. N. Traxler. *Asphalt, Its Composition, Properties, and Uses.* Reinhold, New York, N.Y., 1961.
9. E. T. Severs. *Rheology of Polymers.* Reinhold, New York, N.Y., 1962.



*Publication of this paper sponsored by Committee on Characteristics of Bituminous Materials.*

# Investigation of Laboratory Aging Procedures for Asphalt-Aggregate Mixtures

C. A. BELL, Y. ABWAHAB, AND M. E. CRISTI

A Strategic Highway Research Program project—entitled Performance-Related Testing and Measuring of Asphalt-Aggregate Interactions and Mixtures—includes development of procedures to age mixtures in the laboratory. Two major effects dominate aging of asphalt-aggregated mixtures: (a) loss of volatile components and oxidation in the construction phase (short-term aging) and (b) progressive oxidation of the in-place mixture in the field (long-term aging). Other factors may contribute to aging. In particular, molecular structuring may occur over a long period of time, resulting in steric hardening. Actinic light, primarily in the ultraviolet range, also has an effect, particularly in desert-like climates. Aging may result in hardening (stiffening) of the mixture, which alters the performance of the mixture. This may be beneficial, because a stiffer mixture will have improved load-distribution properties and will be more resistant to permanent deformation. However, aging may also result in embrittlement (increased tendency to crack and ravel) and loss of durability in terms of wear resistance and moisture susceptibility. Preliminary tests to evaluate aging methods for asphalt-aggregate mixtures have been conducted. Short-term methods include oven aging and extended mixing; long-term methods include oven aging and oxygen enrichment. The effects of temperature level and duration of aging are noted. Test specimens were fabricated from two asphalts and two aggregates, representing extreme property levels. The four mixture combinations were prepared at two levels of permeability representing good and moderate compaction conditions. The effects of aging were determined using the diametral resilient modulus test.

With regard to asphalt mixtures, aging is associated with the phenomenon of hardening. Other terms also commonly used include age hardening or embrittlement. The aging process occurs in two stages: short term and long term. The first stage occurs during the construction phase and is primarily attributable to the loss of volatile components and oxidation while the mix is hot. Long-term hardening is primarily attributable to the progressive oxidation of the mixture while in service.

The majority of previous work has investigated the aging effects of asphalt cements rather than the mixture (*1*), and to date no standard procedure exists for aging mixtures. A major objective of this study is to develop standard laboratory procedures simulating field aging conditions.

A preliminary study of laboratory aging procedures for asphalt-aggregate mixtures has been conducted. The study is not yet complete, but a substantial amount of data can be presented. An overview of the aging methods is given together with an outline of test procedures used to evaluate the effect of alternate aging methods. Summary tables of data are presented for those readers interested in specific property levels measured. The authors have not yet completed a detailed statistical evaluation of the data, and therefore this evaluation is based on general trends presented in a series of figures.

Department of Civil Engineering, Oregon State University, Corvallis, Oreg. 97331-4304.

## TEST PROGRAM

A detailed laboratory test program has been presented in a separate document for the Strategic Highway Research Program (SHRP) Project A-003A (*2*). A major objective of the study reported here is to evaluate the most promising aging method(s) to simulate short- and long-term aging effects. Three phases are being undertaken: (a) preliminary test program, (b) expanded test program, and (c) field validation. Only the preliminary program is outlined here. This program involves a limited number of material and test variables. The expanded test program and field validation phases will consider more material and test variables and will be used to develop further those methods appearing to be most appropriate in the preliminary program.

### Aging Methods

The preliminary program involves two groups of aging procedures falling into short- and long-term categories:

| *Short-Term* | *Long-Term* |
|---|---|
| Forced-draft oven aging | Forced-draft oven aging |
| Extended mixing | Pressure oxidation |
| | Triaxial cell aging |

The short-term methods involve conditioning loose mixtures, whereas the long-term methods involve conditioning compacted samples. More details are given for each method in a subsequent section.

### Evaluation Methods

The tests being used to evaluate the effect of each aging method include the following:

| *Mixture Tests* | *Asphalt Tests* |
|---|---|
| Resilient modulus | Rheology tests |
| Dynamic modulus | |
| Tensile test | |

Other tests may be used, such as infrared spectroscopy and size-exclusion chromatography on recovered asphalt. More details are given for each group of tests in a subsequent section.

### Variables Used for Oven Aging and Extended Mixing

The same variables were selected for each of the three short-term aging methods and for the long-term oven aging as shown in Table 1. All mixtures were prepared using the mix design asphalt content and gradations and standard compaction procedures for the California kneading compactor. The program is a 3/4 fraction of the complete factorial with no replicate tests. For each aging method, 36 specimens were prepared and tested according to the combinations of variables shown in Table 1. Two asphalts with substantially different properties and designated with SHRP codes AAK-1 and AAG-1 were used. Similarly, two distinctly different aggregates with SHRP codes RB and RL were used. As shown in Table 1, the two asphalts and two aggregates enabled a total of four mixtures to be tested.

TABLE 1 VARIABLES USED IN OVEN AGING AND EXTENDED MIXING PROGRAMS

| Asphalt and Aggregate Combinations | LOW AIR VOIDS (~4%) | | | | | | MEDIUM AIR VOIDS (~8%) | | | | | |
|---|---|---|---|---|---|---|---|---|---|---|---|---|
| | Temperature | | | | | | Temperature | | | | | |
| | Level 1 | | | Level 2 | | | Level 1 | | | Level 2 | | |
| | Time Period | | | | | | Time Period | | | | | |
| | a | b | c | a | b | c | a | b | c | a | b | c |
| RL + AAK-1 | X | X | X | | | | X | X | X | X | X | X |
| RL + AAG-1 | X | X | X | X | X | X | | | | X | X | X |
| RB + AAK-1 | X | X | X | X | X | X | | | | X | X | X |
| RB + AAG-1 | X | X | X | | | | X | X | X | X | X | X |

### Variables Used for Pressure Oxidation

For the pressure oxidation tests, both oxygen and compressed air were used at pressures of 100 and 300 psi to provide oxygen enrichment. Therefore, a 1/4 factorial experiment was designed requiring 48 specimens as shown in Table 2.

### Variables Used for Triaxial Cell Aging

This approach, which was initiated in June 1990, consisted of forcing either oxygen or air to flow through a mixture specimen, thus providing oxygen enrichment. A 1/2 fraction of the complete factorial requiring 48 specimens with no replicate tests is being used, as shown in Table 3.

TABLE 2 VARIABLES USED IN PRESSURE OXIDATION PROGRAM

| Asphalt and Aggregate Combinations | ATMOSPHERE | | | | | | | | | | | | | | | |
|---|---|---|---|---|---|---|---|---|---|---|---|---|---|---|---|---|
| | Oxygen | | | | | | | | Air | | | | | | | |
| | Low Pressure | | | | High Pressure | | | | Low Pressure | | | | High Pressure | | | |
| | Low Voids | | High Voids | | Low Voids | | High Voids | | Low Voids | | High Voids | | Low Voids | | High Voids | |
| | Temperature (°C) | | | | Temperature (°C) | | | | Temperature (°C) | | | | Temperature (°C) | | | |
| | 60 | | 25 | | 60 | | 25 | | 60 | | 25 | | 60 | | 25 | |
| | Time Period | | | | Time Period | | | | Time Period | | | | Time Period | | | |
| | abc | abc | abc | abc | abc | abc | abc | abc | abc | abc | abc | abc | abc | abc | abc | abc |
| RL + AAK-1 | X-- | -X- | --X | --- | --X | --- | X-- | -X- | -X- | X-- | --- | --X | --- | --X | -X- | X-- |
| RL + AAG-1 | --- | --X | -X- | X-- | -X- | X-- | --- | --X | --X | --- | X-- | -X- | X-- | -X- | --X | --- |
| RB + AAK-1 | --- | --X | -X- | X-- | -X- | X-- | --- | --X | --X | --- | X-- | -X- | X-- | -X- | --X | --- |
| RB + AAG-1 | X-- | -X- | --X | --- | --X | --- | X-- | -X- | -X- | X-- | --- | --X | --- | --X | -X- | X-- |

TABLE 3 VARIABLES USED IN TRIAXIAL CELL AGING PROGRAM

| Asphalt and Aggregate Combinations | ATMOSPHERE | | | | | | | |
|---|---|---|---|---|---|---|---|---|
| | OXYGEN | | | | AIR | | | |
| | Air Voids Low | | Air Voids Medium | | Air Voids Low | | Air Voids Medium | |
| | Temperature (°C) | | Temperature (°C) | | Temperature (°C) | | Temperature (°C) | |
| | 25 | 60 | 25 | 60 | 25 | 60 | 25 | 60 |
| | Time Period | | Time Period | | Time Period | | Time Period | |
| | a b c | a b c | a b c | a b c | a b c | a b c | a b c | a b c |
| RL + AAK-1 | X X X | | | X X X | | X X X | X X X | |
| RL + AAG-1 | | X X X | X X X | | X X X | | | X X X |
| RB + AAK-1 | | X X X | X X X | | X X X | | | X X X |
| RB + AAG-1 | X X X | | | X X X | | X X X | X X X | |

## SAMPLING PREPARATION, AGING, AND TEST PROCEDURES

### Preparation

The preliminary test program used two asphalts with extreme characteristics (AAG-1 and AAK-1). The aggregates (RB and RL) are a crushed granite and a chert gravel. Mixing and compaction followed a protocol established by the study team for SHRP A-003A; they are based on the method used to prepare Hveem samples (ASTM D1560-81a and D1561-81a). The physical properties determined on the mixture samples include bulk specific gravity, maximum theoretical specific gravity, and permeability. The modulus and tensile properties were also determined; they will be described more fully, along with an outline of tests for the recovered asphalt. The tensile strain at yield and tensile strength are determined in an indirect tensile test. The properties of the original and recovered asphalt are being determined using a steady-state rotational viscometer at this stage in the study. However, a dynamic mode of testing is planned for the expanded test program.

### Short-Term Aging Procedures

The short-term aging portion of this investigation involved aging mixtures in their uncompacted state to simulate the precompaction phase of the construction process. Short-term oven aging used a forced-draft oven for either 0, 6, or 15 hr at 135°C or 163°C. The aged mix was then compacted at either 250 or 500 psi compactive effort using a kneading compactor to attain target void levels of approximately 8 and 4 percent, respectively. The actual levels of voids obtained depended on the asphalt-aggregate combination used and vary from the target levels. The bulk specific gravity, permeability, resilient modulus, and tensile properties were determined for all samples.

The extended mixing program involved using a modified rolling thin film oven (RTFO) test. An attachment to the RTFO drum enabled loose mixture to be rolled, thus extending the mixing time. Samples were mixed using the standard procedure and then subjected to 0, 10, 120, or 360 min mixing at 135°C or 163°C. The aged mix was compacted at 250 or 500 psi to attain two void levels. The bulk specific gravity, permeability, resilient modulus, and tensile properties were determined for all samples.

### Long-Term Aging Procedures

The oven aging method used forced-draft ovens, ensuring that the temperature was constant everywhere in the oven as compared to a regular convection oven. The method used is essentially the same as that used in the asphalt-aggregate mixture analysis system study (*3*). Compacted samples were preconditioned for 2 days at 40°C or 60°C. The preconditioning was a measure to ensure the stability of the sample. The specimens were then exposed to conditions of either 0, 2, or 7 days at 107°C. The before-aging and after-aging characteristics were determined.

The pressure oxidation vessel utilized both oxygen and compressed air. The compacted samples were exposed to either environment for 0, 2, or 7 days at 100 or 300 psi at either 25°C or 60°C. The preconditioning step performed with the oven aging method was not required in this procedure. As with other aging methods, tests were performed on the unaged and aged samples to determine effects of aging.

The triaxial cell aging approach involves conditioning a sample while it is positioned in a triaxial test cell as illustrated in Figure 1. For this stage of the study, conventional kneading compactor samples were used (i.e., 4 in. diameter by 2½ in. high). Oxygen or air was passed through the sample and the resilient modulus determined at any time during the conditioning process. A flow rate of 4 $ft^3$/hr was used, which required a pressure of about 50 psi. Tests were run at 25°C and 60°C.

### Test Procedures

The resilient modulus is usually determined using an indirect tensile mode of testing. A triaxial mode of testing is also used where convenient, as in the case of the triaxial aging approach. The dynamic modulus will be determined in the expanded test program with a modified triaxial mode of testing, in which the frequency of loading is varied and the phase lag between the applied load pulse and the strain response is determined. The tangent and loss modulus are obtained at different frequencies to give a thorough characterization of mixture samples. This approach is analogous to the dynamic mechanical analysis of asphalt cement samples.

The modulus tests are nondestructive and yield information on the elasticity (and plasticity, in the case of the dynamic test) of the mixture sample. The tensile test is destructive and, therefore, is not done until all the modulus data have been collected. The test is done at a deformation rate of 2 in./min,

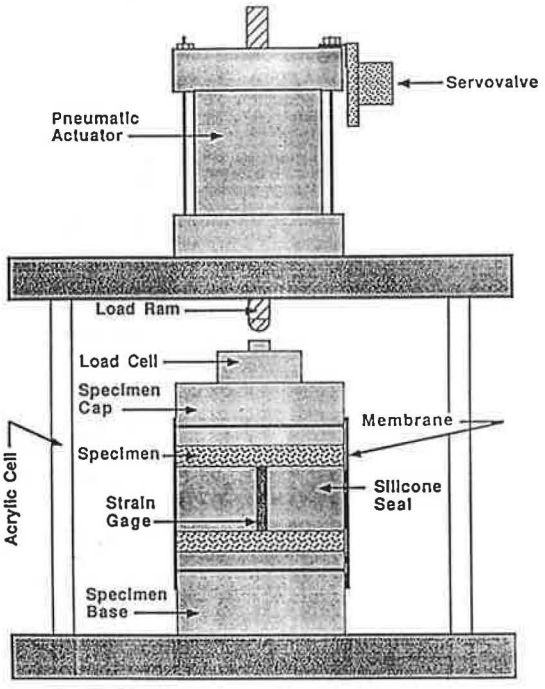


**FIGURE 1 Triaxial aging process.**

and the load and deformation of the sample are monitored, enabling the strength and the strain at yield to be determined. These data indicate the brittleness of the sample. Von Quintus et al. (*3*) suggested that the strain at yield was an indicator of the aging achieved in a mixture sample. Following the tensile test, the mixture portions may be used to obtain recovered asphalt samples.

Only limited tests on the recovered asphalt are being done in the preliminary test program, and the data obtained will not be reported or discussed here because testing is not yet complete. The tests being done include size-exclusion chromatography, infrared spectroscopy, and rheological tests. The rheology is being defined with a plate-to-plate rotational viscometer. This is being used in a steady-state mode during the preliminary test program, but it will be upgraded to enable dynamic measurements to be made in the expanded test program.

## RESULTS

Tables 4–8 show the complete set of data collected for the short-term oven aging, extended mixing, long-term oven aging, pressure oxidation, and triaxial aging respectively. The footnotes to each table explain the code used to identify samples. For the purposes of this paper only, the first three characters are significant, representing the asphalt, aggregate, and air void content of the samples.

The majority of the figures presented herein show resilient modulus ratio versus time plots. This modulus ratio is determined as follows:

$$\frac{\text{resilient modulus after aging}}{\text{resilient modulus before aging}}$$

To date, the majority of the evaluation of the procedures used has been based on the modulus ratios determined. Other data

TABLE 4 SUMMARY OF SHORT-TERM OVEN AGING DATA

| SAMPLE ID | AGING CONDITION | | | ACTUAL VOIDS | MODULUS (ksi) | | | PERMEABILITY, | TENSILE | |
|---|---|---|---|---|---|---|---|---|---|---|
| | PERIOD (hours) | TEMP. (°C) | VOIDS | (%) | BEFORE AGING | AFTER AGING | RATIO | (E-9cm/sec) | STRESS (psi) | STRAIN μ-strain |
| KBLS00O | 0 | LOW | LOW | 4.4 | 304 | 304 | 1.0 | LOW | 127 | 7930 |
| KBLS10O | 6 | LOW | LOW | 4.9 | 304 | 582 | 1.9 | LOW | 205 | 7621 |
| KBLS20O | 15 | LOW | LOW | 6.2 | 304 | 736 | 2.4 | LOW | 244 | 7122 |
| KBLS01O | 0 | HIGH | LOW | 2.6 | 341 | 341 | 1.0 | LOW | 173 | 7959 |
| KBLS11O | 6 | HIGH | LOW | 7.0 | 341 | 807 | 2.4 | LOW | 232 | 5214 |
| KBLS21O | 15 | HIGH | LOW | 14.6 | 341 | 258 | 0.8 | LOW | 90 | 6324 |
| KBMS01O | 0 | HIGH | HIGH | 7.1 | 407 | 407 | 1.0 | LOW | 135 | 10106 |
| KBMS11O | 6 | HIGH | HIGH | 11.7 | 407 | 656 | 1.6 | 6.04 | 150 | 2991 |
| KBMS21O | 15 | HIGH | HIGH | 17.8 | 407 | 228 | 0.6 | 4.66 | 61 | 4499 |
| GBLS00O | 0 | LOW | LOW | 4.6 | 455 | 455 | 1.0 | LOW | 257 | 6927 |
| GBLS10O | 6 | LOW | LOW | 4.2 | 455 | 896 | 2.0 | LOW | 274 | 9278 |
| GBLS20O | 15 | LOW | LOW | 3.9 | 455 | 1224 | 2.7 | LOW | 373 | 3838 |
| GBMS00O | 0 | LOW | HIGH | 7.2 | 364 | 364 | 1.0 | LOW | 195 | 7638 |
| GBMS10O | 6 | LOW | HIGH | 7.0 | 364 | 870 | 2.4 | 3.59 | 244 | 4779 |
| GBMS20O | 15 | LOW | HIGH | 7.2 | 364 | 1206 | 3.3 | 4.68 | 294 | 9885 |
| GBMS01O | 0 | HIGH | HIGH | 6.1 | 368 | 368 | 1.0 | 1.96 | 205 | 8306 |
| GBMS11O | 6 | HIGH | HIGH | 7.2 | 368 | 1445 | 3.9 | 4.34 | 319 | 2312 |
| GBMS21O | 15 | HIGH | HIGH | 13.6 | 368 | 1179 | 3.2 | 6.48 | 190 | 2471 |
| GLLS00O | 0 | LOW | LOW | 6.6 | 193 | 193 | 1.0 | 2.3 | 223 | 8123 |
| GLLS10O | 4 | LOW | LOW | 6.7 | 193 | 651 | 3.4 | 2.1 | 295 | 8751 |
| GLLS20O | 8 | LOW | LOW | 6.9 | 193 | 702 | 3.6 | 4.8 | 288 | 7392 |
| GLMS00O | 0 | LOW | HIGH | 9.4 | 124 | 124 | 1.0 | 13.3 | 171 | 11779 |
| GLMS10O | 4 | LOW | HIGH | 8.6 | 124 | 411 | 3.3 | 19.2 | 243 | 9249 |
| GLMS20O | 8 | LOW | HIGH | 8.5 | 124 | 624 | 5.0 | 14.2 | 277 | 5595 |
| GLMS01O | 0 | HIGH | HIGH | 8.2 | 141 | 141 | 1.0 | 12.0 | 191 | 11768 |
| GLMS11O | 4 | HIGH | HIGH | 9.4 | 141 | 720 | 5.1 | 18.8 | 298 | 3717 |
| GLMS21O | 8 | HIGH | HIGH | 12.8 | 141 | 797 | 5.7 | 70.0 | 193 | 1879 |
| KLLS00O | 0 | LOW | LOW | 5.4 | 236 | 236 | 1.0 | 0.7 | 162 | 7464 |
| KLLS10O | 4 | LOW | LOW | 6.5 | 236 | 394 | 1.7 | 0.7 | 200 | 5977 |
| KLLS20O | 8 | LOW | LOW | 6.4 | 236 | 514 | 2.2 | 1.3 | 244 | 9044 |
| KLLS01O | 0 | HIGH | LOW | 5.2 | 202 | 202 | 1.0 | 1.0 | 173 | 12863 |
| KLLS11O | 4 | HIGH | LOW | 8.1 | 202 | 721 | 3.6 | 7.2 | 223 | 8749 |
| KLLS21O | 8 | HIGH | LOW | 11.2 | 202 | 479 | 2.4 | 2.8 | 149 | 6433 |
| KLMS01O | 0 | HIGH | HIGH | 6.2 | 208 | 208 | 1.0 | 0.5 | 177 | 6440 |
| KLMS11O | 4 | HIGH | HIGH | 12.7 | 208 | 520 | 2.5 | 34.3 | 163 | 7617 |
| KLMS21O | 8 | HIGH | HIGH | 15.2 | 208 | 300 | 1.4 | 34.9 | 78 | 6168 |

KEY FOR SAMPLE IDENTIFICATION:

| | | | |
|---|---|---|---|
| K | ASPHALT | K=AAK-1 | G=AAG-1 |
| L | AGGREGATE | L=RL | B=RB |
| L | VOIDS | L=LOW | M=MEDIUM |
| S | SHORT TERM | S=SHORT TERM | |
| 0 | AGING PERIOD | 0=6/4 HOURS | 1=15/8 HOURS |
| 0 | AGING TEMP. | 0=LOW(135°C) | 1=HIGH(163°C) |
| O | AGING TYPE | O=SHORT TERM OVEN AGING | |

TABLE 5 SUMMARY OF EXTENDED MIXING DATA

| SAMPLE ID | AGING TIME (minutes) | TEMPER-ATURE | VOIDS | ACTUAL VOIDS (%) | MODULUS (ksi) | | | PERMEA-BILITY (E-9cm/sec) | TENSILE | |
|---|---|---|---|---|---|---|---|---|---|---|
| | | | | | BEFORE | AFTER | RATIO | | STRESS | STRAIN |
| KBLS00E | 10 | LOW | LOW | 3.1 | 333 | 333 | 1.00 | LOW | 158.1 | 6892.0 |
| KBLS10E | 120 | LOW | LOW | 2.3 | 333 | 398 | 1.20 | LOW | 209.9 | 6464.0 |
| KBLS20E | 360 | LOW | LOW | 1.8 | 333 | 777 | 2.33 | LOW | 271.1 | 4545.0 |
| KBLS01E | 10 | HIGH | LOW | 5.0 | 301 | 301 | 1.00 | LOW | 158.4 | 8031.0 |
| KBLS11E | 120 | HIGH | LOW | 4.2 | 301 | 818 | 2.72 | LOW | 247.8 | 5159.9 |
| KBLS21E | 360 | HIGH | LOW | 8.3 | 301 | 839 | 2.79 | 14.9 | 205.9 | 4838.7 |
| KBMS01E | 10 | HIGH | HIGH | 7.7 | 279 | 279 | 1.00 | 2.5 | 135.8 | 7691.4 |
| KBMS11E | 120 | HIGH | HIGH | 11.0 | 279 | 558 | 2.00 | HIGH | 154.2 | 3960.7 |
| KBMS21E | 360 | HIGH | HIGH | 7.8 | 279 | 630 | 2.26 | 15.7 | 220.3 | 3724.9 |
| GBLS00E | 10 | LOW | LOW | 4.1 | 491 | 491 | 1.00 | LOW | 218.2 | 6407.0 |
| GBLS10E | 120 | LOW | LOW | 3.7 | 491 | 827 | 1.68 | LOW | 342.5 | 6801.6 |
| GBLS20E | 360 | LOW | LOW | 0.8 | 491 | 810 | 1.65 | LOW | 380.0 | 5150.8 |
| GBMS00E | 10 | LOW | HIGH | 6.1 | 345 | 345 | 1.00 | 1.1 | 207.8 | 10846.9 |
| GBMS10E | 120 | LOW | HIGH | 4.5 | 345 | 557 | 1.61 | LOW | 256.0 | 6039.2 |
| GBMS20E | 360 | LOW | HIGH | 5.9 | 345 | 681 | 1.97 | LOW | 315.4 | 5320.7 |
| GBMS01E | 10 | HIGH | HIGH | 7.5 | 324 | 324 | 1.00 | LOW | 179.2 | 5499.5 |
| GBMS11E | 120 | HIGH | HIGH | 6.5 | 324 | 888 | 2.74 | 3.6 | 293.6 | 3903.2 |
| GBMS21E | 360 | HIGH | HIGH | 3.8 | 324 | 1713 | 5.29 | LOW | 457.6 | 3696.7 |
| GLLS00E | 10 | LOW | LOW | 6.5 | 228 | 228 | 1.00 | 2.1 | 153.3 | 9293.7 |
| GLLS10E | 120 | LOW | LOW | 6.3 | 228 | 447 | 1.96 | 2.9 | 208.2 | 9321.7 |
| GLLS20E | 360 | LOW | LOW | 8.0 | 228 | 699 | 3.07 | HIGH | 213.3 | 7603.7 |
| GLMS00E | 10 | LOW | HIGH | 8.6 | 140 | 140 | 1.00 | 13.2 | 122.7 | 10160.1 |
| GLMS10E | 120 | LOW | HIGH | 10.5 | 140 | 327 | 2.34 | HIGH | 141.3 | 9243.7 |
| GLMS20E | 360 | LOW | HIGH | 10.2 | 140 | 657 | 4.69 | HIGH | 179.9 | 3390.3 |
| GLMS01E | 10 | HIGH | HIGH | 9.3 | 163 | 163 | 1.00 | 21.7 | 113.9 | 17009.4 |
| GLMS11E | 120 | HIGH | HIGH | 11.1 | 163 | 522 | 3.20 | HIGH | 155.1 | 3867.3 |
| GLMS21E | 360 | HIGH | HIGH | 15.5 | 163 | 459 | 2.82 | HIGH | 93.3 | 4642.5 |
| KLLS00E | 10 | LOW | LOW | 0.6 | 291 | 291 | 1.00 | LOW | 154.7 | 8906.5 |
| KLLS10E | 120 | LOW | LOW | 4.6 | 291 | 436 | 1.50 | HIGH | 178.4 | 7220.0 |
| KLLS20E | 360 | LOW | LOW | 6.0 | 291 | 804 | 2.76 | HIGH | 233.1 | 5760.9 |
| KLLS01E | 10 | HIGH | LOW | 0.6 | 273 | 273 | 1.00 | LOW | 154.6 | 8647.9 |
| KLLS11E | 120 | HIGH | LOW | 7.8 | 273 | 523 | 1.92 | HIGH | 158.7 | 7767.3 |
| KLLS21E | 360 | HIGH | LOW | 8.7 | 273 | 662 | 2.42 | HIGH | 180.7 | 4446.1 |
| KLMS01E | 10 | HIGH | HIGH | 2.2 | 215 | 215 | 1.00 | 4.3 | 126.9 | 7325.6 |
| KLMS11E | 120 | HIGH | HIGH | 8.8 | 215 | 660 | 3.07 | HIGH | 169.6 | 6024.4 |
| KLMS21E | 360 | HIGH | HIGH | 4.6 | 215 | 710 | 3.30 | HIGH | 178.2 | 3050.2 |

## KEY FOR SAMPLE IDENTIFICATION:

| | | | |
|---|---|---|---|
| K | ASPHALT | K=AAK-1 | G=AAG-1 |
| L | AGGREGATE | L=RL | B=RB |
| L | VOIDS | L=LOW | M=MEDIUM |
| S | SHORT TERM | S=SHORT TERM | |
| 0 | AGING PERIOD | 0=10 MIN. | 1=120 MIN. 2=360 MIN. |
| 0 | AGING TEMP. | 0=LOW(135°C) | 1=HIGH(163°C) |
| E | AGING TYPE | E=EXTENDED MIXING | |

TABLE 6 SUMMARY OF LONG-TERM OVEN AGING DATA

| SAMPLE ID | AGING TIME (days) | TEMPER-ATURE (°C) | TARGET VOIDS | ACTUAL VOIDS (%) | MODULUS (ksi) BEFORE AGING | MODULUS (ksi) AFTER AGING | MODULUS RATIO | PERM (E-9c/s) BEFORE AGING | PERM (E-9c/s) AFTER AGING | TENSILE STRESS (psi) | TENSILE STRAIN μ-strain |
|---|---|---|---|---|---|---|---|---|---|---|---|
| GLLL00O | 0 | 40 | LOW | 7.38 | 249 | 294 | 1.18 | - | 2.92 | 138 | (2) |
| GLLL10O | 2 | 40 | LOW | 7.99 | 340 | 928 | 2.73 | - | 3.29 | (1) 150 | (2) |
| GLLL20O | 7 | 40 | LOW | 7.42 | 401 | 1547 | 3.86 | - | - | 231 | (2) |
| GLLL01O | 0 | 60 | LOW | 7.91 | 351 | 367 | 1.05 | - | - | 161 | (2) |
| GLLL11O | 2 | 60 | LOW | 7.87 | 290 | 865 | 2.98 | - | - | 204 | (2) |
| GLLL21O | 7 | 60 | LOW | 7.54 | 329 | 1587 | 4.82 | 2.12 | 3.00 | 241 | (2) |
| GLML01O | 0 | 60 | HIGH | 10.00 | 234 | 348 | 1.49 | 3.71 | 3.89 | 144 | (2) |
| GLML11O | 2 | 60 | HIGH | 9.30 | 240 | 679 | 2.83 | 3.50 | 3.97 | 170 | (2) |
| GLML21O | 7 | 60 | HIGH | 10.00 | 258 | 1136 | 4.40 | 3.56 | 2.97 | 170 | (2) |
| KLLL00O | 0 | 40 | LOW | 6.69 | 295 | 328 | 1.11 | 1.37 | 1.59 | 137 | (2) |
| KLLL10O | 2 | 40 | LOW | 7.55 | 308 | 507 | 1.65 | 2.43 | 2.74 | 156 | (2) |
| KLLL20O | 7 | 40 | LOW | 7.23 | 355 | 1593 | 4.49 | 1.81 | 2.86 | 177 | (2) |
| KLML00O | 0 | 40 | HIGH | 9.20 | 198 | 240 | 1.21 | 3.55 | - | 91 | (2) |
| KLML10O | 2 | 40 | HIGH | 9.50 | 185 | 629 | 3.40 | 3.48 | - | 132 | (2) |
| KLML20O | 7 | 40 | HIGH | 9.10 | 208 | 1285 | 6.18 | 3.34 | 3.70 | 192 | (2) |
| KLML01O | 0 | 60 | HIGH | 9.00 | 203 | 344 | 1.69 | 3.62 | 3.36 | 116 | (2) |
| KLML11O | 2 | 60 | HIGH | 9.40 | 190 | 537 | 2.83 | 3.63 | 3.36 | 128 | (2) |
| KLML21O | 7 | 60 | HIGH | 8.90 | 208 | 1318 | 6.34 | 3.71 | 4.10 | 188 | (2) |
| KBLL01O | 0 | 60 | LOW | 6.57 | 303 | 376 | 1.24 | - | - | 141 | (2) |
| KBLL11O | 2 | 60 | LOW | 6.11 | 351 | 563 | 1.60 | 1.41 | - | 178 | (2) |
| KBLL21O | 7 | 60 | LOW | 6.42 | 288 | 894 | 3.10 | LOW | - | (1) 171 | (2) |
| KBLL00O | 0 | 40 | LOW | 6.50 | 314 | 358 | 1.14 | 1.26 | 1.14 | 133 | (2) |
| KBLL10O | 2 | 40 | LOW | 6.82 | 345 | 565 | 1.64 | 0.56 | 1.06 | 166 | (2) |
| KBLL20O | 7 | 40 | LOW | 7.83 | 357 | 894 | 2.50 | 1.76 | 1.88 | 207 | (2) |
| KBML01O | 0 | 60 | HIGH | 9.03 | 296 | 344 | 1.16 | 3.65 | 3.23 | 115 | (2) |
| KBML11O | 2 | 60 | HIGH | 8.74 | 273 | 519 | 1.90 | 2.63 | 3.56 | 144 | (2) |
| KBML21O | 7 | 60 | HIGH | 8.64 | 257 | 994 | 3.87 | 2.57 | 2.66 | 261 | (2) |
| GBLL00O | 0 | 40 | LOW | 3.53 | 530 | 509 | 0.96 | LOW | LOW | 181 | (2) |
| GBLL10O | 2 | 40 | LOW | 2.42 | 511 | 562 | 1.10 | LOW | LOW | 235 | (2) |
| GBLL20O | 7 | 40 | LOW | 2.94 | 578 | 509 | 0.88 | 2.87 | - | 139 | (2) |
| GBML00O | 0 | 40 | HIGH | 8.00 | 312 | 328 | 1.05 | 2.11 | 2.40 | 138 | (2) |
| GBML10O | 2 | 40 | HIGH | 8.20 | 298 | 548 | 1.84 | 1.33 | 2.42 | 168 | (2) |
| GBML20O | 7 | 40 | HIGH | 8.90 | 264 | 1334 | 5.05 | 3.45 | 2.18 | 214 | (2) |
| GBML01O | 0 | 60 | HIGH | 8.40 | 329 | 376 | 1.14 | 2.86 | 3.75 | 121 | (2) |
| GBML11O | 2 | 60 | HIGH | 9.20 | 279 | 529 | 1.90 | 2.52 | 3.16 | 127 | (2) |
| GBML21O | 7 | 60 | HIGH | 8.20 | 346 | 1121 | 3.24 | 3.14 | 2.48 | 184 | (2) |

## NOTES:

(1) Power shut off. Second stress was applied.

(2) No data recorded.

- No data recorded due to either operator or equipment error.

## KEY FOR SAMPLE IDENTIFICATION:

| | | | |
|---|---|---|---|
| K | ASPHALT | K=AAK-1 G=AAG-1 | |
| L | AGGREGATE | L=RL B=RB | |
| L | VOIDS | L=LOW M=MEDIUM | |
| L | LONG TERM | L=LONG TERM | |
| 0 | AGING PERIOD | 0=0 DAYS 1=2 DAYS 2=7 DAYS | DAYS AT 107°C |
| 0 | CONDITION'G TEMP. | 0=LOW(40°C) 1=HIGH(60°C) | TEMP. USED FOR 2 DAYS BEFORE USING 107°C |
| O | AGING TYPE | O=LONG TERM OVEN AGING | |

TABLE 7 SUMMARY OF PRESSURE OXIDATION DATA

## (a) PRESSURIZED WITH OXYGEN

| SAMPLE ID * | AGING CONDITION PER-IOD (days) | TEMP. (°C) | PRES-SURE (psi) | ACTUAL VOIDS (%) | MODULUS (ksi) BEFORE AGING | MODULUS (ksi) AFTER AGING | Mr RATIO | PERMEABILITY (E-9c/s) BEFORE AGING | PERMEABILITY (E-9c/s) AFTER AGING | TENSILE TEST STRESS (psi) | TENSILE TEST STRAIN μ-strain |
|---|---|---|---|---|---|---|---|---|---|---|---|
| GLLL013P | 0 | 60 | 300 | 7.96 | 272 | 249 | 0.92 | 2.06 | 1.81 | 162.9 | 9250 |
| GLLL103P | 2 | 25 | 300 | 8.08 | 272 | 257 | 0.94 | 1.40 | 2.23 | 135.8 | 8175 |
| GLLL211P | 7 | 60 | 100 | 7.15 | 300 | 387 | 1.29 | LOW | 1.39 | 100.5 | 11407 |
| GLML011P | 0 | 60 | 100 | 9.50 | 222 | 279 | 1.26 | 4.95 | 5.49 | 132.4 | 1187 |
| GLML101P | 2 | 25 | 100 | 9.20 | 211 | 337 | 1.60 | 4.21 | 4.69 | 129.8 | 12585 |
| GLML213P | 7 | 60 | 300 | 9.40 | 176 | 128 | 0.73 | 4.60 | HIGH | 67.4 | 25449 |
| KLLL001P | 0 | 25 | 100 | 7.30 | 224 | 194 | 0.87 | 2.07 | 1.91 | 110.0 | 9266 |
| KLLL111P | 2 | 60 | 100 | 7.70 | 294 | 274 | 0.93 | 3.13 | HIGH | 116.8 | 7010 |
| KLLL203P | 7 | 25 | 300 | 7.10 | 237 | 165 | 0.70 | 0.86 | 1.97 | 124.9 | 8249 |
| KLML003P | 0 | 25 | 300 | 8.80 | 283 | 216 | 0.76 | 2.68 | 3.99 | 6.4 | 3247 |
| KLML113P | 2 | 60 | 300 | 8.40 | 334 | 133 | 0.40 | 1.90 | HIGH | 93.0 | 11331 |
| KLML201P | 7 | 25 | 100 | 8.60 | 242 | 219 | 0.90 | 2.94 | 1.39 | 104.7 | 7164 |
| KBLL013P | 0 | 60 | 300 | 4.60 | 455 | 427 | 0.94 | LOW | LOW | 183.3 | 4206 |
| KBLL103P | 2 | 25 | 300 | 4.60 | 420 | 180 | 0.43 | LOW | LOW | 142.5 | 9962 |
| KBLL211P | 7 | 60 | 100 | 5.00 | 488 | 164 | 0.34 | LOW | LOW | 130.4 | 9782 |
| KBML001P | 0 | 25 | 100 | 8.00 | 326 | 239 | 0.73 | 1.70 | 2.00 | 133.9 | 5617 |
| KBML101P | 2 | 25 | 100 | 8.90 | 259 | 180 | 0.69 | 4.28 | 4.42 | 104.9 | 9494 |
| KBML213P | 7 | 60 | 300 | 8.10 | 292 | 73 | 0.25 | 3.05 | HIGH | 71.3 | 28887 |
| GBLL001P | 0 | 25 | 100 | 7.00 | 476 | 418 | 0.88 | 1.76 | 0.74 | 219.1 | 7523 |
| GBLL111P | 2 | 60 | 100 | 7.40 | 458 | 419 | 0.91 | 0.21 | LOW | 221.1 | 9878 |
| GBLL203P | 7 | 25 | 300 | 7.70 | 450 | 228 | 0.51 | 0.54 | 2.14 | 228.2 | 8279 |
| GBML003P | 0 | 25 | 300 | 9.10 | 409 | 420 | 1.03 | 3.02 | 2.35 | 210.7 | 7145 |
| GBML113P | 2 | 60 | 300 | 8.10 | 486 | 167 | 0.34 | 3.37 | 6.31 | 130.2 | 26118 |
| GBML201P | 7 | 25 | 100 | 8.10 | 499 | 387 | 0.78 | 3.14 | 8.69 | 216.0 | 4448 |

## (b) PRESSURIZED WITH AIR

| SAMPLE ID * | AGING CONDITION PER-IOD (day) | TEMP. (°C) | PRES-SURE (psi) | ACTUAL VOIDS (%) | MODULUS (ksi) BEFORE AGING | MODULUS (ksi) AFTER AGING | Mr RATIO | PERMEABILITY (E-9c/s) BEFORE AGING | PERMEABILITY (E-9c/s) AFTER AGING | TENSILE TEST STRESS (psi) | TENSILE TEST STRAIN μ-strain |
|---|---|---|---|---|---|---|---|---|---|---|---|
| GLLL003P | 0 | 25 | 300 | 6.99 | 366 | 413 | 1.13 | 0.99 | 1.17 | 251.9 | 3441 |
| GLLL113P | 2 | 60 | 300 | 8.57 | 488 | 101 | 0.21 | 3.63 | 4.45 | 117.6 | 15739 |
| GLLL201P | 7 | 25 | 100 | 7.68 | 347 | 281 | 0.81 | 1.99 | 3.05 | 182.5 | 7058 |
| GLML001P | 0 | 25 | 100 | 9.06 | 228 | 199 | 0.87 | 4.10 | 3.98 | 167.7 | 10570 |
| GLML111P | 2 | 60 | 100 | 9.35 | 210 | 175 | 0.83 | 4.05 | 4.49 | 164.7 | 13317 |
| GLML203P | 7 | 25 | 300 | 9.08 | 216 | 88 | 0.41 | 3.74 | cracked | 83.7 | 33872 |
| KLLL011P | 0 | 60 | 100 | 6.50 | 263 | 328 | 1.25 | 1.96 | 1.87 | 124.9 | 7074 |
| KLLL101P | 2 | 25 | 100 | 6.70 | 411 | 262 | 0.64 | 1.50 | 1.63 | 133.4 | 5957 |
| KLLL213P | 7 | 60 | 300 | 6.70 | 340 | 66 | 0.19 | 2.68 | 4.34 | 78.1 | 13264 |
| KLML013P | 0 | 60 | 300 | 10.20 | 217 | 148 | 0.68 | 3.58 | 5.53 | 58.4 | 2921 |
| KLML103P | 2 | 25 | 300 | 9.10 | 211 | 70 | 0.33 | 3.58 | 4.87 | 70.8 | 19234 |
| KLML211P | 7 | 60 | 100 | 8.30 | 289 | 138 | 0.48 | 2.53 | 3.82 | 94.5 | 13333 |
| KBLL003P | 0 | 25 | 300 | 4.90 | 455 | 414 | 0.91 | LOW | LOW | 170.9 | 2142 |
| KBLL113P | 2 | 60 | 300 | 5.40 | 387 | 56 | 0.14 | LOW | 1.78 | 68.5 | 27902 |
| KBLL201P | 7 | 25 | 100 | 4.80 | 325 | 125 | 0.38 | LOW | LOW | 109.7 | 16228 |
| KBML001P | 0 | 25 | 100 | 9.00 | 345 | 279 | 0.81 | 2.61 | 3.51 | 123.8 | 6091 |
| KBML111P | 2 | 60 | 100 | 8.00 | 383 | 92 | 0.24 | 1.78 | 2.12 | 92.1 | 21194 |
| KBML203P | 7 | 25 | 300 | 8.90 | 265 | 91 | 0.34 | 2.40 | 3.3 | 79.9 | 16244 |
| GBLL010P | 0 | 60 | 100 | 4.20 | 596 | 430 | 0.72 | LOW | LOW | 249.9 | 5007 |
| GBLL101P | 2 | 25 | 100 | 5.40 | 601 | 300 | 0.50 | 0.84 | 3.73 | 207.5 | 10998 |
| GBLL213P | 7 | 60 | 300 | 5.00 | 817 | 126 | 0.15 | 0.46 | 2.72 | 143.8 | 22602 |
| GBML013P | 0 | 60 | 300 | 9.50 | 332 | 320 | 0.96 | 7.75 | 5.23 | 162.6 | 12450 |
| GBML103P | 2 | 25 | 300 | 7.80 | 531 | 101 | 0.19 | 4.70 | 4.26 | 192.7 | 10474 |
| GBML211P | 7 | 60 | 100 | 8.60 | 642 | 249 | 0.39 | 6.36 | 4.26 | 184.5 | 12058 |

## KEY FOR SAMPLE IDENTIFICATION:

| | | |
|---|---|---|
| K | ASPHALT | K=AAK-1 G=AAG-1 |
| L | AGGREGATE | L=RL B=RB |
| L | VOIDS | L=LOW M=MEDIUM |
| L | LONG TERM | L=LONG TERM |
| 0 | AGING PERIOD | 0=0 DAYS 1=2 DAYS 2=7 DAYS |
| 0 | AGING TEMP. | 0=LOW(25°C) 1=HIGH(60°C) |
| 0 | AGING PRESSURE | 0=ROOM PRESSURE 1=100 PSI 3=300 PSI |
| P | AGING TYPE | P=PRESSURE OXIDATION AGING |

TABLE 8 SUMMARY OF TRIAXIAL AGING DATA

## (a) USING OXYGEN

| SAMPLE ID | AGING COND'N | | ACTUAL | MODULUS (ksi) | | MODULUS RATIO | PERM (E-9c/s) | | TENSILE | |
|---|---|---|---|---|---|---|---|---|---|---|
| | PERIOD (day) | TEMP. (°C) | VOIDS (%) | BEFORE AGING | AFTER AGING | | BEFORE AGING | AFTER AGING | STRESS (psi) | STRAIN μ-strain |
| KLLL00TO | 0 | 25 | 4.9 | 387 | 387 | 1.00 | 0.47 | 0.45 | 188 | 6398 |
| KLLL10TO | 1 | 25 | 5.0 | 416 | 500 | 1.20 | 0.03 | 0.09 | 204 | 5725 |
| KLLL20TO | 3 | 25 | 5.3 | 489 | 550 | 1.12 | 0.38 | 0.67 | 205 | 4912 |
| KLML01TO | 0 | 60 | 7.3 | 407 | 407 | 1.00 | 2.08 | 2.60 | * | * |
| KLML11TO | 1 | 60 | 7.0 | 412 | 396 | 0.96 | 3.75 | 3.38 | 181 | 6358 |
| KLML21TO | 3 | 60 | 7.9 | 336 | 430 | 1.28 | 5.87 | 4.86 | 194 | 6122 |
| KLML31TO | 7 | 60 | 7.4 | 317 | 478 | 1.51 | 3.04 | 3.60 | 198 | 5382 |
| GLLL01TO | 0 | 60 | 6.3 | 421 | 421 | 1.00 | 0.54 | 0.48 | 237 | 5906 |
| GLLL11TO | 1 | 60 | 5.5 | 457 | 549 | 1.20 | LOW | 0.57 | 254 | 6279 |
| GLLL21TO | 3 | 60 | 6.1 | 460 | 593 | 1.29 | 1.07 | 3.67 | * | * |
| GLML00TO | 0 | 25 | 7.1 | 422 | 422 | 1.00 | 0.84 | 1.26 | 200 | 7292 |
| GLML10TO | 1 | 25 | 8.3 | 308 | 390 | 1.27 | 5.01 | 3.69 | 160 | 7933 |
| GLML20TO | 3 | 25 | 8.1 | 404 | 487 | 1.21 | 1.23 | 2.52 | 223 | 5760 |
| GLML31TO | 7 | 60 | 7.8 | 448 | 747 | 1.67 | 3.65 | 3.80 | 298 | 4270 |
| KBLL01TO | 0 | 60 | 5.3 | 334 | 334 | 1.00 | LOW | LOW | * | * |
| KBLL11TO | 1 | 60 | 5.2 | 350 | 465 | 1.33 | LOW | 0.36 | 214 | 6222 |
| KBLL21TO | 3 | 60 | 4.8 | 338 | 500 | 1.48 | LOW | 0.10 | 230 | 5549 |
| KBML00TO | 0 | 25 | 7.8 | 289 | 289 | 1.00 | 0.78 | 1.43 | * | * |
| KBML10TO | 1 | 25 | 6.6 | 280 | 267 | 0.95 | LOW | 1.01 | 169 | 6735 |
| KBML20TO | 3 | 25 | 7.4 | 295 | 320 | 1.08 | 0.07 | 1.48 | 173 | 5772 |
| KBML31TO | 7 | 60 | 6.7 | 284 | 496 | 1.75 | 0.71 | 0.09 | 182 | 7093 |
| GBLL00TO | 0 | 25 | 4.8 | 508 | 508 | 1.00 | 0.03 | 0.04 | 286 | 6589 |
| GBLL10TO | 1 | 25 | 4.8 | 499 | 581 | 1.16 | LOW | 0.14 | 301 | 6762 |
| GBLL20TO | 3 | 25 | 5.1 | 480 | 637 | 1.33 | 0.07 | 0.13 | 277 | 7681 |
| GBML01TO | 0 | 60 | 7.1 | 396 | 513 | 1.30 | 0.33 | 0.53 | 248 | 9415 |
| GBML11TO | 1 | 60 | 7.3 | 437 | 529 | 1.21 | 0.80 | 1.82 | 258 | 6920 |
| GBML21TO | 3 | 60 | 7.0 | 503 | 763 | 1.52 | 0.49 | 1.16 | 248 | 7175 |
| GBML31TO | 7 | 60 | 7.4 | 449 | 744 | 1.66 | 0.71 | 2.49 | 327 | 4818 |

## (b) USING AIR

| SAMPLE ID | AGING COND'N | | ACTUAL | MODULUS (ksi) | | MODULUS RATIO | PERM (E-9cm/s) | | TENSILE | |
|---|---|---|---|---|---|---|---|---|---|---|
| | PERIOD (days) | TEMP. (°C) | VOIDS (%) | BEFORE AGING | AFTER AGING | | BEFORE AGING | AFTER AGING | STRESS (psi) | STRAIN μ-strain |
| KLLL00TA | 0 | 25 | 4.6 | 390 | 390 | 1.00 | 0.63 | 0.43 | 178.8 | 6474.0 |
| KLLL10TA | 1 | 25 | 5.0 | 333 | 393 | 1.18 | 0.14 | 0.15 | 183.4 | 6890.5 |
| KLLL20TA | 3 | 25 | 5.4 | 355 | 403 | 1.14 | LOW | 0.14 | 168.7 | 7239.3 |
| KLML01TA | 0 | 60 | 7.0 | 365 | 365 | 1.00 | 0.51 | 0.71 | 173.5 | 6384.2 |
| KLML11TA | 1 | 60 | 6.2 | 334 | 388 | 1.16 | 0.27 | 2.07 | 152.8 | 6190.1 |
| KLML21TA | 3 | 60 | 7.2 | 299 | 411 | 1.37 | 1.66 | 3.30 | 161.2 | 4525.6 |
| GLLL01TA | 0 | 60 | 5.3 | 596 | 596 | 1.00 | 0.18 | 0.17 | * | * |
| GLLL11TA | 1 | 60 | 5.7 | 594 | 571 | 0.96 | 0.43 | 1.56 | 293.7 | 5485.1 |
| GLLL21TA | 3 | 60 | 6.2 | 520 | 566 | 1.09 | 4.17 | 4.29 | 324.1 | 4361.8 |
| GLML00TA | 0 | 25 | 8.2 | 471 | 473 | 1.00 | 1.60 | 4.13 | 219.3 | 7042.4 |
| GLML10TA | 1 | 25 | 7.3 | 465 | 461 | 0.99 | 1.90 | 2.95 | 252.6 | 4513.1 |
| GLML20TA | 3 | 25 | 7.5 | 451 | 397 | 0.88 | 0.95 | 3.87 | 252.1 | 5646.3 |
| KBLL01TA | 0 | 60 | 5.0 | 353 | 353 | 1.00 | LOW | LOW | 186.5 | 4231.2 |
| KBLL11TA | 1 | 60 | 4.7 | 339 | 376 | 1.11 | LOW | LOW | 214.4 | 6241.5 |
| KBLL21TA | 3 | 60 | 3.8 | 364 | 382 | 1.05 | LOW | LOW | 227.9 | 6095.2 |
| KBML00TA | 0 | 25 | 7.1 | 347 | 347 | 1.00 | LOW | 0.36 | * | * |
| KBML10TA | 1 | 25 | 7.4 | 332 | 317 | 0.95 | 0.76 | 1.15 | 171.7 | 7853.2 |
| KBML20TA | 3 | 25 | 8.1 | 305 | 314 | 1.03 | 3.10 | 3.32 | 158.2 | 7013.0 |
| GBLL00TA | 0 | 25 | 4.8 | 479 | 500 | 1.04 | 0.23 | 0.50 | 297.4 | 6168.9 |
| GBLL10TA | 1 | 25 | 4.8 | 536 | 516 | 0.96 | 0.26 | 0.52 | 291.7 | 5768.8 |
| GBLL20TA | 3 | 25 | 5.1 | 631 | 519 | 0.82 | LOW | LOW | 331.7 | 5711.5 |
| GBML01TA | 0 | 60 | 7.1 | 449 | 449 | 1.00 | 0.71 | 2.49 | * | * |
| GBML11TA | 1 | 60 | 7.3 | 525 | 463 | 0.88 | 2.11 | 2.79 | 253.8 | 5036.8 |
| GBML21TA | 3 | 60 | 7.0 | 570 | 569 | 1.00 | 3.73 | 2.83 | 324.4 | 3716.7 |

## NOTES AND KEY FOR SAMPLE IDENTIFICATION:

* Due to an operator error this data was lost.

| | | | |
|---|---|---|---|
| K | ASPHALT | K=AAK-1 | G=AAG-1 |
| L | AGGREGATE | L=RL | B=RB |
| L | VOIDS | L=LOW | M=MEDIUM |
| L | LONG TERM | L=LONG TERM AGING | |
| 0 | AGING PERIOD | 0=O DAY | 1=1 DAY 2=3 DAYS |
| 0 | AGING TEMP. | 0=LOW(25°C) | 1=HIGH(60°C) |
| TO or TA | AGING TYPE | TO=OXYGEN | TA=AIR |

evaluation has not been done completely and, in the interest of space, will not be attempted here.

The resilient modulus data for the short-term oven aging are shown in Figures 2–5; resilient modulus data for extended mixing test programs are shown in Figures 6–9. In all the figures presented, the key uses a three-character code (similar to those used in Tables 4–8) to indicate the asphalt-aggregate combination used, for example, KBO represents asphalt AAK-1 with aggregate RB prepared at low air voids level (0), and KB1 represents a higher air void level (1).

Figures 10 and 11 show resilient modulus data for the long-term oven aging tests. Note that the modulus ratios shown for 0 days aging are greater than 1 because these samples have undergone conditioning at 40°C or 60°C, which increases their modulus slightly. Figures 12–15 show resilient modulus data for the pressure oxidation tests with oxygen, and Figures 16–19 show similar data for the tests with compressed air.

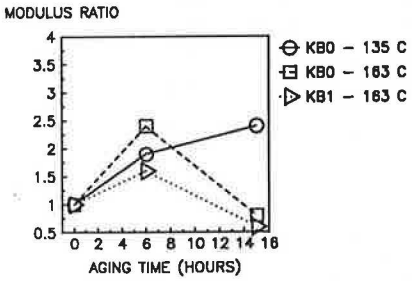


**FIGURE 2 Short-term oven aging results, AAK-1 and RB.**

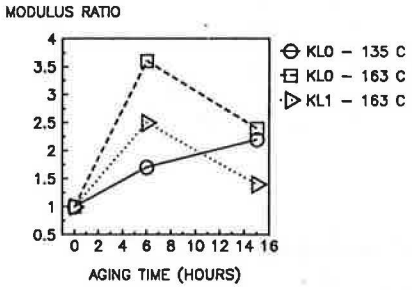


**FIGURE 3 Short-term oven aging results, AAK-1 and RL.**

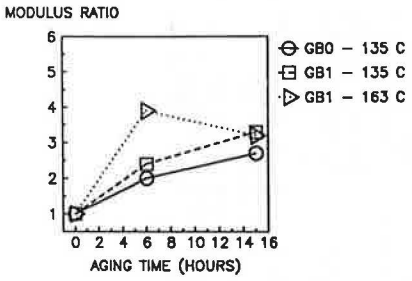


**FIGURE 4 Short-term oven aging results, AAG-1 and RB.**

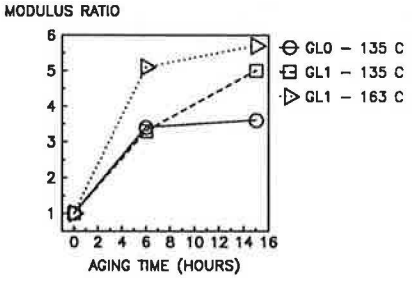


**FIGURE 5 Short-term oven aging results, AAG-1 and RL.**

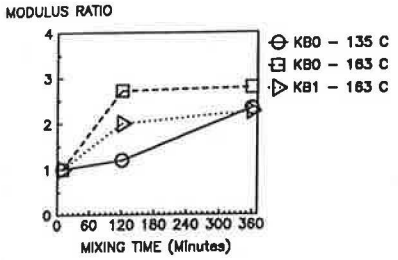


**FIGURE 6 Extended mixing results, AAK-1 and RB.**

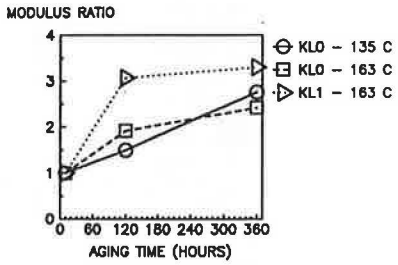


**FIGURE 7 Extended mixing results, AAK-1 and RL.**

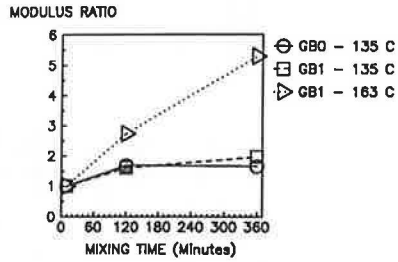


**FIGURE 8 Extended mixing results, AAG-1 and RB.**

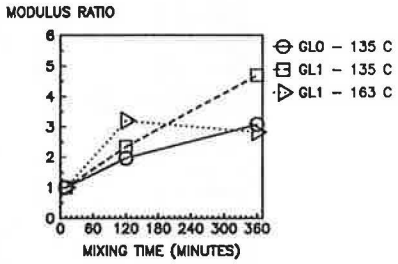


**FIGURE 9 Extended mixing results, AAG-1 and RL.**

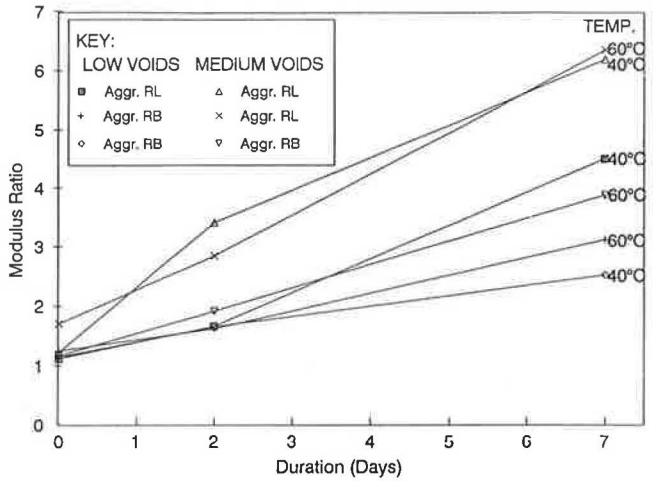


**FIGURE 10 Long-term oven aging results for AAK-1.**

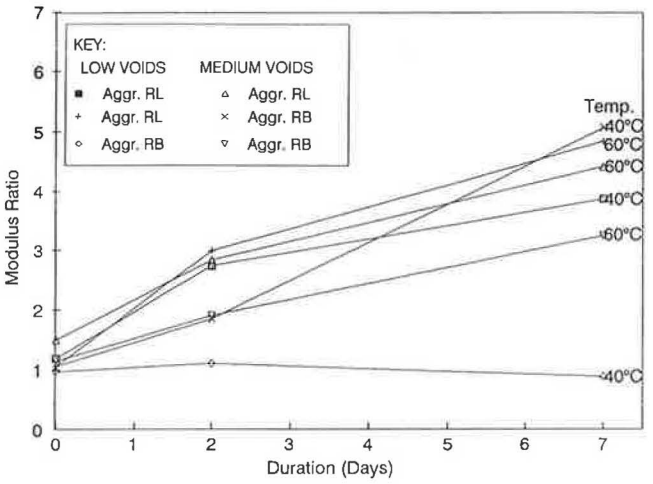


**FIGURE 11 Long-term oven aging results for AAG-1.**

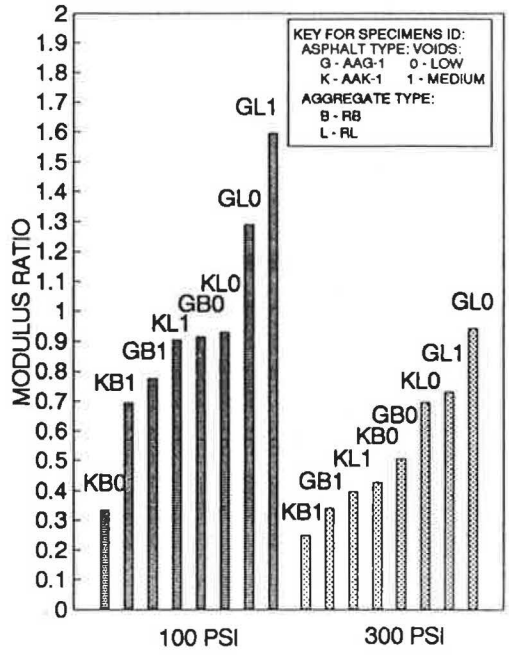


**FIGURE 12 Effect of pressure, pressure oxidation with oxygen.**

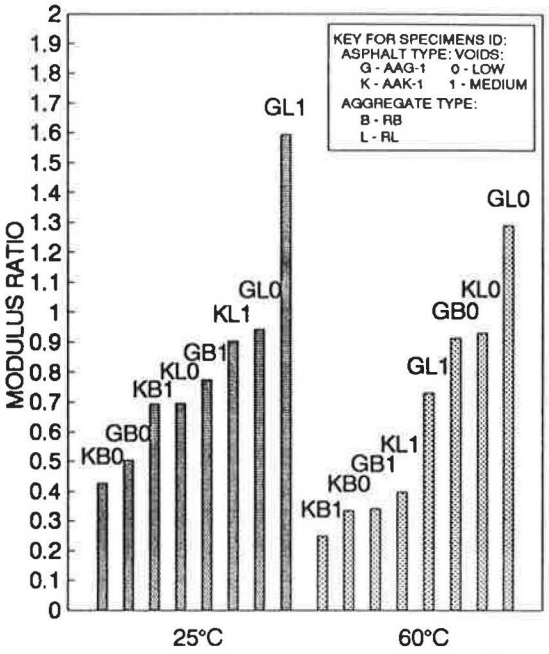


**FIGURE 13 Effect of temperature, pressure oxidation with oxygen.**

Tensile test data are available for all the short- and long-term tests done to date and tend to follow the resilient modulus data in terms of ranking aging procedures. Figures 20 and 21 show sample tensile test data for the pressure oxidation with oxygen tests. These figures show the effect of pressure on tensile strength and strain at yield, respectively.

The test program for the triaxial cell approach was completed recently. Figure 22 shows modulus ratios using oxygen at low pressure. Only the data for the medium air void samples conditioned with oxygen at 60°C are shown. All other samples showed a very low and sporadic increase in modulus.

## DISCUSSION OF RESULTS

### Short-Term Oven Aging

The data from these tests (Figures 2–5) show that significant aging occurs as indicated by an increase in modulus with aging time. In cases in which a temperature of 163°C was used, the modulus ratio for samples aged for 15 hr is lower than for those aged 6 hr. This was attributed to severe aging of the asphalt film in the coated mixture and inability to compact these samples adequately after aging. Table 4 shows that the air voids of these samples were much higher than unaged samples and much higher than with samples aged at 135°C. Compaction of all samples was done at 120°C, as with unaged samples. It may be more appropriate to use an equiviscous compaction temperature in future studies with this approach. Also, subsequent short-term oven aging will be done for shorter periods of time at a temperature of 135°C with a maximum

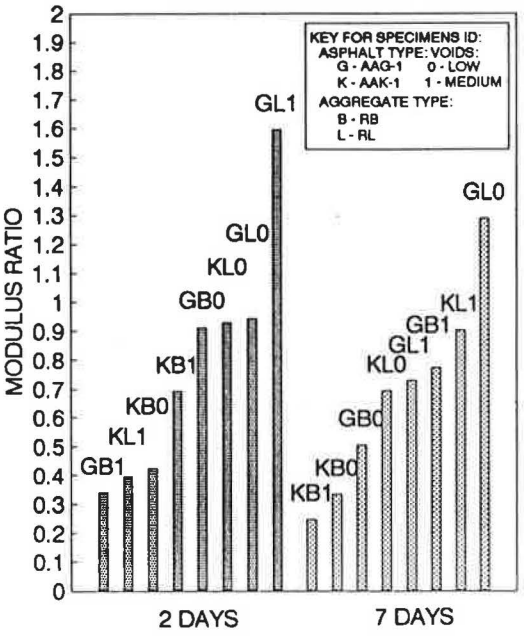


FIGURE 14 Effect of aging period, pressure oxidation with oxygen.

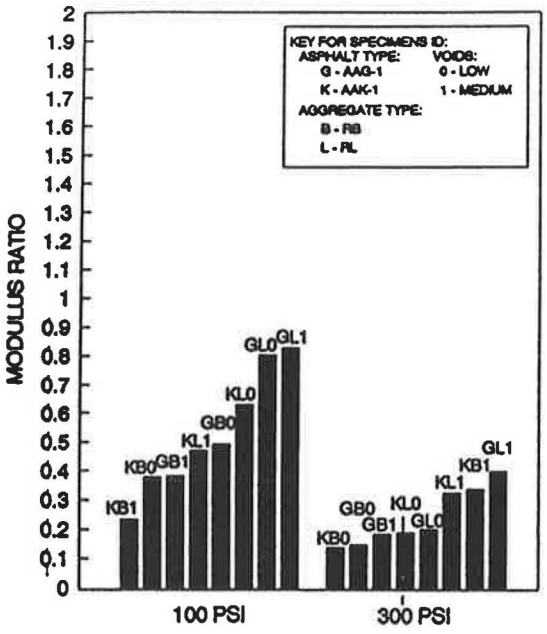


FIGURE 16 Effect of pressure, pressure oxidation with compressed air.

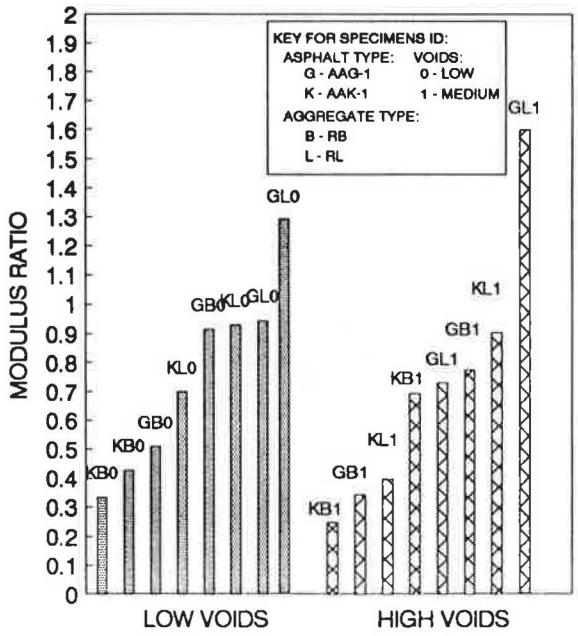


FIGURE 15 Effect of voids, pressure oxidation with oxygen.

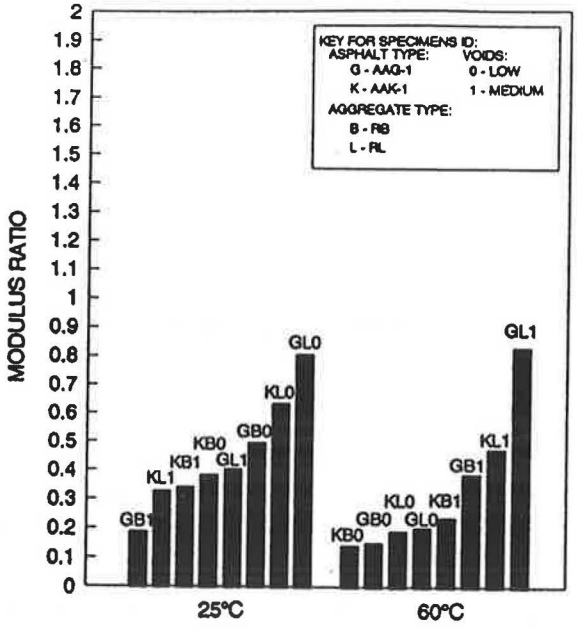


FIGURE 17 Effect of temperature, pressure oxidation with compressed air.

time of around 10 hr. An advantage of this approach is that several trays of material can be aged at the same time.

### Extended Mixing

The data from these tests (Figures 6–9) show that aging increases with aging time, as indicated by increasing modulus ratio. Similar levels of modulus ratio increase were achieved in these tests and the oven aging tests. Although these tests were successful in achieving significant aging, to be viable for production testing, several ovens or significant modification to the RTFO would be needed.

### Long-Term Oven Aging

The oven aging method generally produced an increase in the physical characteristics of the asphalt mixtures. Figures 10 and 11 show that modulus ratio increased as the duration of the

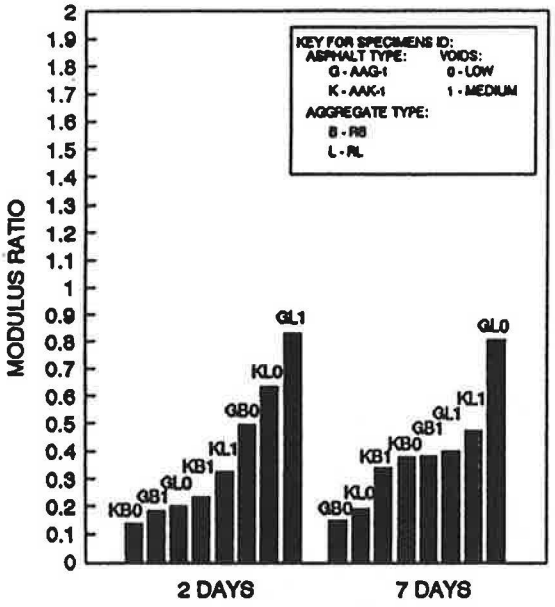


FIGURE 18 Effect of aging period, pressure oxidation with compressed air.

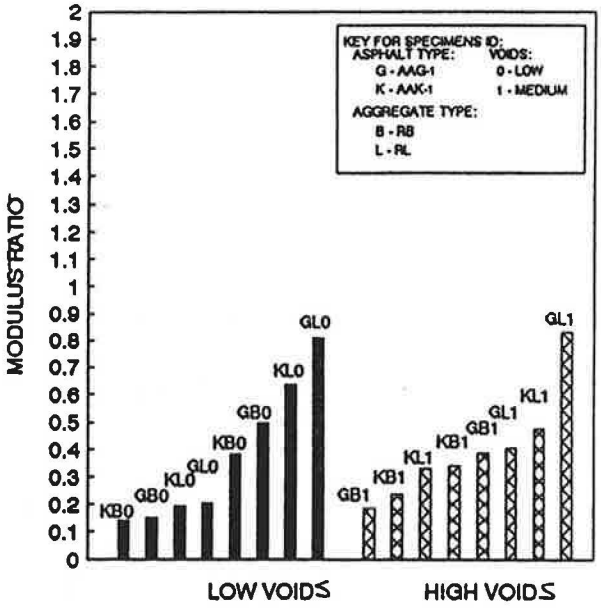


FIGURE 19 Effect of voids, pressure oxidation with compressed air.

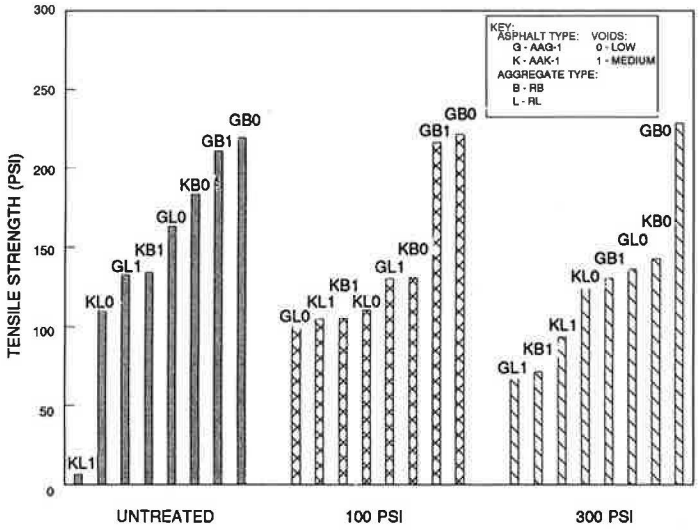


FIGURE 20 Effect of oxygen pressure on tensile strength.

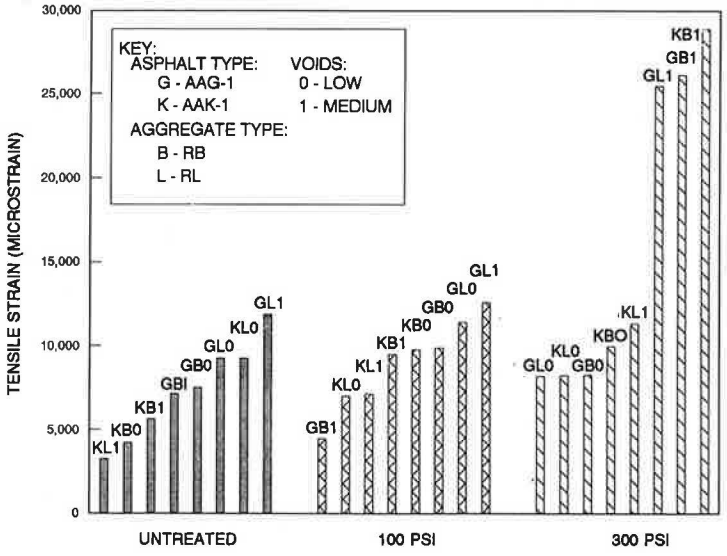


FIGURE 21 Effect of oxygen pressure on tensile strain.

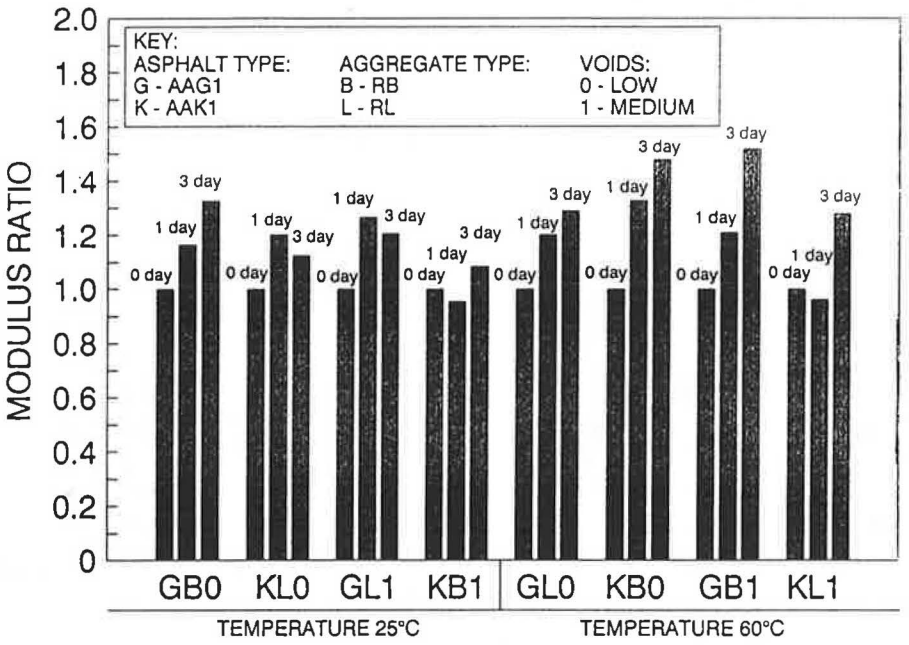


**FIGURE 22 Modulus ratios for low-pressure oxidation with oxygen.**

aging increased. It is apparent that the samples with the higher air voids attained a higher modulus ratio. The two asphalts produced mixes with different aging susceptibility with the AAK-1 mixes exhibiting somewhat greater increase in modulus. Also, aggregate RL tended to produce a higher level of aging than aggregate RB. The exposure temperature also affected the samples. In addition, the permeability tended to increase, although this behavior did not occur for all the samples. The tensile strengths increased as the aging duration increased (Table 6), and the strain at break decreased.

This approach is similar to that recommended by Von Quintus et al. (*3*). It is simple to apply and produces a rapid change in the mixtures within a few days. However, the use of temperatures above 100°C is not representative of the conditions occurring in the field and produces moduli greater than 1,500,000 psi in some mixtures. This is about 50 percent higher than moduli of cores recovered from the field (*4*) or of samples aged in the field (*5*). There is some evidence to suggest that the mechanism of oxidation at high temperatures is different than that at low temperature (*6*), and therefore, a long-term aging method using a lower temperature would be preferable.

### Pressure Oxidation Vessel Using Oxygen

The pressure oxidation vessel using oxygen produced unexpected results. In particular, the modulus ratios decreased with aging treatment, with the effect of pressure being most dramatic. The investigators observed a noticeable change in diameter and thickness for samples exposed to this environment for 7 days at 300 psi at 60°C. Because of this difference, a change in procedure may be necessary to ensure the stability of the samples. Preconditioning similar to that done with oven aging may be an appropriate additional step. The results shown in Figures 12–15 show that pressure was the most significant variable. As the pressure increased from 100 to 300 psi (Figure 12), the modulus ratio tends to decrease. As the temperature (Figure 13) and aging period (Figure 14) or void content (Figure 15) increased, the modulus ratio also tends to decrease. At the extreme conditions of 7 days, 300 psi, and 60°C, the specimens deteriorated most rapidly. Figures 20 and 21 show that the tensile strength deteriorated with level of pressure and the strain at break increased. Again, these trends are contrary to what is expected as samples age. Other data from the tensile tests were similar to those shown in Figures 20 and 21.

More investigation is necessary to understand the effect of oxygen on the asphalt-aggregate mixtures. However, it seems likely that subjecting the samples to a gas at higher pressure disrupts the integrity of the sample, thus reducing the modulus. The disruption probably occurs when pressure is released at the end of the test. An approach using low pressure and/or that confines the sample would be preferable.

### Pressure Oxidation Vessel Using Compressed Air

The pressure oxidation vessel using compressed air produced similar results to the those for pressure oxidation with oxygen. The results for modulus changes are shown in Figures 16–19. Samples subjected to the most extreme conditions of 60°C at 300 psi for 7 days experienced greater deterioration in terms of their physical properties.

### Triaxial Aging

The data shown in Figure 22 indicate that moderate increases in aging manifested by increasing resilient modulus ratio are achieved. It was anticipated that considerably more aging would occur after 7 days with this approach. However, it appears that this method is most viable, perhaps at slightly

higher temperatures, for realistic long-term oxidative aging. It is also a much safer approach than the pressure oxidation approach, because the pressure required is much lower.

## COMPARISON WITH PREVIOUS RESEARCH

Few data are available from previous studies. However, the data obtained from the long-term oven aging tests exhibit similar trends to those reported by Von Quintus et al. (*3*) as shown in Table 9. The results obtained in the pressure oxidation tests by Von Quintus et al. were variable, and some showed a decrease in modulus with aging treatment similar to that observed in this study. Previous work by Kim et al. (*7*) using 60°C and 100 psi oxygen pressure is shown in Figures 23 and 24 and also produced variable results. The general trend was for modulus to increase, although it did decrease in one case for low air-void samples. It appears that higher air-void samples are able to dissipate the pressure.

## CONCLUSIONS

On the basis of the work done to date in this study, the following conclusions can be made:

1. Both short-term oven aging and extended mixing procedures for loose mixtures can cause a fourfold increase in resilient modulus in some mixtures.
2. Extended mixing appears to produce more uniform aging in the mix than oven aging of loose mixtures. However, oven aging is more viable where productivity is of concern, because several samples can be treated in one oven.
3. Subsequent development of the short-term oven aging approach will include adjustment to the maximum exposure

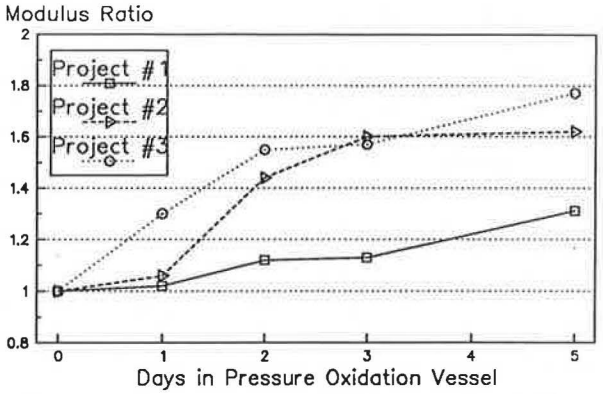


**FIGURE 23 Aging modulus ratios for three asphalt mixtures at 88 percent compaction level (*7*).**

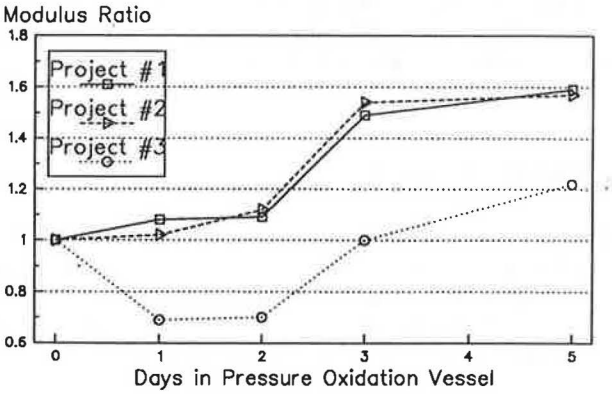


**FIGURE 24 Aging modulus ratios for three asphalt mixtures at 94 percent compaction level (*7*).**

TABLE 9 SUMMARY DATA FOR SPECIMENS CONDITIONED USING DIFFERENT ACCELERATED HARDENING TECHNIQUES (*3*)

| State / Project | Accelerated Aging Method | No. of Days | Penetration (77°F) | Viscosity (140°F) | Indirect Tensile Strength psi | Strain @ Failure mils/in. | Resilient Modulus ksi |
|---|---|---|---|---|---|---|---|
| Michigan MI-0021 | Unaged | 0 | 60 | 2144 | 84 | 14.56 | 482 |
| | Oxygen Bomb | 5 | 63 | 3844 | 111 | 14.04 | 480 |
| | | 10 | 43 | 7542 | 123 | 12.13 | 582 |
| | Forced Draft Oven | 2 | 76 | 2512 | 120 | 9.88 | — |
| | | 7 | 49 | 5897 | 139 | 6.59 | — |
| Texas TX-0021 | Unaged | 0 | 30 | 4388 | 129 | 9.01 | 601 |
| | Oxygen Bomb | 5 | 55 | 3488 | 151 | 8.84 | 738 |
| | | 10 | 64 | 2822 | 167 | 5.98 | 683 |
| | Forced Draft Oven | 2 | 37 | 5654 | 200 | 5.11 | — |
| | | 7 | 30 | 9904 | 241 | 2.69 | — |
| Virginia VA-0621 | Unaged | 0 | 37 | 6000 | 114 | 7.97 | 758 |
| | Oxygen Bomb | 5 | 32 | 28021 | 128 | 10.23 | 569 |
| | | 10 | 35 | 25021 | 121 | 10.66 | 431 |
| | Forced Draft Oven | 2 | 47 | 4401 | 146 | 5.37 | — |
| | | 7 | 27 | 7910 | 177 | 2.69 | — |

time used and possibly adoption of an equiviscous temperature for compaction.

4. Long-term oven aging of compacted mixture samples can cause a sixfold increase in resilient modulus in some mixtures. This increase is regarded as too high, and this approach will only be adopted as a fallback position at a lower temperature than the 107°C used in this study. A temperature of 85°C is probably more appropriate.

5. The results from the pressure oxidation test program for either oxygen or compressed air show a general trend of decreasing modulus with the severity of treatment. This is a trend contrary to that anticipated and is attributed to disruption of the sample when the gas pressure is relieved. Modifications to the test procedure may improve this situation, but a low-pressure technique would be preferable.

6. The triaxial cell aging approach is an alternate method of oxygen enrichment to the pressure oxidation technique. To date, increases of 50 to 100 percent in resilient modulus have been observed with this approach. This is the most likely technique to carry forward for further development. A temperature higher than 60°C will be investigated in the future test program. A temperature of 85°C seems appropriate at this time.

## ACKNOWLEDGMENTS

The work reported herein has been conducted as a part of a SHRP project being conducted by the Institute of Transportation Studies, University of California, Berkeley, with Carl L. Monismith as principal investigator. The support and encouragement of Ian Jamieson is gratefully acknowledged.

## REFERENCES

1. C. A. Bell. *Summary Report on Aging of Asphalt-Aggregate Systems*. SHRP-A/IR-89-004. SHRP, National Research Council, Washington, D.C., 1990.
2. R. G. Hicks, C. L. Monismith, and L. Painter. *Laboratory Study Plan for SHRP Project A-003A*. SHRP Technical Memorandum 89-8. SHRP, National Research Council, Washington, D.C., 1989.
3. H. J. Von Quintus, J. Sherocman, T. Kennedy, and C. S. Hughes. *Asphalt-Aggregate Mixture Analysis System*. Final Report to NCHRP. TRB, National Research Council, Washington, D.C., 1988.
4. G. Thenoux, C. A. Bell, and J. E. Wilson. Evaluation of Physical and Fractional Properties of Asphalt and Their Interrelationship. In *Transportation Research Record 1171*, TRB, National Research Council, Washington, D.C., 1988, pp. 82–97.
5. G. R. Kemp and N. H. Predoehl. A Comparison of Laboratory and Field Environments on Asphalt Durability. *Proc., Association of Asphalt Paving Technologists*, 1981, Vol. 50, pp. 492–537.
6. J. D. Petersen. Effects of Physical and Physicochemical Factors on Asphalt Oxidative Aging, *Proc., 1st Materials Engineering Congress, ASCE*, Denver, Colo., Aug. 1990, pp. 244–253.
7. O-K Kim, C. A. Bell, J. E. Wilson, and G. Boyle. Development of Laboratory Oxidative Aging Procedures for Asphalt Cements and Asphalt Mixtures. In *Transportation Research Record 1115*, TRB, National Research Council, Washington, D.C., 1987, pp. 101–112.



*Publication of this paper sponsored by Committee on Characteristics of Bituminous Materials.*

# Evaluation of Solvents for Extraction of Residual Asphalt from Aggregates

C. A. CIPIONE, R. R. DAVISON, B. L. BURR, C. J. GLOVER, AND J. A. BULLIN

When highway cores and hot mixes are extracted, several percent of the asphalt frequently remains on the aggregate. A variety of solvents were evaluated for their ability to remove this material. They were compared using several aggregates that had been extracted by three procedures. The effectiveness of alcohols as a solvent additive was investigated. Finally a direct comparison of trichloroethylene and toluene containing 15 pecent ethanol using an old road-core material was made. In general, trichloroethylene containing 15 percent ethanol was the best solvent tested. Pyridine is similar but objectionable for other reasons. The residual unextracted material is difficult to remove even with the best solvents.

To study the changes occurring in asphalt as it hardens in the hot-mix plant or roadway and to determine the asphalt content of cores and mixes, asphalt must be extracted from the aggregate. This is done almost exclusively today by either the centrifuge or reflux procedure, usually as specified in ASTM D2172, Methods A and B.

A number of solvents have been used to extract the asphalt. In early years, carbon disulfide was widely used but was largely replaced by benzene. In the 1950s and 1960s, chlorinated solvents became popular. The most common were trichloroethylene, 1,1,1-trichloroethane, and methylene chloride. Abson and Burton (*1*, ASTM D2172-81) tested several of these and found trichloroethylene to be as effective as benzene. Addition of about 10 percent ethanol or methanol to benzene was shown to remove more asphalt from the aggregate (*2*). This has become popular among many researchers. Because benzene has been proven carcinogenic, its use has been phased out and trichloroethylene has been the primary replacement. Pyridine and tetrahydrofuran are used on rare occasions for specialized extractions (*3*,*4*).

Either Method A or B with a variety of solvents is satisfactory for determining the percent asphalt. Round-robin tests of various procedures show no difference in results (*5*). Actually, none of these procedures removes all the asphalt, but the quantity remaining is within the variance of the methods. This does not guarantee that results will be satisfactory when the properties of the recovered asphalt are studied, however.

## INADEQUATE EXTRACTION AND RECOVERY METHODS

Evidence is strong that the present extraction and recovery methods are either inadequate or being performed improperly in the laboratories nationwide. AASHTO conducts interlaboratory proficiency tests periodically to determine the precision of the methods. It sends identical pavement samples to 50 to 100 laboratories. The laboratories extract and recover the asphalt, perform various tests, and send the results to AASHTO. In a February 1989 report, the coefficients of variance on recovered viscosities were about 25 percent. In earlier years, it has been as high as 42 percent (*6*).

In the extraction-recovery discussions, there appear to be three main areas from which errors are likely to stem:

1. The solvent has some hardening effect on the asphalt, which increases with temperature and time of exposure.
2. Solvent is often not completely removed from the asphalt during recovery. This results in viscosities that are lower than the true value.
3. Asphalt is not completely removed from the aggregate. The strongly adsorbed material left on the aggregate has a significantly different composition than the bulk asphalt.

### Solvent Hardening

Solvent hardening of asphalt is particularly severe at higher temperatures such as exist in the reflux method. Though ASTM D1856 specifies that ASTM D2172 Method B is not to be used when asphalt properties will be determined, a survey of the literature indicates this has been ignored as often as followed. Even when using low-temperature extraction, it has been shown that some solvent hardening usually occurs (*7*). Incomplete solvent removal has been studied in detail by Burr et al. (*8*).

### Incomplete Extraction

It is evident that the percentage of total asphalt removed during extraction could also be significant in determining a method's effectiveness. Traxler (*2*) has found that additional asphalt can be removed by adding 10 percent ethanol to benzene. Pyridine has also been used to extract additional asphalt (*9*). Petersen et al. (*10*,*11*) have published several papers that state that up to 4 percent—but usually 2 percent—of the asphalt remains on the aggregate after benzene or trichloroethylene extractions. The asphalt seems to be more strongly adsorbed in old cores than in laboratory mixes.

The strongly adsorbed material is also of a different nature than the bulk asphalt. Glover et al. (*12*) has shown this ma-

Department of Chemical Engineering and the Texas Transportation Institute, Texas A&M University, College Station, Tex. 77843-3122.

terial to be highly oxidized. Petersen (*13*) analyzed this material and found concentrations of carboxylic acids were higher by 12 to 63 times, anhydrides 4 to 32 times, ketones 1 to 6 times, sulfoxides 1 to 4 times, and 2-quinoline types 3 to 10 times in the strongly adsorbed material. Relative affinities of functionalities to the aggregate with respect to the bulk are carboxylic acids > dicarboxylic anhydrides > 2-quinoline types > sulfoxides > other nitrogen groups > ketones. Ketones and sulfoxides can account for 90 percent of the polar compounds in the strongly adsorbed material (*9*). The amount of strongly adsorbed material is a function of the aggregate surface area and not as dependent on aggregate composition (*9*). Apparently, no work has been done to determine the effect on physical properties of adding the strongly adsorbed material back to the bulk asphalt. It is not even clear whether the strongly adsorbed material should be considered part of the asphalt binder. Because of its strong interaction with the aggregate, it may play a stronger role as an aggregate substituent.

Most solvents that have been used for extracting asphalt from aggregates remove the bulk of the asphalt rather quickly but leave some material that is not removed even after repeated or lengthy contacting. The choice of solvent or solvent mixtures, then, should be based on efficiency removing the hard-to-remove material. Pyridine has been indicated to be particularly effective as a single solvent for removing this material. Methanol and ethanol have been shown in this laboratory and in others to improve the ability of commonly used solvents to remove this material with about 15 percent ethanol in trichloroethylene being optimum.

In this work, a number of solvents and mixtures with alcohols are quantitatively compared with respect to their ability to remove the hard-to-remove material from a variety of previously extracted (recovered) aggregates. Because of some objection to chlorinated solvents, direct comparisons between trichloroethylene, toluene, and cyclohexane were made with various alcohol contents.

## PROCEDURES

Pavement cores or hot mixes extracted using ASTM D2172 Method A or Method B or a method using trichloroethylene/ethanol previously recommended by this laboratory (modified Method A) were used. The resulting recovered aggregate material was subsequently contacted by solvents to test their ability to remove any strongly adsorbed residual asphalt material.

The recovered aggregates used in this study were limestone from several sources and were obtained in several ways. First, three recovered aggregates, simply identified by their state of origin—New York (NY), Georgia (GA), and California (CA)—were used. These had all been pavement cores extracted by Method B using trichloroethylene. Second, a composite core (CC) recovered aggregate was formed from a large amount of diverse discarded core material. The core material was divided into three portions, each of which was extracted by a different method—ASTM D2172 Method A using trichloroethylene, Method B using trichloroethylene, and the recommended modified procedure using trichloroethylene/ethanol—to give three more recovered aggregate materials. Third, the recovered aggregate from an Ampet AC-20 hot mix was obtained by an ASTM D2172 Method B extraction and was used in several experiments. In one experiment, this hot-mix recovered aggregate was extracted with pyridine by repeated contacts in a beaker until additional asphalt removal was not evident, and another, a Method B–extracted core, was preextracted with trichloroethylene before the experiment. Finally, a few experiments were made with unidentified Method B–extracted core material. Clean limestone aggregate with no previous contact with asphalt was used as a blank.

To obtain a measure of the relative extraction power of the different solvents or solvent systems, 100- or 150-mesh fines were obtained from each of the recovered aggregates and the blank, and these were used in subsequent extraction experiments with a variety of solvents and conditions. Ten grams of fines were weighed into vials, and 10 mL of the solvent were added. The fines were allowed to soak for 24 hr and then they were filtered. At 650 nm the absorbance was found to vary linearly with whole asphalt content, and this was assumed to be true for all asphalt fractions. Furthermore, in each case the absorbance (650 nm) was normalized by the amount of aggregate contacted to obtain absorbance per gram of aggregate contacted. This provided a basis for comparing the various extracted fine samples. The absorbance measurements were not further converted to an amount of asphalt extracted, however, because of the assumptions that would be required to justify such conversions, that a calibration made with a given whole asphalt would be valid for the hard-to-remove material.

In modified Method A, 15 percent ethanol is added to the solvent and the hot-mix or core material is stirred after each solvent addition. In a final experiment, this procedure was used in a direct comparision of trichloroethylene and toluene.

In all, the following eight sets of experiments were performed:

1. Fines from a Method B–extracted core were equilibrated with 12 solvents to compare their relative abilities to remove the residual hard-to-remove material.
2. Fines from the same Method B–extracted core were further extracted using two successive room-temperature washes, each with 200 mL trichloroethylene, in an Erlenmeyer flask. The fines were then equilibrated with the same 12 solvents as Experiment 1 to compare their relative abilities to remove the residual material.
3. Fines resulting from the different extraction methods or from the different aggregate sources equilibrated with 10 solvents to compare the different methods and sources in their amounts of residual material and to compare the effectiveness of the solvents in removing the residual material.
4. Method B–extracted CC fines containing incremental quantities of water were equilibrated with trichloroethylene and trichloroethylene/15 percent ethanol to evaluate the effect of moisture on these solvents' abilities to remove the residual asphalt material.
5. Method B–extracted hot-mix fines were equilibrated with toluene and cyclohexane containing incremental amounts of methanol and ethanol to evaluate these solvent systems.
6. Method B–extracted hot-mix fines were equilibrated with trichloroethylene and toluene containing incremental amounts

of ethanol and propanol to evaluate the relative abilities of these alcohols to enhance removal of the residual material.

7. Three fines loadings of Method A–extracted CC material were equilibrated with trichloroethylene containing incremental amounts of ethanol to assess the optimum trichloroethylene/ethanol ratio.

8. Both hot-mix and CC aggregate materials were extracted by modified Method A using 15 percent ethanol in either toluene or trichloroethylene. These recovered aggregate materials were then equilibrated in pyridine for several days, and the amount of asphalt thus dissolved in the pyridine was determined gravimetrically so as to establish the fraction of the original asphalt left behind by the extraction method for a solvent.

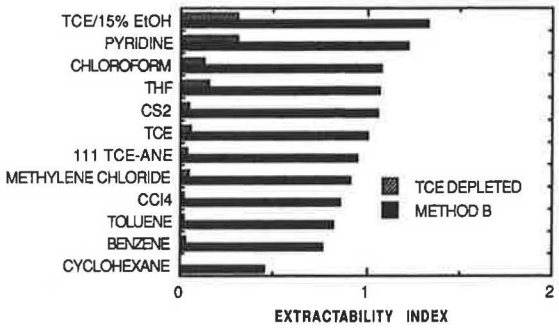


**FIGURE 1 Comparison of solvents for extraction of hard-to-remove material from aggregate.**

In Experiments 1 and 2, the fines loading in the equilibrating solvent was 2 g of 150-mesh material to 10 mL of solvent. In Experiments 3–6, 5 g of 100-mesh fines were used per 10 mL of solvent. In Experiment 7, incremental amounts of 100-mesh fines were used. In Experiment 8, the entire recovered aggregate from a hot-mix or core extraction (approximately 1000 g) was equilibrated with 1 L of pyridine.

## RESULTS

The results of Experiments 1 and 2 are given in Figure 1. The extractability index is defined to be the 650 nm absorbance of that solvent's equilibrated solution relative to the absorbance of the trichloroethylene solution obtained from Experiment 1. In Experiment 2, the same fines were further extracted with trichloroethylene before the 24-hr experiment. As can be seen, trichloroethylene/15 percent ethanol and pyridine are very nearly equal and give the best results in each instance, particularly as more material is removed.

Results for various recovered-aggregate/solvent combinations are given in Table 1 (Experiment 3). Figure 2 compares the solvents on the New York, Georgia, and California Method B–recovered aggregates. Pyridine and trichloroethylene/ethanol are generally best (yield the highest 650 nm absorbance). All absorbance levels were lower for the California aggregate, indicating that it had been much more completely extracted previously.

Figure 3 compares the solvents relative to the method used to preextract the composite recovered aggregate. As can be seen, the modified Method A using trichloroethylene/ethanol was always superior, providing the least amount of asphalt subsequently removed by a solvent wash, followed by Method A, which in turn is superior to Method B. Comparing the solvent systems, trichloroethylene/ethanol is best, extracting the most of the hard-to-remove residual asphalt, except on the material that was preextracted with trichloroethylene/ethanol (modified Method A) on which pyridine was marginally best. On the hot-mix aggregate preextracted with pyridine, however, trichloroethylene/ethanol was clearly superior (Figure 4). It appears that each solvent may selectively remove certain materials.

Six experiments were performed to assess the effect of water on extractability (Experiment 4). Recovered aggregate (CC material, Method B extraction) was used with trichloroethylene and trichloroethylene/15 percent ethanol (absolute). The

TABLE 1 650 nm ABSORBANCES OF SOLVENTS CONTACTED WITH VARIOUS RECOVERED AGGREGATES

| Solvents | 650 nm Absorbance per gm of Recovered Aggregate | | | | | | | |
|---|---|---|---|---|---|---|---|---|
| | | | | | | Composite Core | | |
| | Blank | N Y | GA | CA | Pyridine | Modified A | Method A | Method B |
| Trichlor/Ethanol | 0.0000 | 0.0251 | 0.0437 | 0.0078 | 0.0374 | 0.0268 | 0.0768 | 0.2371 |
| Pyridine | 0.0026 | 0.0307 | 0.0448 | 0.0170 | 0.0128 | 0.0302 | 0.0722 | 0.2291 |
| Chloroform | 0.0000 | 0.0252 | 0.0264 | 0.0012 | 0.0056 | 0.0074 | 0.0330 | 0.1339 |
| Tetrahydrofuran | 0.0006 | 0.0108 | 0.0276 | 0.0010 | 0.0052 | 0.0074 | 0.0370 | 0.1431 |
| Carbon disulfide | 0.0038 | 0.0204 | 0.0200 | 0.0048 | 0.0064 | 0.0094 | 0.0250 | 0.1092 |
| Trichloroethylene | 0.0058 | 0.0212 | 0.0192 | 0.0064 | 0.0078 | 0.0052 | 0.0176 | 0.0923 |
| 111-Trichloroethane | 0.0036 | 0.0192 | 0.0176 | 0.0056 | 0.0076 | 0.0094 | 0.0244 | 0.0934 |
| Methylene Chloride | 0.0044 | 0.0186 | 0.0232 | 0.0048 | 0.0042 | 0.0090 | 0.0154 | 0.0931 |
| Carbon Tetrachloride | 0.0032 | 0.0132 | 0.0122 | 0.0018 | 0.0014 | 0.0024 | 0.0100 | 0.0679 |
| Benzene | 0.0018 | 0.0122 | 0.0094 | 0.0018 | 0.0042 | 0.0050 | 0.0116 | 0.0769 |

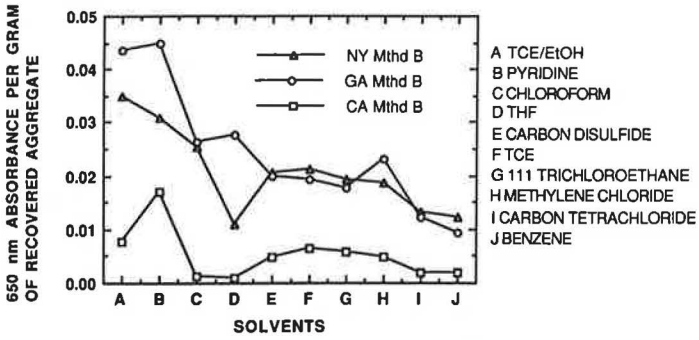


**FIGURE 2 Comparison of solvent systems' abilities to extract hard-to-remove asphalt material remaining on aggregate after ASTM D2172 Method B extraction using trichloroethylene (three sources of pavement core were used).**

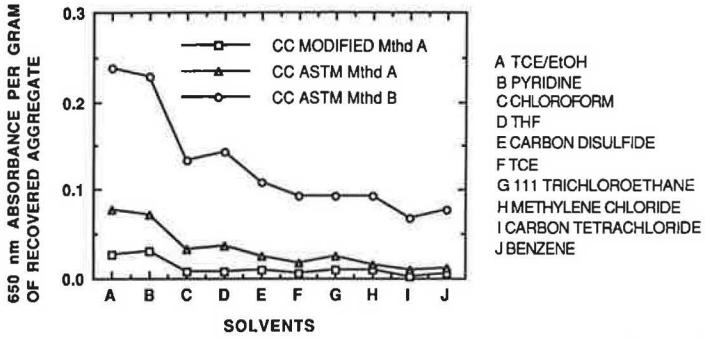


**FIGURE 3 Comparison of solvent systems' abilities to extract hard-to-remove asphalt material and of amount of hard-to-remove material left by three extraction procedures.**

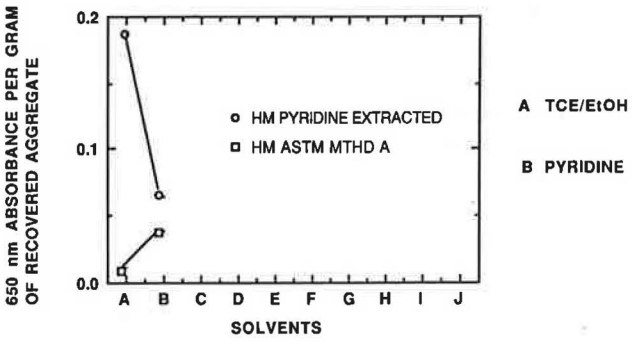


**FIGURE 4 Ability of pyridine to remove material left behind by trichloroethylene/ethanol extraction procedure and vice versa.**

TABLE 2 EFFECT OF WATER ON EXTRACTABILITY FROM THE METHOD B-EXTRACTED CC AGGREGATE

| % Water in Solvent | 650 nm Absorbance per gm of Recovered Aggregate | |
|---|---|---|
| | TCE | TCE/Ethanol |
| 0 | 0.011 | 0.027 |
| 2 | 0.012 | 0.032 |
| 5 | 0.007 | 0.025 |

results in Table 2 suggest that the effect of added moisture to the solvent probably is not significant. This does not, however, assess the effect of prolonged soaking of a pavement core in water (i.e., weathering) on asphalt extraction.

To study the effect of alcohol on the extraction power of nonchlorinated solvents, recovered aggregate (hot-mix material, Method B extraction) was treated with incremental quantities of methanol and ethanol in cyclohexane and toluene (Experiment 5). The results in Table 3 indicate that methanol is relatively ineffective as an additive and that toluene/ethanol is much superior to cyclohexane/ethanol, although inferior to trichloroethylene/ethanol.

Because ethanol was so superior to methanol, it was decided to investigate propanol as an additive in both trichloroethylene and toluene (Experiment 6). New samples of the same recovered aggregate were used. The results are shown in Table 4 and Figure 5. Propanol is seen to be less effective than ethanol, and toluene less effective than trichloroethylene.

Using a different recovered aggregate (CC material, Method A extraction) additional data were obtained to reconfirm the optimum ethanol level in trichloroethylene. This was done at three different recovered aggregate-to-solvent loadings (Experiment 7). The results are shown in Figure 6 and indicate that the alcohol content should be at least 15 percent but that little is gained beyond that.

This multiple testing indicated that for probably any aggregate and at any solvent-to-aggregate ratio, trichloroethylene with 15 percent ethanol was equal or superior to any

TABLE 3 EFFECT OF METHANOL AND ETHANOL ON EXTRACTABILITY OF TOLUENE AND CYCLOHEXANE FOR METHOD B-EXTRACTED HOT-MIX RECOVERED AGGREGATE

| % Alcohol Added | 650 nm Absorbance per gram of Recovered Aggregate | | | |
|---|---|---|---|---|
| | Toluene | | Cyclohexane | |
| | Methanol | Ethanol | Methanol | Ethanol |
| 0 | 0.003 | 0.001 | 0.003 | 0.000 |
| 5 | 0.004 | 0.016 | 0.001 | 0.008 |
| 10 | 0.003 | 0.019 | 0.002 | 0.007 |
| 15 | 0.003 | 0.026 | 0.001 | 0.009 |
| 20 | 0.003 | 0.025 | 0.009 | 0.013 |
| 25 | 0.003 | 0.024 | 0.005 | 0.010 |

TABLE 4 EFFECT OF ETHANOL AND PROPANOL CONCENTRATIONS ON EXTRACTABILITY FOR METHOD B-EXTRACTED HOT-MIX RECOVERED AGGREGATE

| % Alcohol | 650 nm Absorbance Per Gm of Recovered Aggregate | | | |
|---|---|---|---|---|
| | Trichloroethylene | | Toluene | |
| | Ethanol | n-Propanol | Ethanol | n- Propanol |
| 5 | .0548 | .0465 | .0324 | .0244 |
| 10 | .0756 | .0535 | .0429 | .0286 |
| 15 | .0799 | .0586 | .0478 | .0312 |
| 20 | .0871 | .0619 | .0542 | .0352 |
| 25 | .0862 | .0598 | .0687 | .0389 |
| 30 | .0753 | .0597 | .0554 | .0413 |

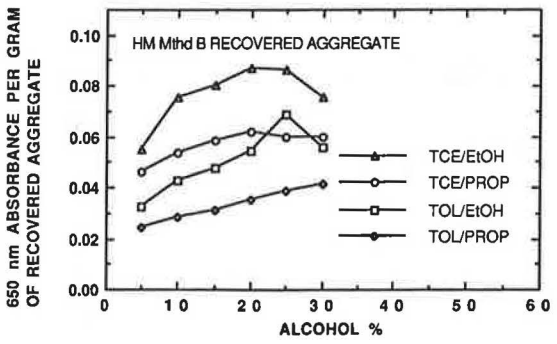


**FIGURE 5 Comparison of ethanol and propanol as additives for improving asphalt extraction.**

other solvent tested. It also indicated that the modified Method A using trichloroethylene/15 percent ethanol with increased agitation removed more material than Method A or B.

The final experiment (Experiment 8) was a direct comparison of toluene/15 percent ethanol and trichloroethylene/15 percent ethanol using modified Method A (which included stirring of the solvent and mix before soaking for improved

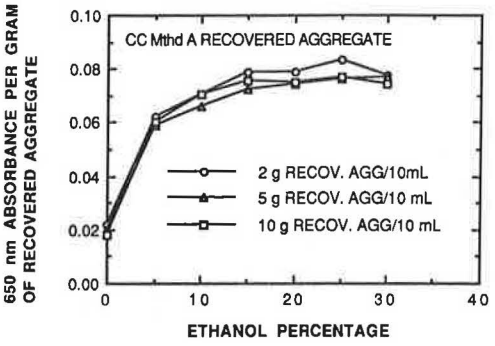


**FIGURE 6 Effectiveness of ethanol in improving asphalt extraction at different alcohol concentrations.**

extraction). The results shown in Figure 7 were obtained by soaking the recovered aggregate in pyridine for several days and quantitatively determining the asphalt material dissolved in the filtered solution by evaporating aliquots to dryness and weighing the residual asphalt. Determinations were made at 1, 3, and 9 days of soaking; the data in Figure 7 are the 9-day determinations. Two separate determinations were made for each (solvent system)/(asphalt core or mix) combination to give the eight data points shown in Figure 7.

The results show estimates of the percentage of the original asphalt that remained after extraction using the modified Method A procedure. The amounts of solvent used on the eight tests vary because of the way in which the procedure is carried out. Solvent contact is continued until the solvent comes out straw-colored, independent of the solvent system used. The data indicate the trichloroethylene/ethanol system more efficiently removes the hard-to-remove material from the recovered aggregate than does the toluene/ethanol system when this variation of solvent volume is taken into account (Figure 7). When the same amount of solvent is used for the two solvent systems, as was the case for the hot-mix material, the trichloroethylene system removes significantly more or leaves significantly less of the hard-to-remove material than does the toluene system. But when the same amount of residual material was left by the extraction procedure by the two solvent systems, the trichloroethylene system achieved its level by using significantly less solvent than the toluene

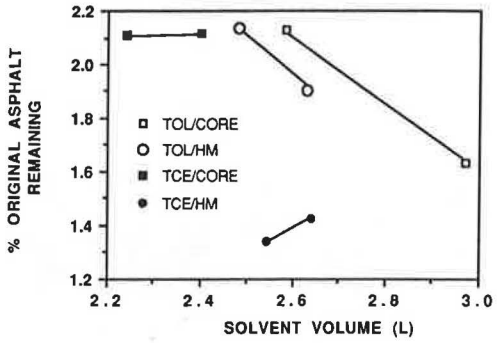


**FIGURE 7 The unextracted material remaining following extraction with trichloroethylene/ethanol and toluene ethanol as a function of the solvent volume used.**

system used. The one toluene extraction on the core material that resulted in the lowest amount of residual asphalt remaining required 50 percent more solvent than the trichloroethylene extractions.

From the pyridine soakings of the eight recovered aggregate samples of Experiment 8 made at the 1-, 3-, and 9-day soak times (Figure 8), it is evident that contact time also plays a significant role in the recovery of this residual material. The total contact time in modified Method A is 2.5 to 3 hr spread over six or seven contacts. The pyridine—which, based on the experiments described earlier, is a considerably better solvent—still extracted additional material after 9 days. Obviously, the trichloroethylene and toluene systems after only 2.5 to 3 hr would have benefited from additional contact time as well.

Finally, it should be recalled that Figure 3 indicates that modified Method A is superior to Method A, but that the increased agitation in the modified method might account for most of the superiority rather than the different solvent systems (trichloroethylene/ethanol versus trichloroethylene).

The data clearly show that no method removes all the asphalt; to take full advantage of the better solvents for hard-to-remove material, more agitation and longer contact is required, but does it matter? Material that is so hard to remove probably affects adhesion but not bulk properties. It might be that the property of only the relatively easily removed material is a better predictor of cracking. Certainly the easily extracted and hard-to-remove material can be extracted and studied separately. Regardless, it is desirable to have an extraction procedure that at least can remove all the material.

## CONCLUSIONS

1. Trichloroethylene with 15 percent ethanol is a superior solvent.
2. Trichloroethylene/ethanol and pyridine are comparable in solvent power for a hard-to-remove material but appear to remove different material preferentially.
3. If only removing the bulk of the material is required, then many solvents and methods will suffice although there are some differences.
4. To recover more than 99 percent of the asphalt material will require the development of better contacting methods.
5. Extraction and recovery procedures also must be designed to minimize solvent hardening and ensure complete solvent removal.

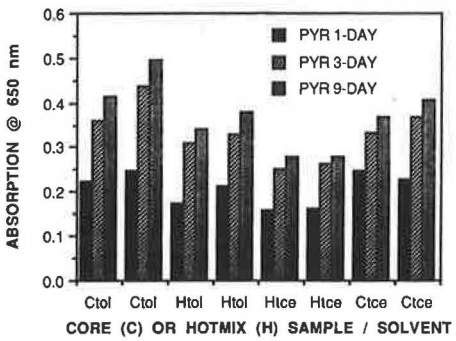


**FIGURE 8 Time required for pyridine to remove hard-to-remove material from extracted core aggregate.**

## ACKNOWLEDGMENTS

Support for this work by the Texas State Department of Highways and Public Transportation, in cooperation with the U.S. Department of Transportation, FHWA, and the Strategic Highway Research Program, is gratefully acknowledged. Helpful discussions with Don O'Connor and Darren Hazlett are greatly appreciated.

## REFERENCES

1. G. Abson and C. Burton. The Use of Chlorinated Solvents in the Abson Recovery Method. *Proc., Association of Asphalt Paving Technologists*, 29, 1990, pp. 246–252.
2. R. N. Traxler. Changes in Asphalt Cements During Preparation, Laying, and Service of Bituminous Pavements. *Proc., Association of Asphalt Paving Technologists*, 36, 1967, pp. 541–561.
3. M. A. Plummer and C. C. Zimmerman, Asphalt Quality and Yield Predictions from Crude Oil Analyses. *Proc., Association of Asphalt Paving Technologists*, 53, 1984, pp. 138–159.
4. P. W. Jennings, J. A. Pribanic, and K. R. Dawson. *Uses of High Pressure Liquid Chromatography to Determine the Effects of Various Additives and Fillers on the Characteristics of Asphalt*. Research Report FHWA-MT-82/001. Montana Department of Highways, Helena, June 1982.
5. M. Stroup-Gardiner, D. E. Newcomb, and J. A. Epps. Precision of Methods for Determining Asphalt Cement Content. In *Transportation Research Record 1228*, TRB, National Research Council, Washington, D.C., 1989, pp. 156–167.
6. *AASHTO Materials Reference Laboratory, Report for Bituminous Concrete Proficiency Samples*. Reports from 1987, 1988, 1989 tests. National Bureau of Standards, Gaithersburg, Md.
7. R. R. Davison, J. A. Bullin, C. J. Glover, B. L. Burr, H. B. Jemison, A. L. G. Kyle, and C. A. Cipione. *Development of Gel Permeation Chromatography, Infrared and Other Tests to Characterize Asphalt Cements and Correlate with Field Performance*. Report FHWA/TX-90/458-1F. Texas Department of Highways and Public Transportation, Austin, Nov. 1989.
8. B. L. Burr, R. R. Davison, C. J. Glover, and J. A. Bullin. Solvent Removal from Asphalt. In *Transportation Research Record 1269*, TRB, National Research Council, Washington, D.C., 1990.
9. H. Plancher, S. M. Dorrence, and J. C. Petersen. Identification of Chemical Types in Asphalts Strongly Adsorbed at the Asphalt-Aggregate Interface and Their Relative Displacement by Water. *Proc., Association of Asphalt Paving Technologists*, Vol. 46, 1977, pp. 151–175.
10. J. C. Petersen, E. K. Ensley, and F. A. Barbour. Molecular Interactions of Asphalt in the Asphalt-Aggregate Interface Region. In *Transportation Research Record 515*, TRB, National Research Council, Washington, D.C., 1974, pp. 67–78.
11. J. C. Petersen. Relationships Between Asphalt Chemical Composition and Performance-Related Properties. Presented at Annual Meeting of the Asphalt Emulsion Manufacturers Association, Las Vegas, Nev., March 1982.
12. C. J. Glover, R. R. Davison, S. M. Ghoreishi, H. B. Jemison, and J. A. Bullin. Evaluation of Oven Simulation of Hot-Mix Aging by an FT-IR Pellet Procedure and Other Methods. In *Transportation Research Record 1228*, TRB, National Research Council, Washington, D.C., 1989, pp. 177–182.



*Publication of this paper sponsored by Committee on Characteristics of Bituminous Materials.*

# Characterization of Age-Hardening Potential of Asphalts by Using Corbett-Swarbrick Asphalt Fractionation Test

JIH-MIN SHIAU, MANG TIA, BYRON E. RUTH, AND GALE C. PAGE

The use of the Corbett-Swarbrick fractionation procedure for characterization of age-hardening potentials of asphalts was studied. The fractionation procedure was used to separate asphalts into four different fractions (asphaltenes, saturates, naphthene-aromatics, and polar-aromatics), to identify trends in the changes of proportions of these asphalt fractions during aging. The technique of infrared spectroscopy was used to examine the changes in the characteristics of these fractions during aging. Analyses were performed to determine the relationship between the properties of these asphalt fractions and the hardening potential of the asphalts. The proportions of fractions in asphalts were found to change during aging: the proportions of the asphaltenes and polar-aromatics increase and the proportions of saturates and naphthene-aromatics decrease. For the asphalts tested, the higher the asphaltene content of an original asphalt, the higher the aging potential as determined by the absolute viscosity ratios after the thin film oven test (TFOT) or the rolling thin film oven test (RTFOT). The proportions of asphalt fractions in the original asphalts were found to correlate fairly well with the absolute viscosity ratios after the TFOT and moderately well after the RTFOT. The results of infrared spectral analyses on the asphalt fractions indicated that the characteristics of the fractions change as an asphalt ages. Anhydrides, carboxylic acids, and ketones develop in asphaltenes; carboxylic acids and ketones develop in polar-aromatics and naphthene-aromatics as a result of aging. No evidence exists that any functional group developed in saturates as a result of aging.

In the selection of an asphalt for paving, it is important to ensure not only that the asphalt has suitable properties at the time of placement but also that it retains these properties to achieve adequate long-term performance. One of the major factors affecting the durability of an asphalt is its rate of hardening in service. When an asphalt binder hardens excessively, it may cause the asphalt mixture to become too brittle, and the pavement will crack prematurely. The age hardening of an asphalt has been known to be caused by oxidation, loss of volatile fractions, and changes in chemical structure (such as polymerization) resulting from exposure to air, heat, and ultraviolet light. Although it is known that construction specifications such as plant mix temperature and compaction of the asphalt mixture have great effects on the hardening of the asphalt (*1*), it has also been recognized that the chemical composition of the asphalt plays a great role in its hardening potential, and many studies have been devoted to this area (*2–4*).

The use of the Corbett-Swarbrick fractionation procedure for characterization of age-hardening potentials of asphalts has been studied. In this study, the Corbett-Swarbrick procedure (ASTM D4124-86, Method B), with modifications as recommended by Thenoux et al. (*5,6*), was used to separate asphalts into four fractions (asphaltenes, saturates, naphthene-aromatics, and polar-aromatics), to identify trends in the changes of proportions of these asphalt fractions during the aging process. The technique of infrared absorption spectroscopy was used to examine the changes in the characteristics of these fractions during aging. Analyses were performed to determine the relationship between the properties of these asphalt fractions and the hardening potential of the asphalts.

## TESTING PROGRAM

Eight asphalts were selected and used to make Marshall specimens that were subjected to an artificial aging process. For each of the asphalts, the thin film oven test (TFOT) (ASTM D1754-78) and the rolling thin film oven test (RTFOT) (ASTM D2872-80) were performed at 325°F. The absolute viscosity at 140°F (60°C) of each asphalt was measured before and after the tests. Three fractionation analyses were performed for each asphalt under different aging conditions, namely, (a) the original asphalt, (b) the asphalt extracted from Marshall specimens that had not been subjected to any aging process, and (c) the asphalt extracted from Marshall specimens that had been aged in a forced-draft oven at 140°F (60°C) for 90 days. The absolute viscosity of each asphalt at these various conditions was also measured.

The infrared absorption spectroscopy was performed on the asphalt fractions from three of the asphalts to examine changes in the characteristics of these fractions during the aging process.

## TEST PROCEDURES

### Fabrication of Marshall Specimens

The Marshall specimens in this study were prepared using a limestone aggregate blend that meets the gradation specifi-

J. M. Shiau, M. Tia, and B. E. Ruth, Department of Civil Engineering, University of Florida, Gainesville, Fla. 32611. G. C. Page, Florida Department of Transportation Bureau of Materials and Research, P.O. Box 1029, Gainesville, Fla. 32601.

cation for a Florida Type S-1 asphalt concrete mix (dense-grade structural surface mix) with an asphalt content of 6.5 percent and compacted by the 50-blow Marshall compaction method. The Marshall specimens were aged in a forced-draft oven in which the temperature was maintained at 140°F (60°C) for 90 days. Results of a previous aging study indicated that aging in a forced-draft oven at 140°F (60°C) for 28 days simulated 1 to 2 years of field aging under Florida conditions (*2*). Aging in the forced-draft oven for 90 days would correspond to 3 to 6 years of field aging. The Abson method (ASTM D1856) was used to extract the asphalt from the Marshall specimens.

### Fractionation Test

The Corbett-Swarbrick procedure of asphalt fractionation (ASTM D4124-86, Method B), with modification recommended by Thenoux et al., was used to separate the asphalt into four different fractions (*5,6*). The procedure is briefly described here. The first step involves the separation of the asphalt into a n-heptane–insoluble asphaltenes and the n-heptane–soluble petrolene. The petrolene is then adsorbed on a calcined F-20 alumnia and further fractionated into the saturate, naphthene-aromatic, and polar-aromatic fractions by downward solvent elution in a glass chromatographic column. Eluted fractions are recovered by solvent removal before final weighing. The column feed volumes used in this test are shown in Table 1.

According to the ASTM D4124-86, the single operator precision of the fractionation test for asphaltenes, saturates, naphthene-aromatics, and polar-aromatics are 0.32, 0.44, 1.03, and 0.78 percent, respectively.

### Infrared Absorption Spectroscopy

Infrared spectroscopic technique was used to measure changes in the structures of the asphalts and asphalt fractions because of aging, in terms of the changes in the amount of certain functional groups in them. The infrared absorption spectrum between 1600 $cm^{-1}$ and 1900 $cm^{-1}$ is of particular interest, because it contains the absorption bands for the functional groups of carboxylic acids, ketones, and anhydrides (*4,7*). Ketones and anhydrides are formed in asphalt on oxidative aging, although carboxylic acids occur naturally in asphalt but increase in amount in oxidative aging.

TABLE 1 COLUMN FEED VOLUMES

| Eluant Solvent | ml | Fraction Received | Approximate ml |
|---|---|---|---|
| n-Heptane | 65 | Saturates | 100 |
| Toluene | 35 | | |
| Toluene | 100 | Naphthene-Aromatics | 200 |
| Methanol/Toluene (50/50) | 100 | | |
| Trichloroethylene | 200 | Polar-Aromatics | 200+ |
| | | | Cleaning Solvent |

The infrared spectroscopy tests were run on a Nicolet 60 SX research-grade Fourier transform infrared (FTIR) spectrophotometer system in the Materials Science and Engineering Laboratory of the University of Florida. The system offers a resolution of 0.25 $cm^{-1}$ throughout the standard range of 5000 to 400 $cm^{-1}$. The components of the FTIR system are arranged into two main groups: the data acquisition system, consisting of the computer, disk drives, and terminal; and the spectrometer, consisting of the optical bench and washer control. Figure 1 depicts a typical 60 SX system configuration.

A 5 percent (wt/vol) solution in high-performance liquid chromatography- (HPLC-) grade tetrahydrofuran was used in the tests. A sealed cell with 1 mm path length and sodium chloride windows was used. The background spectrum for tetrahydrofuran was generated by scanning the pure solvent and stored in computer. Then the spectrum for the solution was generated. Using the computer software of the system, the background spectrum was ratioed out, yielding the spectrum of the sample.

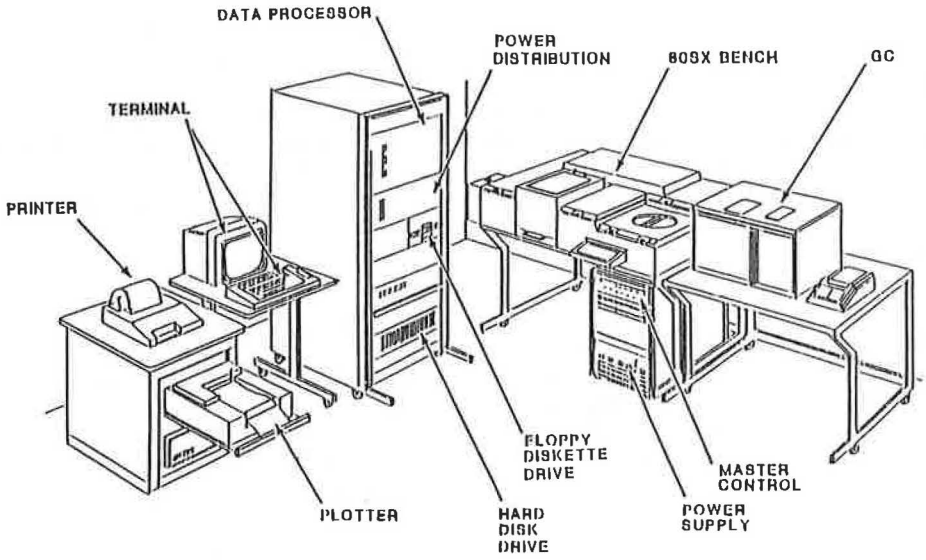


**FIGURE 1 Typical 60 SX FTIR spectrophotometer system.**

## RESULTS

### Results of Absolute Viscosity Test

The results of the absolute viscosity test on the eight asphalts at different aging conditions are shown in Table 2. Table 3 displays the viscosity ratios of these asphalts after the TFOT and RTFOT. It can be seen that the RTFOT procedure produced a slightly higher viscosity ratio than the TFOT procedure.

TABLE 2 ABSOLUTE VISCOSITY OF ASPHALTS AT DIFFERENT AGING CONDITIONS

| | Absolute Viscosity at 140°F (Poises) | | | | |
|---|---|---|---|---|---|
| Asphalt | Original | After TFOT | After RTFOT | Zero day[1] aging | 90 days[2] aging |
| A AC-30 | 3301 | 9760 | 10451 | 7334 | 374433 |
| B AC-30 | 3100 | 9748 | 14389 | 11322 | 132900 |
| D AC-30 | 2967 | 7613 | 8489 | 7096 | 47893 |
| E AC-30 | 2753 | 8894 | 11321 | 8906 | 100829 |
| F Air blown 85-100 pen. | 1931 | 3588 | 3426 | 2392 | 8928 |
| G 85-100 pen. | 1064 | 2327 | 2499 | 2345 | 11466 |
| H 85-100 pen. | 3810 | 17910 | 19090 | 11315 | 73359 |
| I 25-35 pen. | 17885 | 38309 | 48601 | 34021 | 2400000 |

NOTE:

(1) asphalt extracted from Marshall specimens which were not aged.

(2) asphalt extracted from Marshall specimens which were aged for 90 days.

TABLE 3 VISCOSITY RATIO OF ASPHALTS AFTER TFOT AND RTFOT PROCEDURES

| | Absolute Viscosity Ratio | |
|---|---|---|
| Asphalt | After TFOT | After RTFOT |
| A | 2.96 | 3.17 |
| B | 3.14 | 4.64 |
| D | 2.57 | 2.86 |
| E | 3.23 | 4.11 |
| F | 1.86 | 1.77 |
| G | 2.19 | 2.35 |
| H | 4.70 | 5.01 |
| I | 2.14 | 2.72 |

### Results of Fractionation Test

The results of the fractionation test are shown in Table 4. Average percentages of the fractions for paving asphalts (excluding Asphalt I) are shown in Table 5 (Asphalt I is excluded because it is a roofing asphalt). Some trends can be easily identified from the results. The percentage of asphaltenes does not change much between the original and 0-day asphalt, and increases more significantly during the aging process. The

TABLE 4 RESULTS OF ASPHALT FRACTIONATION TEST

| Asphalt | Condition | Asp (%) | Sat (%) | N-A (%) | P-A (%) |
|---|---|---|---|---|---|
| A AC-30 | Original | 23.31 | 9.77 | 44.74 | 22.18 |
| | Zero day | 25.47 | 6.64 | 37.64 | 30.25 |
| | 90 days | 38.23 | 8.54 | 26.62 | 26.61 |
| B AC-30 | Original | 22.22 | 14.93 | 45.14 | 17.71 |
| | Zero day | 22.89 | 11.25 | 40.16 | 25.70 |
| | 90 days | 30.14 | 10.96 | 33.22 | 25.68 |
| D AC-30 | Original | 15.25 | 10.64 | 48.22 | 25.89 |
| | Zero day | 14.28 | 8.22 | 43.57 | 33.93 |
| | 90 days | 26.14 | 7.57 | 35.61 | 30.68 |
| E AC-30 | Original | 23.48 | 13.77 | 45.75 | 17.00 |
| | Zero day | 22.54 | 10.56 | 40.85 | 26.05 |
| | 90 days | 31.61 | 9.63 | 32.64 | 26.12 |
| G 85-100 pen. | Original | 12.75 | 27.49 | 38.25 | 21.51 |
| | Zero day | 12.64 | 10.03 | 39.78 | 37.55 |
| | 90 days | 16.77 | 10.32 | 34.84 | 38.07 |
| F Airblown 85-100 pen. | Original | 7.41 | 23.61 | 43.52 | 25.46 |
| | Zero day* | 6.72 | 25.21 | 33.62 | 34.45 |
| | 90 days | 17.36 | 23.02 | 31.32 | 28.30 |
| I 25-35 pen. | Original | 17.41 | 14.58 | 42.51 | 25.50 |
| | Zero day | 24.14 | 11.73 | 37.24 | 26.89 |
| | 90 days | 29.93 | 12.41 | 31.02 | 26.64 |
| H 85-100 pen. | Original | 25.83 | 10.23 | 45.78 | 18.16 |
| | Zero day | 24.00 | 8.00 | 39.33 | 28.67 |
| | 90 days | 33.58 | 7.66 | 29.93 | 28.83 |

Asp: Asphaltenes

Sat: Saturates

N-A: Naphthene-Aromatics

P-A: Polar-Aromatics

* The amount of asphalt used was only 1.24 grams.

TABLE 5 AVERAGE PERCENTAGES OF ASPHALT FRACTIONS

| | Asp % | Sat % | N-A % | P-A % |
|---|---|---|---|---|
| Original | 18.61 | 15.78 | 44.49 | 21.12 |
| Zero day | 18.36 | 11.42 | 39.28 | 30.94 |
| 90 days | 27.69 | 11.10 | 32.03 | 29.18 |

NOTE: Asphalt I is excluded in the computation.

saturates' fraction decreases slightly after the mixing process and remains steady during the aging process. The naphthene-aromatics' fraction decreases during both the mixing and the aging process. The percentage of polar-aromatics increases during the mixing process, but no significant change occurs after that.

### Relationship Between Asphalt Fractions and Absolute Viscosity

The plots of absolute viscosity at 140°F of the seven paving asphalts versus the percentages of the asphalt fractions present are shown in Figures 2–5. From Figure 2, it can be seen that the absolute viscosity increases when the asphaltenes content is higher. On the contrary, an asphalt with a higher content of saturates has a lower absolute viscosity value (see Figure 3). The trends in naphthene-aromatics and polar-aromatics are not clear. This agrees with the findings reported by Corbett (*8*), which state that asphaltenes contribute much toward temperature susceptibility and to high viscosity.

### Relationship Between Asphalt Fractions and Absolute Viscosity Ratio

The plots of the viscosity ratio (after the TFOT and RTFOT) versus the asphaltenes content of original asphalt are shown in Figures 6 and 7. In both cases, the viscosity ratio increases as the asphaltenes content increases. This indicates that an original asphalt with a higher asphaltenes content tends to produce a higher viscosity ratio after the TFOT or RTFOT (especially the RTFOT). The relationship between the viscosity ratio (after the TFOT and RTFOT) and the other fractions is not so clear.

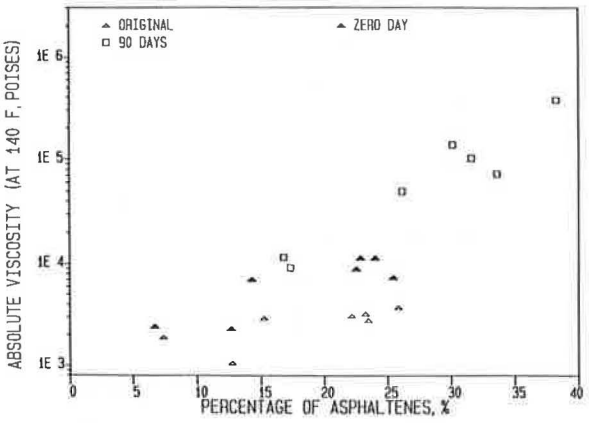


**FIGURE 2 Asphaltenes content versus absolute viscosity.**

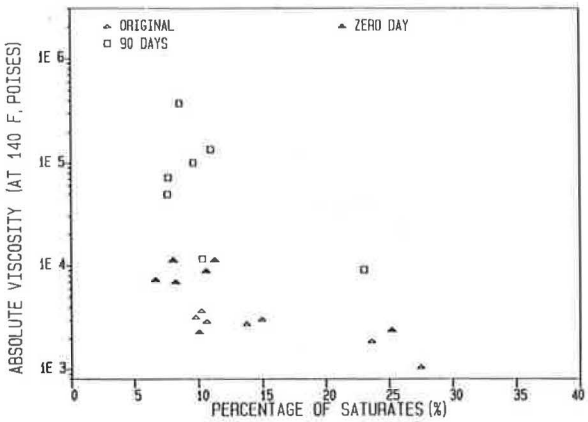


**FIGURE 3 Saturates content versus absolute viscosity.**

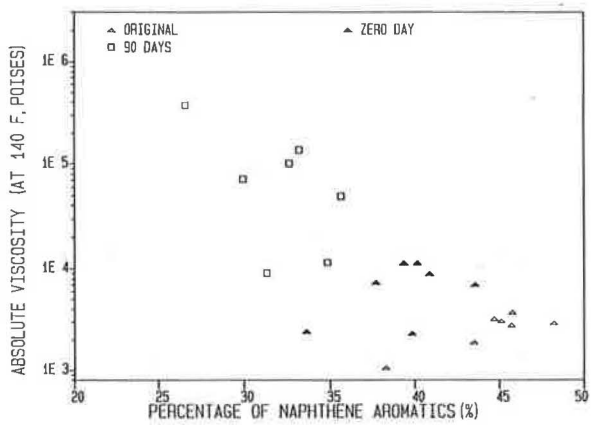


**FIGURE 4 Napthene-aromatics content versus absolute viscosity.**

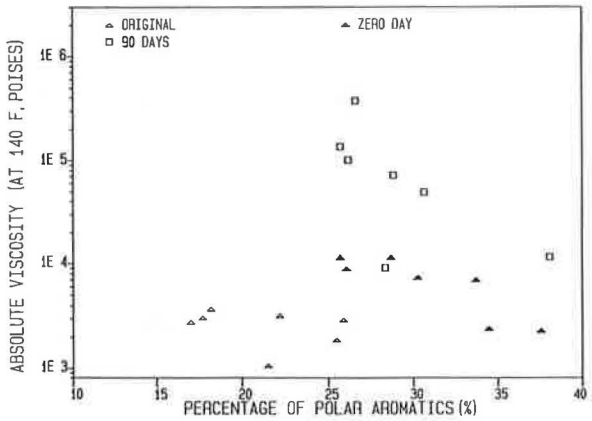


**FIGURE 5 Polar-aromatics content versus absolute viscosity.**

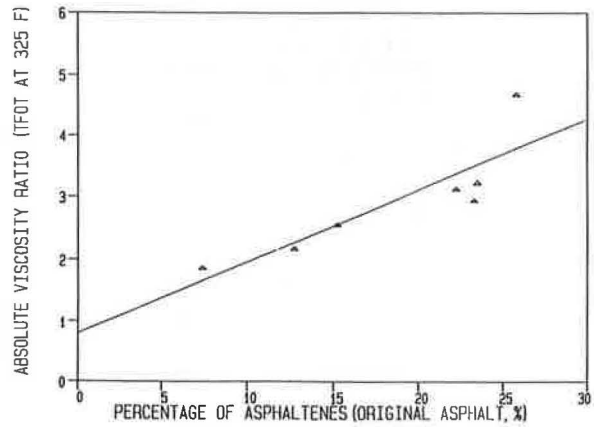


**FIGURE 6 Relationship of asphaltenes content of original asphalt and absolute viscosity ratio (TFOT at 325°F).**

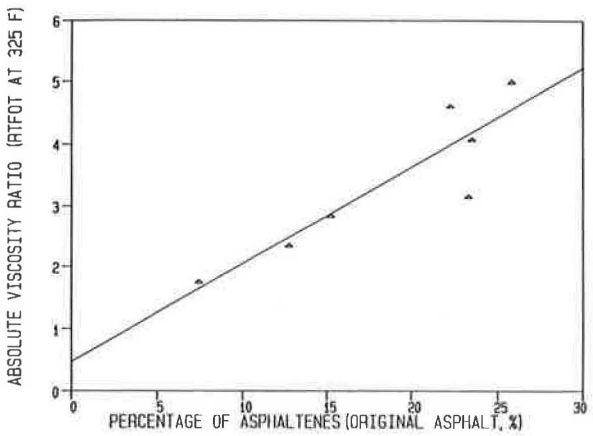


**FIGURE 7 Relationship of asphaltenes content of original asphalt and absolute viscosity ratio (RTFOT at 325°F).**

Regression analyses were performed to relate the percentages of the asphalt fractions present in the original asphalt to the viscosity ratio after the TFOT and RTFOT. The SAS/STAT computer software was used for this purpose. A regression equation of the following form was used:

$$\text{Viscosity ratio (after RTFOT or TFOT)} = \beta_0 + \beta_1(\text{Asp }\%) + \beta_2(\text{Sat }\%) + \beta_3(P - A\,\%) + \text{error}$$

The *R*-square values for the model above were found to be .7531 for TFOT and .9193 for RTFOT. The regression coefficients for the RTFOT case are as follows:

$$\beta_0 = 13.5444$$

$$\beta_1 = -0.0709$$

$$\beta_2 = -0.1229$$

$$\beta_3 = -0.3252$$

It is to be noted that only the percentages of three of the four fractions are needed in this prediction equation. Using the percentage of the fourth fraction in the prediction equation would be redundant, because it is dependent on the percentages of the other three fractions (they add up to 100 percent).

Although the three regression coefficients—$\beta_1$, $\beta_2$, and $\beta_3$—are all negative, $\beta_1$ is less negative than the other two coefficients. An increase in asphaltenes content (Asp %) will result in an increase in viscosity ratio, because an increase in asphaltenes content is accompanied by a decrease in the other fractions, whose corresponding coefficients are more negative than that for the asphaltenes.

Table 6 shows the comparison between the actual and predicted viscosity ratios if this regression equation were used to predict the viscosity ratios after the RTFOT from the percentages of the fractions of the original asphalts. It can be noted that the predicted values are fairly close to the actual ones with a maximum error of 0.55. This indicates that the composition of an asphalt (in terms of the proportions of the four fractions) might be used to predict the hardenability of

TABLE 6 COMPARISON BETWEEN ACTUAL VISCOSITY RATIOS (AFTER RTFOT) AND THOSE PREDICTED BY REGRESSION EQUATION

| Asphalt | Actual | Predicted Value | Residual |
|---|---|---|---|
| 1 | 4.64 | 4.3758 | 0.2642 |
| 2 | 4.11 | 4.6600 | -.550011 |
| 3 | 3.17 | 3.4795 | -.309531 |
| 4 | 2.86 | 2.7375 | 0.1225 |
| 5 | 2.35 | 2.2673 | .0827177 |
| 6 | 1.77 | 1.8384 | -.068374 |
| 7 | 5.01 | 4.5515 | 0.4585 |

the asphalt. The effects of asphalt composition on predicted hardenability are depicted in Figure 8. In this plot, percentage of asphaltenes and percentage of polar-aromatics are used as abscissa and ordinate, respectively. For specified fixed percentages of saturates (10, 15, 20, and 25 percent), lines that represent combinations of percentages of asphaltenes and polar-aromatics that would give a predicted viscosity ratio of 4 are drawn. For a specified saturates content (such as 15 percent), the area above the line represents combinations of percentages of asphaltenes and polar-aromatics that would give a predicted viscosity ratio of less than 4. If the combination of percentages of these two fractions falls below the line, the predicted viscosity ratio would be greater than 4.

### Results of Infrared Absorption Spectroscopy

Fractions from Asphalts A, E, and F at different conditions were used in the infrared absorption spectroscopy test. The characteristic changes of fractions caused by aging are similar for these three asphalts.

Figures 9–12 display the infrared absorption spectra for fractions of Asphalt A in the region between 1900 $cm^{-1}$ and 1500 $cm^{-1}$. Three spectra in each figure are for three different conditions, that is, original 0-days, and 90-days aging. From Figure 9, which shows the spectra of the asphaltenes, anhydrides can be identified at about 1730 $cm^{-1}$ and 1780 $cm^{-1}$.

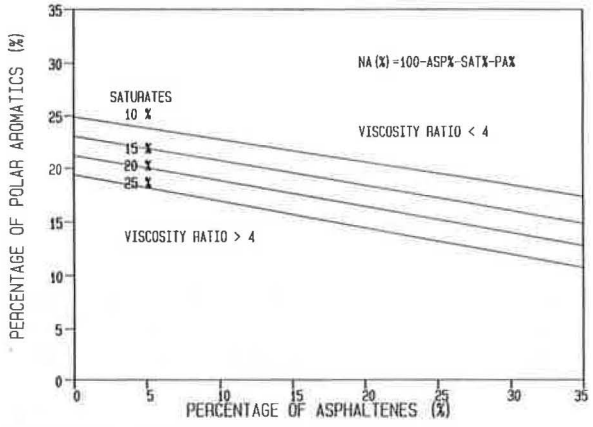


**FIGURE 8 Relationship between compositions of original asphalt and viscosity ratio after RTFOT.**

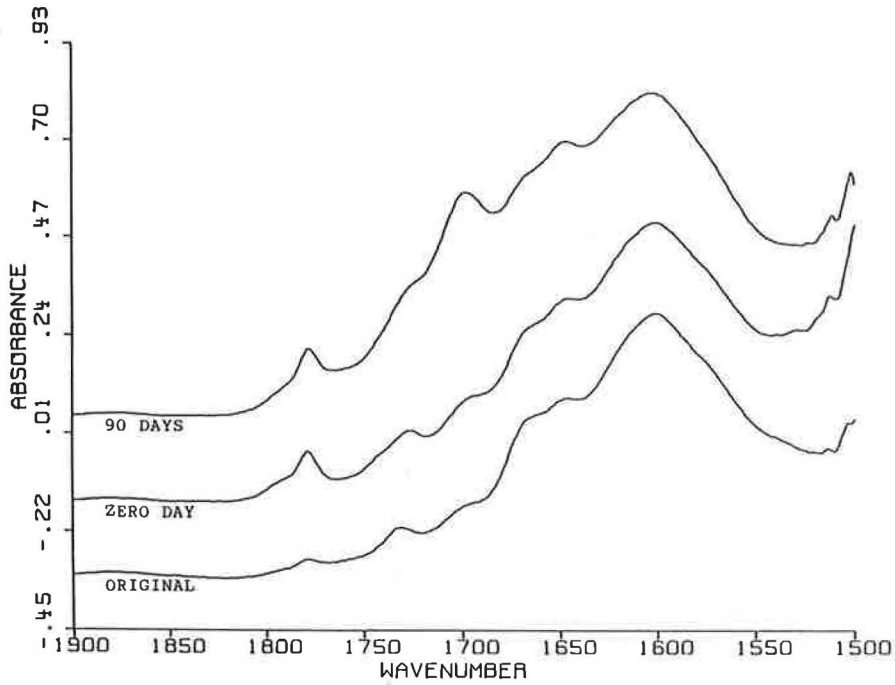


**FIGURE 9 Infrared spectra of asphaltenes for Asphalt A at different conditions.**

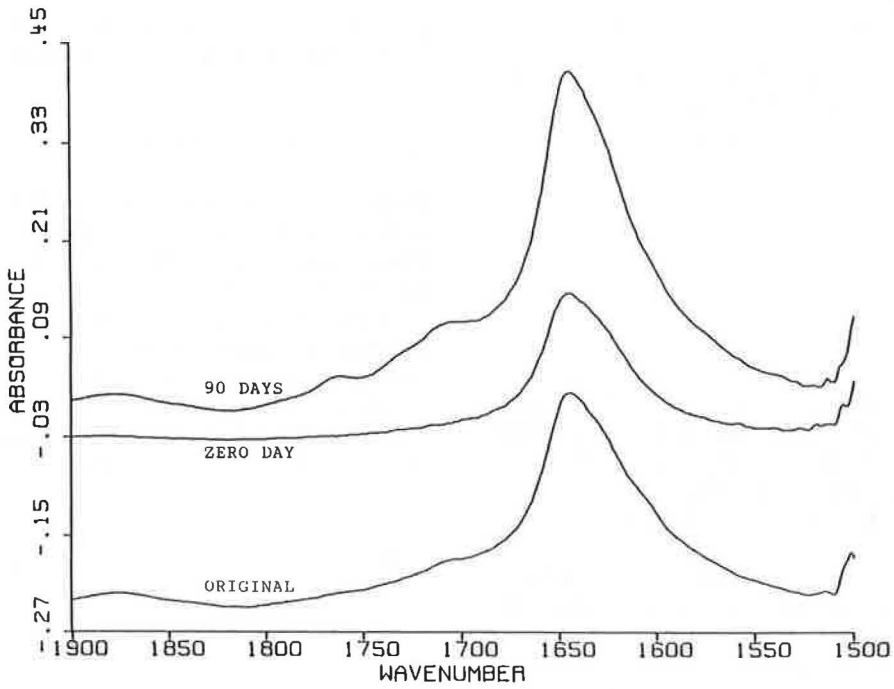


**FIGURE 10 Infrared spectra of saturates for Asphalt A at different conditions.**

The peak at about 1700 $cm^{-1}$ results from the presence of carboxylic acids, ketones, and aldehydes. Anhydrides exist in the asphaltenes of original asphalt and continue to develop during the mixing and aging process. Aldehydes exist in the original spectrum, and do not change much after that. Ketones and carboxylic acids are formed during the mixing and aging process.

The difference between the spectra of saturates at different conditions is primarily in the intensity of the peak at around 1645 $cm^{-1}$ (see Figure 10). In Figure 11, which shows the spectra of the naphthene-aromatics, the peak at around 1700 $cm^{-1}$ develops continously during the mixing and aging process. It results from the forming of ketones and carboxylic acids. No evidence exists of the presence of anhydrides in

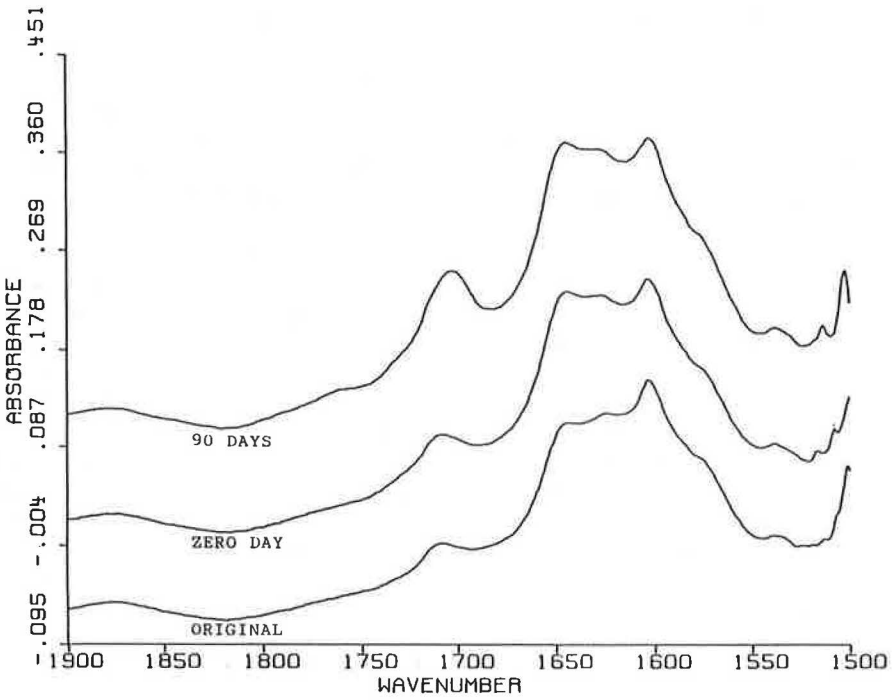


**FIGURE 11 Infrared spectra at naphthene-aromatics for Asphalt A at different conditions.**

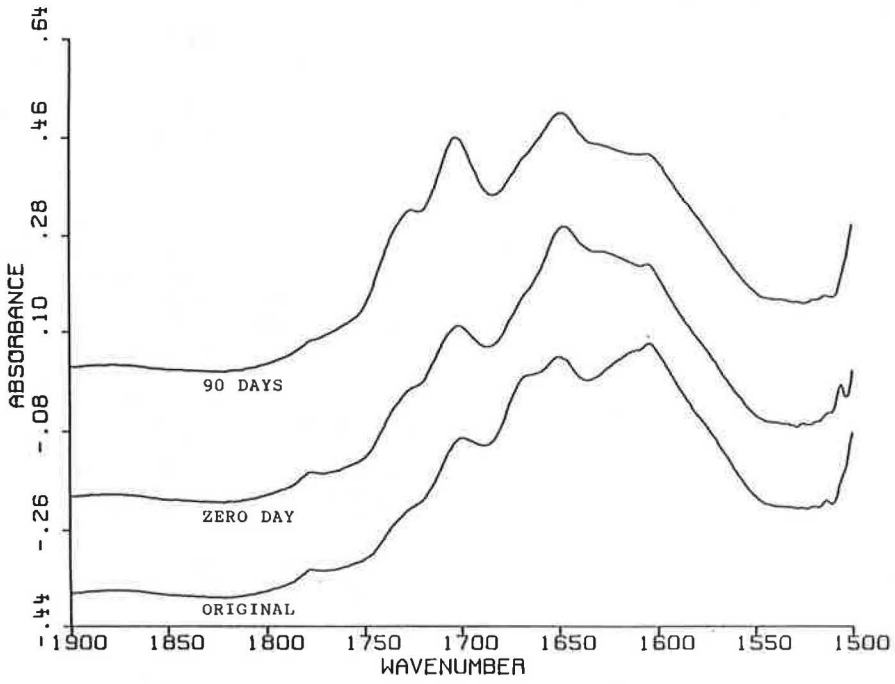


**FIGURE 12 Infrared spectra of polar-aromatics for Asphalt A at different conditions.**

naphthene-aromatics. In the fraction of polar-aromatics (see Figure 12), anhydrides exist in each condition, but no change is found at the different aging conditions. The peak at 1700 $cm^{-1}$ resulting from the ketones and carboxylic acids develops during the mixing and aging process.

The absorption band centering at 1600 $cm^{-1}$, which results primarily from aromatic carbon-carbon double bonds, can be assumed to be fairly constant, because the group is present in highly condensed stable molecules (*2,9*). The absorption band centering at 1375 $cm^{-1}$, resulting primarily from carbon-methyl bond, is also fairly constant (*2*). Therefore, the carbonyl ratio, a ratio of absorbances at 1700 $cm^{-1}$ and 1600 $cm^{-1}$ (CR1) or a ratio of absorbances at 1700 $cm^{-1}$ and 1375 $cm^{-1}$ (CR2), was used as an indicator of the level of oxidation

(*2*). Table 7 presents the carbonyl ratio of each fraction of asphalts. All absorption measurements were with reference to the absorption at 1900 $cm^{-1}$. It is obvious, from the results, that the carbonyl ratios of asphaltenes and polar-aromatics increase significantly during the mixing and aging process. The carbonyl ratios of the naphthene-aromatics increases also but not significantly. The trend of saturates is not clear.

## SUMMARY

The major findings from the results of the study are summarized as follows:

1. The proportions of fractions in asphalts change during aging. The proportion of asphaltenes does not change much during the mixing and increases during the aging process. The proportion of saturates decreases during mixing and changes very little during aging. The naphthene-aromatics content decreases during both mixing and aging. The polar-aromatics portion increases during mixing, but not much change occurs after that.

TABLE 7 CARBONYL RATIOS OF ASPHALT FRACTIONS

| | | | Carbonyl Ratio | | | |
|---|---|---|---|---|---|---|
| Asphalt | Condition | | Asphaltenes | Saturates | Naphthene Aromatics | Polar Aromatics |
| Asphalt A AC-30 | Original | CR1 | 0.2606 | 0.4756 | 0.2701 | 0.6290 |
| | | CR2 | 0.2034 | 0.0807 | 0.1099 | 0.4760 |
| | Zero day | CR1 | 0.3606 | *0.4055 | 0.3362 | 0.7296 |
| | | CR2 | 0.2761 | *0.1368 | 0.1361 | 0.5253 |
| | 90 days | CR1 | 0.6871 | 0.6010 | 0.5163 | 1.0785 |
| | | CR2 | 0.5937 | 0.1323 | 0.2175 | 0.7144 |
| Asphalt E AC-30 | Original | CR1 | 0.2028 | 0.6273 | 0.2469 | 0.5482 |
| | | CR2 | 0.1552 | 0.0852 | 0.1447 | 0.4822 |
| | Zero day | CR1 | 0.3701 | *0.3183 | 0.2713 | 0.7085 |
| | | CR2 | 0.3692 | *0.0884 | 0.1206 | 0.5624 |
| | 90 days | CR1 | 0.6241 | -- | 0.3498 | 0.9644 |
| | | CR2 | 0.5517 | -- | 0.1800 | 0.8032 |
| Asphalt F Airblown 85-100 pen. | Original | CR1 | -- | 0.6040 | 0.4619 | 0.8946 |
| | | CR2 | -- | 0.0552 | 0.2580 | 0.9325 |
| | Zero day | CR1 | -- | 0.6239 | 0.5002 | 1.0530 |
| | | CR2 | -- | -- | 0.3081 | 0.9716 |
| | 90 days | CR1 | -- | 0.4735 | 0.4854 | 1.1986 |
| | | CR2 | -- | 0.0642 | 0.3304 | 1.1444 |

CR1 = Relative Absorbance @ 1700 $cm^{-1}$/Relative Absorbance @ 1600 $cm^{-1}$
CR2 = Relative Absorbance @ 1700 $cm^{-1}$/Relative Absorbance @ 1375 $cm^{-1}$
* = 1% concentration

2. For the asphalts tested, the higher the asphaltenes content of an original asphalt, the higher the viscosity ratio after the TFOT or RTFOT.

3. The proportions of asphalt fractions in the original asphalts correlate fairly well with the absolute viscosity ratios after the RTFOT (with an *R*-square value of .92) and correlate moderately well with that after the TFOT (with an *R*-square value of .75).

4. As noted from the results of infrared spectral analyses on the asphalt fractions, the characteristics of the fractions change as an asphalt ages. Anhydrides, carboxylic acids, and ketones develop in asphaltenes as a result of aging. For naphthene-aromatics and polar-aromatics, carboxylic acids and ketones develop because of aging. No evidence exists for any functional group developed in saturates as a result of aging.

5. The change of the proportions of fractions in an asphalt alone may not be a simple indicator of the degree of oxidation in the asphalt, because not only do the proportions of fractions change but the characteristics of the fractions themselves also change during the oxidation process.

## REFERENCES

1. G. C. Page, K. H. Murphy, B. E. Ruth, and R. Roque. Asphalt Binder Hardening. *Proc., Association of Asphalt Paving Technologists*, Vol. 54, 1985, pp. 140–167.
2. C. T. Chari. *Evaluation of Age Hardening on the Characteristics of Asphalts and Mixtures*. Ph.D. dissertation. University of Florida, Gainesville, April 1988.
3. L. W. Corbett, and H. E. Schweyer. Composition and Rheology Considerations in Age Hardening of Bitumen. *Proc., Association of Asphalt Paving Technologists*, Vol. 50, 1981, pp. 571–582.
4. J. C. Peterson. Chemical Composition of Asphalt as Related to Asphalt Durability: State of the Art. In *Transportation Research Record 999*, TRB, National Research Council, Washington, D.C., 1984, pp. 13–30.
5. G. Thenoux and C. A. Bell. *Test Instruction Manual for Separation of Asphalt into Four Fractions by Corbett-Swarbrick Procedure*. Civil Engineering Department, Oregon State University, Corvallis, Sept. 1985, pp. 1–20.
6. G. Thenoux, C. A. Bell, J. E. Wilson, D. Eakin, and M. Schroeder. Experiences with the Corbett-Swarbrick Procedure for Separation of Asphalt into Four Generic Fractions. In *Transportation Research Record 1171*, TRB, National Research Council, Washington, D.C., 1988, pp. 66–70.
7. J. C. Peterson. Quantitative Functional Group Analysis of Asphalts Using Differential Infrared Spectrometry and Selective Chemical Reactions—Theory and Application. *Transportation Research Record 1096*, TRB, National Research Council, Washington, D.C., 1986, pp. 1–11.
8. L. W. Corbett. Dumbbell Mix for Better Asphalt. *Hydrocarbon Processing*, April 1979, pp. 173–177.
9. A. C. Edler, M. M. Hatting, V. P. Servas, and C. P. Marais. Use of Aging Test to Determine the Efficiency of Hydrated Lime Additions to Asphalt in Retarding its Oxidative Hardening. *Proc., Association of Asphalt Paving Technologists*, Vol. 54, 1985, pp. 118–139.

*Publication of this paper sponsored by Committee on Characteristics of Bituminous Materials.*

# Survey of State Highway Authorities and Asphalt Modifier Manufacturers on Performance of Asphalt Modifiers

ROBERT A. ROMINE, MAGHSOUD TAHMORESSI, R. DAVID ROWLETT, AND D. FRED MARTINEZ

One of the key objectives in the first phase of a Strategic Highway Research Program (SHRP) contract was to identify asphalt modifiers with varying levels of pavement performance. Key pavement distress categories identified by SHRP were fatigue cracking, low-temperature cracking, moisture susceptibility, permanent deformation, and aging. These modifiers will be used in the second phase to evaluate laboratory binder and mixture tests suitable for development of performance-based specifications. Information on asphalt modifiers was obtained from state highway authorities and asphalt modifier manufacturers. The questionnaire results were analyzed, and modifiers with varying levels of performance were identified. Performance ratings for the modifiers evaluated are presented for each pavement distress category.

One of the key objectives in the first phase of a Strategic Highway Research Program (SHRP) contract was to identify asphalt modifiers with varying levels of pavement performance. Key pavement distress categories identified by SHRP were fatigue cracking, low-temperature cracking, moisture susceptibility, permanent deformation, and aging. These modifiers will be used in the second phase to evaluate laboratory binder and mixture tests suitable for development of performance-based specifications. Information on asphalt modifiers was obtained from state highway authorities (SHAs) and modifier manufacturers (MFGs). Information was secured by issuing questionnaires to the SHAs and MFGs. The data gathered were organized into two categories: (a) nonperformance-related data and (b) performance-related data.

Nonperformance-related data were gathered for future use in the second and third phases of the program to assist in developing the following:

1. Cost-benefit relationships,
2. Modifier implementation guidelines, and
3. Specifications.

The primary goal of the questionnaires was to obtain data about the historical performance of modifiers. These data were further separated into three performance categories:

1. Binder test data,
2. Mixture test data, and
3. Test pavement performance data.

Center for Construction Materials Technology, Southwestern Laboratories, Houston, Tex. 77009.

Figure 1 illustrates the approach used to determine modifier performance from the analysis of questionnaire data. The selected performance-related data, the methodology used to analyze the responses, and the questionnaire results are discussed.

The SHAs returned 45 questionnaires, a 90 percent response rate. The MFGs returned 30 questionnaires, a 42 percent response rate.

## NONPERFORMANCE-RELATED DATA

The nonperformance-related inquiries on the SHA questionnaire were designed to collect information on the current uses of asphalt modifiers and to assist in projecting trends in the field.

One of the primary nonperformance-related questions was, What modifiers have been most commonly used by SHAs based on the modifier classification system presented in Table 1? Table 1 details the responses. More than half of the SHAs that responded have used some form of polymers, antistripping agents, and filler/fibers/extenders.

The second question was directed at determining the most common application of asphalt modifiers. Table 2 outlines the results. Based on these data, the construction of hot-mix asphalt concrete (HMAC) overlays is the most common use of asphalt modifiers.

The third inquiry was designed to establish why asphalt modifiers have been used. This was determined by identifying which of the key pavement distresses were expected to be improved by asphalt modifiers. The results in Table 3 indicate that all of the distresses are cited nearly equally. The nearly equal distribution of the responses is most likely because of required design criteria, regional variations in available construction materials, and variable environmental conditions.

The fourth inquiry was developed to give an indication of how modifier performance was being evaluated by SHAs. Many states are actively involved in field research projects designed to determine the long-term performance of modifiers. The responses in Table 4 indicate that detailed high-quality performance evaluations focused on long-term pavement performance are occurring throughout the SHAs.

The types of nonperformance-related data accumulated from the MFG questionnaire include the modifier's physical, chemical, and environmental characteristics; mechanism respon-

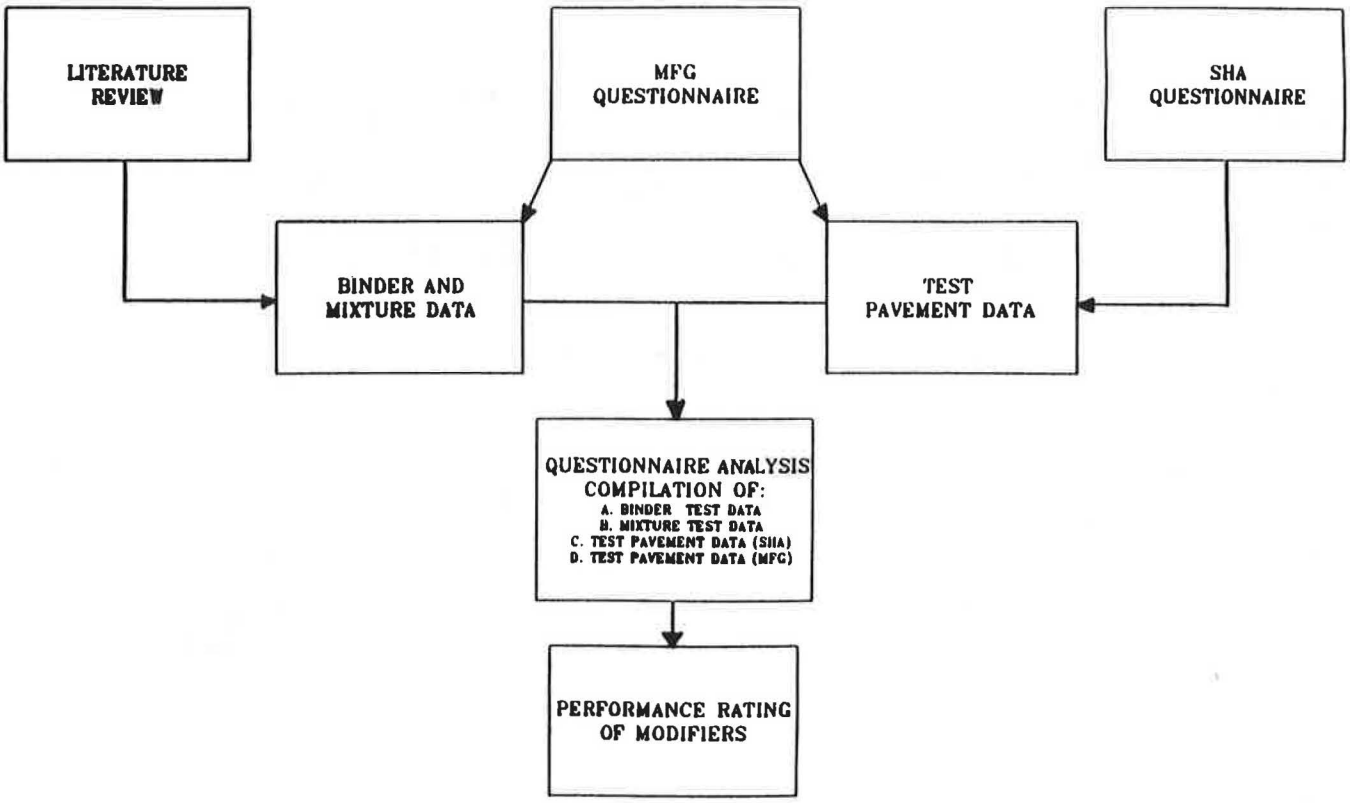


**FIGURE 1 Flow chart for questionnaire data analysis.**

TABLE 1 ANALYSIS OF SHA QUESTIONNAIRES: MODIFIERS MOST COMMONLY USED

| Modifiers | Responses (Percent) |
|---|---|
| A. Polymers | 86 |
| B. Anti-Stripping Agents | 77 |
| C. Fillers/Fibers/Extenders | 59 |
| D. Recycling Agents | 43 |
| E. Catalyst | 25 |
| F. Aging Inhibitors | 16 |
| G. Others: | |
| Ground Tire Rubber | 36 |
| Gilsonite | 9 |
| Trinidad Lake Asphalt | 7 |

TABLE 2 ANALYSIS OF SHA QUESTIONNAIRES: TYPE OF CONSTRUCTION IN WHICH MODIFIERS ARE MOST COMMONLY USED

| Type of Construction | Responses (Percent) |
|---|---|
| A. HMAC Overlays | 49 |
| B. Seal Coats | 36 |
| C. Asphalt Treated Base | 10 |
| D. Others: | |
| Open Graded Friction Course | 4 |
| Intersection Mixes | 1 |

sible for effectiveness; hot-mix production and laydown; cost analysis; and unique beneficial factors. The results from these data will assist in estimating cost-performance relationships and generating guidelines for the effective implementation of asphalt modifiers.

## PERFORMANCE-RELATED DATA

Performance-related data accumulated from the SHA questionnaire, MFG questionnaire, and a literature review were used in the modifier selection process. As described earlier,

TABLE 3 ANALYSIS OF SHA QUESTIONNAIRES: PRIMARY TARGETED PAVEMENT DISTRESS

| Distress | Responses (Percent) |
|---|---|
| A. Permanent Deformation | 24 |
| B. Fatigue Cracking | 20 |
| C. Moisture Susceptibility | 21 |
| D. Low Temperature Cracking | 20 |
| E. Aging | 15 |

TABLE 4 ANALYSIS OF SHA QUESTIONNAIRES: PERFORMANCE EVALUATION METHODS

| TPDS Responses | Responses (Percent) |
|---|---|
| Condition Survey | |
| Visual | 80 |
| Accepted Industry Method | 50 |
| (Rating Index, PCI, etc.) | |
| Method of Performance Evaluation | |
| Lab Evaluation of Cores | 71 |
| Skid Tests | 48 |
| Deflection Measurements | 43 |
| Roughness Measurements | 41 |
| Rut Depth Determinations | 16 |
| Long-Term Evaluation Program | 71 |

TABLE 5 TESTS REPORTED TO CORRELATE TO PAVEMENT PERFORMANCE USED IN MODIFIER EVALUATION PROCESS

| Distress | Binder Test | Mixture Test |
|---|---|---|
| Moisture Susceptibility | | Indirect Tensile Strength Ratio *(1)* |
| | | Immersion Compression *(2)* |
| Low Temperature Cracking | Penetration @ 4°C *(3)* | Resilient Modulus @ 4°C *(8)* |
| | Fraass Brittle Point[1] *(4)* | Creep Stiffness @ 4°C *(8)* |
| | Low Temperature Ductility *(5)* | |
| | PVN *(6,7)* | |
| Aging | Aging Index (Vis. @ 60°C) *(9)* | |
| Fatigue Cracking | Penetration @ 4°C[1] *(3)* | |
| | Asphalt Modulus[1] *(3)* | |
| | Viscosity @ 60°C *(10)* | |
| Permanent Deformation | Viscosity @ 60°C *(10)* | Resilient Modulus @ 25°C, 40°C *(11)* |
| | Penetration @ 4°C[1] *(3)* | Creep Stiffness @ 25°C, 40°C *(12)* |
| | Penetration @ 25°C[1] *(3)* | |

Note: 1. Performed on aged residue.

the accumulated data were categorized into the following performance categories:

1. Binder test data,
2. Mixture test data,
3. Test pavement performance data submitted by SHAs, and
4. Test pavement performance data submitted by MFGs.

One of the initial tasks was to determine which binder and mixture test properties correlated to pavement performance. Numerous physical, chemical, and rheological tests are used to characterize asphalt binders and mixtures. However, only a few tests have been reported to correlate with pavement performance. A literature review was performed to identify binder and mixture test results reported to correlate to field performance.

### Binder and Mixture Test Data

Table 5 provides an overview of binder and mixture tests that were reported in the literature to correlate with pavement performance (*1–11*, ASTM D175). Results from these tests reported in the questionnaires were used in the analysis.

The effect of a given modifier on the identified test result compared with that of the original asphalt was determined for the tests listed in Table 5. It was established whether the change represented a positive or negative influence on the performance of the binder or mixture.

### Test Pavement Performance Data

The most important function of the questionnaires was to secure data on the field performance of modifiers. These data were gathered from test pavement data sheets (TPDSs) contained in the questionnaires. An example of a TPDS is presented in Figure 2. Three categories of information were se-

Test Pavement Data Sheet (TPDS):

A. Location of Test Pavement:

State: _____
Highway: _____ (Example: 2 mi. West of Houston on IH-10)
Lane: _____ (Example: West bound inside lane)
Traffic Volume: ____/____ (ADT/%Trucks)
Structural Cross-section: ____/____/____ (inches HMAC/inches of base/inches of sub-base)
Date test pavement was placed: __/__/__

B. Type of modifier used in the test pavement:
Name: _____

C. Cite the methods used for the conditions survey:

[ ] None
[ ] Visual
[ ] Rating Index, PCI, etc.
[ ] Other, specify: _____

D. Date of the most recent survey: __/__/__

E. Cite the method or methods used to determine roadway performance:

| | | | |
|---|---|---|---|
| [ ] | None | [ ] | Visual |
| [ ] | Evaluation of cores | [ ] | Skid Test |
| [ ] | Deflection measurements | [ ] | Roughness measurements |

F. Is there a long-term evaluation program?

[ ] Yes, specify interval of inspection: _____ [ ] No

G. What was the apparent effect of the modifier on the following performance categories?

| | Adverse Effect | Minor Adverse | No Effect | Minor Positive | Positive Effect |
|---|---|---|---|---|---|
| Fatigue | [ ] | [ ] | [ ] | [ ] | [ ] |
| Low Temp. Cracking | [ ] | [ ] | [ ] | [ ] | [ ] |
| Permanent Deformation | [ ] | [ ] | [ ] | [ ] | [ ] |
| Aging | [ ] | [ ] | [ ] | [ ] | [ ] |
| Moisture Susceptibility | [ ] | [ ] | [ ] | [ ] | [ ] |

**FIGURE 2 Example of test pavement data sheet included in questionnaire.**

cured from the TPDS. The first category of information solicited was qualifying data, such as environment, date of placement, structural cross section, and traffic volume. This type of data aided in the interpretation of results from the modifier performance response in the TPDS. The qualifying data are represented by Item A in Figure 2.

The second type of performance data in the TPDS was used to validate the responses associated with performance. These were condition survey, date of most recent survey, method of performance evaluation, and long-term evaluation program. These are represented by Items C, D, E, and F in Figure 2.

The final type of data solicited from the TPDS was a rating of the actual performance of the test pavement. The inquiry for pavement performance is represented by Item G in Figure 2.

The performance of the pavement was determined for each TPDS submitted. The TPDS results were then collated by modifier. The results for individual modifiers were evaluated to establish a level of performance for the modifiers.

### Data Secured from SHA Questionnaires

Test pavement performance was the only performance-related data requested in the SHA questionnaires.

A total of 337 TPDS were submitted by the SHAs. A data base of SHA TPDSs containing pertinent information associated with the individual test pavements was developed using Lotus-Symphony software. The data base is organized into 11 data fields. The data may be sorted for analysis as follows:

1. Location
   - State
   - Highway
2. Placement date
3. Modifier class
4. Modifier name
5. Modifier performance
   - Fatigue
   - Low-temperature cracking
   - Permanent deformation
   - Aging
   - Moisture Susceptibility
   - Overall

Some of the 337 TPDS submitted were not used in the selection process. These TPDS were eliminated for one or more of the following reasons:

1. Modifier was used in application other than HMAC overlay construction.
2. Pavement had been in service for too short a time for an adequate evaluation of modifier performance.
3. Judgment of performance was not submitted with the TPDS and could not be established through follow-up contracts with the monitoring agency.

Of the 337 TPDSs submitted, 126 TPDSs were used in the evaluation process.

### Data Secured from MFG Questionnaires

#### *Binder and Mixture Test Data*

The results of 580 binder and mixture test results were accumulated for use in the questionnaire evaluations. A total of 254 binder and mixture test results were secured from the MFG questionnaires. This data set was complemented with an additional 326 results secured by the following:

1. Reviewing the available literature on asphalt modifiers,
2. Identifying articles with the appropriate test data, and
3. Converting the data into the format requested in the MFG questionnaires (i.e., percentage change in property).

#### *Test Pavement Performance*

A total of 195 TPDSs were submitted by the MFGs. The information from these TPDSs was organized and managed in the same manner as TPDSs submitted by the SHAs to create an MFG TPDS data base. The data organization and management was described above.

A total of 96 of the 195 MFG TPDSs submitted were used in the modifier evaluation. The remaining 99 MFG TPDSs were eliminated from the selection process for reasons stated in the discussion of the SHA TPDS.

## QUESTIONNAIRE ANALYSIS

The method for analyzing data from the questionnaires is described. The range of scores resulting from the analysis is +100 to −100. Positive scores indicate a positive influence on pavement performance. Negative scores indicate a negative influence on pavement performance.

### Determine Relative Worth of Performance Categories

The following four performance categories described earlier were used in establishing various levels of modifier performance:

1. Test pavement performance evaluations by SHAs,
2. Test pavement performance evaluations by MFGs,
3. Mixture test data, and
4. Binder test data.

Table 6 lists the relative-worth ranking assignments for each of the performance categories. The magnitude of these assigned weights was based on input from SHRP. The test pavement results reported by the SHAs were weighted highest at 40 percent for all pavement distresses except fatigue cracking, where it was weighted at 60 percent. This was done because of a lack of sufficient mixture test data for fatigue cracking

TABLE 6 RELATIVE WORTH ASSIGNED TO PERFORMANCE CATEGORIES

| PERFORMANCE CATEGORY | PAVEMENT DISTRESS | | | | |
|---|---|---|---|---|---|
| | Permanent Deformation | Fatigue Cracking | Thermal Cracking | Aging | Moisture Susceptibility |
| Binder Tests | 10 | 10 | 10 | 30 | 0 |
| Mixture Tests | 20 | (Note 1) | 20 | 0 | 30 |
| Test Pavements (SHA) | 40 | 60 | 40 | 40 | 40 |
| Test Pavements (MFG) | 30 | 30 | 30 | 30 | 30 |
| TOTAL | 100 | 100 | 100 | 100 | 100 |

Note 1: Sufficient test data was not available.

from the MFG questionnaire. The second highest weight was assigned to the test pavement results as reported by the MFGs. This category was assigned a relative worth of 30 percent for all pavement distresses.

The primary factor considered in the analysis was the effect of the modifier on pavement performance. The combined worth for test pavement performance ranged from 70 to 90 percent of the total. Because of uncontrolled variables associated with test pavements, the binder and mixture test data were assigned an appreciable relative worth because they represented a consistent and controlled source of data.

A combined relative worth of 30 percent was assigned to binder and mixture test data. It was determined that assigning this relative worth to the binder and mixture data would not mask the actual results of pavement performance.

In two cases, it was necessary to combine the relative worth of the binder and mixture test data categories. Mixture test data were eliminated from the selection process for aging because aging was primarily considered to be a binder phenomenon. However, it is recognized that air void content influences aging in asphalt mixtures. The binder category was eliminated as a performance indicator for moisture susceptibility. This phenomenon was considered to be primarily controlled by asphalt-aggregate interactions.

### Binder and Mixture Test Data Analysis

The binder and mixture test data available for the evaluation of the modifiers were sorted by individual test properties. A histogram was generated for the available test data for the individual tests.

Figure 3 is an example of a histogram illustrating the percentage change in the penetration of neat asphalts at 4°C resulting from modification with various modifiers. The horizontal axis represents the percentage change in a given property caused by the use of modifiers. The vertical axis labeled "count" represents the number of responses that fall in a given range. The second vertical axis, labeled "proportion per standard unit," is a probability density scale that represents the probability that a given response will occur in any given response range based on the theoretical distribution of the data.

The identical exercise was performed for all of the test procedures listed in Table 5. Generating histograms was the first step in the process for the numerical analysis of the binder and mixture test data.

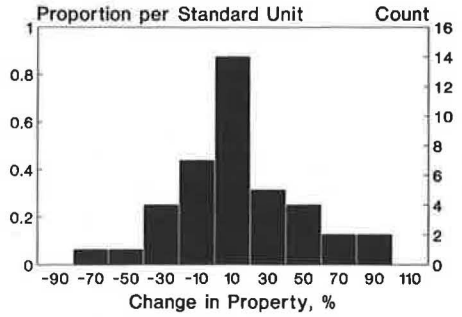


**FIGURE 3 Histogram generated for change in penetration at 4°C, as the result of modification.**

After the histograms were generated, they were reviewed to identify "natural breaks" in the data. These breaks were used to establish the boundaries of the response ranges. The response ranges were incorporated into the ranking guides. The ranking guides are score cards that were filled out from the collected data. Ranking guides were completed for all of the modifiers in each distress category. The score of the binder and mixture data sections were normalized to match the relative worths presented in Table 6.

Figure 4 is a histogram that shows the frequency distribution for percent change in penetration at 4°C as a result of asphalt modification. The histogram is divided into six areas that represent six natural breaks in the data. A decrease in penetration is represented by negative values. An increase in penetration at 4°C is reported to result in a higher susceptibility to permanent deformation (2). Therefore, a score of −8 implies that a modifier has a high susceptibility to permanent deformation. By comparison, a score of +8 implies that a modifier has an increased resistance to permanent deformation.

Three positive ranges and three negative ranges were identified. The exact score depends on the numerical value of the percent change. The ranking guides were developed from this scoring system. The section of the ranking guide for permanent deformation corresponding to penetration at 4°C is shown at the top of Figure 4. The values assigned to the response ranges are transposed into the ranking guide.

### Test Pavement Performance Data Analysis

The questions in the test pavement performance section were divided into three categories to establish the effects of a given

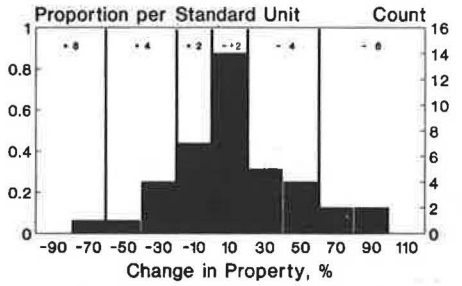


**FIGURE 4 Histogram generated for penetration at 4°C with response ranges identified.**

modifier on pavement performance. The first type of question was designed to solicit qualifying data. These questions aided in the analysis of a questionnaire respondent's judgment of the test pavement performance.

The second type of question was aimed at establishing the reliability or validity of the response. The third type of question was designed to establish an estimate of the modifier performance for each pavement distress category.

### *Questionnaire Responses Associated with Pavement Performance*

To validate the reliability of the test pavement performance response, inquiries from the questionnaires were assigned a numerical value. These values were based on the positive or negative impact of the response on the validation of the performance of the test pavement (Table 7).

Positive responses indicated that a high degree of reliability should be assigned to the pavement performance response. If all responses are positive, the total score ($S$) is 7; if all the responses are negative, corresponding to poor reliability, $S$ is $-4$.

### *Reliability Factor*

Based on the score ($S$) achieved from the validation questions, a reliability factor ($W$) was established, which corresponds to the reliability of the responses discussed above. The reliability factor was based on the following scheme:

if $-4 > S < 0$, then $W = 0.6$
if $0 > S < 3$, then $W = 0.8$
if $3 > S < 7$, then $W = 1.0$

### *Performance Responses*

In both questionnaires, questions associated with determining the influence of modifiers on pavement performance were posed. The potential responses were as follows:

| *Influence* | *Value Assigned to Levels of Performance* |
|---|---|
| No effect | 0 |
| Minor adverse effect | −1 |
| Adverse effect | −2 |
| Minor positive effect | +1 |
| Positive effect | +2 |

The numbers in the brackets represent the value assigned for quantification of the perceived levels of pavement performance. These values were regarded as uncorrected performance scores ($P$). To correct for the effects of reliability on the total ranking score for the test pavement performance, the following relationship was used:

Corrected test pavement performance score $= P \times W$

TABLE 7 VALUES ASSIGNED TO TEST PAVEMENT PERFORMANCE RESPONSES

| Question | Response | Score |
|---|---|---|
| Condition Survey? | PCI, PSI, etc. | +1 |
| | Visual | 0 |
| | None | −1 |
| Roadway Performance Evaluation Methods? | Cores | +1 |
| | Deflection | +1 |
| | Roughness | +1 |
| | Skid Test | +1 |
| | Visual | 0 |
| | None | −1 |
| Long-Term Pavement Performance Monitoring Program? | Yes | +1 |
| | No | −1 |
| Independent Agency Performs Program? | Yes | +1 |
| | No | −1 |

The result of the corrected test pavement performance score was normalized to correspond to the relative worth represented in Table 6.

### Modifier Performance Ranking

The final steps in the analysis of the individual modifiers were as follows:

1. Select the most representative response from the binder and mixture data base available for a given test property and modifier.
2. Select the most representative score from the SHA and MFG TPDSs.
3. Input these results into the ranking guides.
4. Normalize the ranking guide results to correspond to the relative worths of the performance categories listed in Table 6.
5. Compile the scores of the individual performances categories.
6. Assign a final ranking score to the modifier.

A final ranking score for permanent deformation, fatigue cracking, moisture susceptibility, aging, and low-temperature cracking for each modifier was established. Bar charts were generated from the final ranking score data. Figure 5 is an example of a typical modifier ranking chart.

It was necessary to account for the influence that nonresponses (unanswered questionnaire inquiries) had on the final ranking score of the modifiers. Nonresponses were tabulated and reported as part of the total score. Noting nonresponses helped prevent incorrect conclusions on modifier performance (for example, when the primary reason for a low score may be a lack of data). The graphical presentation of the final ranking scores shown in Figure 5 represents the relative influence individual modifiers had on pavement performance. Positive scores indicate a positive influence on pavement performance. Negative scores indicate a negative influence on pavement performance. The number of nonresponses are identified by an "X" next to the numerical score in Figure 5. Modifiers with large numbers of nonresponses were not con-

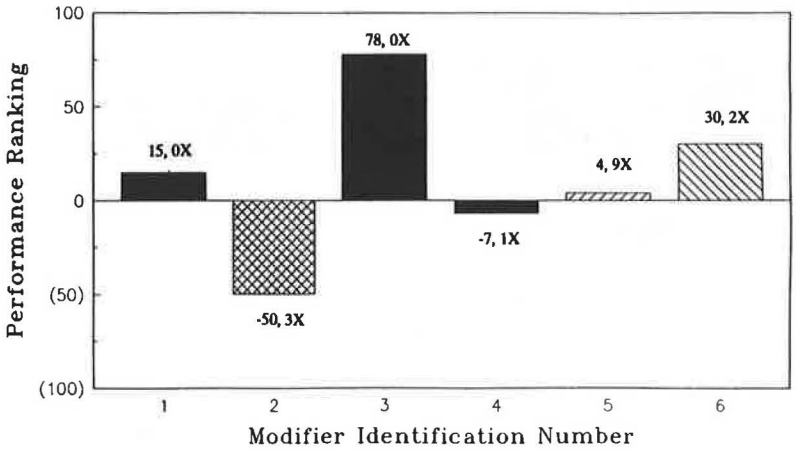


**FIGURE 5 Example of modifier ranking chart for permanent deformation.**

sidered in the questionnaire analysis because of the lack of data.

An example of the final modifier evaluation process is found in Table 8. Table 8 illustrates the steps taken to assign the final ranking score reported for Modifier No. 21 for permanent deformation. Table 8 presents the relative worth assigned to each performance category for permanent deformation and the scores received in the analysis of the data for Modifier No. 21. The final ranking score for Modifier No. 21 for permanent deformation is plotted in Figure 5 along with the other modifiers evaluated in this distress category.

Bar charts were generated ranking the modifiers in fatigue cracking, low-temperature cracking, aging, moisture susceptibility, and permanent deformation performance. Figures 6–10 illustrate the modifier performance rankings in each of the pavement distress categories based on the analysis of questionnaire data.

TABLE 8 EXAMPLE OF THE FINAL MODIFIER EVALUATION FOR MODIFIER NO. 21

| Performance Category | Relative Worth Assigned the Performance Categories for Permanent Deformation [1] | Scores for Modifier No. 21 |
|---|---|---|
| Binder Tests | 10 | 5, 0X [2] |
| Mixture Tests | 20 | 5, 2X |
| Test Pavement Data (SHA) | 40 | 25 |
| Test Pavement Data (MFG) | 30 | 34 |
| TOTAL | 100 | 69, 2X |

Note:
1. See discussion on Table 6
2. X represents number of non-responses

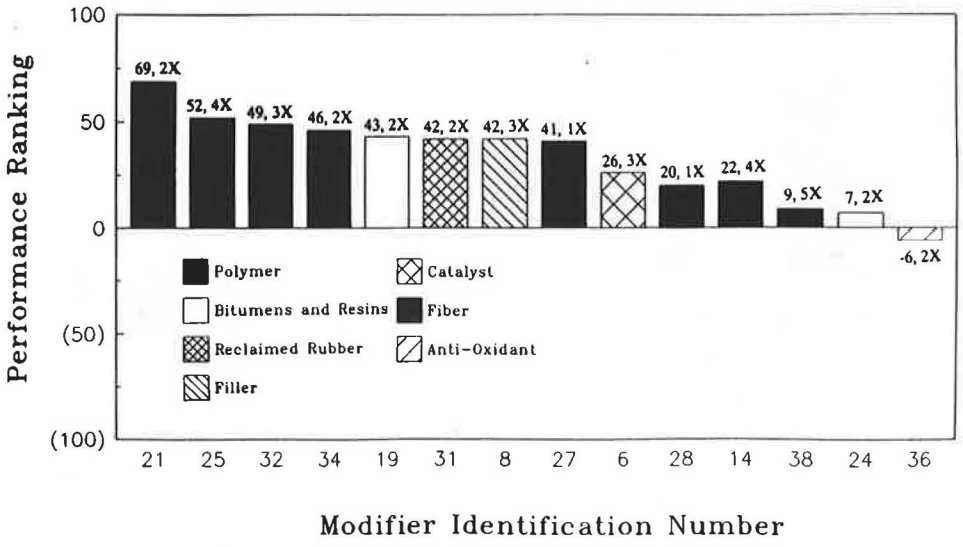


**FIGURE 6 Modifier ranking chart for permanent deformation.**

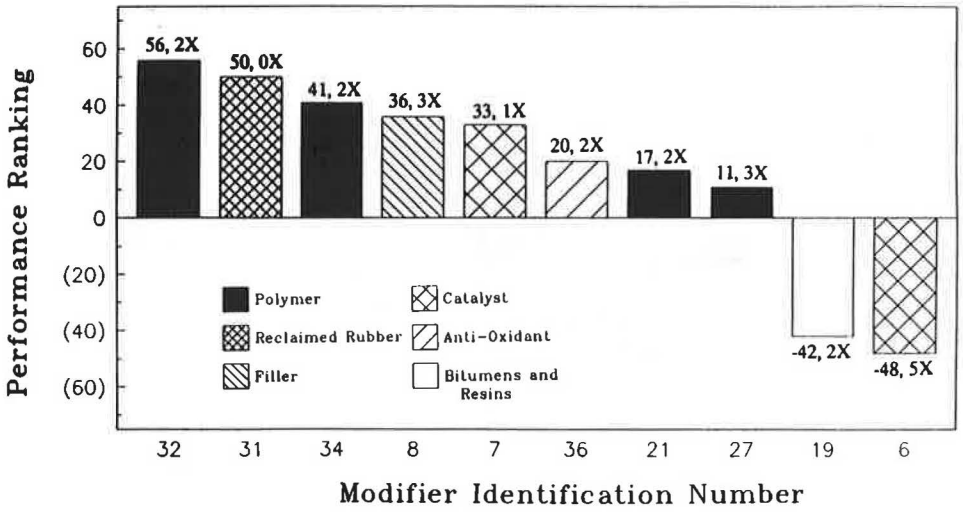


**FIGURE 7 Modifier ranking chart for low-temperature cracking.**

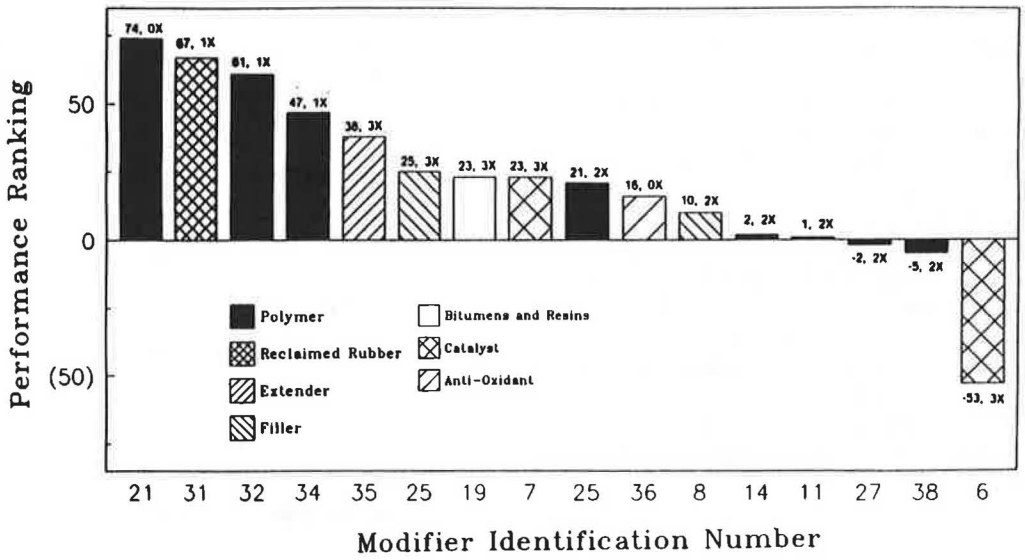


**FIGURE 8 Modifier ranking chart for fatigue cracking.**

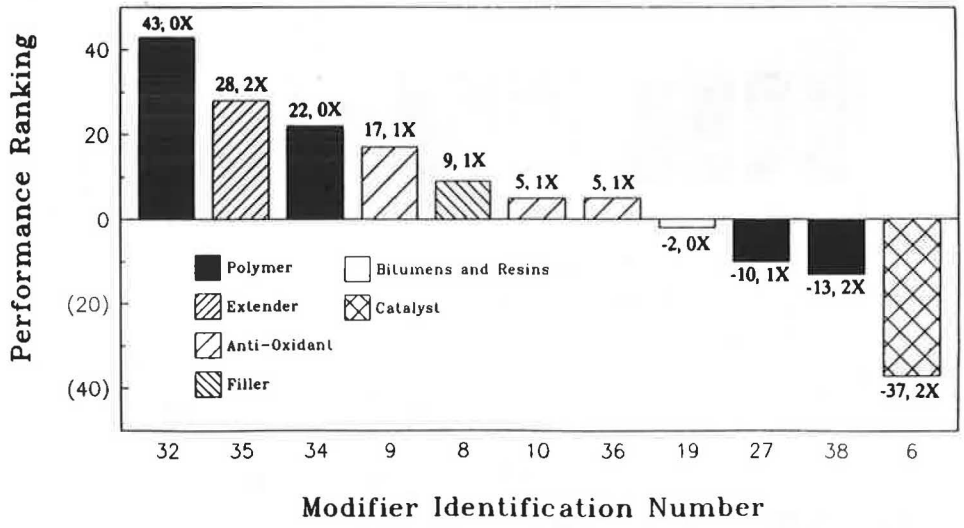


**FIGURE 9 Modifier ranking chart for aging.**

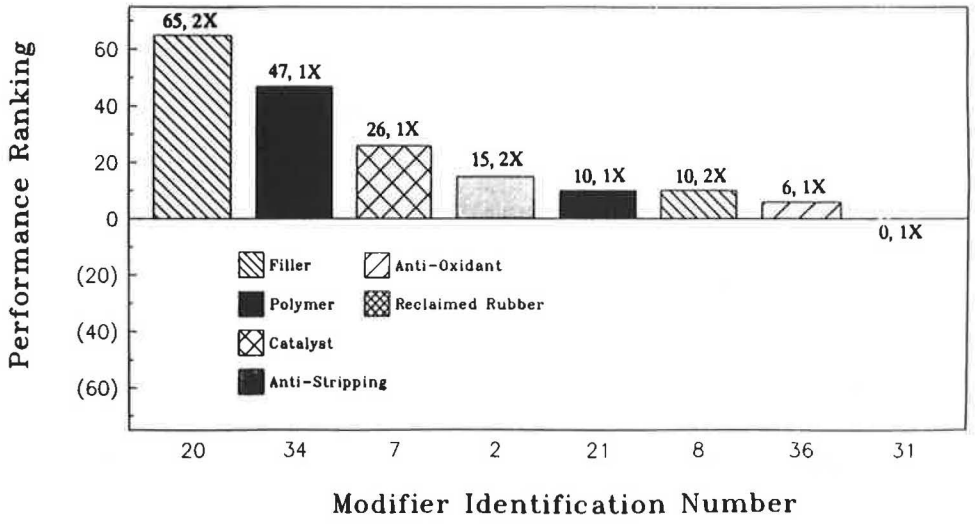


**FIGURE 10 Modifier ranking chart for moisture susceptibility.**

## CONCLUSIONS

The performance of 38 modifiers was evaluated in the questionnaire analysis. Modifiers were classified according to the system outlined in Table 9. The modifiers were assigned an identification number to assist in presenting the questionnaire results in a confidential manner.

Modifiers from the same class were identified as having extremely wide variations in their effect on pavement performance within a particular distress category. This characteristic is illustrated in Figure 8 where eight polymer modifiers were evaluated for their effect on fatigue cracking. The final ranking scores for the polymer classification ranges from 74,0X to −5,2X.

The analysis of the questionnaire data successfully identified modifiers with varying levels of performance within each pavement distress category. Modifiers with positive, negative, and no effect on performance were identified for all of the distress categories, except moisture susceptibility. In this case, only modifiers with a positive or no effect were identified.

SHRP used the questionnaire results, results from a literature survey, and its experience to make the final selection of the asphalt modifiers to be used in the project.

TABLE 9 MODIFIER CLASSIFICATION SYSTEM USED IN QUESTIONNAIRE ANALYSIS

| | |
|---|---|
| I | Polymer |
| II | Reclaimed Rubber Product |
| III | Filler |
| IV | Fiber |
| V | Extender |
| VI | Catalyst |
| VII | Anti-Oxidant |
| VIII | Bitumen and Resin |
| IX | Anti-Stripping Agent |

## ACKNOWLEDGMENT

Work described herein was supported by SHRP.

## REFERENCES

1. *Prediction of Moisture-Induced Damage to Asphalt Mixtures Using Molded Specimens*. Test Method Tex-531-C. Texas State Department of Highways and Public Transportation, Materials and Test Division, Austin, 1986.
2. J. L. Goodrich. Asphalt and Polymer Modified Asphalt Properties Related to Performance of Asphalt Concrete Mixes. *Proc., Association of Asphalt Paving Technologists*, Vol. 57, 1988, pp. 116–175.
3. J. G. Brodnyan. Use of Rheological and Other Data in Asphalt Engineering Problems. *Bulletin 192*, HRB, National Research Council, Washington, D.C., 1958.
4. P. S. Kandhal. Low Temperature Ductility in Relation to Pavement Performance, Low Temperature Properties of Bituminous Materials and Compacted Bituminous Paving Mixtures. ASTM STP 628 (C. R. Marek, ed.), 1977, pp. 95–106.
5. N. W. McLeod. Transverse Pavement Cracking Related to Hardness of Asphalt Cement. *Proc., Canadian Technical Asphalt Association*, 1968.
6. V. P. Puzinauskas. *Properties of Asphalt Cements*. Research Report 20-3, Asphalt Institute, College Park, Md., Nov. 1989.
7. R. J. Schmidt. Use of ASTM Tests to Predict Low Temperature Stiffness of Asphalt Mixes. In *Transportation Research Record 544*, TRB, National Research Council, Washington, D.C., 1975.
8. J. L. Goodrich and L. H. Dimpfl. Performance and Supply Factors to Consider in Asphalt Pavement Specifications. *Proc., Association of Asphalt Paving Technologists*, Vol. 55, 1986, pp. 57–87.
9. C. S. Hughs and G. W. Maupin. Experimental Bituminous Mixes to Minimize Pavement Rutting. *Proc., Association of Asphalt Paving Technologists*, Vol. 56, 1987, pp. 1–32.
10. T. W. Kennedy and J. Moulthrop. *Properties of Modified Asphalt-Aggregate Mixtures Involving a Metal Complex Catalyst*. Canadian Technical Asphalt Association, 1985.
11. Z. Yao and C. L. Monismith. Behavior of Asphalt Mixtures with Carbon Black Reinforcement. *Proc., Association of Asphalt Paving Technologists*, Vol. 55, 1986, pp. 564–585.

*Publication of this paper sponsored by Committee on Characteristics of Bituminous Materials.*

# Asphalt Hardening in Extraction Solvents

B. L. Burr, R. R. Davison, H. B. Jemison, C. J. Glover, and J. A. Bullin

Hardening occurs in asphalts during extraction and recovery, posing a serious problem for research into the properties of hot-mix and road-aged asphalts. Hardening appears to occur in all solvents and, to varying degrees, in all asphalts. The effects of light, oxygen, and temperature on this phenomenon were investigated. All are significant, and the data indicate that reflux methods of extraction should be avoided when the properties of the extracted material are to be investigated. The mechanism of the hardening is still unclear. Infrared spectra show definite chemical changes, but these are quite asphalt-dependent and do not relate clearly to changes in viscosity.

To study the changes that occur in asphalt as it ages during the hot-mix operation or on the road, asphalt must be extracted from the associated aggregate. Today, this is primarily accomplished by ASTM D2172 using either the centrifuge Method A or the reflux Method B.

Strong evidence exists that the present extraction and recovery methods are either inadequate or being performed improperly in the laboratories nationwide. AASHTO conducts interlaboratory proficiency tests periodically to determine the precision of the methods. It sends identical pavement samples to 50 to 100 laboratories. The laboratories extract and recover the asphalt, perform various tests, and send the results to AASHTO. In a February 1989 report, the coefficient of variance on recovered viscosities was about 25 percent. In earlier years, it has been as high as 42 percent (*1*).

Errors appear likely to stem from three main areas:

1. The solvent has some hardening effect on the asphalt that increases with temperature and time of exposure.
2. Solvent is often not completely removed from the asphalt during recovery. This results in viscosities that are lower than the true value.
3. Asphalt is not completely removed from the aggregate. The strongly adsorbed material left on the aggregate has a significantly different composition than the bulk asphalt.

## PROBLEM AREAS

It is believed that the first two areas of error may be particularly serious. Very low viscosities for recovered asphalt are most likely the result of incomplete removal of asphalt as shown by Burr et al. (*2*). The rather widespread use of ASTM D2172 Method B, even though it is known that the reflux method hardens asphalt (ASTM D1856-79), probably accounts for many high viscosity values for recovered material.

Department of Chemical Engineering and Texas Transportation Institute, Texas A&M University, College Station, Tex. 77843-3122.

### Solvent Aging

It has been known for a long time that asphalts do harden upon exposure to solvents. However, little is known about the causes or extent of solvent aging.

Abson (*3*) dissolved a 156-penetration asphalt in benzene and let it sit at room temperature for different times. The penetration was down to 147 after 24 hr and 109 after 48 hr. For this reason, he advised that the extraction-recovery process should be completed within 8 hr. He did not study the effect of different solvents, concentration, or temperature. Bussow (*4*) found that his asphalts did not age when the solvent-asphalt mixture was left in the dark. He suggested that the hardening is due to a photochemical reaction. The literature makes no other mention of this phenomenon.

Abson and Burton (*5*) tested several chlorinated solvents and showed that some induced severe aging. The worst of these was $CCl_4$. An 89-penetration asphalt was dissolved in 4 volumes of $CCl_4$ at room temperature for 2 to 4 hr before recovering. The residue had a penetration of 56. Another solvent, 1,1,1-trichloroethane, also caused severe hardening.

Abu-Elgheit et al. (*6*, p. 823) studied effects of different solvents on an asphalt's 77°F viscosity. After refluxing for 2 hr in 4 volumes of solvent, the viscosity-hardening indexes were 1.15 for benzene, 1.45 for benzene-ethanol, 1.9 for trichloroethylene (TCE), and 2.0 for 1,1,1-trichloroethane. Lottman et al. (*7*) reported a 140°F viscosity index of 1.4 for cold-extracted, Abson-recovered asphalt 16 hr after mixing with trichloroethylene. Bissett (*8*) contradicted this when he reported no aging after 7 days in trichloroethylene at room temperature. Almost certainly these results are incorrect and are affected by solvent contamination, as demonstrated by results of Noureldin and Manke (*9*). They experienced hardening after hot extraction in trichloroethylene and remedied it by reducing the recovery temperature to 311°F and time to 6 min. It is likely that they did not correct the aging that occurred in the extraction step, but corrected for it by leaving an amount of solvent that brought the penetration back to its original value. Currently, the safest way to avoid the solvent aging problem is to use a cold extraction method, as ASTM suggests.

### Objective

The purpose of this study was to quantify solvent hardening with respect to time of exposure, temperature, and concentration of dissolved asphalt. A variety of solvents, as well as a number of asphalts, were included. Extraneous variables such as dissolved oxygen and light were also investigated.

## EXPERIMENTAL METHODS

In general, asphalt was dissolved in solvent at various concentrations such as 20 g in 400 mL (5 percent) or in 800 mL (2.5 percent). These were allowed to stand for a specified period of time either at room temperature or at a controlled temperature. In most instances, the asphalt was recovered, although in some instances the solutions were injected directly into the gel permeation chromatograph (GPC).

A variety of conditions were used to assess the effect of oxygen, light, and preaging on solvent aging. In some instances the solution was deoxygenated by bubbling with $CO_2$ or $N_2$. This was either done to the solvent before dissolution or to the solution just after dissolving the asphalt. In some experiments, oxygen was bubbled through the solvent to achieve $CO_2$ saturation. In other experiments, solvents directly from the bottle were used (designated by "air"). Three levels of light were employed: dark, low hood light, and strong fluorescent light. Several experiments were performed on an Exxon AC-20 that had been air blown to 20,000 poises.

Most recoveries designated "hot" were in a roto-vap at atmospheric pressure. Those designated "cold" were under sufficient vacuum that the solvent temperature was near room temperature. The time and temperature were chosen to ensure complete solvent removal (*2*).

In the GPC analyses, a 500Å/50Å column combination was used. Tetrahydrofuran was used as a solvent with a flow rate of 1 mL/min. Injection volumes were 100 μL. The instrument was an IBM Model LC-9533 high-performance liquid chromatography- (HPLC-) equipped with a Waters refractive index detector.

Infrared analyses were made with a Nicolet 60 SX Fourier transform infrared (FT IR) single-beam spectrometer using an attenuated total reflectance method. In this procedure, the beam passes through a zinc selinide prism and is reflected from the prism-asphalt sample interface back through the prism to the detector. The asphalt is softened and spread directly on the prism surface.

The primary measure used to monitor solvent hardening was the viscosity at 60°C, ASTM D2171.

## RESULTS

It had been observed that GPC chromatograms tend to shift to larger molecular size on standing. It was thought that this might be used as a convenient solvent-aging tool. An American Petrofina AC-10 asphalt was dissolved in a variety of solvents at 7 percent by weight. Samples were aged for up to 5 days at room temperature, 50°C, and 100°C. The results were erratic, but it was clear that increasing temperature increased aging, in all solvents. Typical chromatograms at 100°C and 50°C are shown in Figures 1 and 2.

An extensive set of experiments, shown in Table 1, was conducted with a single asphalt at room temperature. A number of solvents were used, recovery was both hot and cold, and varying levels of light and oxygen exposure were studied. Viscosities at 60°C were run on the recovered asphalt and compared to the viscosity of the original asphalt. Some results for trichloroethylene and for trichloroethylene containing 15 percent ethanol are shown in Figure 3. The samples subjected to high levels of light or oxygen saturation are excluded. Except for one datum, there seems to be no effect from low light or using solvent directly from the bottle without degassing. Some rapid hardening apparently occurs in the beginning or during recovery, though with many asphalts and perhaps all tank asphalts, part of this is loss of volatiles during recovery.

Figure 4 shows the rest of the data. Prehardened asphalt still solvent hardens at about the same rate as tank asphalt. All the solvents appear about equal in hardening except $CCl_4$,

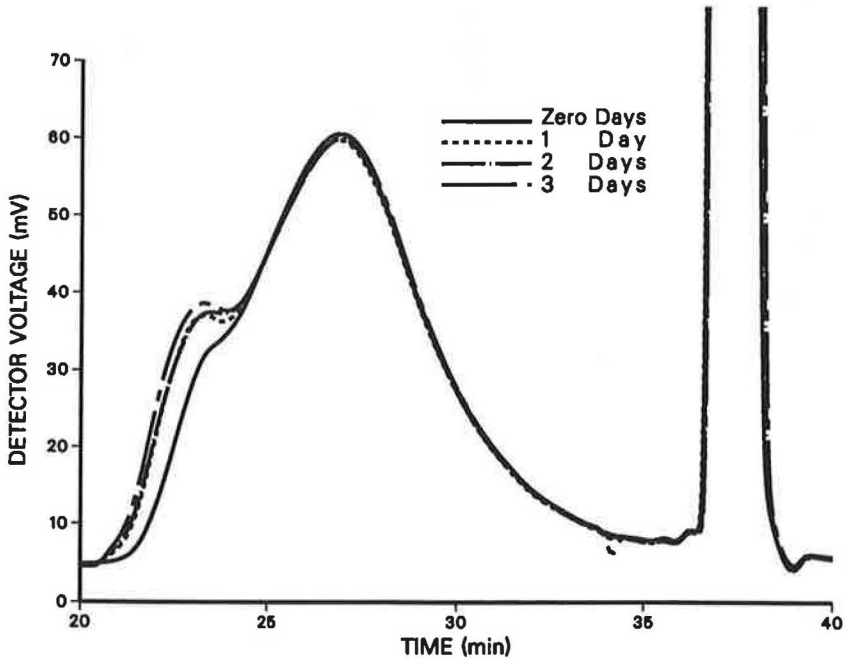


**FIGURE 1 GPC chromatograms accompanying asphalt solvent hardening: 7 percent Ampet AC-10 in toluene at 100°C.**

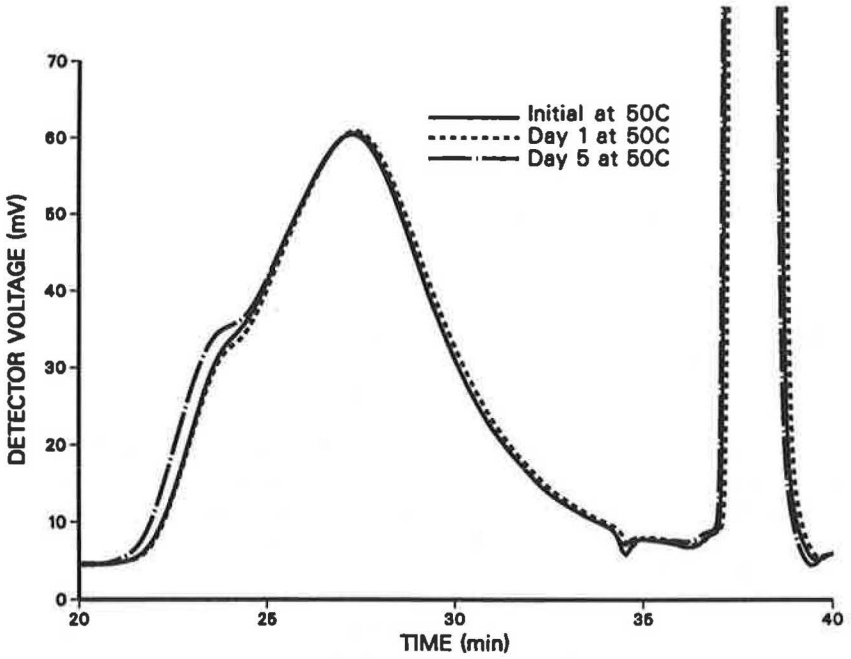


**FIGURE 2 GPC chromatograms accompanying asphalt solvent hardening: 7 percent Ampet AC-10 in toluene at 50°C.**

TABLE 1 SOLVENT HARDENING EXPERIMENTS

| | Asphalt | Solvent % Asphalt | Recovery | Gas | Light | Time(hrs) | %Diff Visc |
|---|---|---|---|---|---|---|---|
| 1 | EXXON AC-20 | TCE 5% | HOT | AIR | LOW | 96.000 | 66.900 |
| 2 | EXXON AC-20 | TCE 5% | HOT | AIR | NO | 7.000 | 21.500 |
| 3 | EXXON AC-20 | TCE 5% | HOT | AIR | NO | 20.000 | 26.800 |
| 4 | EXXON AC-20 | TCE 5% | HOT | AIR | NO | 49.000 | 34.300 |
| 5 | EXXON AC-20 | TCE 5% | HOT | AIR | NO | 116.000 | 43.400 |
| 6 | EXXON AC-20 | TCE 5% | HOT | AIR | NO | 1032.000 | 105.000 |
| 7 | EXXON AC-20 | TCE 5% | HOT | AIR | LOW | 1.000 | 18.600 |
| 8 | EXXON AC-20 | TCE 5% | HOT | AIR | LOW | 0.250 | 13.700 |
| 9 | EXXON AC-20 | TCE 5% | COLD | AIR | LOW | 0.250 | 9.800 |
| 10 | EXXON AC-20 | TCE 5% | HOT | $O_2$ | BRIGHT | 48.000 | 71.600 |
| 11 | EXXON AC-20 | TCE 5% | HOT | $N_2$ | NO | 48.000 | 37.800 |
| 12 | EXXON AC-20 | TCE 5% | COLD | $N_2$ | BRIGHT | 48.000 | 35.000 |
| 13 | EXXON AC-20 | TCE 5% | COLD | $O_2$ | NO | 48.000 | 26.000 |
| 14 | EXXON AC-20 | TCE 5% | HOT | DEGASSED | BRIGHT | 48.000 | 74.700 |
| 15 | EXXON AC-20 | TCE 5% | HOT | DEGASSED | NO | 48.000 | 39.100 |
| 16 | EXXON AC-20 | TCE 5% | HOT | $O_2$ | BRIGHT | 48.000 | 86.800 |
| 17 | EXXON AC-20 | TCE 5% | HOT | $O_2$ | NO | 48.000 | 60.900 |
| 18 | EXXON AC-20 | $CHCL_3$ 5% | HOT | AIR | LOW | 48.000 | 38.700 |
| 19 | EXXON AC-20 | $CH_2CL_2$ 5% | HOT | AIR | LOW | 48.000 | 33.000 |
| 20 | EXXON AC-20 | 111 TCE ane | HOT | AIR | LOW | 48.000 | 34.300 |
| 21 | EXXON AC-20 | TCE/ETOH | HOT | AIR | LOW | 48.000 | 34.700 |
| 22 | EXXON AC-20 | TCE 5% | HOT | AIR | NO | 48.000 | 34.300 |
| 23 | EXXON AC-20 | $CCL_4$ 5% | HOT | AIR | LOW | 48.000 | 91.200 |
| 24 | EXXON AC-20 | TOLUENE | HOT | AIR | LOW | 48.000 | 36.900 |
| 25 | EXXON AC-20 | 12 DCE | HOT | AIR | LOW | 48.000 | 39.600 |
| 26 | EXXON AC-20 | TCE/ETOH | HOT | AIR | NO | 0.250 | 10.800 |
| 27 | EXXON AC-20 | TCE/ETOH | HOT | AIR | NO | 1.300 | 15.700 |
| 28 | EXXON AC-20 | TCE/ETOH | HOT | AIR | NO | 4.750 | 20.100 |
| 29 | EXXON AC-20 | TCE/ETOH | HOT | AIR | NO | 6.670 | 17.800 |
| 30 | EXXON 20kP | TCE 5% | HOT | AIR | NO | 69.000 | 45.200 |
| 31 | EXXON 20kP | TCE 2.5% | HOT | AIR | LOW | 0.250 | 17.200 |
| 32 | EXXON 20kP | TCE 2.5% | COLD | AIR | LOW | 0.250 | 7.990 |
| 33 | EXXON 20kP | TCE 5% | COLD | AIR | LOW | 0.250 | 17.700 |

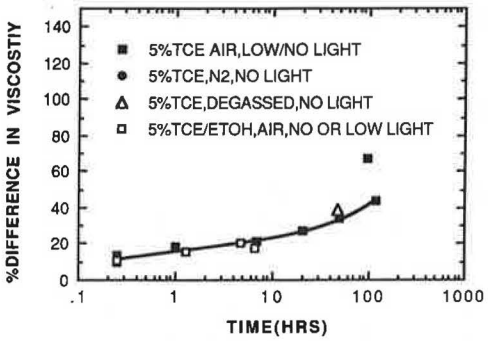


**FIGURE 3 Solvent Hardening (60°C viscosity increases): 5 percent asphalt in trichloroethylene without oxygen or strong light.**

which causes much greater hardening. As would be expected, some of the oxygen-containing samples hardened considerably. Light also seems to accelerate hardening both with and without oxygen. However, Runs 12 and 13 appear inconsistent. There is no proof here that cold recovery under vacuum reduces aging, but it appears logical and needs further study.

The next set of experiments used a single asphalt from the core asphalts of the Strategic Highway Research Program (SHRP) to investigate the effect of asphalt concentration on solvent aging. In addition, the effect of degassing was further explored, and one experiment was conducted at 0°C. Also, a direct comparison is made between the hardening properties of trichloroethylene/15 percent ethanol and toluene/15 percent ethanol.

The solvent aging (hardening index, viscosity at 60°C) results for 48-hr incubation times for SHRP asphalt AAK-1 (Boscan) in a variety of solvent systems and over a range of concentration are shown in Figure 5. For comparison, a result is shown that was obtained at an AAK-1 asphalt concentration of 0.05 g/mL in trichloroethylene/ethanol with zero incubation time. This point is actually three experiments that produced exactly the same result, approximately 11 percent hardening. All other steps of the procedure followed were the same. Based on our results for other asphalts, this is a normal amount of hardening, apparently due to volatiles loss from the virgin or unaged materials.

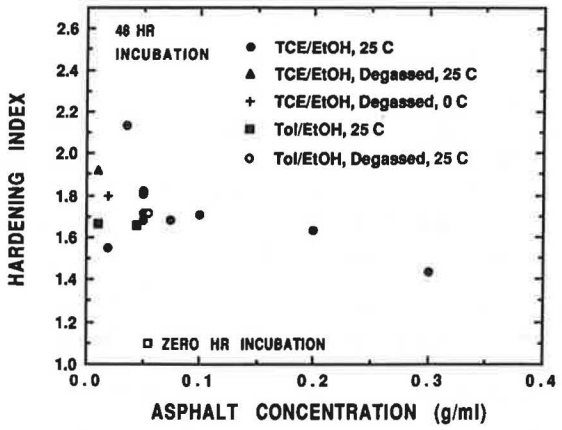


**FIGURE 5 Solvent aging of asphalt AAK-1 in dilute solution.**

The trichloroethylene/15 percent ethanol solvent systems showed gradually increasing hardening with decreasing asphalt concentration over the range of asphalt concentration up to 0.3 g/mL. The increase with decreasing concentration was not great, however; the total range in hardening index rose from about 1.45 to about 1.8. However, the low concentrations may be less reproducible than the higher concentrations. The degree of hardening for the 48-hr incubation time is very significant, much greater than that attributed to volatiles loss.

The comparisons between trichloroethylene/ethanol and toluene/ethanol were made at an asphalt concentration of 0.05 g/mL and at 0.01 g/mL. No significant difference between the toluene system and the trichloroethylene system is observed for these two experiments. The solutions degassed before incubation show no difference from those that were not degassed. Also, the solution that was incubated at 0°C rather than at 25°C shows no difference. These results are somewhat puzzling.

It is interesting to speculate as to what this reveals about the mechanism of solvent hardening. Figures 1 and 2 show that solvent hardening is accompanied by an increase in large molecular size material. If this occurs from multibody collisions, one would expect the hardening to decrease with concentration, but Figure 5 suggests the opposite.

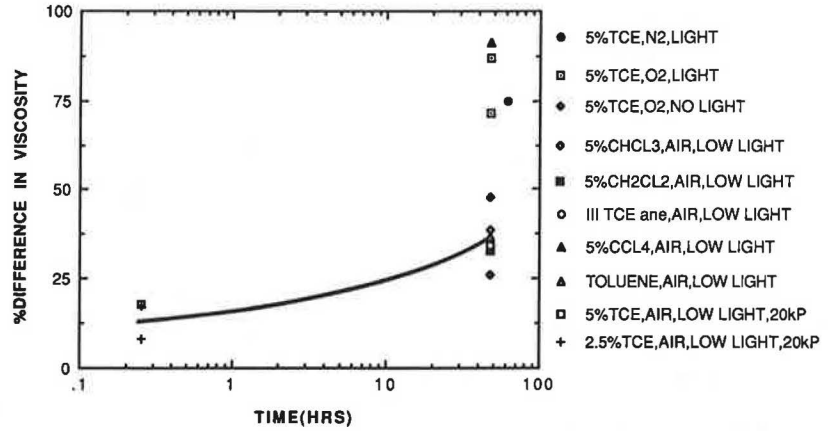


**FIGURE 4 Solvent hardening in various solvents and the effect of oxygen and strong light.**

Figure 6 shows the large molecular size (LMS) region (defined as the fraction of the chromatograph area that elutes before 25 min) plotted as a function of asphalt concentration in tetrahydrofuran. A large number of asphalts were analyzed in this way, and all but the one, which has no asphaltenes, showed the positive slope as in Figure 6. The samples were run immediately following dissolution, so little solvent hardening has occurred. Figure 6 indicates a partial dissociation of LMS material to be occurring at high dilution that evidently increases the reactivity of this material but tells us nothing of the nature of the reactions.

Solvent hardening appears to occur to roughly the same degree in most solvents, so it is not a reaction between asphalt and solvent. It also occurs with all asphalts that have been investigated and is much more asphalt- than solvent-dependent. Figure 7 shows solvent hardening versus time for three asphalts. The contact was in trichloroethylene/15 percent ethanol at room temperature in the dark in contact with air followed by cold recovery. Again aging is rapid in the beginning, partly because of volatiles loss during recovery, and then the effect slows gradually with time. Most significant, however, is the much more rapid hardening of the California Coastal asphalt.

In the next set of experiments, all the SHRP asphalts were hardened for 48 hr in trichloroethylene/15 percent ethanol and toluene/15 percent ethanol at room temperature in the dark in contact with air and cold recovered. Another identical set was recovered immediately. The results are shown in Figure 8, plotted versus SHRP (*10*) values for thin film oven (TFO) aging. The correlation coefficients are $r^2$ = .65 for trichloroethylene, .32 for toluene, and .097 for the instant recovery. Obviously, there is no apparent relation between initial solvent hardening and TFO aging, which is hardly surprising as this includes volatiles loss on recovery. Although there is considerable scatter, it appears that for most of these asphalts a relation exists between solvent and oxidative hardening. If it were not for two very low data for toluene, the correlations would be indistinguishable. Actually, one might expect somewhat lower hardening in toluene because it is a poorer solvent that leads to more aggregation or association in solution (*11,12*, p. 240).

Although solvent aging and oxidative aging must be by different mechanism, they may both be affected by some inherent reactivity of a given asphalt. To further explore the solvent aging mechanism, infrared spectra were run on the SHRP asphalts and a number of others, some of which had been subjected to light and oxygen. It has already been shown above that light and oxygen accelerate solvent hardening; furthermore, infrared changes accompany this hardening and are similar to those observed for oxidative oven aging.

The spectra of asphalts aged in the absence of light and oxygen corresponding to the asphalt aging in Figure 8 are far more interesting. Five of these are shown in Figures 9–13. On each figure, the spectra before and after hardening are shown. The results raise more questions than they answer. For instance, for asphalt AAA-1, Figure 9 shows almost no change in infrared but has a viscosity increase of 52 percent. Asphalt AAC-1 (Figure 10) hardened an almost identical 53 percent but shows a rise in the spectrum over a broad width. Asphalt AAG-1 (Figure 11) also hardened 50 percent but shows a spectral change similar to that of slight oxidative aging, that is, an increase in the carbonyl area at 1,700 and the sulfoxide region at 1,030. Asphalt AAK-1 (Figure 12) hardened 77 percent and shows a spectral change different from the above. The carbonyl area is shifted to about 1,735 and a distinct area appears at about 1,270. These bands correspond well to cyclic anhydrides or certain esters. Asphalt AAD-1 (Figure 13), on the other hand, shows a large change

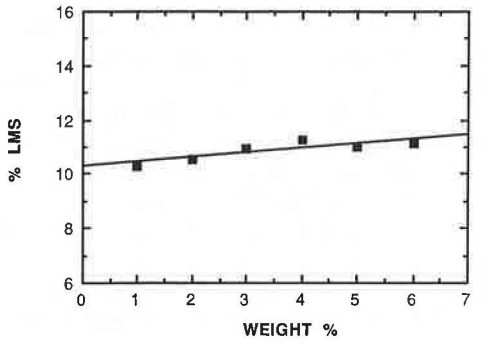


**FIGURE 6 GPC percent LMS versus concentration for 1989 Exxon AC-20.**

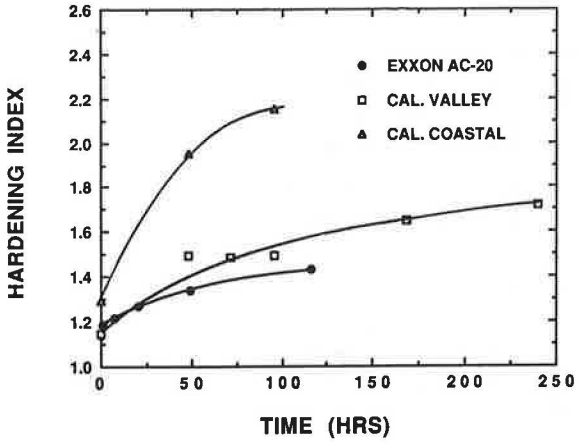


**FIGURE 7 Effects of time on solvent hardening of various asphalts at 5 percent in trichloroethylene/ethanol solutions at 25°C.**

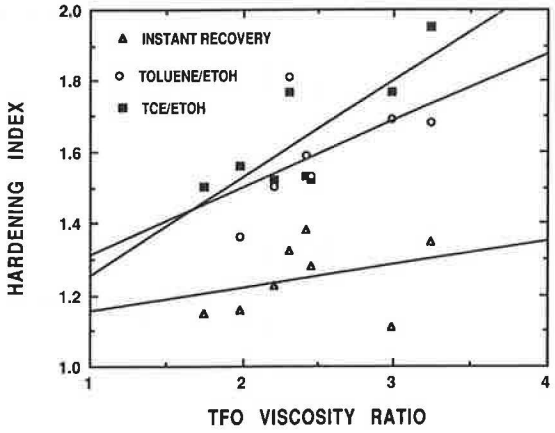


**FIGURE 8 Comparison of SHRP asphalt's solvent aging and volatiles loss hardening to TFO aging.**

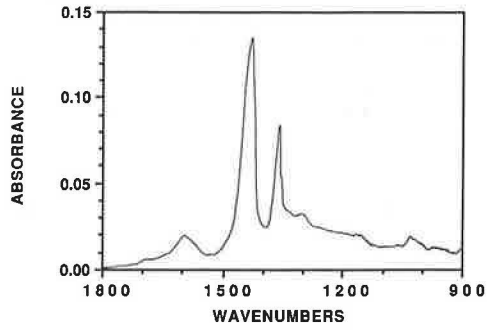


**FIGURE 9 IR spectrum of SHRP AAA-1 asphalt aged at 5 percent in trichloroethylene/ethanol for 2 days at 25°C.**

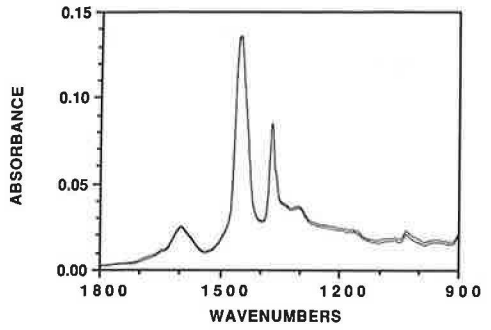


**FIGURE 10 IR spectrum of SHRP AAC-1 asphalt aged at 5 percent in trichloroethylene/ethanol for 2 days at 25°C.**

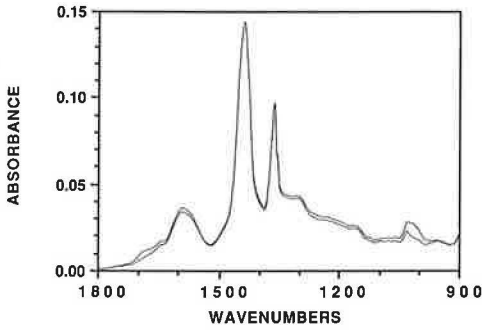


**FIGURE 11 IR spectrum of SHRP AAG-1 asphalt aged at 5 percent in trichloroethylene/ethanol for 2 days at 25°C.**

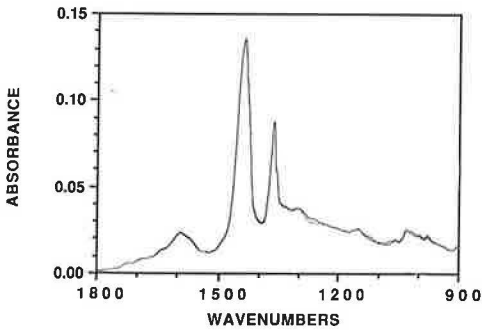


**FIGURE 12 IR spectrum of SHRP AAK-1 asphalt aged at 5 percent in trichloroethylene/ethanol for 2 days at 25°C.**

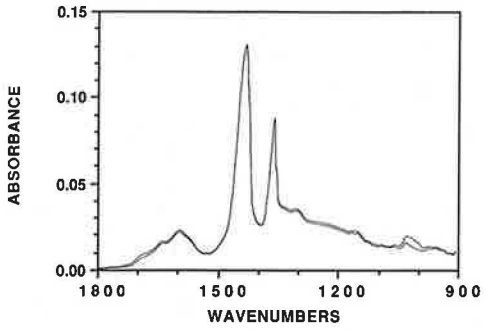


**FIGURE 13 IR spectrum of SHRP AAD-1 asphalt aged at 5 percent in trichloroethylene/ethanol for 2 days at 25°C.**

all across the spectrum and also exhibited the greatest viscosity change of 95 percent.

Chemical changes occur in most but not all asphalts during solvent hardening, and the changes vary with the asphalt. No obvious relation between these chemical changes and the viscosity change is yet evident. The only consistent datum is that the large infrared spectrum change did occur in the most hardened asphalt.

## CONCLUSIONS

Solvent aging appears to occur in all solvents and is, to some extent, unavoidable when extracting asphalt from aggregate. It is definitely a concern when the asphalt is being extracted for a study of properties. It can be minimized by using cold extraction and completing recovery of the resulting solutions as rapidly as possible.

The mechanism is still unclear and is worthy of further study. Like oxidative aging, it involves changes that increase the fraction of large molecular size material, but the mechanism must be quite different, as it occurs in the absence of oxygen, but sensitivity by an asphalt to one seems to correlate with sensitivity to the other. The infrared spectra indicate chemical changes occur, but unlike oxidative hardening, the species formed vary from asphalt to asphalt and do not seem to be related necessarily to the hardening process.

## ACKNOWLEDGMENTS

Support for this work by the Texas State Department of Highways and Public Transportation, in cooperation with FHWA, and by SHRP is gratefully acknowledged. Helpful discussions with Don O'Connor and Darren Hazlett and the technical contributions of Ana Laura G. Kyle are greatly appreciated.

## REFERENCES

1. *AASHTO Materials Reference Laboratory Report for Bituminous Concrete Proficiency Samples*. Reports from 1987, 1988, 1989 tests. National Bureau of Standards, Gaithersburg, Md.
2. B. L. Burr, R. R. Davison, C. J. Glover, and J. A. Bullin. Solvent Removal from Asphalt. In *Transportation Research Record 1269*, TRB, National Research Council, Washington, D.C., 1990.

3. G. Abson. Method and Apparatus for the Recovery of Asphalt. *Proc., ASTM II*, 1933, pp. 704–714.
4. C. Bussow. Notes on a Method of Recovering Bitumen from Paving Materials. *Proc., Association of Asphalt Paving Technologists*, Vol. 7, 1936, pp. 160–164.
5. G. Abson and C. Burton. The Use of Chlorinated Solvents in the Abson Recovery Method. *Proc., Association of Asphalt Paving Technologists*, 29, 1960, pp. 246–252.
6. M. A. Abu-Elgheit, C. K. Hancock, and R. N. Traxler. Effect of Selected Solvents on the Viscosities and Oxygen Contents of Asphalts. *Analytical Chemistry*, 41, May 1969.
7. R. P. Lottman, S. K. Sonawala, and M. Al-Haboobi. Change of Asphalt Viscosity During Mixing with Hot Aggregates. *Proc., Association of Asphalt Paving Technologists*, Vol. 32, 1963, pp. 1–36.
8. J. R. Bissett. Changes in Physical Properties of Asphalt Pavement with Time. *Bulletin 41*, HRB, National Research Council, Washington, D.C., 1962, pp. 211–220.
9. M. S. Noureldin and P. G. Manke. Study of Transverse Cracking in Flexible Highway Pavements in Oklahoma. In *Transportation Research Record 695*, TRB, National Research Council, Washington, D.C., 1978, pp. 28–32.
10. *Properties of Materials Reference Library Asphalt Cements*, Strategic Highway Research Program, National Research Council, Washington, D.C., 1990.
11. G. R. Donaldson, J. A. Bullin, R. R. Davison, C. J. Glover, and M. W. Hlavinka. The Use of Toluene as a Carrier Solvent for Gel-Permeation Chromatography Analysis of Asphalt. *Journal of Liquid Chromatography*, Vol. 11, 1988, pp. 749–765.
12. K. H. Altgelt and O. L. Harle. The Effect of Asphaltenes on Asphalt Viscosity. *Industrial and Engineering Chemistry Product Research and Development*, Vol. 14, 1975.



*Publication of this paper sponsored by Committee on Characteristics of Bituminous Materials.*

# Evaluation of Standard Oven Tests for Hot-Mix Plant Aging

H. B. JEMISON, R. R. DAVISON, C. J. GLOVER, AND J. A. BULLIN

The thin film oven test and the rolling thin film oven test are widely used to simulate the asphalt hardening that occurs in hot-mix plants. Using nine road-collected hot-mix samples and the corresponding tank asphalts, a comparison is made between the oven tests and the hot mix. Comparisons are made on the basis of viscosity at 60°C and 135°C, penetration at 25°C, infrared analysis, and gel permeation chromatography. In general, the two oven tests are in close agreement for all parameters at standard test times. However, if the times are extended, they may diverge. The recovered hot-mix asphalt is generally more aged than the oven-aged material with respect to all parameters although less so with viscosity. The infrared spectra show much greater change in the hot-mix than in the oven-aged material. The hot-mix operation also produces highly oxidized material that is not usually removed from the aggregate in the extraction operation.

When hot asphalt and aggregate are combined in a hot-mix plant, considerable hardening occurs in the asphaltic material. Some of this is caused by a loss of volatile components, but the greater part is the result of oxidation. As the degree of hardening occurring in the hot-mix plant is an important property of asphalt, a number of tests have been devised to simulate this effect. By far the most commonly used are the thin film oven test (TFOT), ASTM D1754, and the rolling thin film oven test (RTFOT), ASTM D2872. The TFOT was designed by Lewis and Welborn (*1*, p. 14) and requires 5 hr. In 1963, Hveem et al. (*2*, p. 271) developed the RTFOT, which cut the time to 75 min and was designed to give results similar to the TFOT. On the basis of viscosity changes, these tests are generally in close agreement. Attempts to relate any test to hot-mix results are often marred by incomplete solvent removal and solvent hardening (*3*) and further complicated by hot-mix plant variability. Considering the variability in hot-mix plant operations, these tests probably reproduce viscosity changes reasonably well. Yet, it was noted many years ago (*4*) that this does not guarantee that what actually occurs in the hot-mix plant from a chemical standpoint is being simulated by the oven test.

Recently, Glover et al. (*5*), in a preliminary study, presented data on two asphalts indicating agreement between the two oven tests but divergence between the oven test asphalts and hot-mix asphalts, particularly with respect to infrared spectra. Chollar et al. (*6*) in a comparison of batch and drum plants also indicate greater hardening in hot-mix plants than usually occurs in oven tests. An ideal simulation should reproduce actual plant changes in every respect as closely as possible. To evaluate the oven tests as hot-mix plant simulators, a variety of chemical and physical parameters for comparing extracted hot-mix and the corresponding oven-aged tank asphalts were employed.

Department of Chemical Engineering and the Texas Transportation Institute, Texas A&M University, College Station, Tex. 77843-3122.

## OBJECTIVE

The objective of this study was to evaluate a more extensive and diverse set of asphalts than the earlier study of Glover et al. (*5*), thereby providing a better picture of the comparisons between the hot-mix and oven-aged materials.

## EXPERIMENTAL DESIGN AND METHODS

Hot-mix samples were obtained along with the corresponding tank asphalts from nine plants, of which two were batch plants and seven drum plants. Six separate suppliers were represented, but the two asphalts designated "Cosden" are plainly from different sources.

The hot-mix asphalt samples were extracted from the aggregate using a modified ASTM D2172 Method A. The asphalt was recovered from the solvent using a modified ASTM D1856. Both of these procedures are described in Davison et al. (*3*); the recovery procedure is also described in Burr et al. (*7*). It has been shown using gel permeation chromatography (GPC) that the standard recovery procedure often failed to remove all the solvent. Time and temperature were increased to ensure complete removal and then confirmed by GPC. The major modification of the extraction procedure was to add 15 percent ethanol by volume to trichloroethylene. This considerably enhances removal of the last few percent of the asphalt. Agitation of the material was also increased, and care was taken to finish the entire extraction and recovery in 8 hr to minimize solvent hardening of the recovered material. Furthermore, filtration of the recovered solution with $<5$ μm filter paper was performed to remove residual fines material. In some cases, additional, very-hard-to-remove material was obtained by further agitation and soaking of the aggregate with a trichloroethylene/ethanol (15 percent) mixture for 2 days. This material was filtered, recovered, and analyzed separately from the material of the primary extraction.

The TFOT and RTFOT were performed on all tank asphalts. These tests were also run at extended times of 14.5 hr for the TFOT (ETFOT) and 3.5 hr for the RTFOT (ERTFOT). The tank and oven-aged asphalts provided a range in which the extracted hot mix would fall and give an indication of the ability of oven tests to predict the chemical and physical properties of the hot mix.

Penetrations (ASTM D5) and viscosities (ASTM D2171) at 140°F and 275°F were run on all samples of tank, oven-aged, and hot-mix asphalts. The samples were also analyzed chemically by GPC and Fourier transform infrared (FTIR) spectroscopy. GPC chromatograms give a molecular size distribution, and FTIR shows the presence of certain chemical groups.

In this work, an IBM LC-9533 liquid chromatograph with a refractive index detector was used in the GPC analyses. Tetrahydrofuran at 1 mL/min was used as the solvent. A 500Å/50Å column combination was used. The injected volume was 100 μL, and the asphalt concentration was 7 percent. The percent large molecular size (LMS), as suggested by Jennings (*8*), was used to characterize each asphalt, and in this work it was defined as the fraction of the chromatogram area between 20 and 25 min.

The infrared analyses were made with a Nicolet 60 SX FTIR single-beam spectrometer using an attenuated total reflectance method (*9*). In this procedure, the asphalt is coated on a zinc selenide prism. The infrared beam passes into and through the prism and is reflected at the sample interface surface back to the detector.

The area under the carbonyl peak around a wave number of 1700 $cm^{-1}$ was used to characterize each asphalt. The height at 1820 $cm^{-1}$ was arbitrarily chosen as the base and the carbonyl peak area was the area above this level from 1820 to 1650 $cm^{-1}$. Hard-to-remove material was obtained for analysis by allowing the previously extracted hot mix to soak in trichloroethylene/15 percent ethanol overnight and then evaporating the solvent.

## RESULTS

The complete experimental results are given in Table 1 along with calculated viscosity-temperature susceptibility (VTS). The times for the two extended tests were chosen because they both approximately doubled the increase in viscosity for a particular asphalt relative to the standard test. It is interesting that, although the viscosities resulting from the two tests are in approximate agreement for the standard times, at the extended times there is close agreement for some asphalts and wide divergence for others.

Chromatograms obtained from the GPC show the shifts in molecular size associated with the oxidative aging of the asphalt. The average molecular size increases with aging, resulting in an increase of the percentage of LMS (Table 1). Some hot-mix samples gave chromatograms that not only differ in molecular size, but also show significantly different shapes. This can not be easily explained, and apparently no amount of oven aging can reproduce the shapes of some hot mixes.

The spectra obtained from the FTIR indicate a definite increase in carbonyl absorption with oxidative aging (Table 1). Changes also occur in other regions representing increases in carbon-oxygen bonds. The sulfoxide absorbance area at a wave number of 1030 $cm^{-1}$ is of interest, but it could be masked by the presence of micron-size dust and aggregate particles whose silicon oxide bands absorb at approximately the same location. This could be the cause of the radically different absorbance of some hot mixes in the sulfoxide region compared with the oven tests. Throughout the rest of the spectrum, however, the changes in chemical compositions attributed to the hot-mix procedure seemed to be proportional to the changes resulting in the oven tests. Using the parameters given in Table 1, a comparison is made between the TFOT and the RTFOT and then between these tests and the hot-mix results.

### Oven Test Comparisons

The two oven tests are similar in design and the temperatures are identical. The RTFOT yields a more homogeneous product than the TFOT because of its constantly renewed surface. The exposure times of the tests differ significantly; the RTFOT's shorter time is generally more desirable. Because these methods were designed to accomplish the identical task of simulating the changes of asphalt properties occurring during the hot-mix process, they would be expected to produce at least similar outputs with identical inputs.

The data in Table 1 and Figures 1–6 show that the TFOT and RTFOT chemical and physical properties are indeed comparable. The diagonal lines represent lines of equality on each plot. The plots of the viscosities at 275°F (135°C), the percentage LMS, the penetration values, and the viscosities at 140°F (60°C) (Figures 1, 2, 3, and 4, respectively) appear to characterize the RTFOT as being a slightly more severe aging test. These differences are small, however, and the carbonyl area and the VTS values shown in Figures 5 and 6 indicate that one test could not be considered different from the other.

Examples of GPC and FTIR may be seen in Figures 7 and 8. Figure 7 shows the identical GPCs for the two oven tests with Ampet AC-20. Figure 8 exhibits almost identical infrared spectra for both tests with the Cosden AC-10.

Considering the inherent error in the oven tests and analysis techniques, and the variability of asphalt samples, the apparent differences between the two oven tests are small and probably insignificant. Indeed, their possible subtle differences do not warrant the use of both tests. Therefore, it is concluded that the TFOT and RTFOT methods are interchangeable and cannot be considered independent.

### Hot-Mix and Oven Test Comparisons

For many years, the TFOT and RTFOT have been used to simulate and predict the chemical and physical changes of asphalt during the hot-mix process. Many factors during plant operation and in sample handling can complicate the comparison, however. Examples of these include solvent aging and insufficient removal of the asphalt from the aggregate during the extraction, as well as incomplete solvent removal and volatiles loss during the recovery. Other variables arise at the hot-mix plant such as different hot-mix plant types, fuels, and operating conditions.

The same parameters that were used to compare the oven tests are used to investigate the hot-mix performance. The hot-mix data are considerably more scattered because, at least in part, of the previously mentioned error contributions. Figures 9–14 show that the hot-mix and oven test data do not show nearly as good agreement as the two oven test comparisons exhibit.

TABLE 1 PROPERTIES OF HOT-MIX STUDY ASPHALTS

| Names | Asphalts | Penetration | Viscosity @ 60°C | Viscosity @ 135°C | %LMS | Carbonyl | VTS |
|---|---|---|---|---|---|---|---|
| AMPET AC-20 | Tank | 69.7 | 1835 | 3.91 | 15.7 | 0.392 | 3.49 |
| 1989 | RTFOT | 47.3 | 3287 | 4.58 | 18.2 | 0.445 | 3.59 |
| Batch | TFOT | 47.9 | 3100 | 4.61 | 18.0 | 0.493 | 3.56 |
| | Hot Mix | 28.7 | 4792 | 5.75 | 20.0 | 0.703 | 3.56 |
| | ERTFOT | 35.0 | 5437 | 5.60 | 20.8 | 0.553 | 3.62 |
| | ETFOT | 29.7 | 7533 | 6.73 | 22.0 | 0.695 | 3.60 |
| COASTAL | Tank | 57.7 | 1998 | 4.19 | 19.4 | 0.522 | 3.47 |
| AC-20 1987 | RTFOT | 39.2 | 5722 | 6.58 | 23.2 | 0.607 | 3.52 |
| | TFOT | 41.1 | 5374 | 6.33 | 22.0 | 0.614 | 3.52 |
| | Hot Mix | 32.1 | 9227 | 6.83 | 26.2 | 0.763 | 3.66 |
| | ERTFOT | 29.5 | 15644 | 12.05 | 25.8 | 0.739 | 3.44 |
| | ETFOT | 27.1 | 27095 | 9.64 | 26.5 | 0.828 | 3.78 |
| COSDEN | Tank | 89.0 | 970 | 2.61 | 11.4 | 0.364 | 3.57 |
| AC-10 1989 | RTFOT | 47.0 | 2571 | 3.33 | 15.2 | 0.488 | 3.76 |
| | TFOT | 50.7 | 2193 | 3.18 | 14.3 | 0.462 | 3.73 |
| | Hot Mix | 27.5 | 9854 | 4.40 | 19.7 | 0.894 | 4.03 |
| | ERTFOT | 27.0 | 7442 | 6.39 | 19.1 | 0.679 | 3.64 |
| | ETFOT | 29.0 | 7078 | 4.94 | 18.6 | 0.773 | 3.82 |
| COSDEN | Tank | 76.7 | 2061 | 3.85 | 26.3 | 0.497 | 3.55 |
| AC-20 1989 | RTFOT | 46.0 | 5763 | 5.96 | 29.6 | 0.624 | 3.60 |
| | TFOT | 50.5 | 4695 | 5.25 | 28.6 | 0.605 | 3.62 |
| | Hot Mix | 47.0 | 5945 | 4.98 | 29.7 | 0.751 | 3.75 |
| | ERTFOT | 33.2 | 12533 | 7.94 | 32.5 | 0.788 | 3.66 |
| | ETFOT | 32.7 | 16620 | 8.80 | 32.8 | 0.793 | 3.68 |
| EXXON | Tank | 61.2 | 1974 | 3.64 | 13.4 | 0.450 | 3.58 |
| AC-20 1987 | RTFOT | 38.8 | 4372 | 4.91 | 15.9 | 0.544 | 3.64 |
| | TFOT | 38.0 | 4195 | 5.02 | 15.2 | 0.552 | 3.61 |
| | Hot Mix | 45.9 | 3304 | 4.13 | 18.3 | 0.571 | 3.68 |
| | ERTFOT | 26.4 | 8539 | 6.58 | 18.5 | 0.641 | 3.66 |
| | ETFOT | 23.5 | 11347 | 7.82 | 19.6 | 0.760 | 3.64 |
| EXXON | Tank | 62.8 | 1809 | 3.12 | 10.9 | 0.377 | 3.67 |
| AC-20 1987 | RTFOT | 46.6 | 2846 | 3.76 | 13.1 | 0.500 | 3.70 |
| BATCH | TFOT | 49.6 | 3004 | 3.68 | 13.0 | 0.517 | 3.74 |
| | Hot Mix | 41.8 | 2902 | 4.02 | 15.6 | 0.521 | 3.65 |
| | ERTFOT | 31.8 | 5056 | 4.69 | 15.6 | 0.607 | 3.74 |
| | ETFOT | 31.1 | 6564 | 5.24 | 16.6 | 0.715 | 3.74 |
| EXXON | Tank | 64.6 | 1864 | 3.43 | 10.9 | 0.421 | 3.60 |
| AC-20 1988 | RTFOT | 47.6 | 3203 | 4.22 | 13.4 | 0.469 | 3.65 |
| | TFOT | 47.5 | 3204 | 4.28 | 13.3 | 0.517 | 3.64 |
| | Hot Mix | 46.6 | 3615 | 4.29 | 16.9 | 0.683 | 3.68 |
| | ERTFOT | 34.6 | 5733 | 5.51 | 15.9 | 0.601 | 3.66 |
| | ETFOT | 31.8 | 7529 | 6.17 | 17.1 | 0.721 | 3.67 |
| TEXACO | Tank | 86.6 | 2070 | 4.24 | 19.3 | 0.411 | 3.47 |
| AC-20 1989 | RTFOT | 58.4 | 4372 | 5.66 | 21.7 | 0.460 | 3.53 |
| | TFOT | 52.0 | 4646 | 5.70 | 21.8 | 0.490 | 3.55 |
| | Hot Mix | 44.7 | 5547 | 6.23 | 23.8 | 0.543 | 3.55 |
| | ERTFOT | 39.1 | 9651 | 7.60 | 24.3 | 0.569 | 3.60 |
| | ETFOT | 40.4 | 13678 | 8.77 | 25.0 | 0.641 | 3.62 |
| TEXAS GULF | Tank | 78.4 | 2209 | 3.58 | 16.5 | 0.472 | 3.64 |
| AC-20 1989 | RTFOT | 40.1 | 6496 | 5.39 | 19.7 | 0.578 | 3.72 |
| | TFOT | 47.1 | 5610 | 5.00 | 19.2 | 0.583 | 3.72 |
| | Hot Mix | 34.8 | 8607 | 5.99 | 21.4 | 0.653 | 3.74 |
| | ERTFOT | 29.3 | 18902 | 7.68 | 22.2 | 0.710 | 3.83 |
| | ETFOT | 28.9 | 29344 | 9.07 | 23.6 | 0.830 | 3.85 |

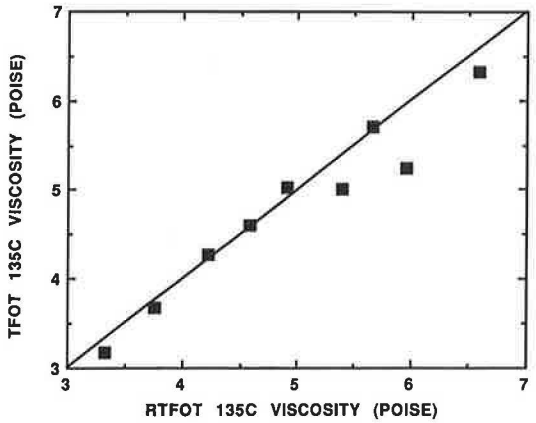


FIGURE 1 Comparisons of TFOT and RTFOT viscosity at 135°C.

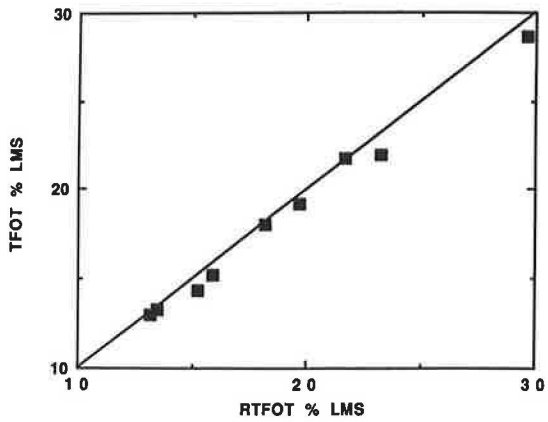


FIGURE 2 Comparison of %LMS for TFOT and RTFOT aged asphalts.

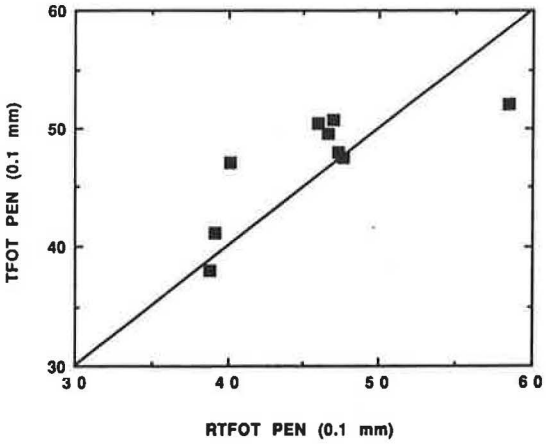


FIGURE 3 Comparison of the penetrations of TFOT and RTFOT aged asphalts.

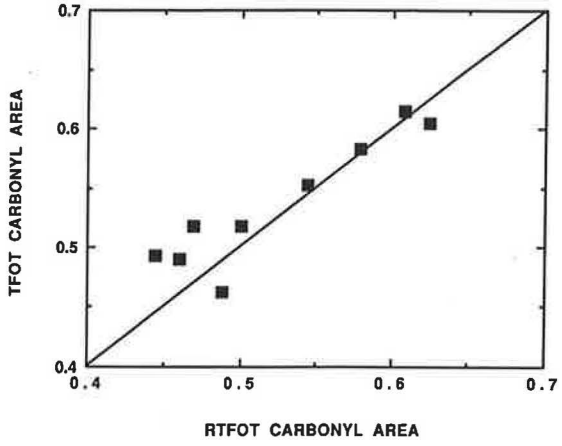


FIGURE 5 Comparison of carbonyl areas of IR spectra of TFOT and RTFOT aged asphalt.

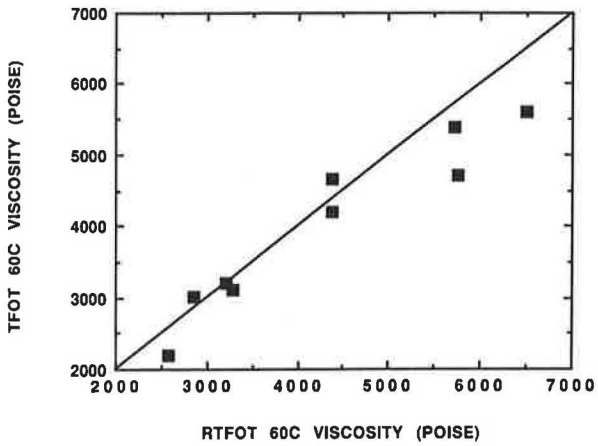


FIGURE 4 Comparison of the 60°C viscosities of TFOT and RTFOT aged asphalts.

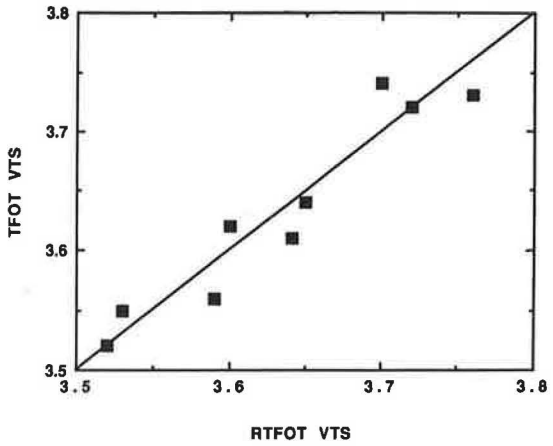


FIGURE 6 Comparison of viscosity temperature susceptibility of TFOT and RTFOT aged asphalts.

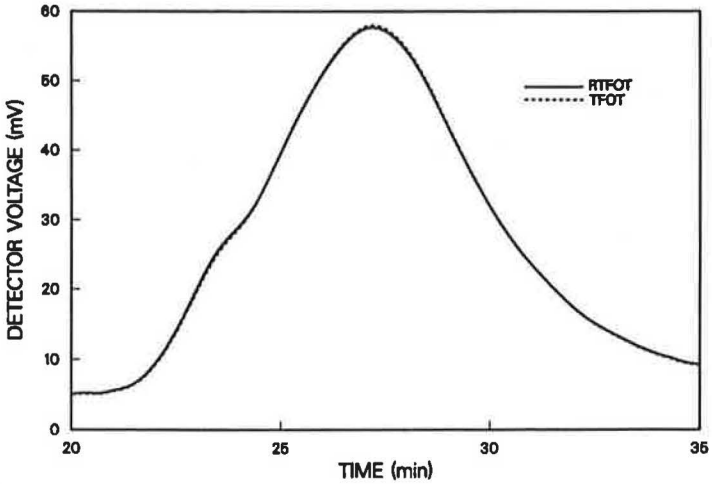


FIGURE 7 GPC chromatograms for TFOT and RTFOT of 1989 Ampet AC-20.

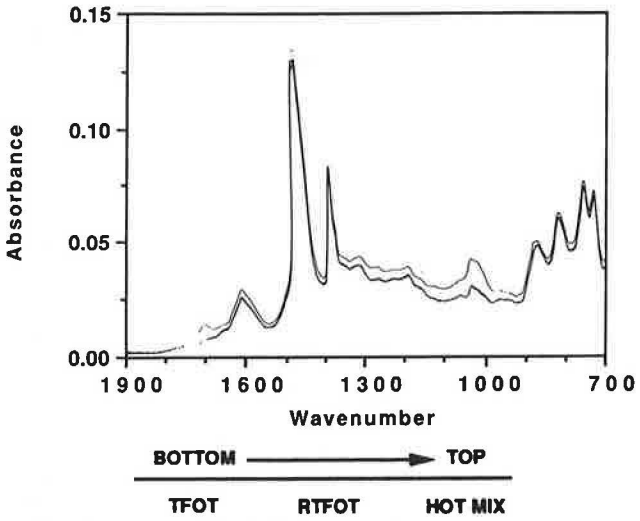


FIGURE 8 Comparison of 60°C viscosities of hot-mix and oven-aged asphalts.

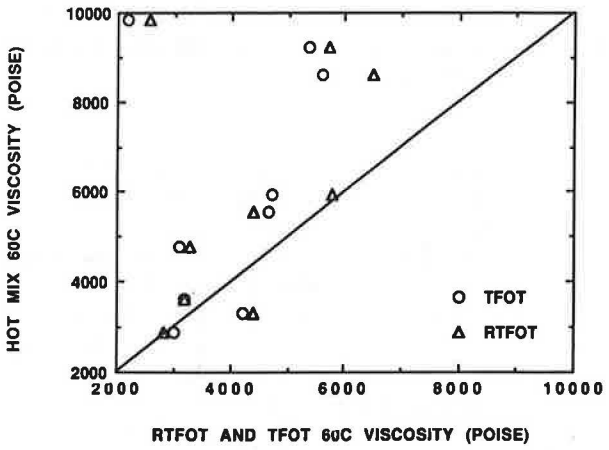


FIGURE 9 Comparison of 135°C viscosities of hot-mix and oven-aged asphalt.

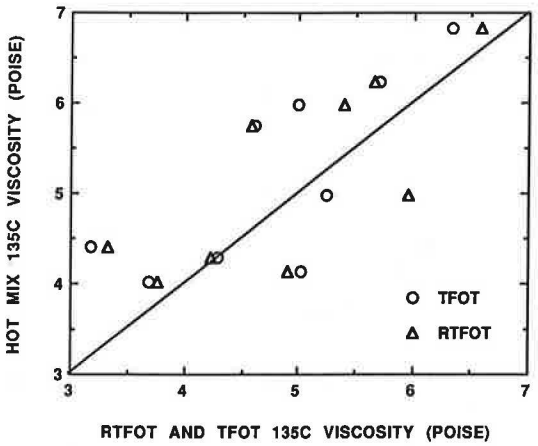


FIGURE 10 Comparison of viscosity temperature susceptibility of hot-mix and oven-aged asphalt.

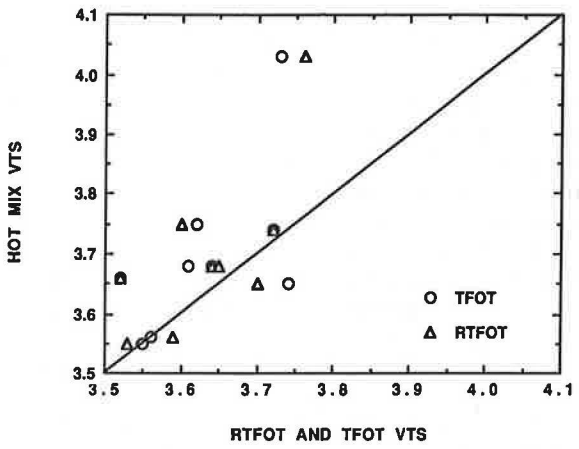


FIGURE 11 Comparison of IR carbonyl areas of hot-mix and oven-aged ashpalt.

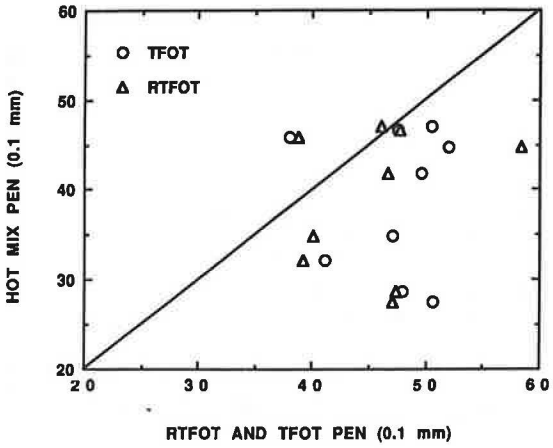


FIGURE 12 Comparison of IR carbonyl areas of hot-mix and oven-aged ashpalt.

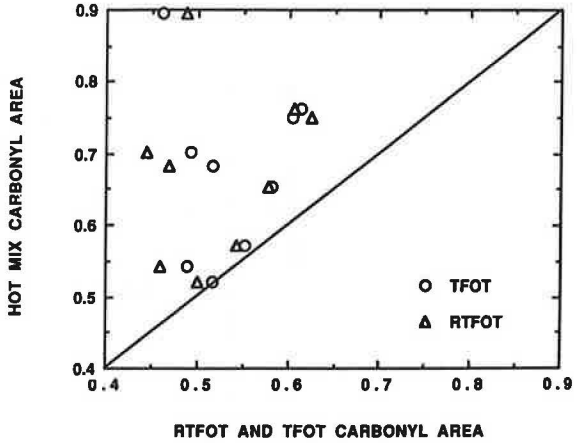


FIGURE 13 Comparison of %LMS for hot-mix and oven-aged asphalts.

Figure 9 indicates that the 60°C (140°F) viscosity is being fairly reproduced for more than half of the samples, but several were badly hardened in the plant. The viscosity at 275°F (135°C), Figure 10, shows better agreement than most properties but has considerable scatter. Both the penetration comparison, Figure 12, and particularly the carbonyl area comparison, Figure 13, show greater change in the hot-mix plant than in the oven tests. In general these comparisons suggest that the hot-mix process is more severe than the oven test.

Only the percent LMS, Figure 14, shows linear variation, but it is displaced to higher hot-mix values. Some of this may be solvent aging. Also percent LMS alone does not reflect all of the aging changes that occur in the GPC chromatograms. Consider the case of the Texaco AC-20. The data in Table 1 show that the percent LMS for the hot mix and the ERTFOT are close, but in Figure 15 the chromatograms are seen to be quite different. The infrared spectra in Figures 8, 16, and 17 are particularly instructive. In Figure 8, the good agreement of the oven tests and their gross disagreement with the hot mix is clearly evident with greater hot-mix aging across the spectrum. Figure 16, however, shows fair agreement in the carbonyl region between the standard oven test and the hot mix but gross divergence in the sulfoxide region. As mentioned earlier, some of this, at least, could be silica contamination, and this is supported by the sharp and unusual peak at about 900, which is probably carbonate. In Figure 17, we see good agreement in the carbonyl region between hot mix and oven test but in the sulfoxide region agreement is best between the ETFOT and the hot mix. The upper curve shows the great hardening for material that is not normally extracted and that is absent from the hot-mix spectra. If this material could be extracted with the rest, the divergence between oven tests and hot mix would be greater.

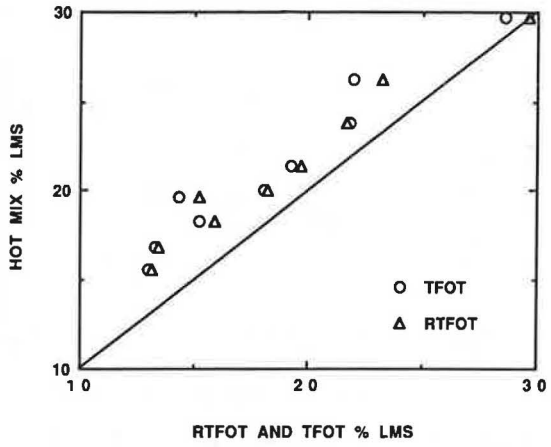


**FIGURE 14 GPC chromatograms of tank, TFOT, ETFOT, and hot-mix: 1989 Texaco AC-20.**

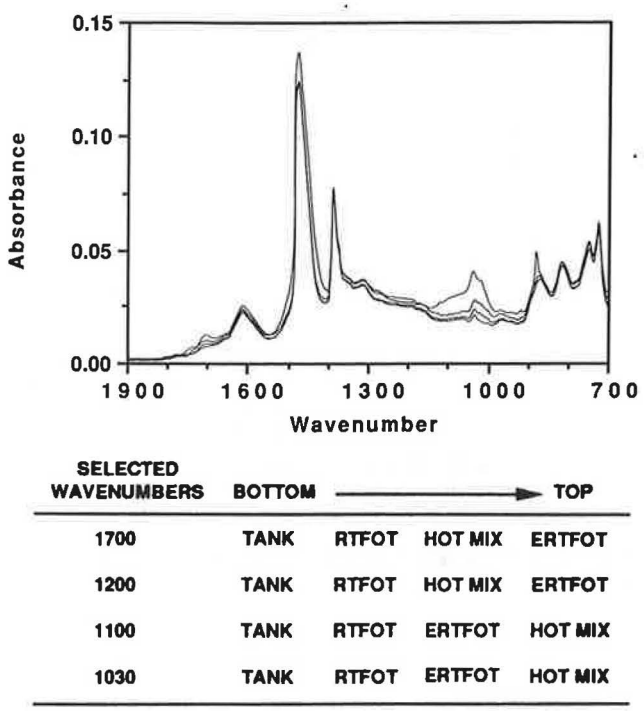


**FIGURE 16 Comparison of IR spectra RTFOT, ERTFOT, and hot-mix: 1989 Cosden AC-20.**

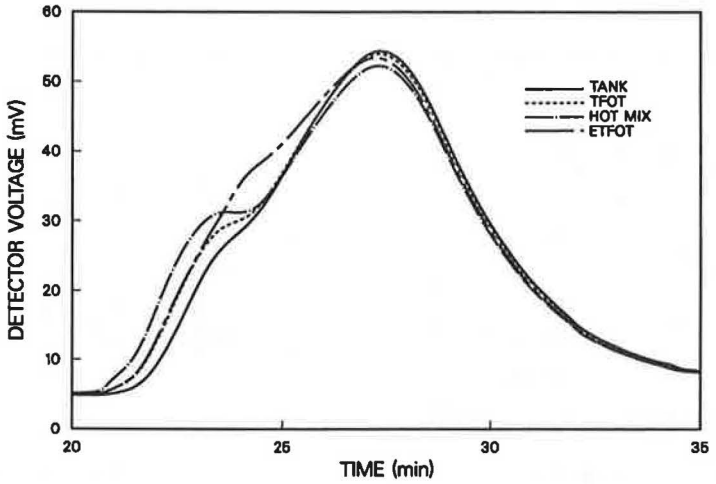


**FIGURE 15 Comparison of IR spectra for TFOT, RTFOT, and hot-mix: 1989 Cosden AC-10.**

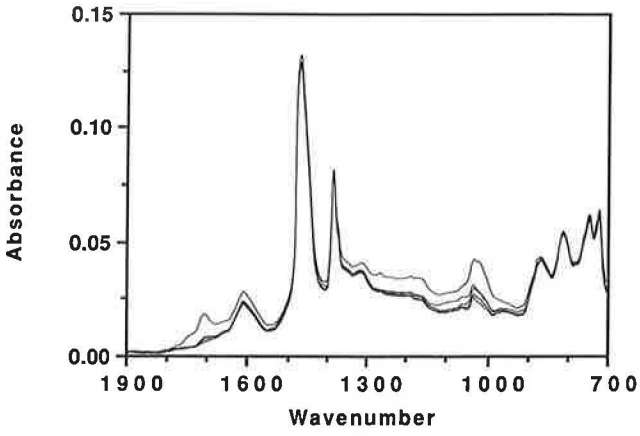


| SELECTED WAVENUMBERS | BOTTOM → TOP | | | | |
|---|---|---|---|---|---|
| 1700 | TANK | RTFOT | HOT MIX | ERTFOT | HARD TO REMOVE |
| 1200 | TANK | RTFOT | HOT MIX | ERTFOT | HARD TO REMOVE |
| 1100 | TANK | RTFOT | ERTFOT | HOT MIX | HARD TO REMOVE |
| 1030 | TANK | RTFOT | ERTFOT | HOT MIX | HARD TO REMOVE |

**FIGURE 17 Comparison of IR spectra for oven test and extended oven test with hot-mix and hard-to-remove material: 1987 Exxon AC-20 (drum).**

### Relation Between Carbonyl Area and Viscosity

Martin et al. (*10*) obtained a very strong correlation between FTIR carbonyl peak height and the viscosity of asphalt extracted from road cores. For a given asphalt, log viscosity varied linearly with the carbonyl peak. A similar correlation was attempted with log viscosity at 60°C and carbonyl area data given in Table 1. The results for all three Exxon asphalts are shown in Figure 18. Even though these asphalts are not identical, being produced at different times, the agreement for the tank and oven-aged samples is not bad. The hot-mix samples appear to form a different population. The same thing is seen in Figure 19 where a very good relation exists for all but the hot-mix point. To a varying degree, this was true for

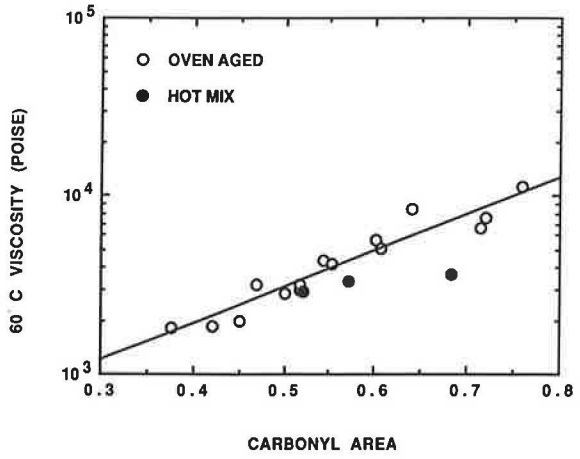


**FIGURE 18 Correlation of 60°C viscosity with IR carbonyl area for hot-mix and oven-aged Exxon AC-20.**

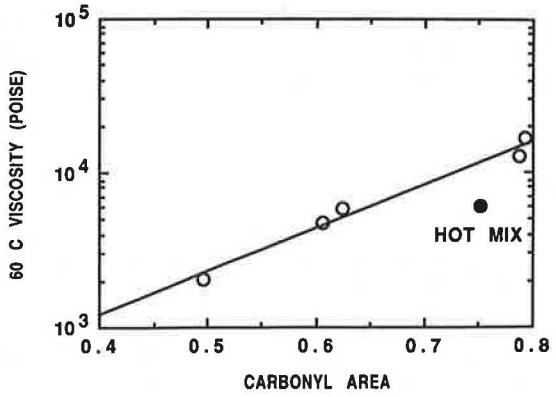


**FIGURE 19 Correlation of 60°C viscosity with IR carbonyl area for hot-mix and oven-aged Cosden AC-20.**

all asphalts with the hot-mix point invariably below the least square fit of the remaining data.

No identifiable source of error could have produced this. All extracted asphalts were solvent free, and either solvent hardening or fines contamination would tend to produce higher, rather than lower, viscosities. It seems reasonable to postulate that oxidation is occurring by a different mechanism in the hot-mix plant to give a different relation between carbonyl production and viscosity change.

## CONCLUSION

As mentioned earlier, the TFOT and RTFOT run at specified standard times would appear to be identical, so that there is little point in running both. On the other hand, the data strongly indicate that the oven tests do not accurately predict the chemical and physical changes occurring in the asphalts during the hot-mix process and, in particular, the FTIR data indicate that different mechanisms may be involved during oxidation.

Problems sometimes arise because the properties of the extracted asphalt are changed during the extraction and recovery processes. Incomplete solvent removal or solvent hardening during extraction and recovery can affect the properties of the recovered hot-mix asphalt, but considerable care was exercised to minimize these effects. Leaving small amounts of asphalt on the aggregate during the extraction can affect the resulting bulk properties, because the asphalt closest to the aggregate surface tends to be more oxidized. The hot-mix properties may also be influenced by the source of the asphalt. In Figure 8, of the 60°C viscosities, the lowest three hot-mix values result from Exxon AC-20 asphalts with which the oven-test values coincide. For this asphalt, using the 60°C viscosity, the oven tests seem to predict the hot-mix properties, but this is not so for the other asphalts. Consequently, the hot-mix properties may be extremely difficult to simulate without accounting for differences in asphalts, the presence of aggregate, and in some cases, incomplete extraction.

## ACKNOWLEDGMENTS

Support for this work by the Texas State Department of Highways and Public Transportation, in cooperation with FHWA,

and by SHRP is gratefully acknowledged. Helpful discussions with Don O'Connor and Darren Hazlett and the technical contributions of Monica Daly are greatly appreciated.

## REFERENCES

1. R. H. Lewis and J. Y. Welborn. Report on the Properties of the Residues of 50–60 and 85–100 Penetration and Ductility at Plant Mix Temperatures. *Proc., Association of Asphalt Paving Technologists*, Vol. 12, 1940.
2. F. N. Hveem, E. Zube, and J. Skog. Proposed New Tests and Specifications for Paving Grade Asphalts. *Proc., Association of Asphalt Paving Technologists*, Vol. 32, 1963.
3. R. R. Davison, J. A. Bullin, C. J. Glover, B. L. Burr, H. B. Jemison, A. L. G. Kyle, and C. A. Cipione. *Development of Gel Permeation Chromatography, Infrared and Other Tests to Characterize Asphalt Cements and Correlate with Field Performance*. Report FHWA/TX-90/458-1F. Texas Department of Highways and Public Transportation, Austin, Nov. 1989.
4. E. H. Chipperfield, J. L. Duthie, and R. B. Girdler. Asphalt Characteristics in Relation to Road Performance. *Proc., Association of Asphalt Paving Technologists*, Vol. 39, 1970.
5. C. J. Glover, R. R. Davison, S. M. Ghoreishi, H. B. Jemison, and J. A. Bullin. Evaluation of Oven Simulation of Hot-Mix Aging by an FT-IR Pellet Procedure and Other Methods. In *Transportation Research Record 1228*, TRB, National Research Council, Washington, D.C., 1989, pp. 177–182.
6. B. H. Chollar, J. A. Zenewitz, J. G. Boone, K. T. Tran, and D. T. Anderson. Changes Occurring in Asphalts in Drum Dryer and Batch (Pug Mill) Mixing Operations. In *Transportation Research Record 1228*, TRB, National Research Council, Washington, D.C., 1989, pp. 145–155.
7. B. L. Burr, R. R. Davison, C. J. Glover, and J. A. Bullin. Solvent Removal from Asphalt. In *Transportation Research Record 1269*, TRB, National Research Council, Washington, D.C., 1990.
8. P. W. Jennings. *Chemical Composition of Commercial Asphalt Cement as Determined by High Pressure Liquid Chromatography*. Report FHWA-MT-7929. FHWA, U.S. Department of Transportation, Dec. 1977.
9. H. B. Jemison, B. L. Burr, R. R. Davison, J. B. Bullin, and C. J. Glover. Application and Use of the ATR FT-IR Method to Asphalt Aging Studies. Presented at 200th ACS National Meeting, Washington, D.C., Aug. 1990.
10. K. L. Martin, R. R. Davison, C. J. Glover, and J. A. Bullin. Asphalt Aging in Texas Roads and Test Sections. In *Transportation Research Record 1269*, TRB, National Research Council, Washington, D.C., 1990.



*Publication of this paper sponsored by Committee on Characteristics of Bituminous Materials.*

# Modulus Properties of Plasticized Sulfur Mixtures

ADLI H. AL-BALBISSI, DALLAS N. LITTLE, CHUCK GREGORY, AND BARRY RICHEY

Plasticized sulfur is a total replacement for asphalt cement. As a result, the potential for using plasticized sulfur in lieu of asphalt cement in paving mixtures is attractive in this day of capricious supply and pricing of petroleum products. The modulus properties of selected plasticized sulfur mixtures were studied. The plasticized sulfur binders consist of about 70 percent elemental sulfur and 30 percent of a combination of hydrocarbons that chemically react with molten sulfur. The results of modulus characterization include resilient modulus, creep stiffness, dynamic modulus, flexural modulus, and relaxation modulus. They also include a comparison with asphalt cement modular properties. The study concluded that plasticized sulfur mixtures exhibit similar modulus properties and are stiffer than asphalt concrete. They also exhibit well-defined viscoelastic response at higher temperatures. These conclusions were consistently substantiated by each of the moduli evaluated.

The modulus properties of the materials that make up flexible pavement layers are an indispensable part of most up-to-date structural pavement design techniques. In fact, the most commonly used failure criteria in flexible pavement design are tensile strain in the stiffest layer and vertical compressive strain in the subgrade layer. These criteria are extremely sensitive to the respective modulus properties of the pavement layers. Thus, the pavement engineer must not only seek an accurate estimate of the modulus but also the proper definition of modulus for the intended purpose.

Viscoelastic materials such as plasticized sulfur concrete and asphalt concrete add another dimension of difficulty to the task of selecting the correct modulus. These materials have modulus properties that are affected by time (duration of loading) and temperature. Detailed description of the properties and uses of several plasticized sulfur binders and mixtures, including those used in this work, are available elsewhere (*1–5*).

Van der Poel (*6*) has defined the modulus of asphalt cement as stiffness:

$$S(t,T) = \text{stress/strain} \quad (1)$$

where $t$ is the time of loading and $T$ is the temperature.

Figure 1 is a simplified illustration of the time of loading dependency of idealized asphalt concrete at a selected temperature. It is easy to trace the change in behavior from an elastic response at short loading times, through a delayed elastic behavior zone, and finally to a region where the stiffness is totally a function of the viscous properties of the binder. Because of the time-temperature superposition properties of asphalt and plasticized sulfur, the abscissa in Figure 1 could be changed to temperature if stiffness were measured at a selected duration of loading.

In this study, the modulus properties were measured in five forms:

1. Resilient modulus ($M_R$),
2. Creep stiffness,
3. Dynamic modulus ($E_{flex}$),
4. Flexural modulus, and
5. Relaxation modulus.

## RESILIENT MODULUS

The resilient moduli, defined as the ratio of induced stress to recoverable strain, were measured by the Mark IV device developed by Schmidt (*7*). The device applies a 0.1-sec load pulse once every 3 sec across the vertical diameter of a cylindrical specimen (Marshall-type specimen) and senses by linear variable transformers the resultant deformation across the horizontal diameter. The shape of the load impulse is shown in Figure 2.

The resilient modulus was used throughout as a quality assurance measure. Resilient moduli data were recorded from aging studies, water susceptibility studies, and mixture design studies. In this study, laboratory mixtures prepared with different binders were aged for 6 days at 50°F and tested at four temperatures: −10°F, 32°F, 73°F, and 104°F. The 6-day cure period was selected based on an aging study that revealed that the resilient modulus does not appreciably change in the laboratory following 6 days of curing at 50°F. The properties of the different binders used are summarized in Table 1.

In addition to the laboratory-molded specimens, field cores from a project in San Antonio, Texas (Loop 1604), were tested over the same temperature range. These data are plotted in Figure 3 and summarized in Table 2.

Table 2 and Figure 3 indicate that the resilient modulus versus temperature relationship is very similar for binders Mix 1, Mix 2, Mix 3, and the field cores from Loop 1604. These cores were 2 months old at the date of testing.

Table 2 and Figure 3 also indicate that mixtures with Mix 4 and Mix 5 proved to have lower resilient moduli than the other plasticized sulfur binders across the test temperature range.

A. H. Al-Balbissi, Civil Engineering Department, Jordan University of Science and Technology, Irbid, Jordan. D. N. Little, C. Gregory, and B. Richey, Texas Transportation Institute, Texas A&M University, College Station, Tex. 77843-3122.

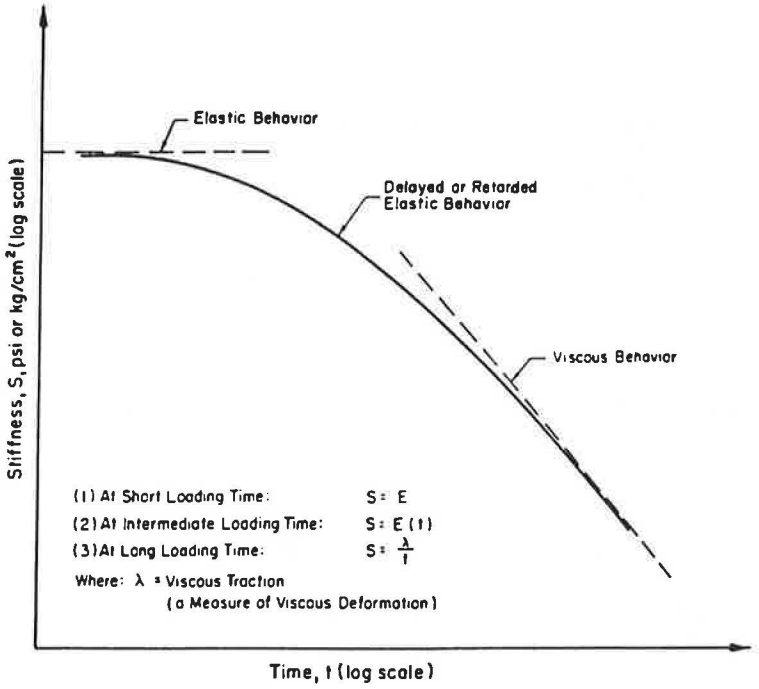


**FIGURE 1 Simplified illustration of components of stiffness: elastic, viscoelastic, and viscous.**

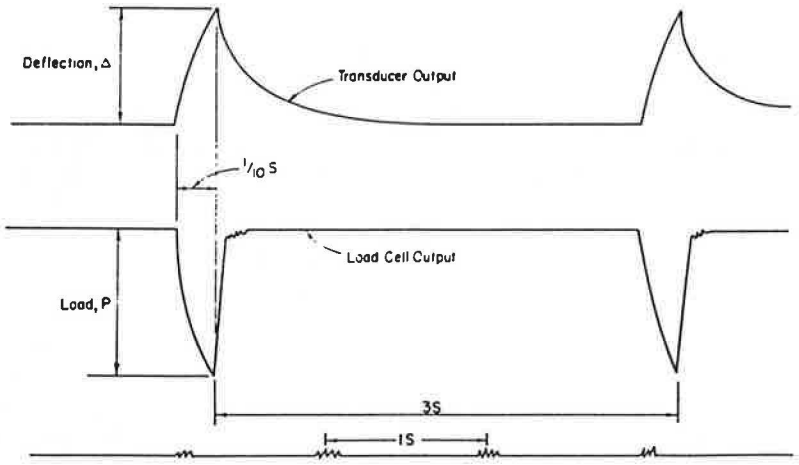


**FIGURE 2 Load pulse of resilient modulus device.**

The data also indicate that both the laboratory mixture of AC-10 plus crushed limestone and the field cores from Loop 1604 of AC-20 and crushed limestone produced similar $M_R$ versus temperature relationships. It is clear that the plasticized sulfur mixtures are substantially stiffer across the temperature range. Obviously, resilient moduli will vary based on the effects of aggregate type, gradation, void content, and such, but the unmistakable trend is that plasticized sulfur mixtures under rapid load rates are much stiffer than asphalt concrete. However, plasticized binders display a very definite temperature susceptibility and viscoelastic response. It should be mentioned that variations in the number of specimens tested in the various cases tested should not cast doubt on the accuracy of comparing the different materials because a minimum of three specimens will provide adequate accuracy.

Figure 3 indicates that the viscoelastic behavior of plasticized sulfur mixtures actively begins at about 32°F. Below about 32°F, the modulus is probably very nearly linearly elastic. However, the accuracy of diametral resilient moduli determinations at low temperatures (32°F) is poor (7). The resilient modulus data in Figure 3 indicate a dominating viscous response at high temperatures, perhaps above 100°F. The stiffness data for all mixtures containing crushed limestone and basaltic aggregate indicate substantial decrease in stiffness with increased time of loading, which reflects the dominating viscous response at high temperatures because high-

TABLE 1 FORMULATION AND PROCESSING CONDITIONS FOR BINDERS ANALYZED

| Binder Identification | Formulation | Reaction Temperature, °F | Reaction Time, Hours | Penetration at 77°F, (1 Day old), dmm | Viscosity at 275°F, (1 day old), poises |
|---|---|---|---|---|---|
| Mix 1 | 68% Sulfur<br>12% DCPD**<br>12% DP***<br>8% Vinyl Toluene<br>Catalyst (1% of mix) | 302 | 6.5 | 35 | 10.2 |
| Mix 2 | 70% Sulfur<br>12% DCPD<br>10% DP<br>8% Vinyl Toluene<br>Catalyst (1% of mix) | 338 | 6.5 | 165 | 4.0 |
| Mix 3 | 70% Sulfur<br>12% DCPD<br>10% DP<br>8% Vinyl Toluene<br>Catalyst (1% of mix) | 302 | 6.5 | 22 | 5.8 |
| Mix 4 | 70% Sulfur<br>12% DCPD<br>10% DP<br>8% Vinyl Toluene<br>Catalyst ( 1% of mix) | 320 | 6.5 | 78 | 2.5 |
| Mix 5 | 68% Sulfur<br>12% DCPD<br>10% Solvenol<br>10% Vinyls Toluene<br>Catalyst ( 1% of mix) | 300-350 | 4.5 | 40 | 11.0 |

* Expressed as percent by weight.
** DCPD = Dicyclopentadiene
*** DP = Dipentene

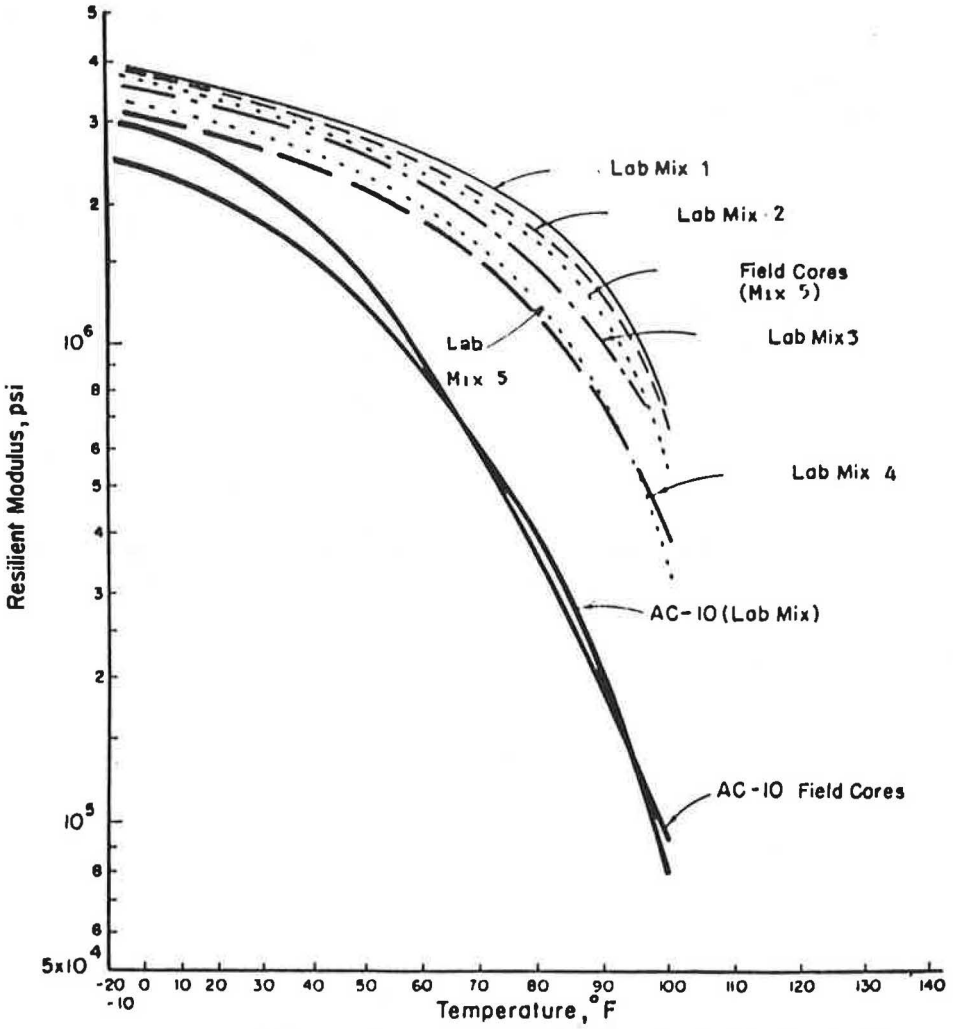


**FIGURE 3 Resilient moduli versus temperature for all mixtures fabricated with crushed limestone.**

TABLE 2 SUMMARY OF RESILIENT MODULI

| Binder | Aggregate | Type of Mixture | Mean Resilient Modulus, psi x $10^6$ -10 F | 73°F | 104°F | No. of Spec. |
|---|---|---|---|---|---|---|
| Mix 1 | CLS* | Lab | 4.01 | 2.22 | 0.790 | 50 |
| Mix 2 | CLS | Lab | 4.00 | 2.16 | 0.699 | 50 |
| Mix 3 | CLS | Lab | 3.62 | 1.82 | 0.670 | 20 |
| Mix 4 | CLS | Lab | 3.19 | 1.29 | 0.540 | 20 |
| Mix 5 | Basalt | Lab | 3.29 | 1.50 | 0.300 | 9 |
| Mix 5 | CLS | Field | 3.81 | 2.01 | 0.710 | 20 |
| AC-10 | CLS | Lab | 2.66 | 0.489 | 0.077 | 20 |
| AC-10 | Basalt | Lab | 2.51 | 0.321 | 0.102 | 9 |
| AC-20 | CLS | Field | 3.00 | 0.501 | 0.092 | 20 |

*CLS : Crushed limestone

temperature effect on viscous materials can be viewed as similar to the effect of long duration of loading. Another point of interest is the generally lower stiffness values of mixtures prepared by using basalt aggregates. This is also true, but to a lesser extent, of field versus laboratory data. General conclusions related to the effect of aggregate type on moduli and stiffness values will not be justified here because of the limited available data related to this specific factor. The lower stiffness and moduli values associated with field data may be attributed to the lesser degree of control in the preparation of field mixtures.

The argument has often been put forth that plasticized sulfur layers should be designed as rigid pavement layers because they probably crystallize rapidly in the thin-film arrangement found in mixtures, and they are probably very nearly linearly elastic in normal pavement conditions. However, the pronounced viscous effects at higher temperatures and longer loading rates and especially a combination of the two effects demand thoughtful consideration of the consequences of these effects in pavement design applications.

## CREEP STIFFNESS

The diametral resilient modulus is often subjected to criticism because of the light load used, the conditions of biaxial stressing, and the rigid assumptions that should be but are not closely adhered to in order for the cylindrical, diametrally loaded specimen to respond elastically. To more precisely establish the modular properties of plasticized sulfur under different conditions of loading and different states of stress, other forms of moduli were computed.

Creep stiffness is simply the inverse of the creep compliance. For purposes of comparison creep stiffness was calculated at 0.1 sec of load duration at 40°F, 70°F, and 100°F during the compression creep test. The resulting values are tabulated in Table 3.

As expected, these moduli do not closely agree with the resilient moduli. However, the same trends are evident as were established with resilient moduli data. These moduli are plotted in Figure 4.

## DYNAMIC MODULUS AND FLEXURAL MODULUS

The dynamic moduli and flexural moduli are also presented in Table 3. The dynamic modulus is defined here as the ratio of stress applied during repeated load permanent deformation testing to the dynamic strain at the 200th load application. The flexural modulus is defined as the modulus of the flexural fatigue beams at the 200th load application. The modulus is more clearly defined as follows:

TABLE 3 SUMMARY OF CREEP STIFFNESSES, DYNAMIC MODULI, AND FLEXURAL MODULI FOR ALL MIXTURES

| Binder | Aggregate | Creep Stiffness, psi x $10^6$ 40 °F | 70°F | 100°F | Dynamic Modulus, psi x $10^6$ 40°F | 70°F | 100°F | Flexural Modulus psi x $10^6$ 70°F |
|---|---|---|---|---|---|---|---|---|
| Mix 1 | CLS** | 3.51* | 1.90 | 0.320 | 4.00 | 2.69 | 0.290 | 0.350 |
| Mix 2 | CLS | 8.00 | 2.90 | 0.300 | 4.76 | 2.22 | 0.495 | 0.675 |
| Mix 4 | CLS | 2.20 | 1.30 | 0.210 | 2.75 | 1.30 | 0.190 | 0.330 |
| Mix 5 | Basalt | 5.00 | 2.00 | 0.150 | 4.00 | 1.02 | 0.200 | ------ |
| AC-10 | CLS | 1.10 | 0.310 | 0.060 | 2.10 | 0.397 | 0.086 | 0.056 |
| AC-10 | Basalt | 1.50 | 0.400 | 0.059 | 2.50 | 0.700 | 0.090 | ------ |

* Each Value represents the mean of three data points.

** CLS : Crushed Limestone

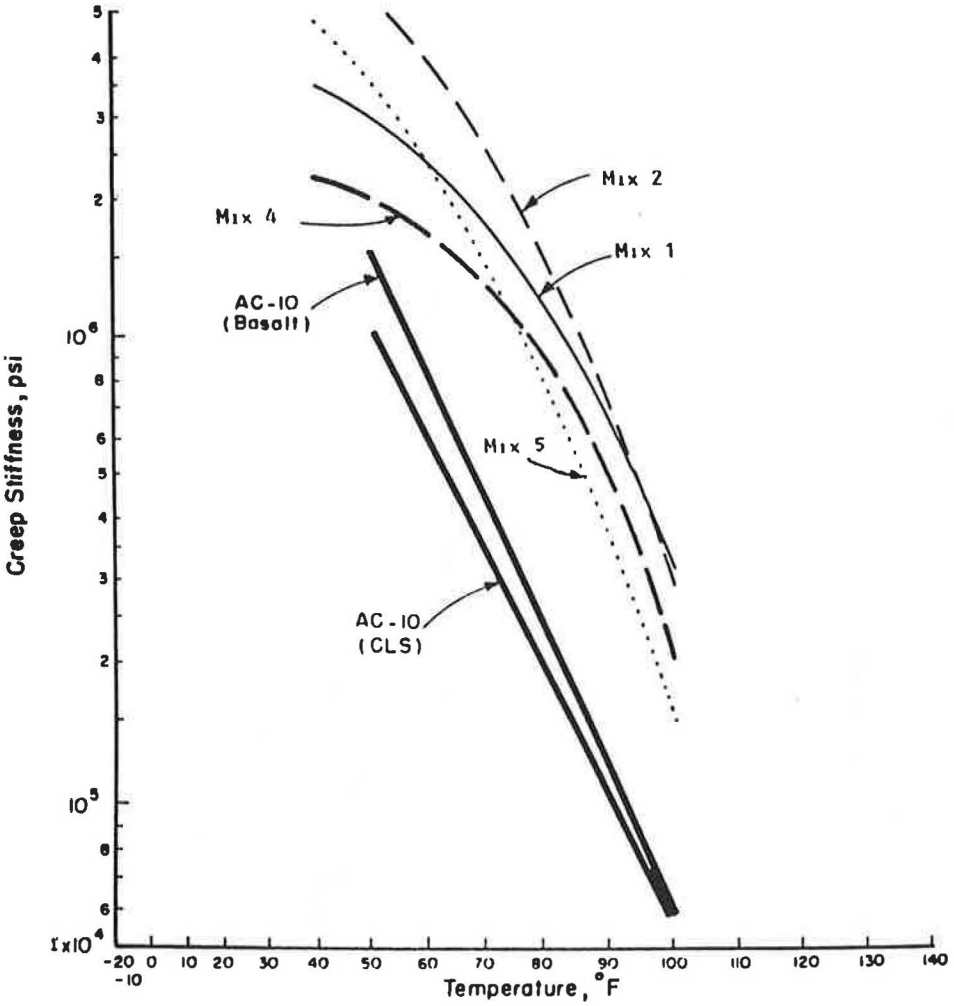


**FIGURE 4 Creep stiffness versus temperature for all mixtures.**

$$E_{flex} = \frac{Pa(3L^2 - 4a^2)}{48\ (I)(DELTA)} \quad (2)$$

where

$P$ = dynamic load applied to deflect the beam,
$a$ = $1/(2L-4)$,
$L$ = reaction span length,
$I$ = specimen moment of inertia, and
$DELTA$ = dynamic beam deflection at the center point.

The dynamic moduli are plotted in Figure 5.

## RELAXATION MODULI

The relaxation modulus was measured by applying a compressive stress that induced an initial strain of 100 μin./in. in specimens 4 in. in diameter and 8 in. high. Strains were measured with linear variable transformers. Strains were monitored across the middle 4 in. of the cylindrical specimens. The resulting relaxation moduli are presented in Table 4.

## MIXTURE PROPERTIES

Although the purpose here is to compare differences in binders, it is appropriate to indicate average mixture properties as a point of reference. For this purpose, aggregates gradation curves, Marshall stability, Marshall flow, percent air voids, and percent voids in mineral aggregate (VMA) for mixtures tested are shown in Figures 6, 7, 8, 9, and 10, respectively.

## SUMMARY

From this study of modulus properties, the following conclusions are established:

1. Plasticized sulfur binders Mix 1, Mix 2, Mix 3, and Field Mix 5 generally exhibit very similar modulus properties over the temperature range that a typical pavement is expected to experience.
2. Although substantially stiffer than asphalt concrete over the normal pavement temperature range, all plasticized sulfur binders exhibit well-defined viscoelastic response as well as dominant viscous response at higher temperatures. These

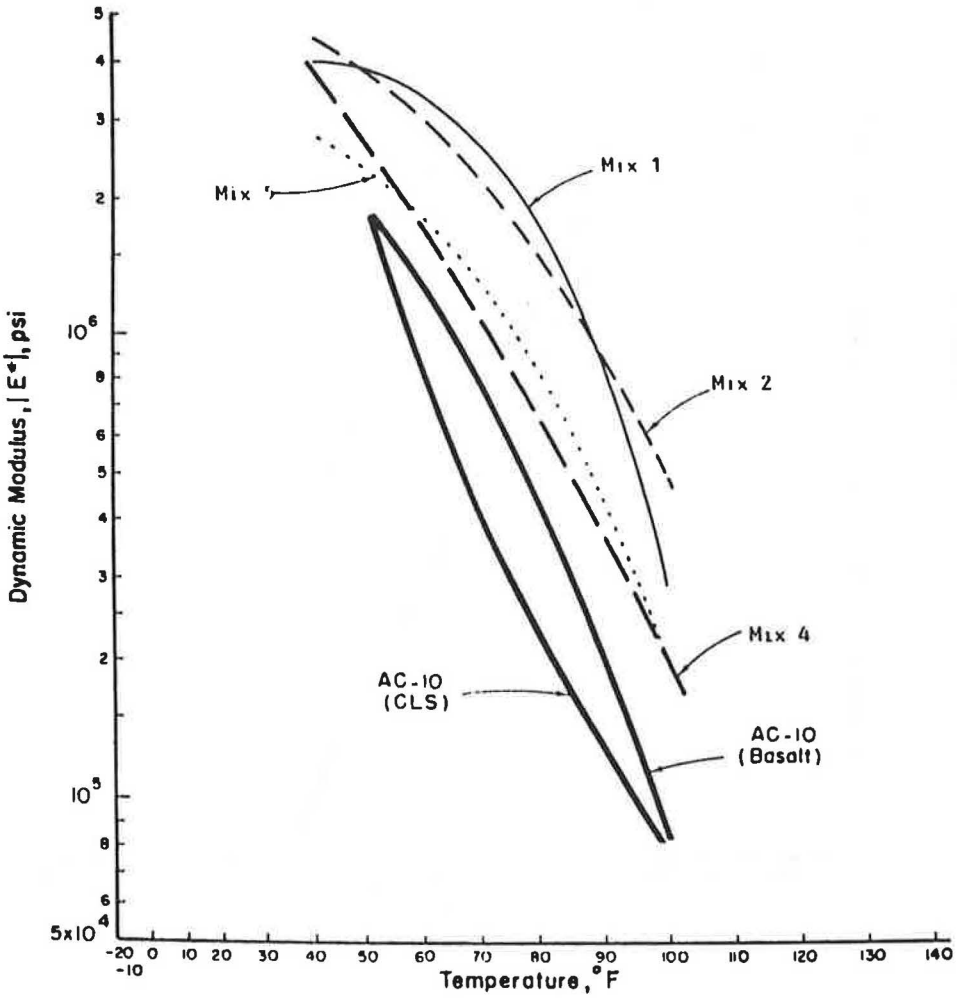


**FIGURE 5 Dynamic moduli versus temperature for all mixtures.**

TABLE 4 RELAXATION MODULI AT 73°F, 0.1-sec LOAD DURATION

| Binder | Relaxation Modulus, Psi x $10^6$ Mean Value | Standard Deviation | Number of Samples |
|---|---|---|---|
| Mix 1 | 1.129 | 0.180 | 3 |
| Mix 2 | 0.637 | 0.010 | 3 |
| Mix 3 | 1.449 | 0.023 | 3 |
| Mix 4 | 0.557 | 0.158 | 3 |
| AC-10 | 0.433 | 0.095 | 3 |

*CLS: Crushed limestone

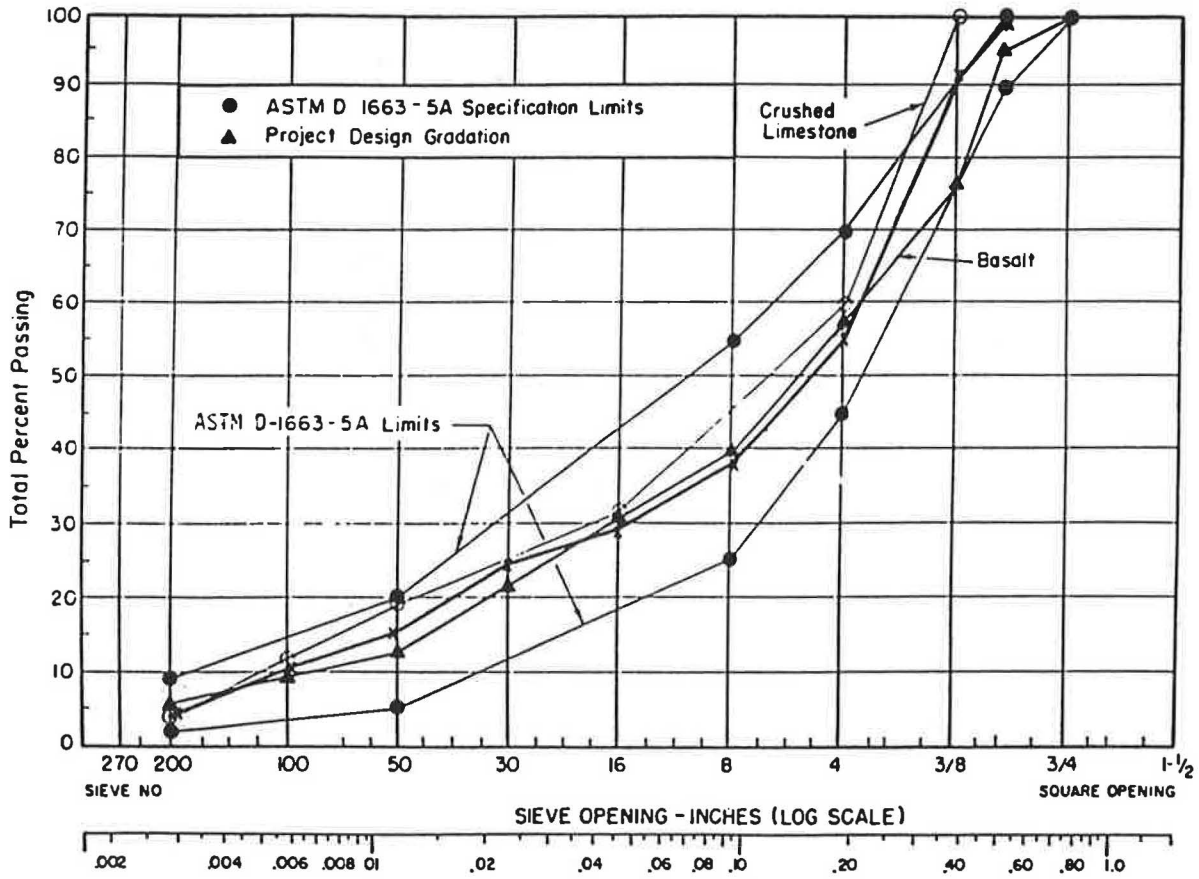


**FIGURE 6 Gradation curves for aggregates used in mixtures.**

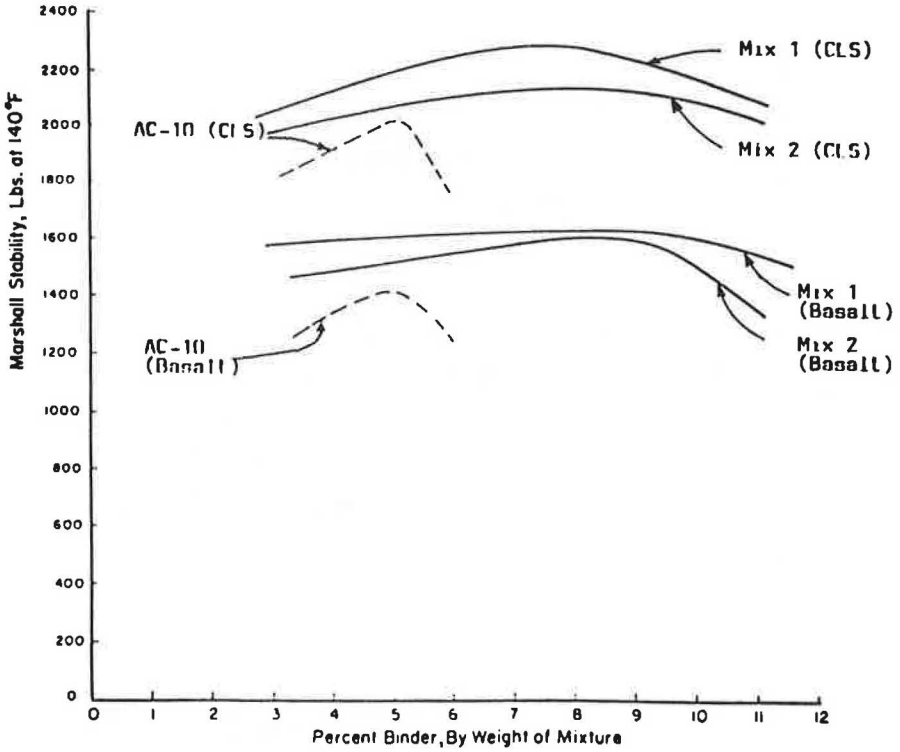


**FIGURE 7 Marshall stability versus binder content for mixtures tested.**

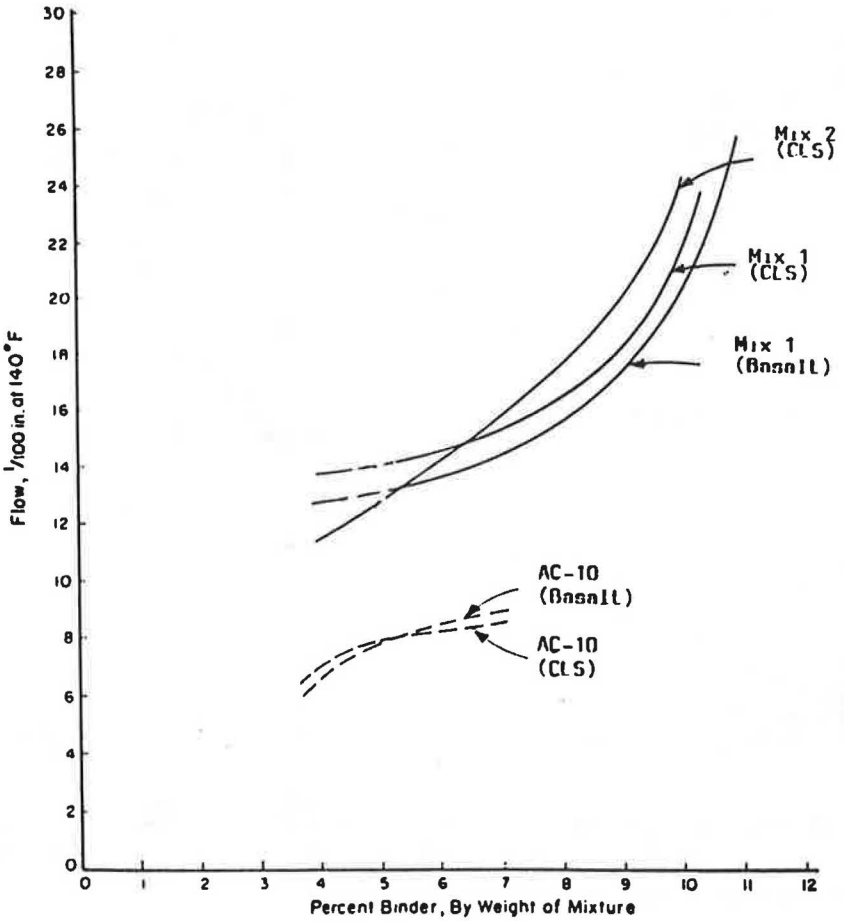


**FIGURE 8 Marshall flow versus binder content for mixtures tested.**

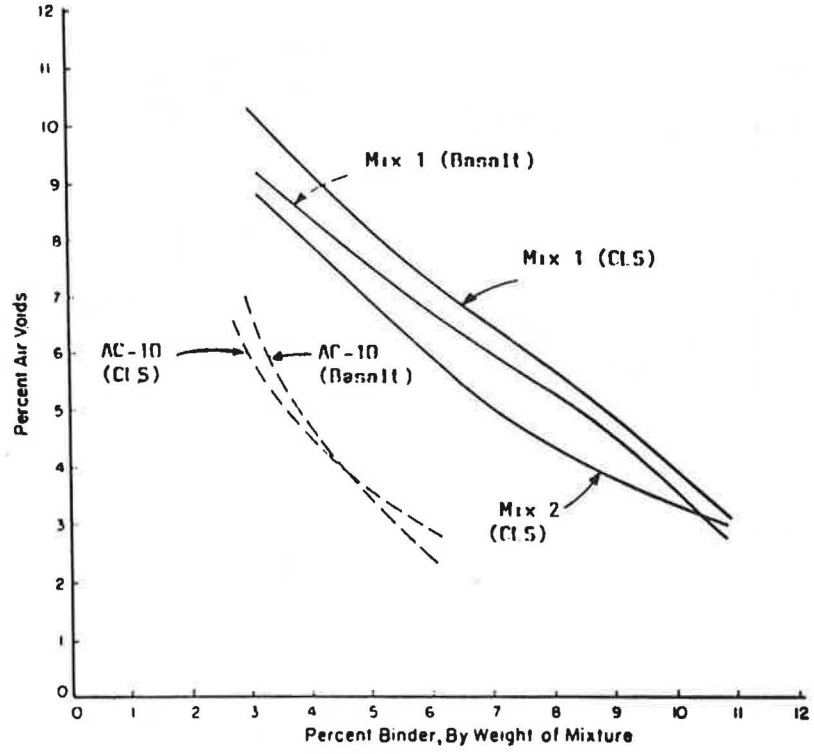


**FIGURE 9 Percentage air voids versus binder content for mixtures tested.**

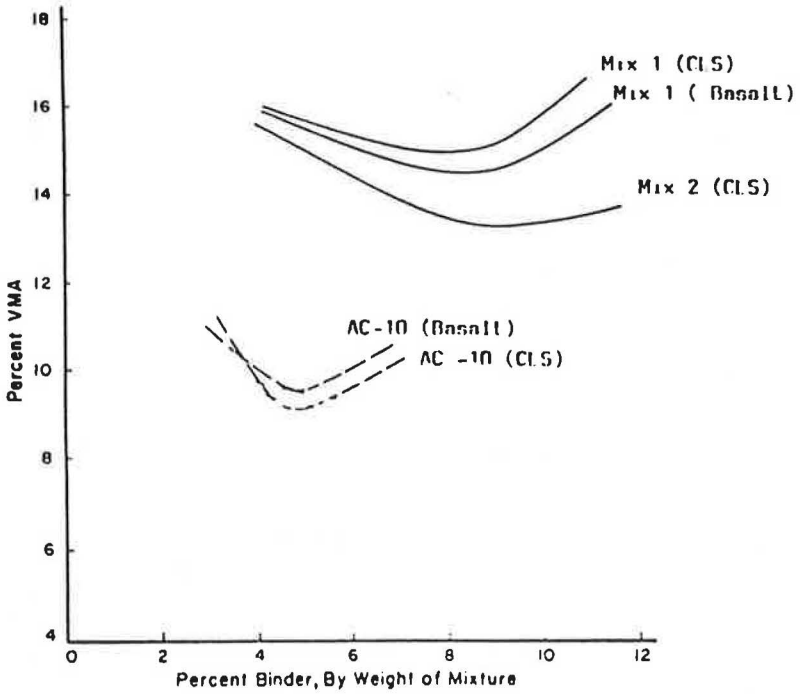


**FIGURE 10 Percentage VMA for mixtures tested.**

properties must be accounted for in structural pavement design considerations.

3. Binder Mix 4 is significantly softer than other plasticized sulfur binders across the temperature range to which pavements are normally subjected. Laboratory mixtures prepared with Mix 5 are also as soft as those prepared with Mix 4. However, the use of basalt aggregates in these mixtures may have contributed to their softness.

4. Resilient moduli, stiffness moduli, dynamic moduli, flexural moduli, and relaxation moduli were evaluated for each binder and the conclusions stated above consistently substantiated by each of the moduli versus temperature data.

## REFERENCES

1. A. C. Ludwig, Gerhardt, and J. Dale. *Materials and Techniques for Improving the Engineering Properties of Sulfur—Interim Report*. Report FHWA-RD-80-023. March 1980.
2. H. E. Haxo, C. J. Busso, M. Gage, J. Miedema, H. Newey, and R. M. White. *Design and Characterization of Paving Mixtures Based on Plasticizers Sulfur Binder-Chemical Characterization*. FHWA Contract D7FH-61-80-C-0048. Matrecon Inc., Oakland, Calif., 1984.
3. Pickett et al. *Extension and Replacement of Asphalt Cement with Sulfur*. Report FHWA-RD-78-95. FHWA, U.S. Department of Transportation, March 1978.
4. H. J. Lentz and E. T. Harrigan. *Laboratory Evaluating of Sulfur Binder Properties and Mix Design*. Report FHWA-RD-80-146. Jan. 1981.
5. T. L. Smith. *Stress-Strain–Time-Temperature Relationships for Polymers*. ASTM STP 325. 1962.
6. C. Van der Poel. A General System Describing the Viscoelastic Properties of Bitumens and the Relation to Routine Test Data. *Shell Bitumen Reprint 9*. Shell Laboratorium-Koninklijike, 1954.
7. R. J. Schmidt. A Practical Method for Measuring the Resilient Modulus of Asphalt-Treated Mixes. In *Highway Research Record 404*, HRB, National Research Council, Washington, D.C., 1972.

*Publication of this paper sponsored by Committee on Nonbituminous Components of Bituminous Paving Mixtures.*

# Comparison Study of Moisture Damage Test Methods for Evaluating Antistripping Treatments in Asphalt Mixtures

THOMAS W. KENNEDY AND W. VIRGIL PING

Moisture damage is a major problem for asphalt concrete pavements constructed throughout much of the United States, as well as other areas in the world. A number of test methods and procedures have been developed to evaluate the moisture damage potential of asphalt-aggregate mixtures; however, these different test methods and variations do not yield the same results. A study of the relationships among various moisture damage test values for a range of mixtures using different antistripping additives compared two basic moisture damage test methods, that is, the wet-dry indirect tensile test (the Lottman test) and the boiling test. A number of variations of the wet-dry indirect tensile test were also compared. On the basis of the results of the test program, the moisture susceptibility test methods are ranked in the decreasing order of severity: (a) original Lottman method, (b) modified Lottman method, and (c) Tunnicliff-Root method. Correlations have been obtained between the moisture damage test values of the modified Lottman method and the other test methods. The relationships between the boiling test results and the wet-dry indirect tensile strength ratio values have also been established.

Moisture damage is a major problem for asphalt pavements constructed throughout much of the United States. The seriousness of the problem, which has been studied for decades, is evidenced by the large number of research efforts conducted in the United States during the past 10 to 15 years.

As a result of the research, a number of tests and test procedures have been developed to evaluate the moisture damage potential of asphalt-aggregate mixtures. Unfortunately, although a limited number of basic tests are currently used, many variations of each test and many different acceptance criteria are being used. It is also apparent that these different tests and test variations do not yield the same results and thus do not predict the same amount of moisture damage potential.

In recognition of these factors, research was undertaken to evaluate the relationships between various moisture damage test values for a range of mixtures and antistripping agents. Two basic moisture susceptibility test methods were selected for laboratory evaluation, that is, the wet-dry indirect tensile test (the Lottman test) and the boiling test. However, a number of variations of the wet-dry indirect tensile test were compared.

T. W. Kennedy, Department of Civil Engineering, University of Texas, Austin, Tex. 78712. W. V. Ping, Department of Civil Engineering, FAMU/FSU College of Engineering, P.O. Box 2175, Tallahassee, Fla. 32310.

## EXPERIMENTAL PROGRAM

The objective of this study was to evaluate the relationships between various moisture damage test methods for a range of mixture and antistripping agents. To achieve the objective, the experimental program used aggregates and asphalts from eight highway districts in Texas (Figure 1), and 13 commercially available antistripping additives and the hydrated lime. Two basic moisture damage tests were performed on treated and untreated mixtures, which were plant mixtures (mixed in the plant and compacted in the laboratory) and laboratory mixtures (mixed and compacted in the laboratory).

### Materials

#### *Plant Mixtures*

Loose samples of the hot asphalt mixtures used in actual field construction were obtained at the eight asphalt mixing plants. The loose samples were reheated and compacted in the laboratory using a compaction procedure that produced an air

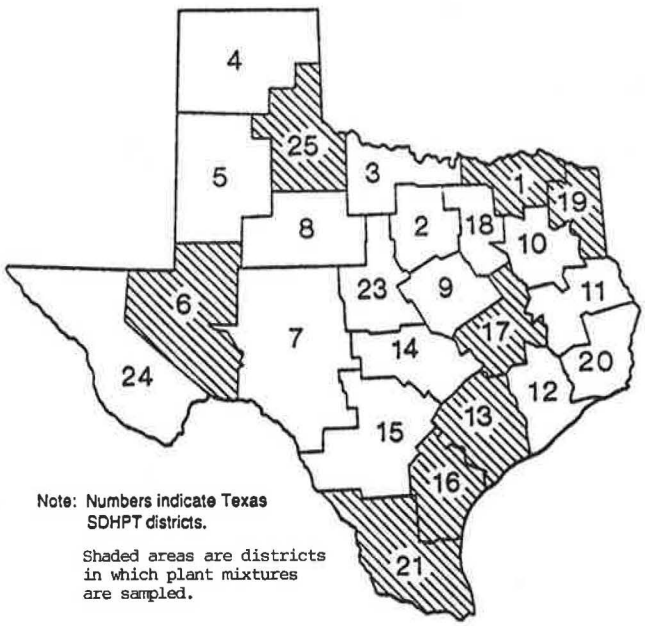


**FIGURE 1 Sampling location of plant mixtures.**

void content of about 7 percent. The types of aggregate and the source and amount of asphalt cement for the plant mixtures are summarized in Table 1. Two or more liquid antistripping additives and hydrated lime were used in each type of plant mixture with identical raw material sources (aggregates and asphalt cement). Fourteen antistripping additives, including hydrated lime, were used in the eight plant mixtures. The actual additive dosages are summarized in Table 2. The percentage of lime is by the total weight of dry aggregates, whereas the percentage of liquid additives is by the weight of asphalt cement.

*Laboratory Mixtures*

The asphalt cements, aggregates, liquid antistripping additives, and hydrated lime were obtained at the asphalt mixing plants. In the laboratory these materials were prepared and mixed using the laboratory mixing procedures in accordance with the mixture design established for the plant mixture. The asphalt cement and additive dosages are summarized in Table 3 for the laboratory-prepared mixtures. The laboratory additive dosage levels are essentially the same as those for the plant mixtures. The liquid additives were blended with the

TABLE 1 SUMMARY OF MATERIALS FOR PLANT MIXTURES

| Location of Field Project | Aggregates | Asphalt | Asphalt Content, % Field + | Design ++ |
|---|---|---|---|---|
| Dist. 17 | .Processed gravel 55%<br>.Washed sand 25%<br>.Coarse sand 10%<br>.Fine sand 10% | .AC-20<br>.Texas Gulf Refinery | 4.9 | 4.9 |
| Dist. 16 | .Field sand 20%<br>.Limestone Screenings 22%<br>.Coarse Limestone 58% | .AC-20<br>.Gulf States Refinery | 5.1 | 4.3 |
| Dist. 13 | .Crushed gravel 50%<br>.Limestone 10%<br>.Limestone screenings 20%<br>.Field Sand 20% | .AC-20<br>.Texas Fuels & Asphalt Refinery | 5.0 | 5.0 |
| Dist. 6 | .Rhyolite 56%<br>.Screening 37%<br>.Field Sand 7% | .AC-20<br>.American Petrofina Refinery | 6.2 | 6.2 |
| Dist. 25 | .Coarse Aggr. 20%<br>.Inter. aggr. 34%<br>.Screening 46% | .AC-20<br>.Diamond Shamrock Refinery | 5.2 | 5.2 |
| Dist. 1 | .Coarse sandstone 55%<br>.Unwashed screenings 30%<br>.Field sand 15% | .AC-20<br>.Total Petroleum Refinery | 5.5 | 6.0 |
| Dist. 19 | .Coarse Aggregate 20%<br>.Inter. Aggregate 40%<br>.Screening 20%<br>.Field sand 20% | .AC-20<br>.Lion Oil Refinery | 5.6 | 5.3 |
| Dist. 21 | .Coarse Aggregate 35%<br>.Uncrushed aggregate 20%<br>.Screening 25%<br>.Field sand 20% | .AC-10<br>.Texas Fuel & Asphalt Coastal Refinery | 5.2 | 5.2 |

\+ Actual asphalt content used for the plant mixtures.
++ Laboratory design optimum asphalt content for the mixture design.

TABLE 2 SUMMARY OF ANTISTRIPPING ADDITIVE DOSAGES FOR PLANT-PREPARED MIXTURES

| Location of Field Project | Additives | Additive Dosage*, % |
|---|---|---|
| District 17 | .Control | 0 |
| | .Lime | 1.5 |
| | .BA 2000 | 1.0 |
| | .Perma-Tac | 1.0 |
| District 16 | .Control | 0 |
| | .Lime | 1.0 |
| | .Aquashield | 0.5 |
| | .Dow Anti-Strip | 0.41 |
| | .Pavebond LP | 0.5 |
| District 13 | .Control | 0 |
| | .Lime | 2.0 |
| | .BA 2000 | 1.0 |
| | .Perma-Tac Plus | 1.0 |
| District 6 | .Control | 0 |
| | .Lime | 1.0 |
| | .Pavebond LP | 1.0 |
| | .Perma-Tac | 1.0 |
| | .Unichem | 0 |
| District 25 | .Control | 0 |
| | .Lime | 1.0 |
| | .Aquashield II | 1.0 |
| | .Fina-A | 1.0 |
| | .Perma-Tac | 1.0 |
| | .Unichem | 1.0 |
| District 1 | .Control | 0 |
| | .Lime | 1.5 |
| | .ARR-MAZ | 0.75 |
| | .Dow Anti-Strip | 0.45 |
| | .Fina-A | 1.0 |
| | .Indulin AS-1 | 1.0 |
| | .Pavebond Special | 1.0 |
| | .Perma-Tac Plus | 1.0 |
| District 19 | .Control | 0 |
| | .Lime | 1.0 |
| | .ARR-MAZ | 1.0 |
| | .Aquashield II | 0.8 |
| | .BA 2000 | 0.5 |
| | .Perma-Tac | 1.0 |
| District 21 | .Control | 0 |
| | .Lime | 1.0 |
| | .ARR-MAZ | 1.0 |
| | .Aquashield II | 0.41 |
| | .Dow Anti-Strip | 0.5 |
| | .Fina-B | 0.41 |
| | .Pavebond LP | 1.0 |
| | .Perma-Tac | 1.0 |

* The percentage of lime is by the total weight of dry aggregates; percentage of liquid additives is by the weight of asphalt cement.

TABLE 3 SUMMARY OF ASPHALT CONTENT AND ADDITIVE DOSAGES FOR LABORATORY-PREPARED MIXTURES

| SDHPT District | Additives | Additive Dosage, * % | Asphalt Content,* * % |
|---|---|---|---|
| 17 | .Control | 0 | |
| | .Lime | 1.5 | 4.9 |
| | .BA 2000 | 1.0 | |
| | .Perma-Tac | 1.0 | |
| 16 | .Control | 0 | |
| | .Lime | 1.0 | |
| | .Aquashield | 0.5 | 4.3 |
| | .Dow Anti-Strip | 0.41 | |
| | .Pavebond LP | 0.5 | |
| 13 | .Control | 0 | |
| | .Lime | 2.0 | 5.0 |
| | .BA 2000 | 1.0 | |
| | .Perma-Tac Plus | 1.0 | |
| | .Control | 0 | |
| | .Lime | 1.0 | |
| 6 | .Pavebond LP | 1.0 | 6.2 |
| | .Perma-Tac | 1.0 | |
| | .Unichem | 0 | |
| 25 | .Control | 0 | |
| | .Lime | 1.0 | |
| | .Aquashield II | 1.0 | 5.2 |
| | .Fina-A | 1.0 | |
| | .Perma-Tac | 1.0 | |
| | .Unichem | 1.0 | |
| 1 | .Control | 0 | |
| | .Lime | 1.5 | |
| | .ARR-MAZ | 0.75 | |
| | .Dow Anti-Strip | 0.45 | 6.0 |
| | .Fina-A | 1.0 | |
| | .Indulin AS-1 | 1.0 | |
| | .Pavebond Special | 1.0 | |
| | .Perma-Tac Plus | 1.0 | |
| 19 | .Control | 0 | |
| | .Lime | 1.0 | 5.3 |
| | .ARR-MAZ | 1.0 | |
| | .Aquashield II | 0.8 | |
| | .BA 2000 | 0.5 | |
| | .Perma-Tac | 1.0 | |
| 21 | .Control | 0 | |
| | .Lime | 1.0 | |
| | .ARR-MAZ | 1.0 | |
| | .Aquashield II | 0.41 | 5.2 |
| | .Dow Anti-Strip | 0.5 | |
| | .Fina-B | 0.41 | |
| | .Pavebond LP | 1.0 | |
| | .Perma-Tac | 1.0 | |

* The percentage of hydrated lime is based on the total weight of dry aggregates: the percentage of liquid additive is based on the weight of the asphalt cement.

* * Asphalt content is percent by weight of total mixture.

preheated asphalt; however, the hydrated lime was placed on the aggregates in a slurry form for all of the lime-treated laboratory mixtures. The specimens were compacted using a procedure that produced an air void content of about 7 percent.

### Moisture Susceptibility Test Methods

The two basic moisture susceptibility test methods compared were the wet-dry indirect tensile test, often referred to as the Lottman test, and the boiling test. There are, however, variations of the wet-dry indirect tensile test. Thus, the following specific test methods were selected for evaluation.

#### *Wet-Dry Indirect Tensile Test*

The indirect tensile test (*1, 2*) was used by Lottman et al. (*3, 4*) for measuring the potential for moisture damage in asphalt mixtures (Figure 2). Subsequently, several techniques for moisture conditioning were developed as modifications of the original Lottman procedure. All methods, however, use the indirect tensile test to determine the tensile strength ratio (*TSR*) of wet and dry specimens as follows:

$$TSR = \frac{S_T(\text{Conditioned})}{S_T(\text{Unconditioned})} \quad (1)$$

where $S_T$ is the indirect tensile strength.

The wet-dry indirect tensile test methods selected for evaluation were as follows:

- Tex-531-C method, a modified Lottman (*5*),
- Modified Tex-531-C method,
- Original Lottman method (*3*), and
- Tunnicliff-Root method (*6, 7*).

The test procedures are described below and are summarized in Table 4.

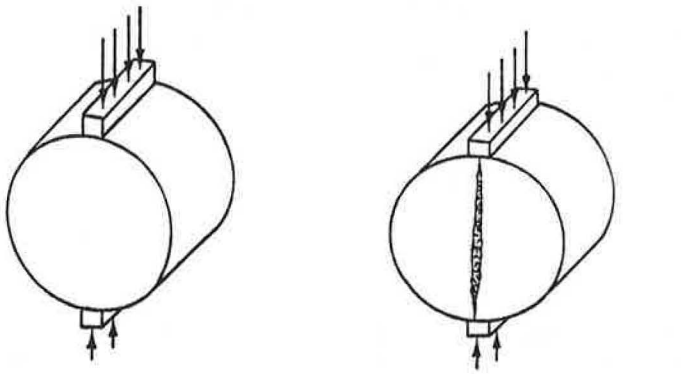

(a) Compressive load being applied. (b) Specimen failing in tension.

**FIGURE 2 Indirect tensile test loading and failure.**

TABLE 4 SUMMARY OF MOISTURE-CONDITIONING PROCEDURE

| Test Method | | |
|---|---|---|
| Tex-531-C | Original Lottman | Tunnicliff-Root |
| .Vacuum saturation to 60-80% filled voids. | .Vacuum saturation using 26-in Hg for 30 min. | .Vacuum saturation to 60-80% filled voids. |
| .Freezing at 0 F for 15 hours. | .Conditioning at 77 F (water bath) for 30 min. | .Soaking at 140 F (water bath) for 24 hours. |
| .Thawing at 140 F (water bath) for 24 hours. | .Freezing at 0 F for 15 hours. | .Conditioning at 77 F (water bath) for 3 hours prior to testing. |
| .Conditioning at 77 F(water bath) for 3 hours prior to testing. | .Thawing at 140 F(water bath) for 24 hours. | |
| | .Conditioning at 77 F (water bath) for 3 hours prior to testing. | |

**Tex-531-C Method** The test method currently used by the Texas State Department of Highways and Public Transportation (SDHPT), the Tex-531-C method, utilizes laboratory-compacted specimens with air void contents of approximately 7 percent. A group of specimens were prepared and compacted using the design aggregates and asphalt. Half of the specimens were tested dry or unconditioned. The other half were conditioned by vacuum saturation with water. A partial vacuum (approximately 15 to 17 in. of mercury) was applied long enough to achieve a degree of saturation of about 70 percent.

The conditioned specimens were placed in a freezer at 0°F for 15 hr, and then placed in a 140°F water bath for 24 hr. After a complete freeze-thaw cycle, the moisture-conditioned specimens were cooled to room temperature in a 77°F water bath for approximately 3 hr before testing. All of the specimens were tested to determine their indirect tensile strength. The ratio of the conditioned strength to the unconditioned (dry) tensile strength is calculated using Equation 1.

**Modified Tex-531-C Method** The Tex-531-C method includes a procedure to account for asphalt absorption. This procedure requires an additional 2 days for curing. Thus, it would be desirable to eliminate this extra time. The mixing and compaction procedures of the Tex-531-C method, with cure and without cure, are summarized in Table 5. The conditioning and testing procedures of the compacted specimens were exactly the same as for the Tex-531-C method.

**Original Lottman Method** In the original Lottman method, the laboratory specimens were fabricated and compacted in the same fashion as for the modified Tex-531-C method. The conditioned specimens, however, were partially saturated under a vacuum of 26 in. of mercury for 30 min rather than for a period of time required to achieve a specified degree of saturation. Subsequently, the wet specimens were placed in a 77°F water bath for 30 min before being subjected to a freeze-thaw cycle. The specimens were frozen at 0°F for 15 hr and then thawed in a 140°F water bath for 24 hr. After a complete freeze-thaw cycle, the wet specimens were cooled to room temperature in a 77°F water bath for approximately 3 hr before testing. All of the wet and dry specimens were then tested to determine their indirect tensile strength.

TABLE 5 SUMMARY OF MIXING AND COMPACTION PROCEDURE

| Procedure | Test Method | |
|---|---|---|
| | Tex-531-Method with Cure (Method A) | Modified Tex-531-C Method without Cure (Method B) |
| Mixing | . Mixing at 300 F<br>. Cooling at room temperature for 2.5 hours<br>. Curing at 140 F for 15 hours | . Mixing at 275 F |
| Molding | . Heating at 250 F for 2 hours<br>. Compacting specimens to 7.0 +/- 1.0% air voids<br>. Cooling the specimens to room temperature | . (Same as Method A) |

**Tunnicliff-Root Method** In the Tunnicliff-Root procedure, the freeze cycle (0°F for 15 hr) used in the Tex-531-C method was eliminated because it was felt that the freeze cycle could cause additional specimen damage over and above that produced by the moisture (*6, 7*). The laboratory specimens were fabricated and compacted to about 7 percent air voids as in the Tex-531-C method. Half of the specimens were partially vacuum-saturated with water to 55 to 80 percent saturation. The conditioned specimens were soaked in a 140°F water bath for 24 hr and then cooled to room temperature in a 77°F water bath for approximately 3 hr before testing. The wet and dry specimens were then tested to determine their indirect tensile strength.

### *Texas Boiling Test*

The Texas boiling test (*5, 8*) involved a visual determination of the extent of stripping of the asphalt from aggregate surfaces after the mixture had been subjected to the action of boiling water for a specified time. To perform this test, an asphalt mixture was prepared at 325°F and boiled in distilled water for 10 min. After boiling, the mixture was allowed to cool, the water was drained, and the mixture was allowed to dry. The mix was examined the following day to estimate the degree of stripping present in the mixture. The stripping test results were reported as the percentage of asphalt retained after boiling.

## Laboratory Testing Program

Moisture susceptibility tests were performed on both the laboratory and plant mixtures. The following tests were conducted on all laboratory mixtures:

- Four wet-dry indirect tensile test methods, and
- Texas boiling test.

Because in plant-prepared mixtures no option exists to account for curing, the procedure is the same with or without cure. Thus, the following tests were used for the plant-mixed and laboratory-compacted samples:

- Three of the wet-dry indirect tensile tests, and
- Texas boiling test.

The treated and untreated mixtures were compacted in the laboratory, and the specimens were prepared for the dry and/or wet conditioning. Eighteen laboratory-mixed and 12 plant-

mixed specimens were prepared for each treatment (or control). Any of the specimens that had air voids outside the 6 to 8 percent range were discarded, and new specimens were prepared and compacted.

The Texas boiling test was performed on the loose laboratory-prepared mixtures and the reheated plant mixtures.

### Engineering Properties Analyzed

The engineering properties analyzed were the indirect tensile strength, tensile strength ratio, and percentage of asphalt retained (boil test).

#### *Tensile Strength*

The indirect tensile strength is the maximum tensile stress the specimen can withstand. For 4-in.–diameter specimens and the load-deformation information obtained from the static test, tensile strength can be calculated from the following relationship:

$$S_T = \frac{0.156P}{t} \tag{2}$$

where

$S_T$ = tensile strength (psi),
$P$ = the maximum load carried by the specimen (lb), and
$t$ = thickness or height of the specimen (in.).

#### *Tensile Strength Ratio*

The tensile strength ratio was defined in Equation 1.

#### *Boil Value*

The boiling test value is expressed as the percentage of asphalt retained after boiling. The value is visually estimated by two independent operators according to the degree of stripping present in the mixture.

## EXPERIMENTAL RESULTS

The test results obtained for the laboratory-prepared mixtures and the plant-mixed/laboratory-compacted mixtures are summarized as follows.

### Wet-Dry Indirect Tensile Test Results

#### *Laboratory Mixture*

The four test methods (Tex-531-C with cure, Tex-531-C without cure, original Lottman, and Tunnicliff-Root) were conducted for the laboratory mixture. Tensile strength ratios (TSRs) were obtained for these test methods by dividing the average tensile strength of the three wet specimens by the average tensile strength of the three dry specimens. These TSR values are summarized in Table 6.

#### *Plant Mixture*

Three test methods (Tex-531-C without cure, original Lottman, and Tunnicliff-Root) were used to evaluate the plant mixture. TSRs were obtained for these test methods by dividing the average tensile strength of the three wet specimens by the average tensile strength of the three dry specimens. These TSR values are summarized in Table 7.

### Texas Boiling Test Results

#### *Laboratory Mixture*

For the boiling test, the boiled mixture was allowed to dry and examined the following day. The percentage of asphalt retained after boiling was estimated independently by two operators at different times. The average value of the two ratings was reported as the degree of stripping present in the mixture. The test results are summarized in Table 8.

#### *Plant Mixture*

Representative loose plant mixtures were used for the boiling test. The same procedure was followed as described for the laboratory mixture. These test results are also summarized in Table 8.

### Comparison of Moisture Damage Test Values

Because of the concern with asphalt absorption during the mixing stage of sample preparation in the laboratory, the effect of curing on the moisture susceptibility of the laboratory mixture was analyzed and is discussed first here for the modified Lottman (Tex-531-C) procedure.

#### *Effect of Curing for Modified Lottman (Tex-531-C) Procedure*

The results from the Tex-531-C method with and without cure are compared in Figures 3–10 for the eight projects. Test values from the Tex-531-C method with cure and the Tex-531-C method without cure are essentially equal with the exception of the values for lime-treated material in District 19. The test values for all laboratory mixtures are compared in Figure 11. These data indicate that curing the laboratory mixtures does not have a significant effect on the estimated moisture susceptibility values (TSR values). Thus, the time required for testing in the laboratory can possibly be shortened significantly. The linear regression relationship between the two sets of TSR values approximates the line of equality, and the $R^2$ value of .86 indicates a reasonably good correlation.

TABLE 6 SUMMARY OF TSR TEST RESULTS FOR LABORATORY MIXTURES

| District | Additive Name | Tensile Strength Ratio (TSR) | | | |
|---|---|---|---|---|---|
| | | Tex-531-C with Cure | Tex-531-C w/o Cure | Original Lottman | Tunnicliff-Root |
| 17 | No Additive | 0.51 | 0.51 | 0.47 | 0.52 |
| | Lime | 1.18 | 1.19 | 1.12 | 1.23 |
| | BA 2000 | 0.82 | 0.96 | 0.88 | 1.09 |
| | Perma-Tac | 0.82 | 0.94 | 0.91 | 0.97 |
| 16 | No Additive | 0.44 | 0.47 | 0.44 | 0.53 |
| | Lime | 0.74 | 0.83 | 0.77 | 0.93 |
| | Aquashield | 0.56 | 0.62 | 0.60 | 0.70 |
| | Dow | 0.53 | 0.58 | 0.45 | 0.68 |
| | Pavebond LP | 0.60 | 0.55 | 0.57 | 0.67 |
| 13 | No Additive | 0.43 | 0.55 | 0.53 | 0.70 |
| | Lime | 1.42 | 1.27 | 1.22 | 1.26 |
| | BA 2000 | 0.64 | 0.66 | 0.79 | 0.29 |
| | Perma-Tac | 0.61 | 0.69 | 0.78 | 0.88 |
| 6 | No Additive | 0.20 | 0.23 | 0.15 | 0.32 |
| | Lime | 0.78 | 0.62 | 0.58 | 0.78 |
| | Pavebond LP | 0.40 | 0.35 | 0.26 | 0.42 |
| | Perma-Tac | 0.49 | 0.37 | 0.30 | 0.42 |
| | Unichem | 0.37 | 0.42 | 0.30 | 0.54 |
| 25 | No Additive | 0.67 | 0.62 | 0.46 | 0.64 |
| | Lime | 1.30 | 1.23 | 0.93 | 1.07 |
| | Aquashield II | 1.19 | 1.23 | 0.82 | 1.01 |
| | Fina-A | 0.98 | 1.18 | 0.82 | 1.01 |
| | Perma-Tac | 1.03 | 0.97 | 0.70 | 0.86 |
| | Unichem | 0.92 | 1.02 | 0.72 | 0.87 |
| 1 | No Additive | 0.74 | 0.96 | 0.80 | 1.01 |
| | Lime | 1.06 | 1.22 | 1.14 | 1.24 |
| | ARR-MAZ | 1.14 | 1.26 | 1.14 | 1.29 |
| | Dow | 0.70 | 0.85 | 0.82 | 0.95 |
| | Fina-A | 1.10 | 1.10 | 1.10 | 1.20 |
| | Indulin AS-1 | 1.07 | 1.14 | 1.17 | 1.22 |
| | PVBD Special | 1.21 | 1.37 | 1.50 | 1.42 |
| | Perma-Tac Plus | 1.15 | 1.15 | 0.94 | 1.13 |
| 19 | No Additive | 1.12 | 1.07 | 0.93 | 0.98 |
| | Lime | 1.07 | 1.53 | 1.45 | 1.64 |
| | ARR-MAZ | 1.19 | 1.09 | 0.99 | 1.20 |
| | Aquashield II | 1.25 | 1.24 | 1.11 | 1.36 |
| | BA2000 | 1.16 | 1.07 | 1.22 | 1.30 |
| | Perma-Tac | 0.93 | 1.17 | 1.03 | 1.03 |
| 21 | No Additive | 0.24 | 0.28 | 0.22 | 0.77 |
| | Lime | 1.04 | 1.06 | 1.04 | 21.07 |
| | ARR-MAZ | 0.52 | 0.48 | 0.39 | 0.55 |
| | Aquashield II | 0.73 | 0.76 | 0.54 | 0.74 |
| | Dow | 0.35 | 0.37 | 0.30 | 0.37 |
| | Fina-B | 0.45 | 0.88 | 0.59 | 0.78 |
| | Pavebond LP | 0.51 | 0.55 | 0.53 | 0.58 |
| | Perma-Tac | 0.47 | 0.52 | 0.39 | 0.49 |

TABLE 7 SUMMARY OF TSR TEST RESULTS FOR PLANT-MIXED/ LABORATORY-COMPACTED MIXTURES

| District | Additive Name | Tensile Strength Ratio (TSR) | | |
|---|---|---|---|---|
| | | Tex-531-C Method | Original Lottman | Tunnicliff-Root |
| 17 | No Additive | 0.64 | 0.51 | 0.61 |
| | Lime | 1.18 | 1.01 | 1.09 |
| | BA 2000 | 1.07 | 0.98 | 1.01 |
| | Perma-Tac | 0.51 | 0.43 | 0.50 |
| 16 | No Additive | 0.79 | 0.72 | 0.87 |
| | Lime | 1.02 | 0.87 | 1.01 |
| | Aquashield | 0.87 | 0.76 | 0.87 |
| | Dow | 0.75 | 0.72 | 0.87 |
| | Pavebond LP | 0.77 | 0.75 | 0.90 |
| 13 | No Additive | 1.03 | 1.02 | 0.98 |
| | Lime | 1.03 | 1.02 | 0.97 |
| | BA 2000 | 1.08 | 0.96 | 0.99 |
| | Perma-Tac | 1.00 | 0.98 | 0.96 |
| 6 | No Additive | 0.47 | 0.38 | 0.54 |
| | Lime | 0.54 | 0.43 | 0.66 |
| | Pavebond LP | 0.83 | 0.66 | 0.80 |
| | Perma-Tac | 0.78 | 0.65 | 0.85 |
| | Unichem | 0.64 | 0.61 | 0.78 |
| 25 | No Additive | 0.60 | 0.44 | 0.64 |
| | Lime | 0.89 | 0.76 | 0.90 |
| | Aquashield II | 0.60 | 0.48 | 0.63 |
| | Fina-A | 0.85 | 0.79 | 0.96 |
| | Perma-Tac | 0.76 | 0.63 | 0.76 |
| | Unichem | 0.75 | 0.67 | 0.78 |
| 1 | No Additive | 1.06 | 0.97 | 1.07 |
| | Lime | 1.12 | 1.27 | 1.12 |
| | ARR-MAZ | 1.10 | 1.23 | 1.16 |
| | Dow | 0.97 | 0.95 | 0.96 |
| | Fina-A | 1.12 | 1.20 | 1.15 |
| | Indulin AS-1 | 1.10 | 1.22 | 1.19 |
| | PVBD Special | 1.15 | 1.24 | 1.19 |
| | Perma-Tac Plus | 1.02 | 1.07 | 1.12 |
| 19 | No Additive | 0.73 | 0.75 | 0.80 |
| | Lime | 1.11 | 1.16 | 1.21 |
| | ARR-MAZ | 1.12 | 1.08 | 1.08 |
| | Aquashield II | 1.16 | 1.24 | 1.17 |
| | BA 2000 | 1.21 | 1.26 | 1.27 |
| | Perma-Tac | 1.01 | 1.14 | 1.15 |
| 21 | No Additive | 0.23 | 0.28 | 0.26 |
| | Lime | 0.17 | 0.19 | 0.19 |
| | ARR-MAZ | 0.39 | 0.41 | 0.40 |
| | Aquashield II | 0.47 | 0.53 | 0.50 |
| | Dow | 0.30 | 0.30 | 0.29 |
| | Fina-B | 0.56 | 0.65 | 0.56 |
| | Pavebond LP | 0.51 | 0.59 | 0.51 |
| | Perma-Tac | 0.42 | 0.49 | 0.44 |

TABLE 8 SUMMARY OF TEXAS BOILING TEST RESULTS

| District | Additive Name | Asphalt Retained After Boiling, % | |
|---|---|---|---|
| | | Lab Mix | Plant Mix |
| 17 | No Additive | 50.0 | 52.5 |
| | Lime | 85.0 | 94.0 |
| | BA 2000 | 92.5 | 92.5 |
| | Perma-Tac | 90.0 | 50.0 |
| 16 | No Additive | 77.5 | 82.5 |
| | Lime | 75.0 | 82.5 |
| | Aquashield | 77.5 | 85.0 |
| | Dow | 77.5 | 85.0 |
| | Pavebond LP | 77.5 | 85.0 |
| 13 | No Additive | 77.5 | 77.5 |
| | Lime | 96.5 | 96.5 |
| | BA 2000 | 97.5 | 96.5 |
| | Perma-Tac | 96.5 | 95.0 |
| 6 | No Additive | 50.0 | 70.0 |
| | Lime | 72.5 | 72.5 |
| | Pavebond LP | 60.0 | 85.0 |
| | Perma-Tac | 65.0 | 80.0 |
| | Unichem | 67.5 | 85.0 |
| 25 | No Additive | 50.0 | 77.5 |
| | Lime | 85.0 | 87.5 |
| | Aquashield II | 96.5 | 77.5 |
| | Fina-A | 94.0 | 94.0 |
| | Perma-Tac | 90.0 | 92.5 |
| | Unichem | 94.0 | 87.5 |
| 1 | No Additive | 82.5 | 90.0 |
| | Lime | 92.5 | 92.5 |
| | ARR-MAZ | 90.0 | 97.5 |
| | Dow | 82.5 | 91.5 |
| | Fina-A | 92.5 | 95.0 |
| | Indulin AS-1 | 92.5 | 96.5 |
| | PVBD Special | 92.5 | 95.0 |
| | Perma-Tac Plus | 92.5 | 95.0 |
| 19 | No Additive | 85.0 | 85.0 |
| | Lime | 94.0 | 90.0 |
| | ARR-MAZ | 92.5 | 90.0 |
| | Aquashield II | 92.5 | 94.0 |
| | BA 2000 | 92.5 | 96.5 |
| | Perma-Tac | 92.5 | 90.0 |
| 21 | No Additive | 37.5 | 25.0 |
| | Lime | 81.0 | 37.5 |
| | ARR-MAZ | 55.0 | 57.5 |
| | Aquashield II | 77.5 | 67.5 |
| | Dow | 57.5 | 52.5 |
| | Fina-B | 80.0 | 75.0 |
| | Pavebond LP | 65.0 | 67.5 |
| | Perma-Tac | 55.0 | 61.0 |

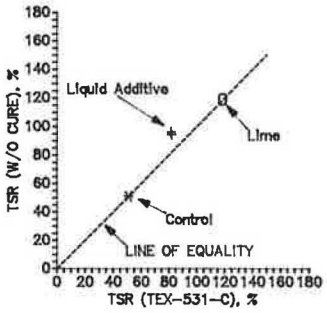


**FIGURE 3 Effect of curing on TSR values for Tex-531-C procedure, District 17 (river gravel aggregate).**

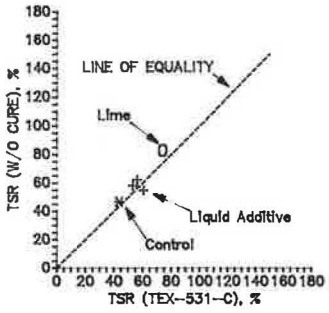


**FIGURE 4 Effect of curing on TSR values for Tex-531-C procedure, District 16 (limestone aggregate).**

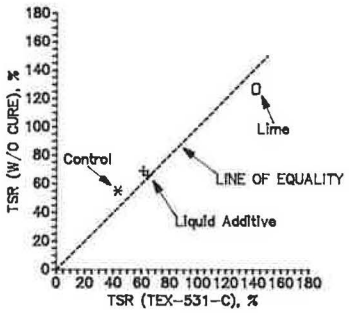


**FIGURE 5 Effect of curing on TSR values for Tex-531-C procedure, District 13 (crushed gravel aggregate).**

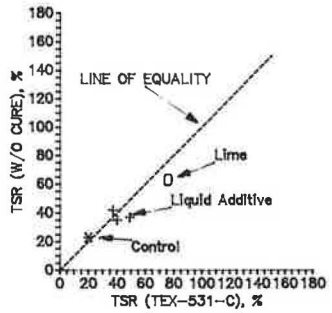


**FIGURE 6 Effect of curing on TSR values for Tex-531-C procedure, District 6 (rhyolite aggregate).**

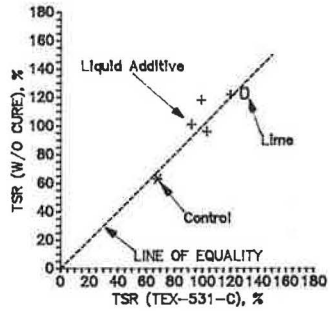


**FIGURE 7 Effect of curing on TSR values for Tex-531-C procedure, District 25 (crushed gravel aggregate).**

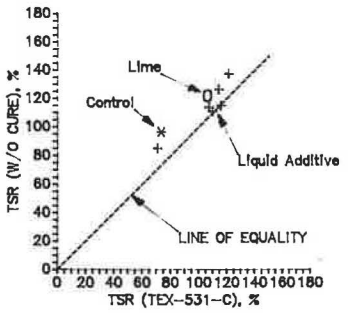


**FIGURE 8 Effect of curing on TSR values for Tex-531-C procedure, District 1 (crushed sandstone aggregate).**

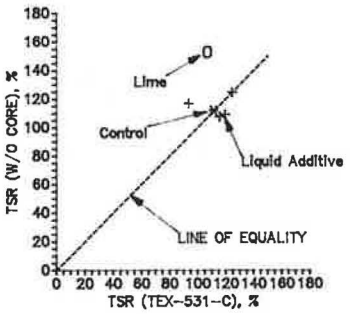


**FIGURE 9 Effect of curing on TSR values for Tex-531-C procedure, District 19 (crushed gravel aggregate).**

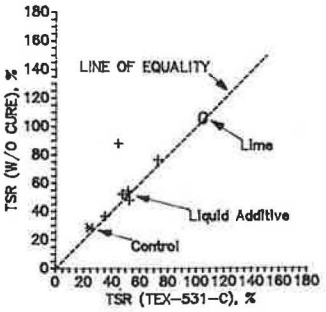


**FIGURE 10 Effect of curing on TSR values for Tex-531-C procedure, District 21 (crushed gravel aggregate).**

*Comparison of Tensile Strength Ratios*

The TSR values obtained using the various wet-dry indirect tensile test methods were evaluated and compared.

Comparisons of the TSR values for laboratory mixtures are shown in Figures 12–19 for the modified Lottman (Tex-531-C), the original Lottman, and the Tunnicliff-Root test methods. All tests were compared to the modified Lottman procedure used by the Texas SDHPT. As shown in the figures, the original Lottman test procedure was more severe than the other test methods evaluated as evidenced by the lower TSR values. The TSR values for the Tunnicliff-Root procedure tended to be approximately equal to or slightly less than the TSR values for the modified Lottman procedure.

For the plant mixture, the results were similar to the results obtained for the laboratory mixtures (Figures 20–27). Thus, the test methods, ranked in decreasing order of severity are as follows:

1. Original Lottman,
2. Modified Lottman, and
3. Tunnicliff-Root.

The severity of the original Lottman test is attributed to the high degree of saturation of the specimens produced by

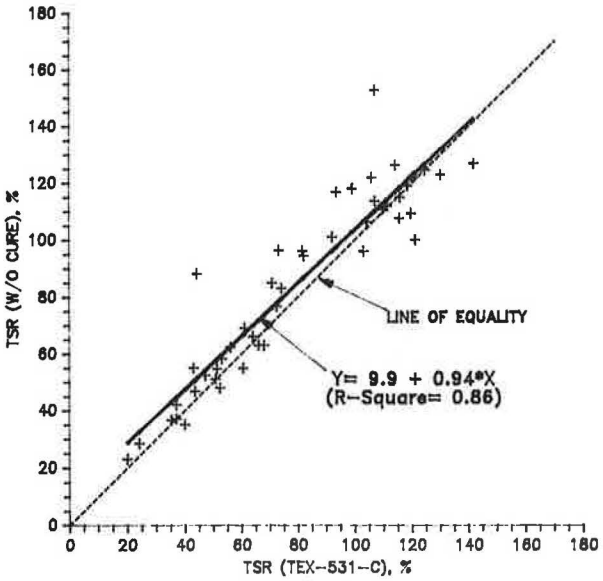


**FIGURE 11 Effect of curing on TSR values for Tex-531-C procedure, all projects.**

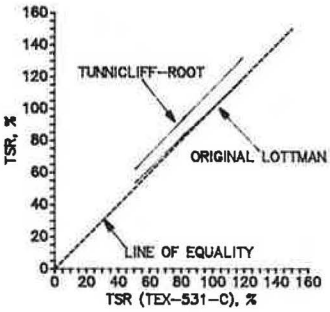


**FIGURE 12 Comparison of TSR values for laboratory mixtures, District 17 (river gravel aggregate).**

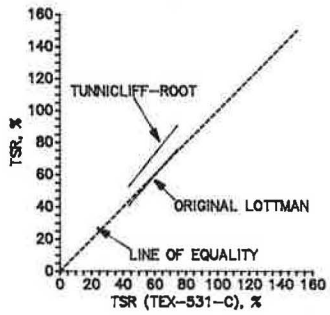


**FIGURE 13 Comparison of TSR values for laboratory mixtures, District 16 (limestone aggregate).**

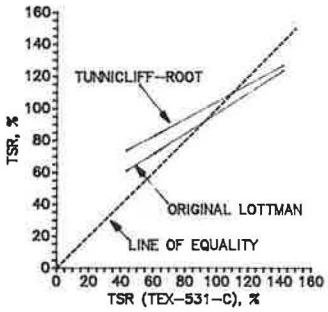


**FIGURE 14 Comparison of TSR values for laboratory mixtures, District 13 (crushed gravel and limestone).**

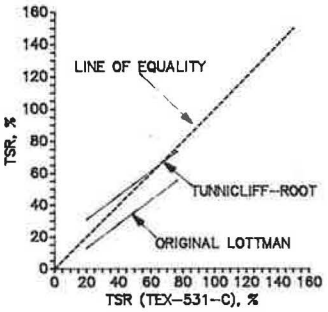


**FIGURE 15 Comparison of TSR values for laboratory mixtures, District 6 (rhyolite aggregate).**

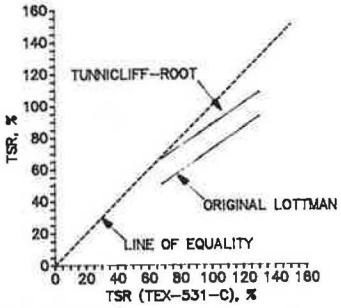


**FIGURE 16 Comparison of TSR values for laboratory mixtures, District 25 (crushed gravel aggregate).**

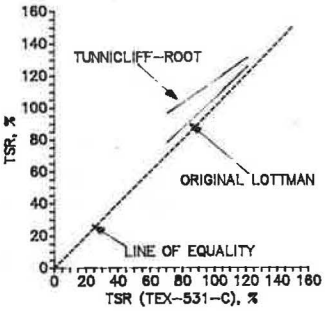


**FIGURE 17 Comparison of TSR values for laboratory mixtures, District 1 (crushed sandstone aggregate).**

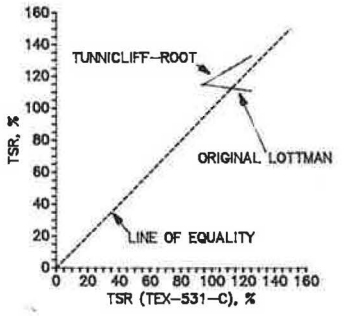


**FIGURE 18 Comparison of TSR values for laboratory mixtures, District 19 (crushed gravel aggregate).**

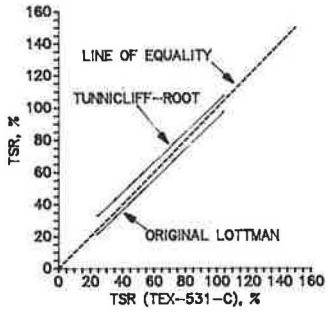


**FIGURE 19 Comparison of TSR values for laboratory mixtures, District 21 (crushed gravel aggregate).**

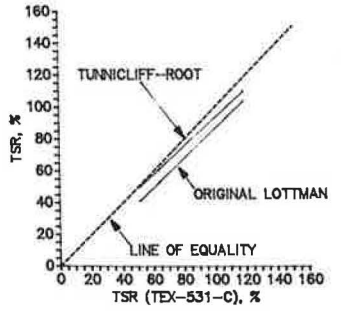


**FIGURE 20 Comparison of TSR values for plant mixtures, District 17 (river gravel aggregate).**

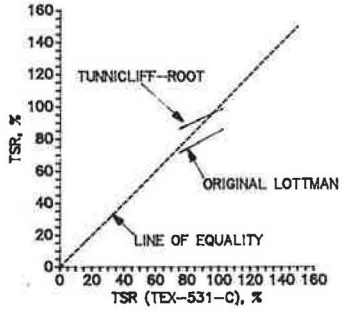


**FIGURE 21 Comparison of TSR values for plant mixtures, District 16 (limestone aggregate).**

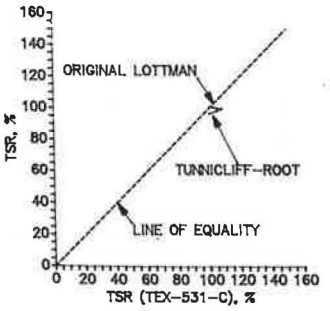


**FIGURE 22 Comparison of TSR values for plant mixtures, District 13 (crushed gravel and limestone).**

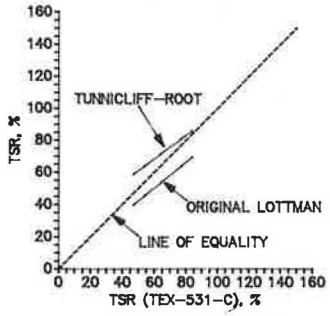


**FIGURE 23 Comparison of TSR values for plant mixtures, District 6 (rhyolite aggregate).**

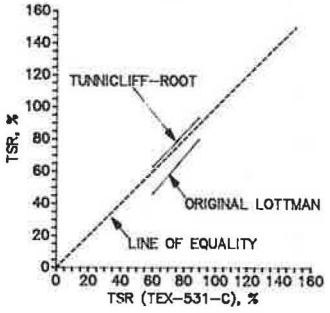


**FIGURE 24 Comparison of TSR values for plant mixtures, District 25 (crushed gravel aggregate).**

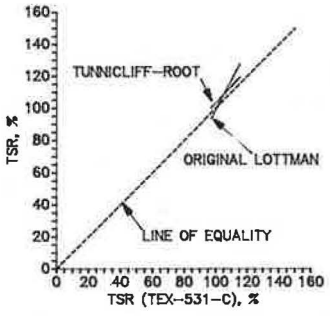


**FIGURE 25 Comparison of TSR values for plant mixtures, District 1 (crushed sandstone aggregate).**

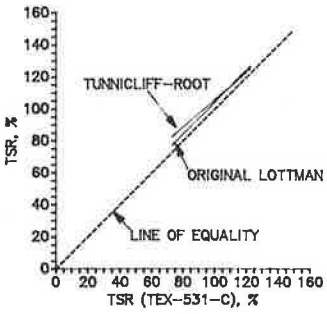


**FIGURE 26 Comparison of TSR values for plant mixtures, District 19 (crushed gravel aggregate).**

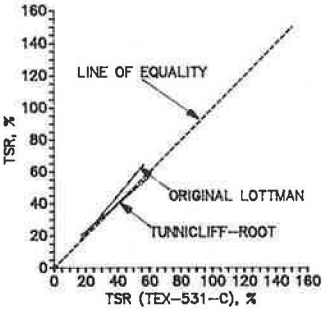


**FIGURE 27 Comparison of TSR values for plant mixtures, District 21 (crushed gravel aggregate).**

the vacuum saturation procedure. In the modified Lottman test (Tex-531-C), the degree of saturation is controlled between 60 and 80 percent and thus results in less damage. In the Tunnicliff-Root method, the degree of saturation is also controlled between 55 and 80 percent, but no freeze cycle is used, and the specimens are conditioned with only a warm (140°F) water bath; thus, damage due to freezing is eliminated.

### *Correlations of TSR Values with Modified Lottman TSR Values*

**Laboratory Mixtures** The laboratory mixture TSR values for the original Lottman and Tunnicliff-Root methods were correlated with the modified Lottman (Tex-531-C) TSR values as shown in Figures 28 and 29. For each comparison (e.g., the original Lottman versus the modified Lottman) there are two correlation relationships shown for the two sets of data. One regresses the original Lottman data on the modified Lottman data. The other regresses the modified Lottman data on the original Lottman data. These correlations are reasonably good. The $R^2$ values range from .67 to .79.

**Plant Mixtures** The TSR values for the original Lottman and Tunnicliff-Root procedures are compared with the modified Lottman TSR values as shown in Figures 30 and 31. For each comparison, two regression equations are shown as previously discussed. The $R^2$ values are very high, ranging from

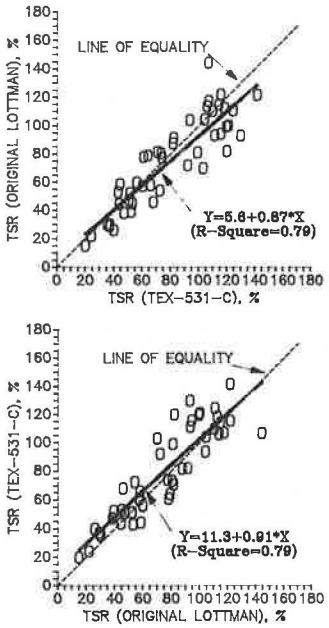


**FIGURE 28 Correlation of original Lottman TSR values with Tex-531-C TSR values, laboratory mixtures.**

.91 to .95. Excellent correlations are obtained between the original Lottman, the Tunnicliff-Root, and the modified Lottman methods for the plant mixtures.

**Laboratory and Plant Mixtures** Combining the TSR values from the laboratory and plant mixtures for all eight proj-

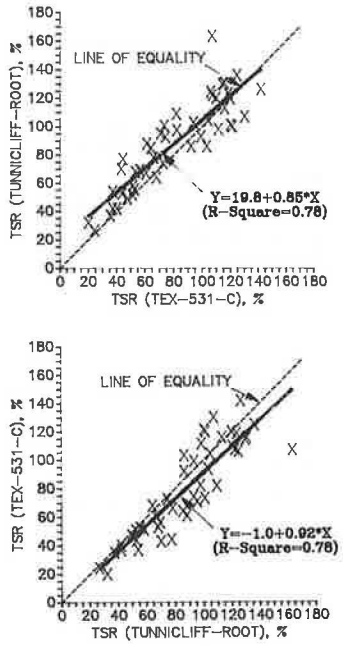


**FIGURE 29 Correlation of Tunnicliff-Root TSR values with Tex-531-C TSR values, laboratory mixtures.**

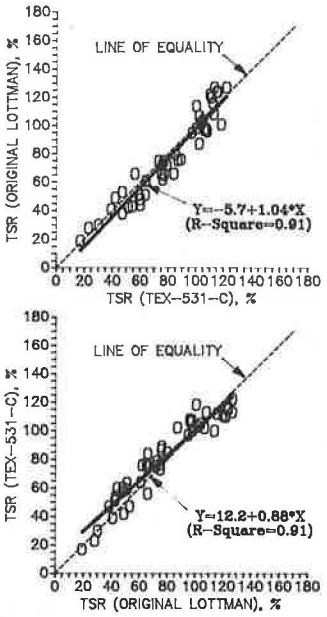


**FIGURE 30 Correlation of original Lottman TSR values with Tex-531-C TSR values, plant mixtures.**

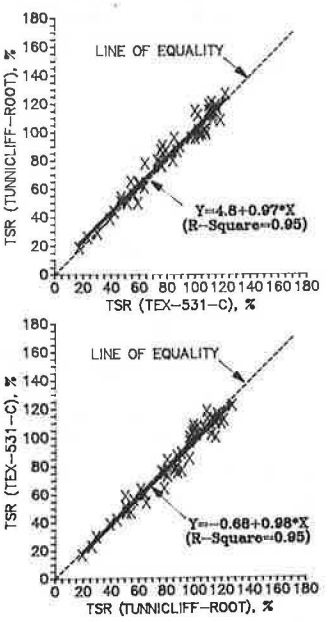


**FIGURE 31 Correlation of Tunnicliff-Root TSR values with Tex-531-C TSR values, plant mixtures.**

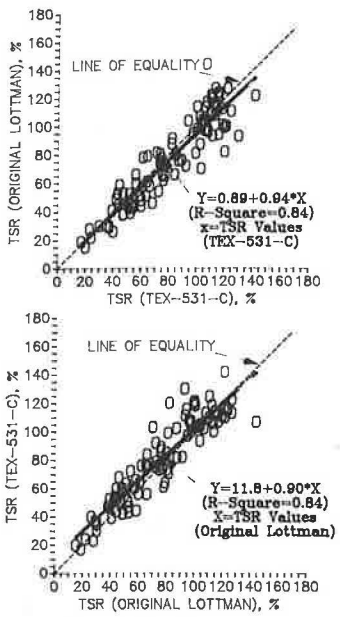


**FIGURE 32 Correlation of original Lottman TSR values with Tex-531-C TSR values, all projects.**

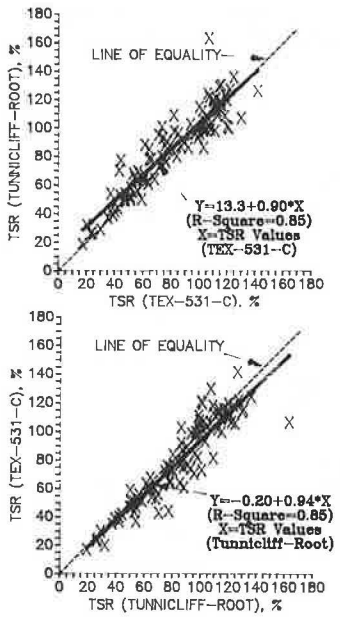


**FIGURE 33 Correlation of Tunnicliff-Root TSR values with Tex-531-C TSR values, all projects.**

ects produces correlations between the TSR values for both the original Lottman and Tunnicliff-Root procedures and the modified Lottman values, as shown in Figures 32 and 33. The correlation equations are also summarized in Table 9 for the comparisons between the original Lottman, the Tunnicliff-Root, and the modified Lottman methods. Good correlations appear, with the $R^2$ values ranging from .84 to .85. Therefore, the TSR values for the modified Lottman procedure can be estimated using the TSR values obtained from either the original Lottman or the Tunnicliff-Root procedures, and vice versa, according to the equations in Table 9.

### *Comparison of Boil Values with TSR Values*

Two types of correlations were developed between the boiling test results and the TSR values; the first regresses the TSR values on the boil values (Figures 34–37 and 38–40), and the

TABLE 9 SUMMARY OF CORRELATION EQUATIONS OF TSR VALUES FOR VARIOUS TEST METHODS

| Correlation | Correlation Equation | $R^2$ Value |
|---|---|---|
| Original Lottman vs. Modified Lottman | C (TSR) = 0.89 + 0.94*A(TSR) or A (TSR) = 11.8 + 0.90*C(TSR) | 0.84 |
| Tunnicliff-Root vs. Modified Lottman | D (TSR) = 13.3 + 0.90*A(TSR) or A (TSR) = 0.20 + 0.94*D(TSR) | 0.85 |

A(TSR) = TSR values of the modified Lottman (Tex-531-C) method, %
C(TSR) = TSR values of the original Lottman method, %
D(TSR) = TSR values of the Tunnicliff-Root method, %

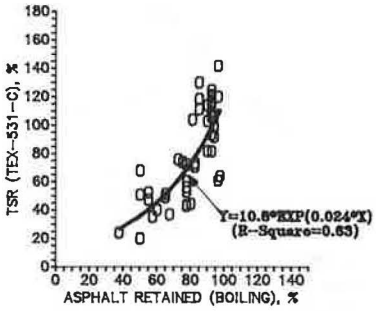


FIGURE 34 Correlation of Tex-531-C TSR values with boiling test results, laboratory mixtures.

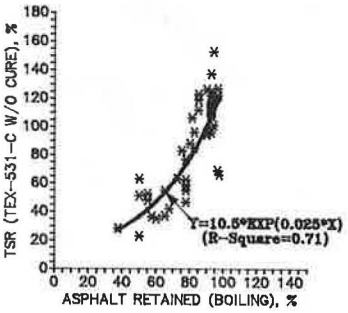


FIGURE 35 Correlation of Tex-531-C (without cure) TSR values with boiling test results, laboratory mixtures.

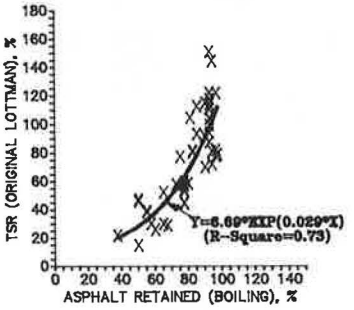


FIGURE 36 Correlation of original Lottman TSR values with boiling test results, laboratory mixtures.

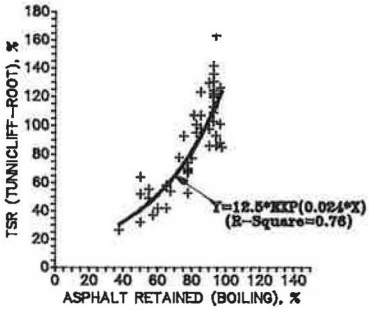


FIGURE 37 Correlation of Tunnicliff-Root TSR values with boiling test results, laboratory mixtures.

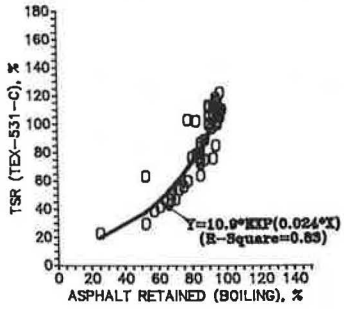


FIGURE 38 Correlation of boiling test results with Tex-531-C TSR values, plant mixtures.

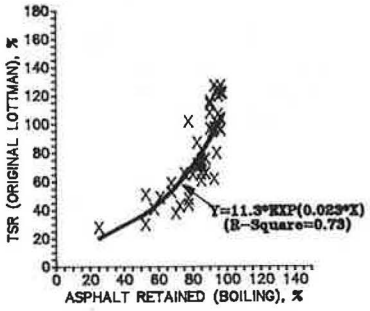


FIGURE 39 Correlation of boiling test results with original Lottman TSR values, plant mixtures.

second regresses the boil values on the TSR values (Figures 41–44 and 45–47). The correlation relationships were developed using the logarithmic transformation of the TSR data and correlating it with the boil values using linear regression.

**Laboratory Mixtures** The relationships between the boiling test results and each of the three TSR test methods for the laboratory mixture are shown in Figures 34–37 and 41–44. The $R^2$ values range from .63 to .76.

**Plant Mixtures** The relationships between the boiling test results and each of the three TSR test methods are shown

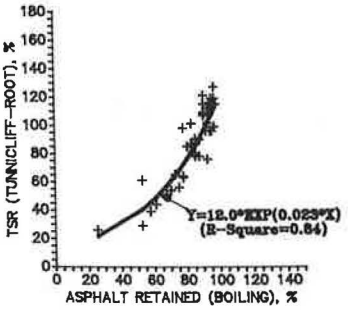


**FIGURE 40 Correlation of boiling test results with Tunnicliff-Root TSR values, plant mixtures.**

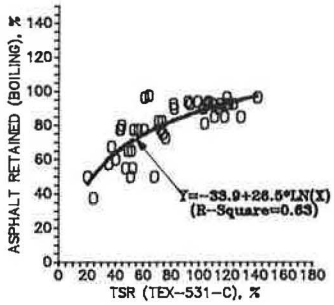


**FIGURE 41 Correlation of Tex-531-C TSR values with boiling test results, laboratory mixtures.**

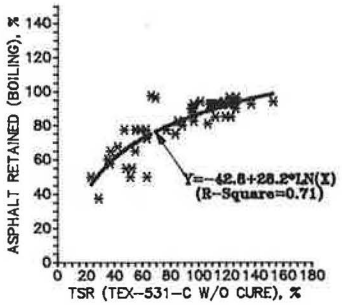


**FIGURE 42 Correlation of Tex-531-C (without cure) TSR values with boiling test results, laboratory mixtures.**

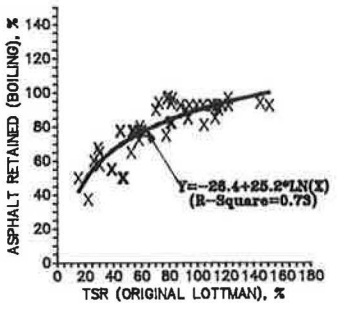


**FIGURE 43 Correlation of original Lottman TSR values with boiling test results, laboratory mixtures.**

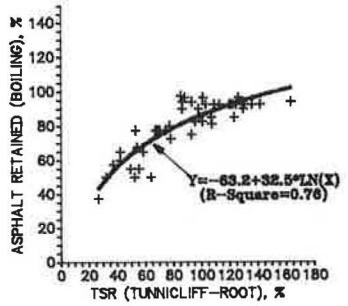


**FIGURE 44 Correlation of Tunnicliff-Root TSR values with boiling test results, laboratory mixtures.**

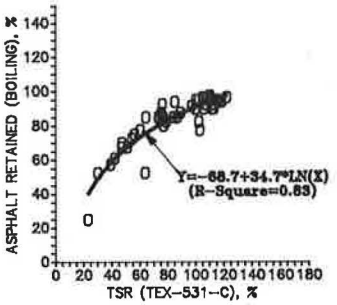


**FIGURE 45 Correlation of Tex-531-C TSR values with boiling test results, plant mixture.**

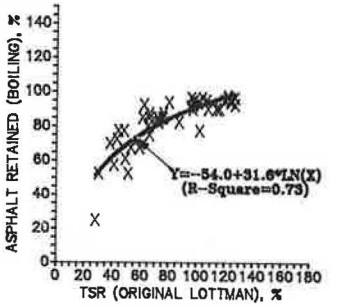


**FIGURE 46 Correlation of original Lottman TSR values with boiling test results, plant mixtures.**

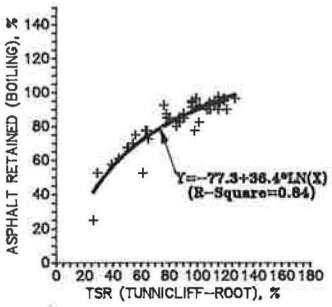


**FIGURE 47 Correlation of Tunnicliff-Root TSR values with boiling test results, plant mixtures.**

in Figures 38–40 and 45–47. The $R^2$ values range from .73 to .84.

**Laboratory and Plant Mixtures** The correlations between the boiling test results and the TSR values were developed using the test values from both the laboratory and plant mixtures for all eight projects. The first type of correlation is shown in Figures 48–50, and the second type is shown in Figures 51–53 for each of the three TSR test methods. The $R^2$ values range from .71 to .79. Therefore, the correlations are reasonably good between the TSR values and the boil values using the logarithmic transformation of the TSR data.

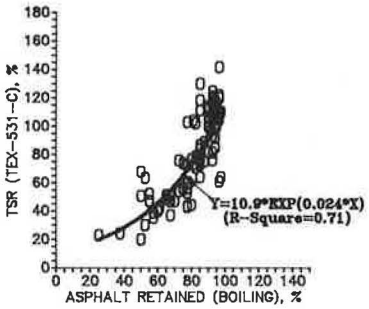


**FIGURE 48 Correlation of boiling test results with Tex-531-C TSR values, all projects.**

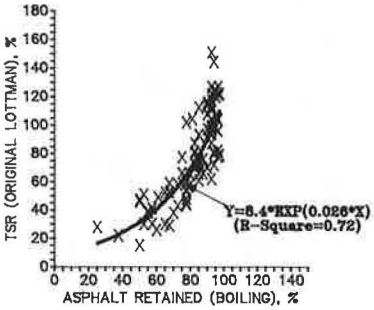


**FIGURE 49 Correlation of boiling test results with original Lottman TSR values, all projects.**

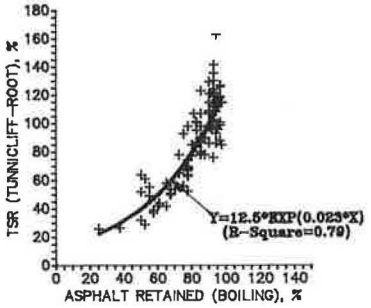


**FIGURE 50 Correlation of boiling test results with Tunnicliff-Root TSR values, all projects.**

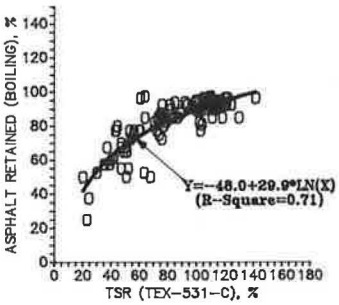


**FIGURE 51 Correlation of Tex-531-C TSR values with boiling test results, all projects.**

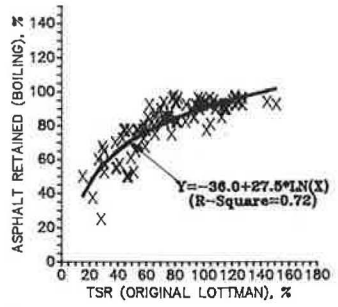


**FIGURE 52 Correlation of original Lottman TSR values with boiling test results, all projects.**

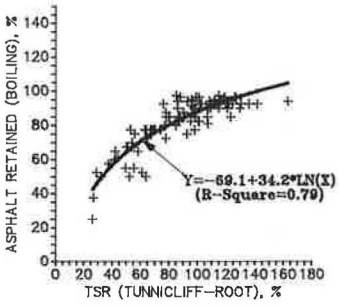


**FIGURE 53 Correlation of Tunnicliff-Root TSR values with boiling test results, all projects.**

## CONCLUSIONS

The conclusions based on the data and analyses from this study are summarized.

- The moisture susceptibility test methods in the decreasing order of severity were as follows:

1. Original Lottman method,
2. Tex-531-C method, and
3. Tunnicliff-Root method.

- Good correlations were obtained between the TSR values of the modified Lottman and both the original Lottman and the Tunnicliff-Root procedures. The $R^2$ values ranged from .84 to .85.
- With regard to the asphalt absorption during the mixing stage of sample preparation in the laboratory, the effect of curing on TSR values specified by the modified Lottman procedure was not significant. Thus, the time required for testing moisture damage could possibly be shortened significantly.
- The correlations between the boiling test results and the TSR values were reasonably good. The $R^2$ values ranged from .71 to .79.
- Because the various test methods produce different levels of damage as measured by the tensile strength ratios, the acceptance criteria should be different for evaluating the moisture damage potential of asphalt-aggregate mixtures.

## ACKNOWLEDGMENTS

Funding for this research was provided by the Texas SDHPT and FHWA. The study was conducted at the Center for Transportation Research of the University of Texas, Austin. The research reported here was part of the second author's Ph.D. dissertation on the evaluation of stripping and moisture damage in asphalt pavements.

## REFERENCES

1. T. W. Kennedy. Characterization of Asphalt Pavement Materials Using the Indirect Tensile Test. *Proc., Association of Asphalt Paving Technologists*, Vol. 46, 1977.
2. J. N. Anagnos and T. W. Kennedy. *Practical Method for Conducting the Indirect Tensile Test.* Research Report 98-10. Center for Highway Research, University of Texas, Austin, Aug. 1972.
3. R. P. Lottman. *Predicting Moisture-Induced Damage to Asphalt-Concrete.* Report 192. NCHRP, 1978.
4. R. P. Lottman. Laboratory Test Method for Predicting Moisture-Induced Damage to Asphalt Concrete. In *Transportation Research Record 843*, TRB, National Research Council, Washington, D.C., 1982.
5. *Manual of Testing Procedures.* Bituminous Section. Texas State Department of Highways and Public Transportation, Austin, 1983.
6. D. G. Tunnicliff and R. E. Root. Antistripping Additives in Asphalt Concrete for Effectiveness of Antistripping Additives. *Proc., Association of Asphalt Paving Technologists*, Vol. 53, 1983.
7. D. G. Tunnicliff and R. E. Root. *NCHRP Report 274: Use of Antistripping Additives in Asphaltic Concrete Mixtures—Laboratory Phase.* TRB, National Research Council, Washington, D.C., 1984.
8. T. W. Kennedy, F. L. Roberts, and K. W. Lee. Evaluating Moisture Susceptibility of Asphalt Mixtures Using the Texas Boiling Test. In *Transportation Research Record 968*, TRB, National Research Council, Washington, D.C., 1984.

*Publication of this paper sponsored by Committee on Characteristics of Bituminous Materials.*

# Evaluation of Effectiveness of Antistrip Additives Using Fuzzy Set Procedures

KWANG W. KIM AND SERJI AMIRKHANIAN

Asphalt concrete pavement layers are sometimes weakened by moisture when the adhesive bond between the aggregate surface and the asphalt cement is broken. The problem of stripping, or disbonding of asphalt cement from aggregates in asphaltic concrete mixtures, has produced serious pavement distress, has increased pavement maintenance, and has resulted in poor pavement performance. Use of antistrip additive is often necessary to prevent stripping in asphaltic concrete pavements. The selection of an appropriate antistrip additive for a particular project is not an easy task because of the many factors involved. Most highway agencies perform tests on an asphaltic concrete mixture to determine its moisture-susceptibility performance. Some of these tests may include indirect tensile strength, resilient modulus test, boiling test, and moisture-susceptibility tests (e.g., Lottman or Tunnicliff-Root). The results obtained from some or all of these tests are used to determine the moisture susceptibility of a mixture. However, depending upon the agency or individuals involved, each test property may be evaluated differently. Therefore, fuzzy set theory is introduced for selecting the best-performance antistrip additive based on the performance of several asphaltic concrete mixture properties. The Tunnicliff-Root procedure was used to evaluate the effect of antistrip additives on the strength of 960 Marshall specimens. The average dry and wet indirect tensile strength ratio, visual stripping, and the price of the antistrip additives were used in a computer program developed to analyze the data using the fuzzy set theory. In this research project, it was shown that fuzzy sets can be successfully used for evaluating the effectiveness of antistrip additives in asphaltic concrete mixtures.

In recent years, more highway agencies have been requiring the use of antistrip additives because of increasing awareness of asphaltic concrete pavement failures caused by moisture damage. Antistrip additives are primarily used to reduce stripping and to increase mixture strength in the presence of moisture. Stripping involves disbonding of asphalt cement from aggregate surfaces, often in the presence of moisture.

Many antistrip additives (ASAs) are on the market. Performance of these ASAs in asphaltic concrete mixtures varies depending on many factors (e.g., the source of asphalt cements and aggregates used). There is, therefore, a need to identify the best-performing ASA for each asphaltic concrete mixture.

Many methods are available, for example, Tunnicliff-Root (*1*) and Lottman (*2*), to measure the performance and moisture susceptibility of asphaltic concrete mixtures. The Tunnicliff-Root procedures recommend saturating a Marshall sample between 55 and 80 percent by applying a vacuum (20 in. Hg, for 5 min). The sample is then placed in water (77°F) for 1 hr, and the indirect tensile strength of the specimen is determined. The ratio of moisture-conditioned specimen to dry-conditioned (stored for 24 hr, 77°F) specimen is determined and is referred to as tensile strength ratio (TSR).

Although methods are available to examine a particular mixture property that is known to be a measure of ASA performance, comprehensive evaluation of ASA performance requires the consideration of many properties. For example, in these evaluations, the interrelationship of tensile strength (TS) ratio (wet TS/dry TS) and visual stripping rating is not clear.

Because the interrelationship among properties is vague, the comparison of one property with another is "fuzzy." Sometimes, comparison of the same property among different mixtures is also fuzzy. For example, because TSR is a function of the TS of dry- and wet-conditioned mixtures, a mixture of lower wet TS can have a higher TSR than a mixture with higher wet TS. In such a case, comparison of TSR alone does not yield meaningful results. Even though it is generally known that stripping has some correlation with weakening of tensile strength (*3,4*), some stripped mixtures show higher strength values than unstripped mixtures. Therefore, an unstripped mixture does not necessarily exhibit high tensile strength. Detailed examples are explained in a subsequent section.

Organizing information for many properties in the way that will lead to a conclusive performance evaluation may involve many subjective judgments. Especially, because interrelation of data is ambiguous, rating individual value and weighing each factor for integration of information are difficult. The result of using conventional methods or simple numerical-ranking comparison for this type of problem may still be ambiguous. The major advantage of using fuzzy procedure is that the result is easy to understand, because fuzzy weighted average operation can quantify the ambiguous values and translate them into illustrative expressions. Therefore, fuzzy set procedures have been applied to the evaluation of the potential performance of antistrip additives.

In this research, fuzzy sets were used to determine the moisture susceptibility of laboratory-prepared Marshall specimens. The materials (aggregates, asphalt cements, and ASAs) used in the lab were typical of those widely used in South Carolina. Four AC-20 ashalt cement sources, designated as I, II, III, and IV, were used. In addition, three liquid ASAs, designated as 1, 3, and 4, and a hydrated lime, designated as 2, were used to evaluate the effectiveness of ASAs on indirect tensile strength (ITS) of Marshall specimens. Aggregates used in this research (designated as A, B, and C) were typical of those used for Type 3 surface mixtures in South Carolina.

K. W. Kim, Agricultural and Civil Engineering Department, Kangweon National University, Chun Chon, 200-701, Republic of Korea. S. Amirkhanian, Civil Engineering Department, Clemson University, Clemson, S.C. 29634-0911.

Aggregates A and C were predominantly crushed granitic aggregates; Aggregate B consisted of siliceous coastal plains sand and gravel (*3*).

## FUZZY SET THEORY

Zadeh, in 1965, introduced the notion of fuzzy sets (*5*). Zadeh (*6*) suggested that the closer one investigates a "real-life" complex problem, the fuzzier the manner of solution becomes. He therefore developed the theory of fuzzy sets to obtain meaningful solutions to complex problems.

The mathematics of fuzzy sets were developed over a decade. However, only a few applications of the approach were implemented. In recent years, fuzzy sets have been used in engineering, medicine, and other areas of science as a tool for the expression of professional judgments (*7–11*). The following sections briefly explain the mathematics involved with fuzzy set theory.

A set is defined as a collection of objects having a general property, for example, a set of asphaltic concrete mixtures or a group of paving contractors. If an engineer works as a paving contractor (i.e., belongs to a group of contractors), then he or she has a membership of 1 in the set of paving contractors. However, if he or she is not a paving contractor, his or her membership is 0 and he or she does not belong to the set. Therefore, in general, the set has a clear and crisp boundary. A fuzzy set, on the other hand, is a set with members having a continuum of grades of membership from 0 to 1, rather than having discrete membership of 0 or 1 (*12*).

Let $U$ denote a space of objects. A fuzzy set $A$ in $U$ is set of

$$A = \{x,\mu_A(x)\}, \qquad X \subset \mathrm{A} \quad \text{and} \quad A \in U \tag{1}$$

in which $\mu_A(x)$ is the grade of membership of $x$ in $A$ ($0 \leq \mu_A(x) \leq 1$). Practical expressions for two fuzzy sets (e.g., $A$ and $B$) are as follows (*13*, p. 192).

$$A = \{x(i)|i;\ 1 < i < n\} \tag{2}$$

$$B = \{y(j)|j;\ 1 < j < n\} \tag{3}$$

where

$i$, $j$, and $n$ = domain elements, expressed as integers, and
$x(i)$ and $y(j)$ = membership functions that characterize $A$ and $B$, respectively.

### Fuzzy Weighted Average Operation

The fuzzy weighted average (FWA) is defined as follows (*13*, p. 192):

$$R = \frac{\Sigma(R_i \times W_i)}{\Sigma W_i} \tag{4}$$

where

$R$ = fuzzy set that represents the overall rating of an alternative,
$R_i$ = fuzzy set that represents rating of an alternative based on a particular criterion, and
$W_i$ = fuzzy set that represents the weight assigned to the particular criterion.

The fuzzy operations—addition, multiplication, and division—for the two fuzzy sets $A$ and $B$, are defined as

$$\text{Addition: } A + B = \{\min[x(i), y(j)]|(i + j);\ 1 < i, j < n\} \tag{5}$$

$$\text{Multiplication: } A * B = \{\min[x(i), y(j)]|(i * j);\ 1 < i, j < n\} \tag{6}$$

$$\text{Division: } A/B = \{\min[x(i), y(j)]|(i/j);\ 1 < i, j < n\} \tag{7}$$

For practical use, the result of the fuzzy division defined in Equation 7 can be rearranged according to the Clements algorithm. The Clements algorithm involves two assumptions: (a) any division of $(i/j)$ that does not result in an integer is deleted, and (b) any division that results in a quotient greater than $n$ is discarded (*14*).

Whether or not the fuzzy normalization is required must be determined after each fuzzy operation. Normalization gives more reasonable results in the fuzzy set operations (*13,15*). The fuzzy normalization, NOR, for a fuzzy set $X$ is defined as follows:

$$\text{if } Z = \mathrm{NOR}(X), \qquad \text{then } Z = \{[z(i)]/i;\ 1 < i < n\} \tag{8}$$

$$\text{where } z(i) = x(i)/\max[x(i),\ 1 < i < n]. \tag{9}$$

The normalization for the fuzzy set obtained after each operation (addition, multiplication, or division) should be conducted by Equations 8 or 9 if max $x(i)$ does not equal max $z(i)$.

### Ranking Index

Expression of FWA result is not by a single numerical value, but by a set that contains a series of domain element and degree of support for each element. The set from FWA operation can be graphically expressed for visual evaluation, or quantitatively expressed with ranking index (RI) for numerical evaluation.

RI can be defined to represent a quantitative measure of the fuzzy set ($R$ in Equation 4) for each alternative. In this study, the RI was defined to increase as the alternative becomes better. The arithmetic expression of the RI is (*14*):

$$\mathrm{RI} = a_l - a_r + c \tag{10}$$

where

$a_l$ = area enclosed to the left of the membership function,
$a_r$ = area enclosed to the right of the membership function, and
$c$ = a constant that is the area enclosed by the universe.

Figure 1 (top) illustrates $a_l$ and $a_r$. In Figure 1 (bottom), for example, RI for the fuzzy set of $X$ = {0|4, 0.5|5, 1.0|6, 0.5|7,

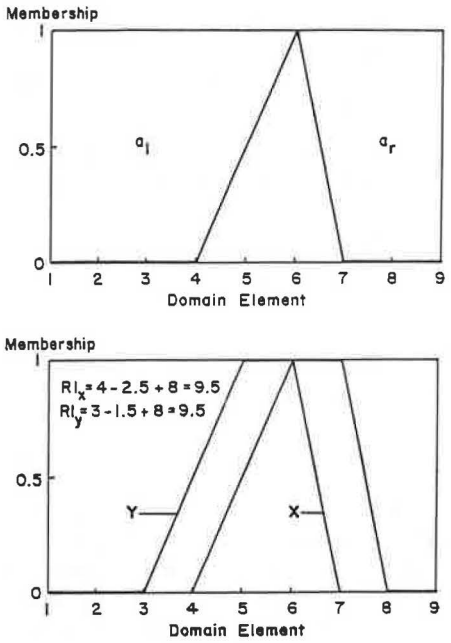


**FIGURE 1 Illustration of ranking index for Fuzzy Sets *X* and *Y*.**

0|8} is the same as that for fuzzy set $Y$ = {0|3, 0.5|4, 1.0|5, 1.0|6, 1.0|7, 0.5|8, 0|9}, where values of $a_l$ for fuzzy set $X$ and $Y$ are 4 and 3, and values of $a_r$ for $X$ and $Y$ are 2.5 and 1.5, and value of RI is 9.5, respectively.

## TESTING PROCEDURES

The Tunnicliff-Root (*1,16,17*) procedure was used to evaluate the effect of ASAs on the strength of asphaltic concrete mixtures. This procedure recommends an air voids content of 7 ± 1 percent for each specimen. After several trials, it was found that a compactive effort of 20 blows per face produced the recommended degree of air voids and saturation (55 to 80 percent). An automatic recording Marshall machine (which conforms to ASTM D1559) was used to measure the ITS of all specimens (*18*). The rate of deformation was 2 in./min and the test temperature was 77 ± 2°F. TSRs of the specimens were calculated. Immediately after tensile strength tests were completed, the surface condition of the exposed aggregates was examined. The visual strip rating ($S$) was calculated by obtaining the mean value of $C$ and $F$, percentage of stripping for coarse ($C$) and fine ($F$) aggregates, respectively. Values of $C$ and $F$ are defined in Table 1.

TABLE 1 VALUES OF COARSE AND FINE AGGREGATES

| Aggregate | Value | Definition |
|---|---|---|
| $C$ | 1 | Less than 10% stripping |
| | 2 | 10–40% stripping |
| | 3 | More than 40% stripping |
| $F$ | 1 | Less than 10% stripping |
| | 2 | 10–25% stripping |
| | 3 | More than 10% stripping |

## EXPERIMENTAL RESULTS

A total of 960 Marshall specimens were made and tested. The means and standard deviations of dry and wet ITS and TSR values for all specimens are shown in Tables 2–5. These tables indicate that the specimens made with Aggregate A and various asphalt cements and ASAs produced the highest values of dry ITS compared with specimens prepared with other aggregate sources. However, the TSR values of the same specimens generally produced lower values than specimens made with Aggregates B and C.

The following examples will demonstrate the fuzziness of the data. For Mixture A0 in Table 2, TSR was found to be 65.7 percent and its wet ITS was 44.1 psi. However, for Mixture B4, TSR was more than 100 percent and its wet ITS was 44.8 psi, which is approximately the same value of wet ITS for Mixture A0 (44.1). Therefore, in this case, simply comparing numerical values of TSR between the two mixtures is not meaningful to comparing mixture performance.

Another fuzzy example can be shown with Aggregate B in Table 3. When only the values of TSR were compared, TSR for Mixture B4 (88.7 percent) appeared to be improved (because an antistrip additive was used), compared with TSR of Control Mixture B0 (87.0 percent). However, ITS wet of B4 (45.8) was actually lower than that of B0 (47.1).

In addition, Table 4 indicates that the values of ITS dry for Aggregate A were, in general, higher than those for Aggregate B. However, TSR values for Aggregate A were lower than those for Aggregate B. Based on this result, neither wet ITS nor TSR gives clear comparison of ASA performance in the mixtures. This result may suggest an analogy that Aggregate A produced stronger mixture than Aggregate B, but was more moisture-susceptible than Aggregate B.

## APPLICATION OF FUZZY SETS FOR EVALUATION OF BEST-PERFORMING ANTISTRIPPING ADDITIVE

In this section, the application of fuzzy set for evaluating ASAs is illustrated using several examples. It is important to note that the fuzzy sets selected in this study to define the rating scale and weighing for each criterion are arbitrary. Criteria for fuzzy evaluation are also selected arbitrarily. These ratings and evaluations were selected only for demonstration purposes. Any other fuzzy set can be defined and applied for similar cases.

### Selection of Fuzzy Sets

Fuzzy sets $A$, $B$, $C$, $D$, and $E$ were defined to represent ratings of excellent, very good, good, fair, and poor, respectively. Each fuzzy set was defined with only three membership functions (0, 0.5, or 1) over a domain of 9 elements ($n$ = 9 in Equations 2 and 3) for easy computation. Fuzzy sets $A$, $B$, $C$, $D$, and $E$ are arithmetically expressed in Equations 11–15 and are illustrated in Figure 2.

$$A = \{0|1, 0|2, 0|3, 0|4, 0|5, 0|6, 0|7, 0.5|8, 1.0|9\} \quad (11)$$

TABLE 2 STATISTICAL RESULTS OF ANALYSES FOR MARSHALL SPECIMENS MADE WITH ASPHALT CEMENT I

| Aggregate Source | ANTISTRIP AGENT | ITS DRY (PSI) | STD. DEV. (PSI) | ITS WET (PSI) | STD. DEV. (PSI) | TSR (%) | STD. DEV. (%) |
|---|---|---|---|---|---|---|---|
| A | 0 | 67.7 | 8.4 | 44.1 | 4.8 | 65.7 | 7.9 |
| | 1 | 65.2 | 7.5 | 57.3 | 10.3 | 87.8 | 10.4 |
| | 2 | 62.3 | 8.7 | 55.8 | 11.0 | 89.2 | 10.5 |
| | 3 | 65.0 | 11.0 | 58.3 | 14.8 | 89.3 | 12.6 |
| | 4 | 65.7 | 9.3 | 52.6 | 11.4 | 79.7 | 10.5 |
| B | 0 | 50.5 | 6.8 | 45.1 | 4.2 | 90.3 | 12.0 |
| | 1 | 51.7 | 9.7 | 46.3 | 4.7 | 92.4 | 20.0 |
| | 2 | 48.8 | 9.6 | 46.2 | 8.2 | 97.5 | 24.8 |
| | 3 | 52.4 | 6.9 | 41.4 | 18.5 | 77.8 | 32.4 |
| | 4 | 44.9 | 7.1 | 44.8 | 5.8 | 102.3 | 25.1 |
| C | 0 | 58.9 | 10.2 | 29.4 | 8.2 | 52.0 | 22.7 |
| | 1 | 57.9 | 11.4 | 51.0 | 8.7 | 89.8 | 17.9 |
| | 2 | 62.6 | 6.8 | 65.4 | 5.7 | 105.7 | 15.0 |
| | 3 | 57.6 | 6.8 | 48.5 | 8.1 | 83.9 | 5.7 |
| | 4 | 57.4 | 9.5 | 42.1 | 8.4 | 75.5 | 20.9 |

Note: Each Cell is Based on an Average of Eight Specimens.

TABLE 3 STATISTICAL RESULTS OF ANALYSES FOR MARSHALL SPECIMENS MADE WITH ASPHALT CEMENT II

| Aggregate Source | ANTISTRIP AGENT | ITS DRY (PSI) | STD. DEV. (PSI) | ITS WET (PSI) | STD. DEV. (PSI) | TSR (%) | STD. DEV. (%) |
|---|---|---|---|---|---|---|---|
| A | 0 | 69.3 | 15.8 | 46.2 | 9.8 | 68.7 | 16.3 |
| | 1 | 73.3 | 9.4 | 60.8 | 10.2 | 82.9 | 8.3 |
| | 2 | 71.4 | 12.7 | 61.4 | 9.1 | 87.2 | 12.8 |
| | 3 | 71.6 | 12.7 | 64.8 | 9.2 | 91.6 | 11.9 |
| | 4 | 63.1 | 8.4 | 59.3 | 10.3 | 94.1 | 11.6 |
| B | 0 | 54.7 | 8.7 | 47.1 | 5.6 | 87.0 | 9.6 |
| | 1 | 56.0 | 8.1 | 53.7 | 7.8 | 97.2 | 16.5 |
| | 2 | 55.3 | 6.3 | 46.9 | 9.8 | 85.4 | 19.3 |
| | 3 | 54.9 | 8.2 | 51.3 | 3.5 | 94.9 | 12.2 |
| | 4 | 52.2 | 7.1 | 45.8 | 9.3 | 88.7 | 17.5 |
| C | 0 | 66.3 | 8.2 | 26.2 | 3.7 | 40.2 | 7.8 |
| | 1 | 67.8 | 10.3 | 56.8 | 8.1 | 84.8 | 12.6 |
| | 2 | 64.3 | 11.9 | 61.9 | 9.8 | 97.7 | 15.8 |
| | 3 | 65.3 | 8.7 | 53.1 | 6.0 | 81.7 | 7.0 |
| | 4 | 58.6 | 12.6 | 53.5 | 7.0 | 94.6 | 22.7 |

Note: Each Cell is Based on an Average of Eight Specimens.

TABLE 4 STATISTICAL RESULTS OF ANALYSES FOR MARSHALL SPECIMENS MADE WITH ASPHALT CEMENT III

| Aggregate Source | ANTISTRIP AGENT | ITS DRY (PSI) | STD. DEV. (PSI) | ITS WET (PSI) | STD. DEV. (PSI) | TSR (%) | STD. DEV. (%) |
|---|---|---|---|---|---|---|---|
| A | 0 | 81.9 | 5.3 | 61.2 | 7.8 | 74.8 | 8.8 |
| | 1 | 86.3 | 12.9 | 75.2 | 9.9 | 87.5 | 6.9 |
| | 2 | 81.9 | 14.6 | 74.3 | 9.4 | 92.7 | 17.1 |
| | 3 | 85.6 | 11.6 | 72.0 | 10.7 | 85.0 | 13.1 |
| | 4 | 73.7 | 12.4 | 68.0 | 9.3 | 93.1 | 9.1 |
| B | 0 | 58.4 | 5.9 | 57.8 | 7.1 | 99.1 | 9.1 |
| | 1 | 63.6 | 10.2 | 66.3 | 8.5 | 105.3 | 14.3 |
| | 2 | 64.9 | 9.9 | 63.3 | 5.2 | 98.8 | 10.8 |
| | 3 | 64.6 | 9.8 | 58.2 | 11.3 | 89.8 | 8.9 |
| | 4 | 60.3 | 8.5 | 56.6 | 5.9 | 95.4 | 15.1 |
| C | 0 | 72.2 | 13.9 | 45.9 | 5.2 | 64.9 | 8.9 |
| | 1 | 71.9 | 10.4 | 63.9 | 8.9 | 90.4 | 16.4 |
| | 2 | 72.6 | 12.9 | 71.6 | 9.0 | 100.6 | 16.6 |
| | 3 | 71.5 | 9.9 | 64.5 | 6.0 | 91.5 | 11.9 |
| | 4 | 68.0 | 11.6 | 62.0 | 6.9 | 93.2 | 16.6 |

Note: Each Cell is Based on an Average of Eight Specimens.

TABLE 5 STATISTICAL RESULTS OF ANALYSES FOR MARSHALL SPECIMENS MADE WITH ASPHALT CEMENT IV

| Aggregate Source | ANTISTRIP AGENT | ITS DRY (PSI) | STD. DEV. (PSI) | ITS WET (PSI) | STD. DEV. (PSI) | TSR (%) | STD. DEV. (%) |
|---|---|---|---|---|---|---|---|
| A | 0 | 76.5 | 14.4 | 61.6 | 12.8 | 82.3 | 18.8 |
| | 1 | 78.0 | 11.6 | 71.2 | 6.8 | 92.9 | 14.4 |
| | 2 | 78.9 | 15.2 | 73.4 | 8.1 | 95.4 | 15.7 |
| | 3 | 76.2 | 14.7 | 77.9 | 7.5 | 104.9 | 16.5 |
| | 4 | 79.8 | 17.0 | 66.4 | 12.9 | 84.5 | 13.9 |
| B | 0 | 61.2 | 12.6 | 58.0 | 9.9 | 96.4 | 14.9 |
| | 1 | 61.2 | 12.8 | 63.9 | 7.8 | 107.5 | 20.3 |
| | 2 | 66.5 | 14.9 | 55.4 | 6.3 | 86.6 | 16.9 |
| | 3 | 56.0 | 10.9 | 58.1 | 11.9 | 104.7 | 16.0 |
| | 4 | 57.8 | 11.9 | 57.0 | 8.1 | 101.3 | 18.7 |
| C | 0 | 73.5 | 17.2 | 35.7 | 3.8 | 50.9 | 12.9 |
| | 1 | 74.6 | 17.8 | 63.8 | 8.6 | 90.5 | 27.5 |
| | 2 | 77.6 | 13.3 | 73.1 | 9.9 | 95.4 | 13.9 |
| | 3 | 71.9 | 17.3 | 68.9 | 10.1 | 101.2 | 30.2 |
| | 4 | 68.5 | 11.8 | 59.7 | 6.3 | 89.9 | 20.8 |

Note: Each Cell is Based on an Average of Eight Specimens.

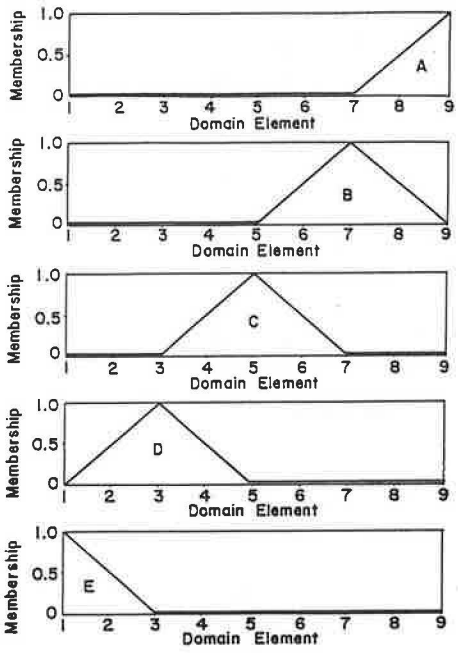


**FIGURE 2 Graphical illustration of Fuzzy Sets *A*, *B*, *C*, *D*, and *E*.**

$$B = \{0|1, 0|2, 0|3, 0|4, 0|5, 0.5|6, 1.0|7, 0.5|8, 0|9\} \quad (12)$$

$$C = \{0|1, 0|2, 0|3, 0.5|4, 1.0|5, 0.5|6, 0|7, 0|8, 0|9\} \quad (13)$$

$$D = \{0|1, 0.5|2, 1.0|3, 0.5|4, 0|5, 0|6, 0|7, 0|8, 0|9\} \quad (14)$$

$$E = \{1.0|1, 0.5|2, 0|3, 0|4, 0|5, 0|6, 0|7, 0|8, 0|9\} \quad (15)$$

The weight or relative importance of one criterion to the other, expressed as $W_i$ in Equation 4, was also defined as fuzzy sets $A$, $B$, $C$, $D$, and $E$ to represent weights for extremely important, very important, important, less important, and unimportant, respectively. The same fuzzy sets, previously defined for rating each alternative, were used for each of the five weights for easy computation. Ranking indexes for the five fuzzy sets, defined as $A$, $B$, $C$, $D$, and $E$, are 15, 12, 8, 4, and 1, respectively (Figure 2). The ranking index of the FWA for any two of the five fuzzy sets can be calculated by Equations 4–15.

### Criteria for Fuzzy Evaluation of ASA Performance

Many properties can be used for evaluation of ASA performance in an asphaltic concrete mixture. Properties used here (for demonstration purposes only) for evaluating performance of ASAs include (a) dry tensile strength (DTS), (b) tensile strength of wet-conditioned mixtures (WTS), (c) tensile strength ratio [$TSR = 100\% \times (WTS/DTS)$], and (d) visual strip rating of the mixture (VSR). The price ($P$) of additive may be important from an economic point of view. Therefore, in some examples, the price was added as the fifth major criterion.

If several different sources of aggregates with one asphalt cement are used for a project and an ASA needs to be selected for the entire project, the aggregate can be used as subcriteria. If several asphalt cements are used with one aggregate and an ASA needs to be selected for the entire project, the asphalt cements can be used as subcriteria. However, if an ASA for each aggregate or asphalt cement is to be selected, there is no need to use aggregates or asphalt cement as subcriteria.

### Converting Real Values to Fuzzy Data

Real data (mean value of each group) collected for the major and subcriteria must be converted to the fuzzy rating system (i.e., fuzzy sets $A$, $B$, $C$, $D$, or $E$). The rating scale and weight for each criterion and subcriterion can be selected on the basis of relative comparison of mean values, variation of data, or the engineer's judgment. This is explained more in example problems.

A computer program was developed to compare the test results for several asphaltic concrete mixtures to determine the mixture that produced the best results (higher TSR, lower value of visual strip rating, lowest cost, etc.). This program produces numerical values of RI for each alternative so that the engineer can obtain the order of mixture performance from the best to the worst. A simplified flow chart of the computer program developed for this study is illustrated in Figure 3.

### Example Problems

Several example problems using the fuzzy sets defined previously are illustrated in the following sections. Data in this study were based on three aggregates, five ASAs (including control) and four asphalt cements, as shown in Tables 2–5. Aggregates were used as subcriteria for each of the first four major criteria for example problems 1–4, and asphalts were used as subcriteria for Example Problem 5. For Example Problems 1–4, the input data were organized as following major criteria and subcriteria. For Example Problem 5, four asphalt cements were used as subcriteria instead of three aggregates.

Major Criterion 1: DTS
  Subcriterion a: Aggregate A
  Subcriterion b: Aggregate B
  Subcriterion c: Aggregate C
Major Criterion 2: WTS
  Subcriterion a: Aggregate A
  Subcriterion b: Aggregate B
  Subcriterion c: Aggregate C
Major Criterion 3: TSR
  Subcriterion a: Aggregate A
  Subcriterion b: Aggregate B
  Subcriterion c: Aggregate C
Major Criterion 4: VSR
  Subcriterion a: Aggregate A
  Subcriterion b: Aggregate B
  Subcriterion c: Aggregate C
Major Criterion 5: Price ($P$)
  No Subcriteria

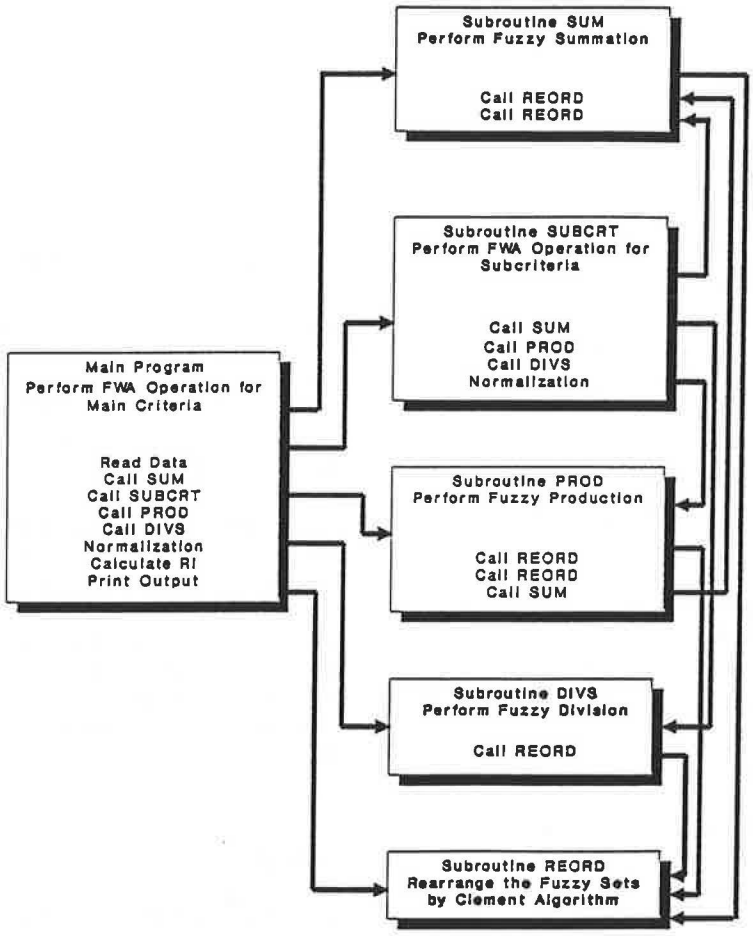


**FIGURE 3 Simplified flow chart of computer program developed for example problems.**

A control (denoted as 0) and four additives (denoted as 1, 2, 3, and 4) were compared using the FWA operation to select the best-performing additive. In Example Problems 1–4, the data shown in Table 2 (Asphalt Cement I and Aggregates A, B, and C) were used. However, for Example Problem 5, the data for Aggregate C and the four asphalt cements mentioned in Tables 2–5 were used. The arbitrarily selected rating scale for each criterion for this study is shown in Table 6. The relative importance of one criterion to the others (weight) can be assigned by the engineer. Therefore, if a criterion is considered more important than the others, then a higher weight (e.g., *A*) can be given to that criterion. Several different weights were assigned in each example analysis to show the effect on the results. The developed computer program was used to obtain the RI values and the ranking of ASAs for each example problem (Figure 3).

### *Example Problem 1*

Five asphaltic concrete mixtures containing five ASAs (including control) made with three different aggregate sources were evaluated based on DTS, WTS, TSR, and VSR. The value for each criterion and rating converted by the rating scale in Table 6 is listed in Table 7. The value for each criterion in Table 7 is the mean value of eight laboratory-prepared specimens. An equal weight *A* was assigned for all the criteria and subcriteria in this example for illustration purposes.

Rating values are represented by numerical values of 1 through 5, which correspond to the fuzzy sets of *A* through *E*, respectively. The RI values obtained by the result of the FWA operation are shown in Table 7. ASAs 1, 2, and 3 tied as the best choice (RI = 12.75 out of possible maximum of 15); control (0) was the worst choice (RI = 8.5) in this case.

### *Example Problem 2*

For this example problem, the same data used in example problem 1 were used, except for different weights for the main criteria. WTS and VSR are weighted as extremely important (*A*), because the purpose of using an ASA is to reduce stripping (VSR) and, at the same time, to improve WTS of the mixture. Weight *B*, very important, was assigned to DTS because DTS is the base of TSR and is the mixture's intrinsic strength that is not affected in the presence of moisture or ASA. Weight *C*, important, is given to TSR because, even though the higher the TSR the better the moisture susceptibility of mixtures, the magnitude of TSR is sometimes less important in evaluating performance of an asphaltic concrete

TABLE 6 RATING SCALE FOR MAIN CRITERIA

| Rating | Criteria: DTS, WTS | TSR | VSR[1] | Price[2] |
|---|---|---|---|---|
| A | R[3] > 0.9 | > 90% | 1.0 - 1.50 | P = 0 |
| B | 0.8 < R < 0.9 | 90 - 80% | 1.50 - 2.50 | P = 1 |
| C | 0.7 < R < 0.8 | 80 - 70% | 2.50 - 3.50 | 1 < P < 2 |
| D | 0.6 < R < 0.7 | 70 - 60% | 3.50 - 4.50 | 2 < P < 3 |
| E | R < 0.6 | < 60% | > 4.50 | P > 3 |

1. VSR: 1.0: S = 1.0; 2.0: S = 1.5C, 1.5F; 3.0: S = 2, 2C, 2F; 4.0: S = 2.5C, 2.5F; 5.0: S = 3

   where, S = (C + F) /2; value of C and F, coarse and fine aggregate stripping, respectively are defined as:

| Value of C | Value of F |
|---|---|
| 1 = less than 10% stripping | 1 = less than 10% stripping |
| 2 = 10-40% Stripping | 2 = 10-25% Stripping |
| 3 = greater than 40% stripping | 3 = greater than 25% stripping |

2. P = price / (cheapest price of the additives (except for control)) For one ton of asphaltic concrete mixture

3. R = (Tensile Strength) /(Max. Tensile Strength)

TABLE 7 INFORMATION FOR FWA INPUT AND RESULTS FOR EXAMPLE 1

FWA Input Information

| Main Criteria (Weight) | ASA No. | Subcriteria Agg A Mean | Agg A Rating | Agg B Mean | Agg B Rating | Agg C Mean | Agg C Rating |
|---|---|---|---|---|---|---|---|
| DTS (psi) (A) | 0 | 67.7* | 1 | 50.6 | 2 | 58.9 | 2 |
| | 1 | 65.2 | 1 | 51.7 | 3 | 58.0 | 2 |
| | 2 | 62.3 | 1 | 48.8 | 3 | 62.6 | 1 |
| | 3 | 65.0 | 1 | 52.4 | 3 | 57.6 | 2 |
| | 4 | 65.7 | 1 | 45.0 | 4 | 57.4 | 2 |
| Weight for Subcriteria | | | A | | A | | A |
| WTS (psi) (A) | 0 | 44.1 | 4 | 45.1 | 4 | 29.4 | 5 |
| | 1 | 57.3 | 2 | 46.3 | 3 | 51.0 | 3 |
| | 2 | 55.8 | 2 | 46.2 | 3 | 65.4* | 1 |
| | 3 | 58.3 | 2 | 47.6 | 3 | 48.6 | 3 |
| | 4 | 52.6 | 2 | 44.8 | 4 | 42.1 | 4 |
| Weight for Subcriteria | | | A | | A | | A |
| TSR (%) (A) | 0 | 65.7 | 4 | 90.3 | 1 | 52.1 | 5 |
| | 1 | 87.8 | 2 | 92.4 | 1 | 89.8 | 2 |
| | 2 | 89.3 | 2 | 97.5 | 1 | 105.7 | 1 |
| | 3 | 89.3 | 2 | 91.0 | 1 | 83.9 | 2 |
| | 4 | 79.7 | 3 | 102.3 | 1 | 75.5 | 3 |
| Weight for Subcriteria | | | A | | A | | A |
| VSR (A) | 0 | 4.13 | 4 | 2.38 | 2 | 1.88 | 2 |
| | 1 | 1.63 | 2 | 1.88 | 2 | 1.00 | 1 |
| | 2 | 1.13 | 1 | 2.00 | 2 | 1.13 | 1 |
| | 3 | 1.25 | 1 | 1.86 | 2 | 1.00 | 1 |
| | 4 | 2.50 | 2 | 1.88 | 2 | 1.13 | 1 |
| Weight for Subcriteria | | | A | | A | | A |

Result of FWA Operation

| ASA | 0 | 1 | 2 | 3 | 4 |
|---|---|---|---|---|---|
| RI value | 8.5 | 12.75 | 12.75 | 12.75 | 10.50 |

*: highest value in each criterion

mixture. A high value of TSR does not necessarily mean high strength of the wet mixture if DTS is low to begin with. Therefore, a lower weight ($C$) was assigned to TSR than to the other three criteria.

It was expected that ratings based on criteria WTS and VSR would be the dominant factors in the evaluation because of the high weights assigned to these two criteria. A different result, compared with Example Problem 1, was obtained (Table 8). ASA 2 showed the highest RI value, ASAs 1 and 3 showed the second highest, and control (0) showed the lowest. The results of this example problem indicate the importance of assigning weight for each criterion to determine the RI.

### *Example Problem 3*

In this example problem, the price of ASA was added as a criterion to the FWA operation. Market price of ASA for 1 ton of asphaltic concrete mixture was used for the price criterion. No subcriteria were given to the price main criterion. The price for ASAs 1, 3, and 4 was assumed to be \$0.50/ton of mixture; the price for ASA No. 2 was taken as \$1.50/ton of mixture. The price of control, ASA 1, was zero. Because prices of the ASA are small compared with the prices of other materials such as asphalt cement and aggregate, a weight $E$, unimportant, was assigned to the price in this example.

Rating for the price was determined based on the scale shown in Table 6. Table 9 shows the input information and the results obtained for this example problem. Because the price of ASA 2 was the highest (lowest rating), RI for ASA 2 was reduced from 12.75 to 12.25. RI values for ASAs cheaper than ASA 2 were somewhat increased (from 11.75 to 12 for ASA 1 and 3, from 8.5 to 10.75 for ASA 0, and from 11 to 11.25 for ASA 4) even though a weight of $E$ was assigned to

TABLE 8 INFORMATION FOR FWA INPUT AND RESULTS FOR EXAMPLE 2

FWA Input Information

| Main Criteria (Weight) | ASA No. | Subcriteria Agg A Mean | Agg A Rating | Agg B Mean | Agg B Rating | Agg C Mean | Agg C Rating |
|---|---|---|---|---|---|---|---|
| | 0 | 67.7* | 1 | 50.6 | 2 | 58.9 | 2 |
| | 1 | 65.2 | 1 | 51.7 | 3 | 58.0 | 2 |
| DTS (psi) | 2 | 62.3 | 1 | 48.8 | 3 | 62.6 | 1 |
| (B) | 3 | 65.0 | 1 | 52.4 | 3 | 57.6 | 2 |
| | 4 | 65.7 | 1 | 45.0 | 4 | 57.4 | 2 |
| Weight for Subcriteria | | | A | | A | | A |
| | 0 | 44.1 | 4 | 45.1 | 4 | 29.4 | 5 |
| | 1 | 57.3 | 2 | 46.3 | 3 | 51.0 | 3 |
| WTS (psi) | 2 | 55.8 | 2 | 46.2 | 3 | 65.4* | 1 |
| (A) | 3 | 58.3 | 2 | 47.6 | 3 | 48.6 | 3 |
| | 4 | 52.6 | 2 | 44.8 | 4 | 42.1 | 4 |
| Weight for Subcriteria | | | A | | A | | A |
| | 0 | 65.7 | 4 | 90.3 | 1 | 52.1 | 5 |
| | 1 | 87.8 | 2 | 92.4 | 1 | 89.8 | 2 |
| TSR (%) | 2 | 89.3 | 2 | 97.5 | 1 | 105.7 | 1 |
| (C) | 3 | 89.3 | 2 | 91.0 | 1 | 83.9 | 2 |
| | 4 | 79.7 | 3 | 102.3 | 1 | 75.5 | 3 |
| Weight for Subcriteria | | | A | | A | | A |
| | 0 | 4.13 | 4 | 2.38 | 2 | 1.88 | 2 |
| | 1 | 1.63 | 2 | 1.88 | 2 | 1.00 | 1 |
| VSR | 2 | 1.13 | 1 | 2.00 | 2 | 1.13 | 1 |
| (A) | 3 | 1.25 | 1 | 1.86 | 2 | 1.00 | 1 |
| | 4 | 2.50 | 2 | 1.88 | 2 | 1.13 | 1 |
| Weight for Subcriteria | | | A | | A | | A |

Result of FWA Operation

| ASA | 0 | 1 | 2 | 3 | 4 |
|---|---|---|---|---|---|
| RI value | 8.5 | 11.75 | 12.75 | 11.75 | 11.00 |

*: highest value in each criterion

TABLE 9 INFORMATION FOR FWA INPUT AND RESULTS FOR EXAMPLE 3

FWA Input Information

| Main Criteria (Weight) | ASA No. | Subcriteria Agg A Mean | Agg A Rating | Agg B Mean | Agg B Rating | Agg C Mean | Agg C Rating |
|---|---|---|---|---|---|---|---|
| | 0 | 67.7* | 1 | 50.6 | 2 | 58.9 | 2 |
| | 1 | 65.2 | 1 | 51.7 | 3 | 58.0 | 2 |
| DTS (psi) | 2 | 62.3 | 1 | 48.8 | 3 | 62.6 | 1 |
| (B) | 3 | 65.0 | 1 | 52.4 | 3 | 57.6 | 2 |
| | 4 | 65.7 | 1 | 45.0 | 4 | 57.4 | 2 |
| Weight for Subcriteria | | | A | | A | | A |
| | 0 | 44.1 | 4 | 45.1 | 4 | 29.4 | 5 |
| | 1 | 57.3 | 2 | 46.3 | 3 | 51.0 | 3 |
| WTS (psi) | 2 | 55.8 | 2 | 46.2 | 3 | 65.4* | 1 |
| (A) | 3 | 58.3 | 2 | 47.6 | 3 | 48.6 | 3 |
| | 4 | 52.6 | 2 | 44.8 | 4 | 42.1 | 4 |
| Weight for Subcriteria | | | A | | A | | A |
| | 0 | 65.7 | 4 | 90.3 | 1 | 52.1 | 5 |
| | 1 | 87.8 | 2 | 92.4 | 1 | 89.8 | 2 |
| TSR (%) | 2 | 89.3 | 2 | 97.5 | 1 | 105.7 | 1 |
| (C) | 3 | 89.3 | 2 | 91.0 | 1 | 83.9 | 2 |
| | 4 | 79.7 | 3 | 102.3 | 1 | 75.5 | 3 |
| Weight for Subcriteria | | | A | | A | | A |
| | 0 | 4.13 | 4 | 2.38 | 2 | 1.88 | 2 |
| | 1 | 1.63 | 2 | 1.88 | 2 | 1.00 | 1 |
| VSR | 2 | 1.13 | 1 | 2.00 | 2 | 1.13 | 1 |
| (A) | 3 | 1.25 | 1 | 1.86 | 2 | 1.00 | 1 |
| | 4 | 2.50 | 2 | 1.88 | 2 | 1.13 | 1 |
| Weight for Subcriteria | | | A | | A | | A |
| | 0 | | | 0 | 1 | | |
| | 1 | | | 0.5 | 2 | | |
| Price (E) | 2 | | | 1.5 | 4 | | |
| ($/ton) | 3 | | | 0.5 | 2 | | |
| | 4 | | | 0.5 | 2 | | |

Result of FWA Operation

| ASA | 0 | 1 | 2 | 3 | 4 |
|---|---|---|---|---|---|
| RI value | 10.75 | 12.00 | 12.25 | 12.00 | 11.25 |

*: highest value in each criterion

the price. Therefore, the difference between the highest RI and the lowest RI was reduced. However, ASA 0 was still the worst and ASA 2 was the best. If a higher weight is assigned to the price, a different result, which may show better RI values for lower-priced ASA, would be expected.

### *Example Problem 4*

For this example problem, all information is the same as given in example problem 3 except for different weights assigned for each of the three subcriteria. The weight for each subcriterion (aggregate) in each main criterion can be determined based on the value of the coefficient of variation (CV), and the weighing scale can be selected arbitrarily.

The CV of DTS, WTS, and VSR ranged up to more than 60 percent. Weight *A* was given for the first 15 percent of CV, *B* for the next 15 percent, and so forth for *C*, *D*, and *E*. Therefore, the following scales were defined to assign the weight to each subcriterion (aggregate) based on CV.

*A*: CV $\leq$ 15%,
*B*: 15% $<$ CV $\leq$ 30%,
*C*: 30% $<$ CV $\leq$ 45%,
*D*: 45% $<$ CV $\leq$ 60%, and
*E*: CV $>$ 60%.

The input information and results are shown in Table 10. In this example problem, RI values for ASA 1, 2, and 3 were the same as for example problem 3. However, RI for ASA 0 was improved to fourth place and RI for ASA 4 was moved to the last choice. ASA 2 was determined to be the best choice.

### *Example Problem 5*

In this example problem, FWA operation was conducted based on five main criteria, used previously, with four subcriteria (four asphalt cements), instead of three aggregates. Weighing for the five main criteria was the same as for Example Problem 4. Weighing for subcriteria was based on CV, which is the same procedure explained in Example Problem 4.

The input information and FWA operation results are shown in Table 11. Similar results to the previous example problems were obtained: ASA 2 was the best choice and ASA 0 was the last.

TABLE 10 INFORMATION FOR FWA INPUT AND RESULTS FOR EXAMPLE 4

FWA Input Information

| Main Criteria (Weight) | ASA No. | Subcriteria Agg A Mean | Agg A Rating | Agg B Mean | Agg B Rating | Agg C Mean | Agg C Rating |
|---|---|---|---|---|---|---|---|
| | 0 | 67.7* | 1 | 50.6 | 2 | 58.9 | 2 |
| | 1 | 65.2 | 1 | 51.7 | 3 | 58.0 | 2 |
| DTS (psi) | 2 | 62.3 | 1 | 48.8 | 3 | 62.6 | 1 |
| (B) | 3 | 65.0 | 1 | 52.4 | 3 | 57.6 | 2 |
| | 4 | 65.7 | 1 | 45.0 | 4 | 57.4 | 2 |
| Wt for Subcr. | CV | 13.4 | A | 16.4 | B | 15.1 | B |
| | 0 | 44.1 | 4 | 45.1 | 4 | 29.4 | 5 |
| | 1 | 57.3 | 2 | 46.3 | 3 | 51.0 | 3 |
| WTS (psi) | 2 | 55.8 | 2 | 46.2 | 3 | 65.4* | 1 |
| (A) | 3 | 58.3 | 2 | 47.6 | 3 | 48.6 | 3 |
| | 4 | 52.6 | 2 | 44.8 | 4 | 42.1 | 4 |
| Wt for Subcr. | CV | 21.7 | B | 13.4 | A | 29.7 | B |
| | 0 | 65.7 | 4 | 90.3 | 1 | 52.1 | 5 |
| | 1 | 87.8 | 2 | 92.4 | 1 | 89.8 | 2 |
| TSR (%) | 2 | 89.3 | 2 | 97.5 | 1 | 105.7 | 1 |
| (C) | 3 | 89.3 | 2 | 91.0 | 1 | 83.9 | 2 |
| | 4 | 79.7 | 3 | 102.3 | 1 | 75.5 | 3 |
| Wt for Subcr. | CV | 16.4 | B | 20.0 | B | 29.9 | B |
| | 0 | 4.13 | 4 | 2.38 | 2 | 1.88 | 2 |
| | 1 | 1.63 | 2 | 1.88 | 2 | 1.00 | 1 |
| VSR | 2 | 1.13 | 1 | 2.00 | 2 | 1.13 | 1 |
| (A) | 3 | 1.25 | 1 | 1.86 | 2 | 1.00 | 1 |
| | 4 | 2.50 | 2 | 1.88 | 2 | 1.13 | 1 |
| Wt for Subcr. | CV | 60.5 | E | 19.9 | B | 34.5 | C |
| | 0 | | | 0 | 1 | | |
| | 1 | | | 0.5 | 2 | | |
| Price (E) | 2 | | | 1.5 | 4 | | |
| ($/ton) | 3 | | | 0.5 | 2 | | |
| | 4 | | | 0.5 | 2 | | |

Result of FWA Operation

| ASA | 0 | 1 | 2 | 3 | 4 |
|---|---|---|---|---|---|
| RI value | 11.75 | 12.00 | 12.25 | 12.00 | 11.00 |

*: highest value in each criterion

TABLE 11 INFORMATION FOR FWA INPUT AND RESULTS FOR EXAMPLE 5

FWA Input Information

| Main Criteria (Weight) | ASA No. | Subcriteria Asp I Mean | Asp I Rating | Asp II Mean | Asp II Rating | Asp III Mean | Asp III Rating | Asp IV Mean | Asp IV Rating |
|---|---|---|---|---|---|---|---|---|---|
| | 0 | 58.9 | 3 | 66.3 | 2 | 72.2 | 1 | 73.5 | 1 |
| | 1 | 58.0 | 3 | 67.8 | 2 | 71.9 | 1 | 74.6 | 1 |
| Dts (psi) | 2 | 62.6 | 2 | 64.3 | 2 | 72.6 | 1 | 77.7 | 1 |
| (B) | 3 | 57.6 | 3 | 65.3 | 2 | 71.5 | 1 | 71.9 | 1 |
| | 4 | 57.4 | 3 | 58.7 | 3 | 68.0 | 2 | 68.6 | 2 |
| Wt for Subcr. | CV | 15.1 | B | 16.2 | B | 15.9 | B | 20.7 | B |
| | 0 | 29.4 | 5 | 26.2 | 5 | 45.9 | 4 | 35.7 | 5 |
| | 1 | 51.0 | 4 | 56.8 | 3 | 64.0 | 2 | 63.8 | 2 |
| WTS (psi) | 2 | 65.4 | 2 | 61.9 | 2 | 71.6 | 1 | 73.0 | 1 |
| (A) | 3 | 48.6 | 4 | 53.1 | 3 | 64.5 | 2 | 68.9 | 1 |
| | 4 | 42.1 | 5 | 53.5 | 3 | 62.0 | 2 | 59.7 | 2 |
| Wt for Subcr. | CV | 29.7 | B | 28.5 | B | 18.0 | B | 25.4 | B |
| | 0 | 52.1 | 5 | 40.2 | 5 | 64.9 | 4 | 50.9 | 5 |
| | 1 | 89.8 | 2 | 84.5 | 2 | 90.4 | 1 | 90.5 | 1 |
| TSR (%) | 2 | 105.7 | 1 | 97.7 | 1 | 100.7 | 1 | 95.4 | 1 |
| (C) | 3 | 83.4 | 2 | 81.7 | 2 | 91.5 | 1 | 101.2 | 1 |
| | 4 | 75.5 | 3 | 94.6 | 1 | 93.2 | 1 | 89.9 | 2 |
| Wt for Subcr. | CV | 30.0 | B | 31.3 | C | 20.9 | B | 32.4 | C |
| | 0 | 1.88 | 2 | 1.88 | 2 | 1.63 | 2 | 2.13 | 2 |
| | 1 | 1.00 | 1 | 1.00 | 1 | 1.00 | 1 | 1.00 | 1 |
| VSR | 2 | 1.13 | 1 | 1.00 | 1 | 1.00 | 1 | 1.00 | 1 |
| (A) | 3 | 1.00 | 1 | 1.00 | 1 | 1.00 | 1 | 1.00 | 1 |
| | 4 | 1.13 | 1 | 1.00 | 1 | 1.00 | 1 | 1.00 | 1 |
| Wt for Subcr. | CV | 34.5 | C | 38.0 | C | 35.9 | C | 47.1 | D |
| | 0 | | | 0 | 1 | | | | |
| | 1 | | | 0.5 | 2 | | | | |
| Price (E) | 2 | | | 1.5 | 4 | | | | |
| ($/ton) | 3 | | | 0.5 | 2 | | | | |
| | 4 | | | 0.5 | 2 | | | | |

Result of FWA Operation

| ASA | 0 | 1 | 2 | 3 | 4 |
|---|---|---|---|---|---|
| RI value | 9.50 | 10.50 | 13.50 | 12.75 | 12.50 |

*: highest value in each criterion

## DISCUSSION AND CONCLUSIONS

Using the fuzzy set analysis method, a procedure for evaluating the effectiveness of ASAs for asphaltic concrete mixtures was presented. The procedure uses selected mixture properties (e.g., dry and wet tensile strength, TSR, VSR) that can be obtained by simple laboratory testing. Because of the vague interrelationship among the mixture properties, a simple comparison of one value to another is fuzzy and sometimes does not give a clear answer. Moreover, selecting the best-performing mixture by comparing many factors (criteria) is not achieved simply, because subjective judgments are involved in organizing much of the data. Therefore, the fuzzy set theory was introduced, and it was shown that it can be successfully incorporated into a solution procedure.

From example problems, it was shown that the best-performing ASA can be selected from among many additives. This was accomplished from FWA operation based on real data, arbitrarily selected fuzzy sets, and weighing scales determined by the engineer's judgment.

The selection of the best-performing ASA is based on a reasonable performance evaluation of the mixtures because the fuzzy weighted average is a combined result of the following considerations:

1. The mean values of engineering properties and moisture susceptibility of each group of mixtures for rating,
2. The engineer's judgment for weight of main criteria, and
3. The variation of the data for weight of each subcriterion.

More properties such as resilient modulus and fatigue resistance modulus can be added to the main criteria, if available. In addition, field mixtures can be used to evaluate the performance of ASAs in the field. In that case, if samples are collected from extensive sections of highway, construction quality and traffic condition can be made additional criteria to obtain a more reasonable result.

It should be noted that fuzzy sets used in this study were arbitrarily selected. Other fuzzy sets can be established for similar types of problems with any number of criteria and subcriteria.

## REFERENCES

1. D. G. Tunnicliff and R. E. Root. *NCHRP Report 274: Use of Antistripping Additives in Asphalt Concrete Mixtures—Laboratory Phase*. TRB, National Research Council, Washington, D.C., 1984.
2. R. P. Lottman. *NCHRP Report 246: Predicting Moisture-Induced Damage to Asphaltic Concrete—Field Evaluation*. TRB, National Research Council, Washington, D.C., 1982.
3. H. W. Busching, J. L. Burati, and S. N. Amirkhanian. *An Investigation of Stripping in Asphalt Concrete in South Carolina*. Report FHWA-SC-86-02. FHWA, U.S. Department of Transportation, July 1986.
4. K. W. Kim. *Determination of Critical Tensile Strength for Bituminous Concrete Surface Course*. Ph.D. dissertation. Clemson University, Clemson, S.C., Aug. 1989.
5. L. Zadeh. Fuzzy Sets. *Information and Control*, Vol. 8, 1965, pp. 338–353.
6. L. Zadeh. Outline of a New Approach to the Analysis of Complex Systems and Decision Processes. *IEEE Transactions on Systems, Man, and Cybernetics*, Vol. SMC-3, No. 1, 1973, pp. 28–44.
7. C. B. Brown and J. T. P. Yao. Fuzzy Sets and Structural Engineering. *Journal of Structural Engineering, ASCE*, Vol. 109, No. 5, May 1983, pp. 1,211–1,225.
8. M. Fishbein and I. Ajzen. *Belief Attitude, Intention and Behavior: An Introduction to Theory and Research*. Addison-Wesley, Reading, Mass., 1975.
9. R. R. Yager. Satisfaction and Fuzzy Decision Function. In *Fuzzy Sets: Theory and Applications to Policy Analysis and Information Systems*, Plenum Press, 1980, pp. 171–194.
10. L. A. Neitzel and L. J. Hoffman. Fuzzy Cost and Benefit Analysis. In *Fuzzy Sets: Theory and Applications to Policy Analysis and Information Systems*, Plenum Press, 1980, pp. 171–194.
11. R. E. Bellman and L. A. Zadeh. Decision-Making in a Fuzzy Environment. *Management Science*, Vol. 17, No. 4, 1970, pp. 141–154.
12. V. U. Nguyen. Tender Evaluation by Fuzzy Set. *Journal of Construction Engineering and Management*, Vol. 111, No. 3, Sept. 1985, pp. 231–243.
13. K. J. Schmucker. *Fuzzy Sets, Natural Language Computations, and Risk Analysis*. Computer Science Press, Rockville, Md., 1984.
14. C. H. Juang and S. N. Kalidindi. *BETS Program Documentation*. Engineering Report. Clemson University, Clemson, S.C., May 1987.
15. P. W. Mullarkey and S. J. Fenves. Fuzzy Logic in a Geotechnical Knowledge-Based System: CONE. *Proc., NSF Workshop on Civil Engineering Application of Fuzzy Sets*, Purdue University, West Lafayette, Ind., Oct. 1985.
16. D. G. Tunnicliff and R. E. Root. Antistripping Additives in Asphalt Concrete, State of the Art. *Proc., Association of Asphalt Paving Technologists*, Vol. 51, 1982, pp. 265–293.
17. D. G. Tunnicliff and R. E. Root. Testing Asphalt Concrete for Effectiveness of Antistrip Additives. *Proc., Association of Asphalt Paving Technologists*, Vol. 52, 1983.
18. T. W. Kennedy. Characterization of Asphalt Pavement Materials Using the Indirect Tensile Test. *Proc., Association of Asphalt Paving Technologists*, Vol. 46, 1977.

*Publication of this paper sponsored by Committee on Nonbituminous Components of Bituminous Paving Mixtures.*

# Properties of Fly Ash–Extended Asphalt Concrete Mixes

ABDULRAHMAN S. AL-SUHAIBANI AND EGON T. TONS

Fillers added to asphalt concrete mixes have long been used as stiffening, extending, or otherwise void-filling materials, depending on their type and particle size. Fly ash, a by-product of the coal-burning process for power generation, is a filler that can serve one or more of the above-mentioned functions. The role of fly ash in asphalt concrete mixes has been investigated. Three sizes of fly ash (coarse, medium, and fine) were used. The effect of these fly ash sizes on the resilient modulus, rutting potential, and water resistance of these mixes was investigated. It was found that the medium-size fly ash was the best size for an asphalt extender.

Fly ash is a finely divided residue that results from furnace-burned pulverized bituminous coal. Electrical generation is the prime consumer of coal produced in the United States and, consequently, the prime producer of fly ash. In the United States, the annual production of fly ash increased from about 43 million tons in 1975 to about 60 million tons in 1979; the utilized amount during that time increased from about 5 million tons, or 10.6 percent of the production, to about 10.0 million tons, or 17.4 percent (*1*). From these figures, it is clear that there is a huge amount of unused fly ash that must be disposed of each year. This not only costs power companies money but also creates a disposal problem.

Asphalt pavement usually consists of three components: asphalt, aggregates, and air. Because nearly all asphalts used in road construction are of crude oil origin, the increase in crude oil prices in recent years has resulted in an increase in asphalt prices. The dwindling world resources of oil have increased concerns about the asphalt supply for highway pavements. In addition, a considerable portion of asphalt-type highways in the United States are deteriorating as a result of heavy loads and unfavorable weather conditions. All of this has led many researchers and agencies to look for ways of reducing the amount of the required asphalt and improving pavement resistance against loading and moisture damage.

One method that has recently received much attention is the partial substitution, or replacement, of asphalt with other materials. Some mineral fillers have been known to work as integral parts (extenders) of asphalt if thoroughly mixed with it, resulting in an increase in binder content and, therefore, decreasing the amount of asphalt required for optimum conditions.

Fly ash has been used successfully as a filler for asphalt mixes for a long time. It has the advantage of increasing the resistance of asphalt mixes to moisture damage. In addition to filling voids, fly ash reportedly works as an asphalt extender (*2*). It is the main purpose of this investigation to study the possibility of using wasted fly ash as an asphalt extender in bituminous paving mixes.

A. S. Al-Suhaibani, Civil Engineering Department, College of Engineering, King Saud University, P. O. Box 800, Riyadh 11421, Saudi Arabia. E. T. Tons, Civil Engineering Department, University of Michigan, Ann Arbor, Mich. 48104.

## LITERATURE REVIEW

As finely pulverized bituminous coal is burned, particles of fly ash are suspended in the gas stream that reaches the boiler. As hot gases pass into the atmosphere, the particles of fly ash collect on the plates of electrostatic precipitators within the heating system. Fly ash is then processed or filtered and finally accumulated and stored (*3,4*).

Fly ash is characterized by its low specific gravity, which is a function of its chemical composition and varies between 2.3 and 2.6, averaging 2.4 (*5*). The particle size distribution generally depends on the collector used. It has been found that the ash collected by the electrostatic precipitator contains a greater percentage of very small particles (<1.5 μ) (*4*). In general, a typical fly ash particle size ranges between 0.5 μ and 100 μ (*4*). Fly ash particles are generally spherical (*4,6*); however, a minor fraction consists of irregularly shaped particles (*6*).

Most types of fly ash have been used successfully as mineral fillers in hot asphalt mixes (*4–6*). It has been reported that fly ash does not differ materially from Trinidad Asphalt's mineral filler (*7*). In another study, fly ash was used as a replacement for limestone dust in asphalt concrete mixes with good results (*8*). The suitability of fly ash as a filler in sheet asphalt mixes was investigated by the Detroit Edison Company and reported by Zimmer (*9*). It was found that stabilities of mixes containing fly ash are comparable to those containing limestone dust when proportions are based on weight, and that fly ash has virtually the same void-reducing properties as limestone dust.

The resistance of asphalt mixes containing fly ash to water action has been found to be equal or superior to those containing other types of filler (*6,10*). The strength retention for eight fly ashes ranges between 85 and 100 percent—all above the 75 percent figure considered to be the critical minimum.

A report by Rosner et al. indicates that the addition of up to 6 percent fly ash by weight of aggregate to asphalt concrete produces an acceptable mix (*11*). At the same time, asphalt requirements and voids in mineral aggregates (VMA) values are lower than those for mixes containing portland cement or hydrated lime.

Tons et al. investigated the use of fly ash as a replacement for asphalt cement in asphalt concrete mixes (*2*). The three

types of fly ash used in the study were found to have positive effects on the physical properties of the evaluated mixes. Furthermore, the replacement of up to 30 percent of asphalt cement by fly ash improved most of the mix's physical properties when a practical asphalt content was used.

Concerning other types of fillers, Kallas and Puzinauskas found that 9 of the 11 fillers investigated were effective in replacing a portion of the asphalt required to produce minimum VMA (*12*). Other reports also point out that some mineral fillers can serve as asphalt extenders, and that they may actually decrease the stiffness of the asphalt (*13,14*). Baghouse fines, also, were reported to act as asphalt extenders (*15–18*).

Finally, it has been found that mixing fine fly ash particles (passing Sieve #325) with asphalt cement causes the highest increase in viscosity compared with coarser fly ash sizes (*19*).

## STUDY OBJECTIVES

This investigation had two objectives:

1. To study the effect of fly ash particle size, aggregate gradation, and binder content on the resilient modulus and rut-depth characteristics of asphalt concrete mixes.
2. To evaluate the use of fly ash as an asphalt extender in asphalt concrete mixes.

## EXPERIMENTAL WORK

### Materials

#### *Asphalt Cement*

AC-20 asphalt cement was used for this study. It was obtained from Marathon Petroleum Company in Detroit, Michigan. The results of tests conducted on the asphalt are shown in Table 1.

#### *Fly Ash*

Fly ash used in this study was obtained from Consumer's Power Company, Michigan. The fly ash was dry-sieved on Sieves #270 and #325 for 15 min. Because fly ash has practically no particles finer than 1 μ, silica fume (microsilica), which is 100 percent finer than 0.5 μ, was mixed with the fly ash fraction passing Sieve #325 in a 50/50 ratio by weight to form the fine fraction. This was done to study the stiffening effect of very fine materials. Table 2 summarizes the specific gravities and particle size distribution of the three fractions.

#### *Aggregate*

The coarse aggregate was a crushed gravel obtained from Thompson-McCully Asphalt Paving Company in Whitmore Lake, Michigan. The fine aggregate was a concrete sand obtained locally.

The coarse aggregate was sieved and divided into different sizes as follows: ¾ in.–½ in., ½ in.–⅜ in., ⅜ in.–#4, #4–#8. Each size was then thoroughly washed, dried, and stored until usage. The fine aggregate was divided into the following sizes: #8–#16, #16–#30, #30–#50, #50–#100, #100–#200.

The coarse and fine aggregate fractions were combined with the desired proportions according to the gradation curves A, B, and C. The three gradations were chosen in such a way that the sand content was different for each one; however, they were all within the specification limits of the Michigan Department of Transportation. The fine gradation (C) represents the finest, and the coarse gradation (A) represents the coarsest. The medium gradation (B) falls between the two. An important property of these aggregate gradations is that they possess different surface areas. This is important because the larger the surface area of aggregates, the larger the amount of asphalt needed to coat such aggregates. The three gradation curves are shown in Figure 1, and their specific gravities and absorptions are shown in Table 3.

TABLE 1 SUMMARY OF ASPHALT CEMENT PROPERTIES

| Test | ASTM Test Designation | Test Results |
|---|---|---|
| Specific Gravity (77/77° F) | D 70-76 | 1.022 |
| Viscosity x $10^6$, poises (77° F) | D 3570-77 | 1.504 |
| Penetration (77° F) 0.1 mm, 100 g, 5 sec | D 5-73 | 74 |
| Penetration (95° F) 0.1 mm, 100 g, 5 sec | D 5-73 | (143)* |
| Softening Point, of (R & B) | D 36-76 | 122 (129)* |
| P.I. | | (-0.7)* |

* For Recovered Asphalt

TABLE 2 PROPERTIES OF FLY ASH FRACTIONS

| Grain Size Analysis | Fly Ash Fraction Coarse | Medium | Fine* |
|---|---|---|---|
| Sieve Size: | | | |
| # 30 (595 μ) | 99.9 | 100 | 100 |
| # 100 (144 μ) | 93 | 100 | 100 |
| # 200 ( 75 μ) | 64 | 100 | 100 |
| # 270 ( 54 μ) | 54 | 100 | 100 |
| Hydrometer Analysis | | | |
| # 325 (44 μ) | 47 | 100 | 100 |
| 30 | 36 | 94 | 97 |
| 20 | 25 | 79 | 90 |
| 13 | 18 | 54 | 77 |
| 9 | 13 | 41 | 70 |
| 7 | 10 | 30 | 65 |
| 3.5 | 4 | 10 | 55 |
| 1.5 | 0 | 2 | 51 |
| 1 | 0 | 0 | 50 |
| 0.5 | 0 | 0 | 50 |
| 0.2 | 0 | 0 | 48 |
| 0.1 | 0 | 0 | 35 |
| 0.084 | 0 | 0 | 25 |
| .05 | 0 | 0 | 10 |
| .01 | 0 | 0 | 2 |
| Specific Gravity | 2.012 | 2.383 | 2.259 |

*50 percent by weight silica fume

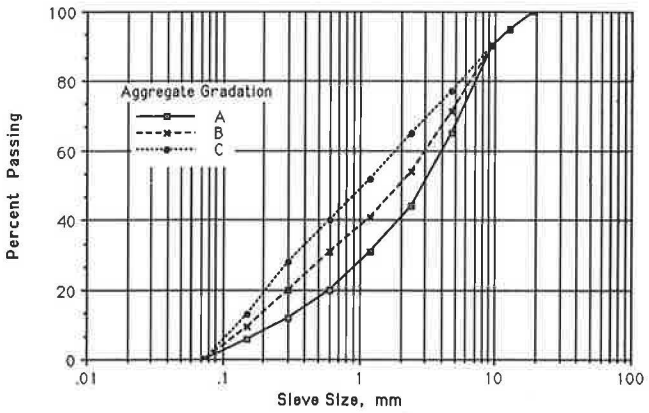


**FIGURE 1 Particle size distribution of aggregates.**

### Test Variables and Specimens Preparation

A set of variables was chosen for this study. In addition to the fly ash sizes and aggregate gradations already mentioned, two other variables—asphalt content and percentage of replacement—were used.

Because asphalt content is not constant in the replacement process, the term "asphalt equivalent," which represents the asphalt content for control mixes, was used instead. Three asphalt equivalents were used in this study—namely, 4, 5, and 6 percent. The asphalt cement at each asphalt equivalent was replaced by an equal volume of fly ash in five replacement percentages: 0, 10, 20, 30, and 40 percent. The asphalt cement was partially replaced by fly ash so that the total volume of binder (asphalt + fly ash) was kept constant and equal to the original asphalt volume before the addition of fly ash.

All specimens used were Marshall size and were cast according to ASTM standards with 50 blows on each side of the specimen.

Either one or two specimens were prepared for each mix, as shown in Table 4. For control mixes (no fly ash), two specimens were prepared. This experimental design was used to reduce the quantity of materials needed and the time necessary for preparing and testing specimens.

## CHARACTERIZATION OF MIXES

### Resilient Modulus

Resilient modulus test before and after immersion was conducted on the same specimen; the nondestructive nature of the test made this possible.

Specimens were immersed in water at 140°F for 24 hr. Testing for resilient modulus was then done for the purpose of evaluating the effect of test variables (mainly fly ash size and quantity) on resistance of mixes to water action. By testing the same specimen before and after immersion, errors owing to material variability were eliminated. At the same time, a reduction in materials' quantities, time, and effort was achieved.

It should be mentioned that although only samples of the results are reported here, the conclusions were based on the results of the entire study (*19*).

### Dry Resilient Modulus

Dry resilient modulus results for 6 percent asphalt equivalent are shown in Figure 2. These results show that, in general and for a given aggregate gradation and binder content, fine fly ash causes the most stiffening of the three fly ash fractions. This is consistent with the results of viscosity testing of asphalt–fly ash mixes (*19*), which show that the fine fly ash causes the highest stiffening effect among the three fly ash sizes. Medium fly ash ranks second; coarse fly ash gave the

TABLE 3 SPECIFIC GRAVITIES AND ABSORPTIONS OF AGGREGATE GRADATIONS

| Parameter | Aggregate Gradation A | B | C |
|---|---|---|---|
| Bulk Sp. Gr. | 2.599 | 2.600 | 2.600 |
| Bulk Sp. Gr. (SSD) | 2.645 | 2.643 | 2.640 |
| Apparent Sp. Gr. | 2.725 | 2.717 | 2.709 |
| Percent Absorption | 1.775 | 1.662 | 1.554 |

TABLE 4 MIX VARIABLES AND NUMBER OF SPECIMENS

| | Aggregate Gradation | | | | | | | | |
|---|---|---|---|---|---|---|---|---|---|
| | A | | | B | | | C | | |
| | Fly Ash Size | | | Fly Ash Size | | | Fly Ash Size | | |
| | F | M | C | F | M | C | F | M | C |
| Asphalt - Equivalent 4 Percent of Asphalt Replaced | | | | | | | | | |
| 0 percent | 2 | 2 | 2 | 2 | 2 | 2 | 2 | 2 | 2 |
| 10 percent | 1 | 2 | 1 | 2 | 1 | 2 | 1 | 2 | 1 |
| 20 percent | 2 | 1 | 2 | 1 | 2 | 1 | 2 | 1 | 2 |
| 30 percent | 1 | 2 | 1 | 2 | 1 | 2 | 1 | 2 | 1 |
| 40 percent | 2 | 1 | 2 | 1 | 2 | 1 | 2 | 1 | 2 |
| Asphalt - Equivalent 5 Percent of Asphalt Replaced | | | | | | | | | |
| 0 percent | 2 | 2 | 2 | 2 | 2 | 2 | 2 | 2 | 2 |
| 10 percent | 2 | 1 | 2 | 1 | 2 | 1 | 2 | 1 | 2 |
| 20 percent | 1 | 2 | 1 | 2 | 1 | 2 | 1 | 2 | 1 |
| 30 percent | 2 | 1 | 2 | 1 | 2 | 1 | 2 | 1 | 2 |
| 40 percent | 1 | 2 | 1 | 2 | 1 | 2 | 1 | 2 | 1 |
| Asphalt - Equivalent 6 Percent of Asphalt Replaced | | | | | | | | | |
| 0 percent | 2 | 2 | 2 | 2 | 2 | 2 | 2 | 2 | 2 |
| 10 percent | 1 | 2 | 1 | 2 | 1 | 2 | 1 | 2 | 1 |
| 20 percent | 2 | 1 | 2 | 1 | 2 | 1 | 2 | 1 | 2 |
| 30 percent | 1 | 2 | 1 | 1 | 1 | 2 | 1 | 2 | 1 |
| 40 percent | 2 | 1 | 2 | 1 | 2 | 1 | 2 | 1 | 2 |

lowest modulus values. This kind of behavior is expected because the fine fraction (contains an appreciable amount of submicron particles), when combined with asphalt, caused its viscosity to increase to values higher than those caused by the other two fractions. This translates into a high resilient modulus in asphalt–fly ash concrete mixes. As for coarse fly ash, given its large particle size, it creates more voids in the mix, hence producing a less stiff mix than the other two.

For a given aggregate gradation and asphalt equivalent, dry resilient modulus increases as the percent of replacement increases for fine and medium fly ash, but it remains the same or decreases for coarse fly ash. The increase in the resilient modulus in the case of fine fly ash appears to be logical, given its high stiffening effect. The ineffectiveness or the negative effect of coarse fly ash is mainly attributable to the increase in voids in mixes made with this fraction as its quantity increases.

For a given aggregate gradation, increasing asphalt equivalent from 4 to 6 percent has little or no effect on dry resilient modulus. The details of this effect can be found elsewhere (*19*).

In general, for a certain asphalt equivalent, changing the aggregate gradation from A to C shifted the resilient modulus values downward. This was more pronounced for mixes containing coarse fly ash and mixes with low replacement percentages. Grain interlock, which is more pronounced for Gradation A, could be the reason for this behavior.

Estimates of the main effects of the four independent variables on dry resilient modulus are shown in Table 5. These effects seem to strengthen the previous conclusions. These

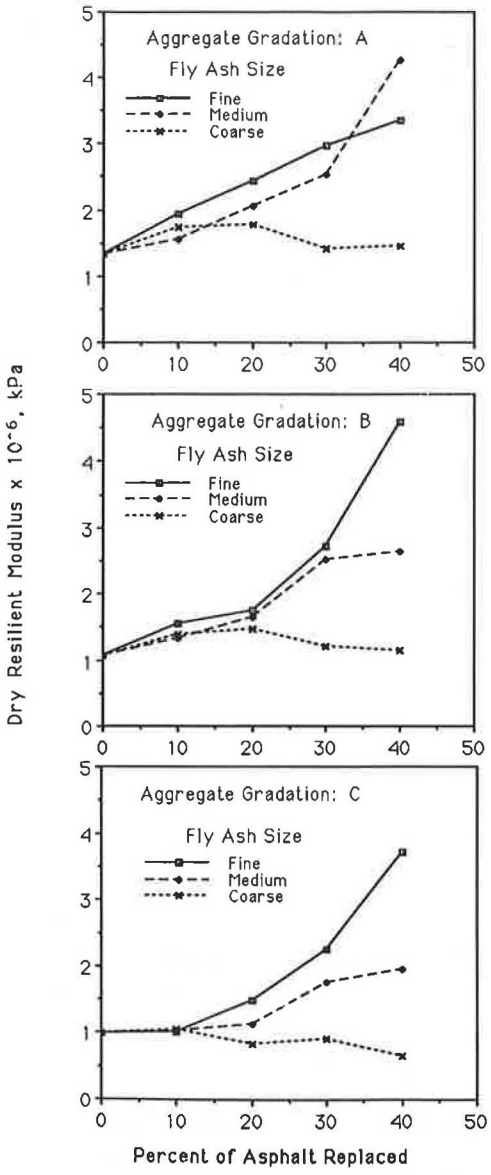


**FIGURE 2 Dry resilient modulus versus percentage of asphalt replaced for 6 percent A.E.**

effects are represented by $\alpha$, $\beta$, $\gamma$, and $\lambda$ in the prediction model shown below.

$$Y_{ijklm} = \mu + \alpha_i + \beta_j + \gamma_k + \lambda_l + \varepsilon_{ijklm} \quad (1)$$

where

$Y_{ijklm}$ = the predicted value of the dependent variable for a given set of levels of the independent variables,
$\mu$ = the grand mean (the constant in Table 5),
$\alpha_i$ = estimated main effect of the $i$th level of the asphalt equivalent,
$\beta_j$ = estimated main effect of the $j$th level of the aggregate gradation,
$\gamma_k$ = estimated main effect of the $k$th level of the percentage of asphalt replaced,
$\lambda_l$ = estimated main effect of the $l$th level of fly ash size, and
$\varepsilon_{ijklm}$ = an error term.

These parameters indicate the effect of each level of a given independent variable on the predicted values. A plus sign indicates a positive effect; a minus sign indicates a negative effect. A very low value (approximately zero) indicates little or no effect. In other words, the estimated main effects show the contribution of each level of the independent variable toward the predicted values. Table 5 also shows the standard deviation of these main effects.

## Immersion Effect

To study the effect of water on asphalt–fly ash concrete mixes, the index of retained stiffness (IRS) was used. IRS is the ratio of resilient modulus after and before water immersion. It indicates the resistance of a given mix to water action.

Figure 3 shows a sample of the results of soaked resilient modulus. Corresponding IRS values are shown in Figure 4. Tables 6 and 7 show the statistically estimated main effects for soaked resilient modulus and IRS, respectively. These results show that, in general, IRS value gets lower as the aggregate gets finer and as the asphalt equivalent gets lower. However, much lower IRS values were obtained for mixes made with Gradation A and fine fly ash at 40 percent replacement. In fact, all mixes made with fine fly ash at 40 percent replacement show lower IRS values than those mixes made with medium or coarse fly ashes. This was expected, because these mixes were not completely coated with asphalt, allowing water to easily strip asphalt films from aggregate surface, thus reducing IRS values below those of other mixes.

## Rut Depth Prediction

One of the major distresses that occur in bituminous pavement is permanent deformation, or rutting. Permanent deformation has received considerable attention from researchers and pavement technologists. Several methods have been introduced in pavement design to address the problem of rutting. These methods are divided into two main categories: indirect and predictive (*20*). Indirect methods are based on limiting layer thickness and component material strengths, stability, or density to a minimum, or limiting the vertical compressive strain on the subgrade surface to some maximum level. Predictive methods are based on predicting rut depth for a given set of conditions and redesigning the pavement if necessary until a satisfactory rut depth value is obtained.

A predictive method that relates pavement permanent deformation to creep test results was developed by Shell Oil Company Laboratories. Because of its simplicity as a tool for comparing different mixes and the availability of the needed equipment to run the creep test, this method has been adopted here to evaluate the rutting potential of asphalt–fly ash concrete mixes (*21*).

To predict rut depth, the static creep test—as suggested by Shell—was conducted on Marshall specimens representing

TABLE 5 ESTIMATED MAIN EFFECTS FOR DRY RESILIENT MODULUS $\times 10^6$ (kPa)

| Parameter | Estimated Main Effects | Standard Deviation |
|---|---|---|
| Constant | 1.88 | 0.03 |
| Asphalt Equivalent | | |
| 6 Percent | 0.02 | 0.06 |
| 5 Percent | 0.03 | 0.06 |
| 4 Percent | -0.06 | 0.06 |
| Aggregate Gradation | | |
| A | 0.36 | 0.06 |
| B | 0.09 | 0.06 |
| C | -0.45 | 0.06 |
| Percent of Asphalt Replaced | | |
| 10 Percent | -0.48 | 0.06 |
| 20 Percent | -0.19 | 0.06 |
| 30 Percent | 0.10 | 0.06 |
| 40 Percent | 0.57 | 0.06 |
| Fly Ash Size | | |
| Fine | 0.53 | 0.06 |
| Medium | 0.10 | 0.12 |
| Coarse | -0.63 | 0.06 |

different mixes. Each mix was represented by either one or two specimens (see Table 4), which were made and tested at random. The test was performed for 1 hr in a temperature-controlled chamber maintained at about 104°F (40°C). The time-dependent deformation was measured using a pair of linear variable differential transformers (LVDTs) that were connected to a computer to take readings, calculate the mix stiffness, and store the data. Time-dependent mix stiffness ($S_{mix}$) was later plotted in a log-log scale against the stiffness of recovered asphalt ($S_{bit}$). The scale, obtained from a Van der Poel nomograph (*22*), was for the same conditions as those of $S_{mix}$.

For rut depth calculation, pavement must be divided into layers and sublayers; then, for a given air temperature, the asphalt effective viscosity is calculated for each sublayer. Effective viscosity, the slope of the $S_{mix}$-$S_{bit}$ relationship, and traffic data were used thereafter to calculate the viscous part of the asphalt stiffness ($S_{bit}$, visc). This value was then used to obtain the viscous part of the mix stiffness from the $S_{mix}$-$S_{bit}$ relationship.

The rut depth was then calculated using the following equation:

$$\Delta h_i = C_m h_i \frac{Z_i \times 6 \times 10^5}{S_{mix,i}} \quad (2)$$

$$\Delta h = \sum \Delta h_i \quad (3)$$

where

$\Delta h_i$ = rut depth in the $i$th sublayer,
$\Delta h$ = total rut depth,
$C_m$ = correction factor for dynamic effect,
$h_i$ = sublayer thickness,
$S_{mix,i}$ = mix stiffness for the $i$th sublayer, obtained from the $S_{mix}$-$S_{bit}$ relationship, and
$Z_i$ = proportionality factor between average stress and contact stress.

The factor $Z$ in the equation is a function of mix stiffness in the high-stiffness region (short loading time), the sublayer thickness, the stiffness and the thickness of other sublayers, the modulus and thickness of the base course, and the subgrade modulus. The values of $Z$ were calculated using the elastic layer theory and tabulated for different combinations of the previously mentioned variables.

The expected rut depth in each mix was calculated for the conditions shown in Table 8.

The results of the calculated rut depth are plotted in Figures 5 and 6. It is worth mentioning that most mixes made with Gradation C failed under the static load, some after only a few minutes of loading, so no data were obtained for thse mixes. As the results show, the general trend for all mixes containing fine and medium fly ash fractions is that the rut depth decreases as the replacement increases. Mixes made with Gradation A and coarse fly ash show similar results. However, mixes made with Gradation B and coarse fly ash show an increase in rut depth as the percent of replacement increases. The reason that the coarse fly ash increases the rut depth as the replacement increases for Gradation B and not A is probably that the aggregates' interlocking—and hence the mix's resistance to loading—is reduced by increasing the percentage of replacement in the case of Gradation B, which contains a larger amount of sand. On the other hand, Gradation A contains a small amount of sand; hence, even with

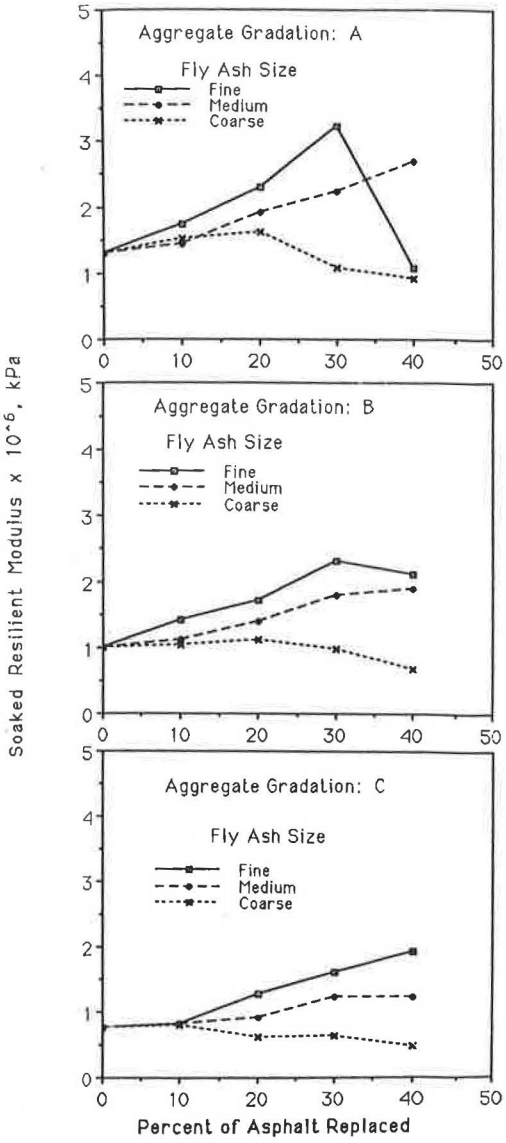


**FIGURE 3 Soaked resilient modulus versus percentage of asphalt replaced for 6 percent A.E.**

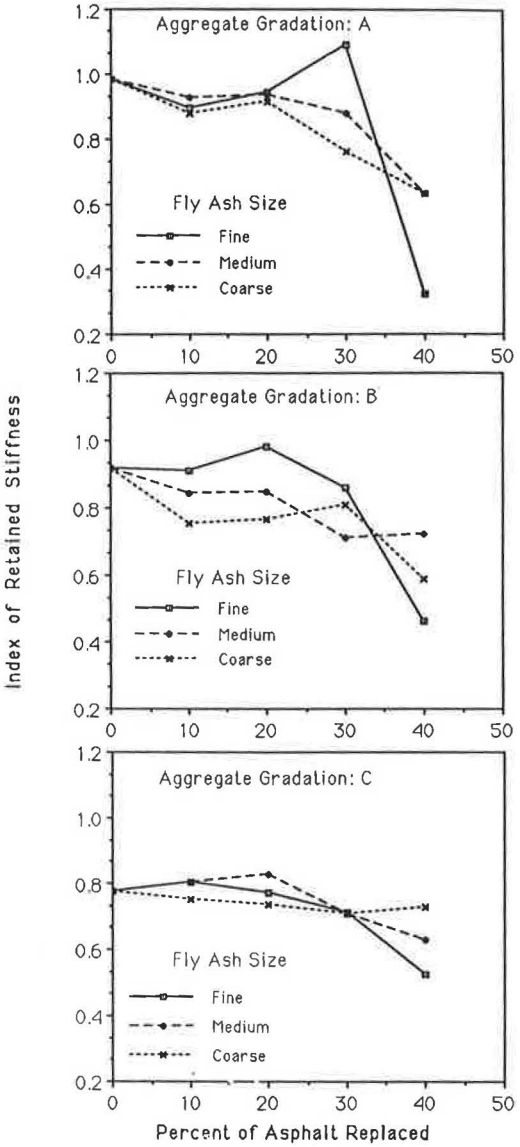


**FIGURE 4 Index of retained stiffness versus percentage of asphalt replaced for 6 percent A.E.**

the addition of coarse fly ash, the interlocking among large aggregate particles—and, in turn, the rut depth—is not much affected by the replacement process.

For a given aggregate gradation and asphalt equivalent, fine, medium, and coarse fly ash fractions gave the lowest, intermediate, and highest rut depth, respectively, when compared at the same percentage of replacement. However, there are a few exceptions. Ranking mixes containing the three fly ash fractions in the order mentioned is expected, given the stiffening effect of each one as was shown in the discussion of resilient modulus results.

The rut depth results for the three fly ash fractions are generally the same in the case of Gradation A but not B. This could be attributed to differences in residual asphalt, unit weight, and air voids between mixes made with Gradation A and those made with B.

When mixes are compared at the same aggregate gradation, the results indicate, although not very obviously, that increasing asphalt equivalent from 4 to 6 percent increases rut depth for control mixes (no fly ash added) and steepens slopes for curves representing the rut depth versus percentage of replacement. The first observation could be explained as follows: for control mixes, the residual asphalt is more at high than that at low asphalt equivalent. Consequently, the strength of high asphalt equivalent depends more on viscosity (resistance to flow) of the asphalt film than on particle-to-particle contact. This results in weaker mixes and, consequently, higher rut values in case of mixes made with high asphalt equivalent. The association of steeper slopes with higher asphalt equivalent could be attributed to the fact that, at a certain percentage of replacement, the higher the asphalt equivalent, the higher the amount of fly ash that should be added to the mix to replace asphalt at a given percentage of replacement. This, in turn, produces mixes with lower asphalt/aggregate ratios, resulting in stiffer mixes as the percentage of replacement increases in case of high asphalt equivalent.

TABLE 6 ESTIMATED MAIN EFFECTS FOR SOAKED RESILIENT MODULUS $\times 10^6$ (kPa)

| Parameter | Estimated Main Effects | Standard Deviation |
|---|---|---|
| Constant | 1.24 | 0.03 |
| Asphalt Equivalent | | |
| 6 Percent | 0.17 | 0.03 |
| 5 Percent | 0.01 | 0.03 |
| 4 Percent | -0.16 | 0.03 |
| Aggregate Gradation | | |
| A | 0.17 | 0.03 |
| B | 0.13 | 0.03 |
| C | -0.30 | 0.03 |
| Percent of Asphalt Replaced | | |
| 10 Percent | -0.17 | 0.05 |
| 20 Percent | -0.05 | 0.05 |
| 30 Percent | 0.17 | 0.05 |
| 40 Percent | -0.04 | 0.05 |
| Fly Ash Size | | |
| Fine | 0.26 | 0.03 |
| Medium | 0.10 | 0.03 |
| Coarse | -0.36 | 0.03 |

TABLE 7 ESTIMATED MAIN EFFECTS FOR INDEX OF RETAINED STIFFNESS

| Parameter | Estimated Main Effects | Standard Deviation |
|---|---|---|
| Constant | 0.69 | 0.008 |
| Asphalt Equivalent | | |
| 6 Percent | 0.08 | 0.01 |
| 5 Percent | -0.03 | 0.01 |
| 4 Percent | -0.05 | 0.01 |
| Aggregate Gradation | | |
| A | -0.03 | 0.01 |
| B | 0.02 | 0.01 |
| C | 0.01 | 0.01 |
| Percent of Asphalt Replaced | | |
| 10 Percent | 0.08 | 0.01 |
| 20 Percent | 0.06 | 0.01 |
| 30 Percent | 0.02 | 0.01 |
| 40 Percent | -0.16 | 0.01 |
| Fly Ash Size | | |
| Fine | -0.02 | 0.01 |
| Medium | 0.001 | 0.01 |
| Coarse | 0.02 | 0.01 |

TABLE 8 CONDITIONS FOR CALCULATING EXPECTED RUT DEPTH (*23*)

| Condition | Measurement |
|---|---|
| Asphalt-fly ash concrete layer thickness | 180 mm |
| Sublayer-1 thickness | 40 mm |
| Sublayer-2 thickness | 40 mm |
| Sublayer-3 thickness | 100 mm |
| Unbound base course thickness | 300 mm |
| Subgrade modulus | $10^8$ N/m$^2$ |
| Axle loads/lane/day | 2,000 |
| Design period | 15 years |
| Traffic growth/year | 2 percent |
| Ann Arbor weather data for 1984 | |

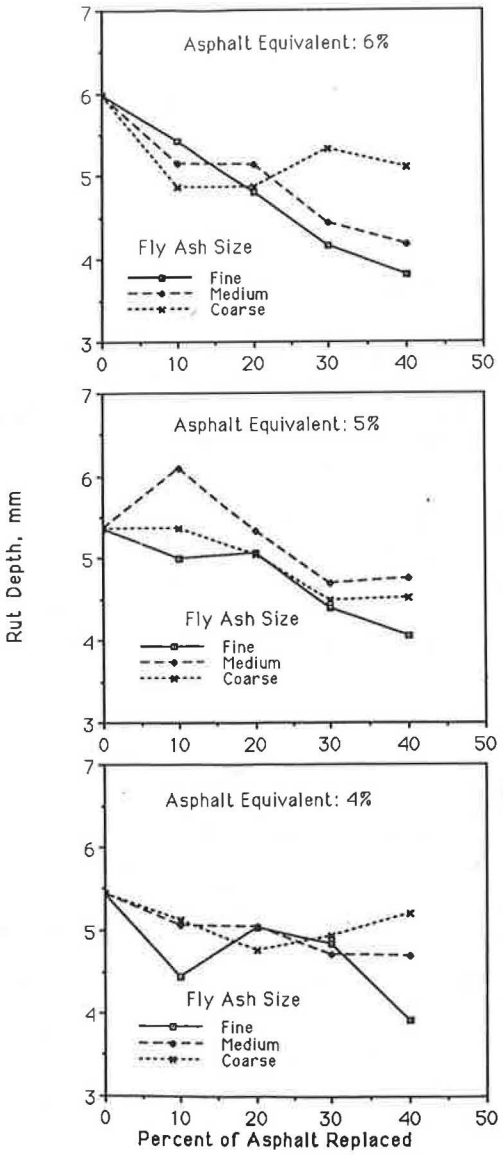


**FIGURE 5 Estimated rut depth versus percentage of asphalt replaced for Aggregate A.**

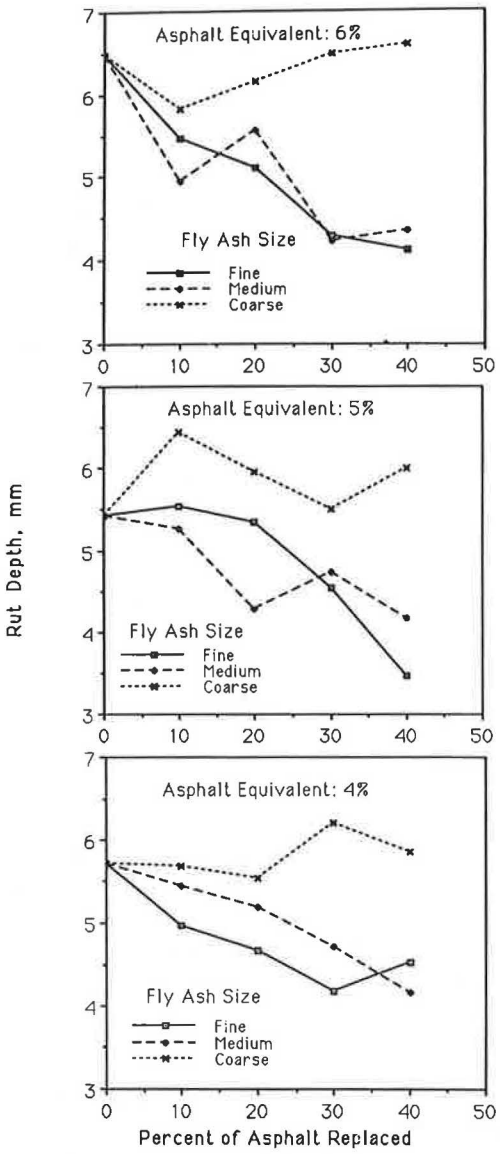


**FIGURE 6 Estimated rut depth versus percentage of asphalt replaced for Aggregate B.**

For 4 and 6 percent asphalt equivalents, the use of Gradation B resulted in a higher rut depth for control mixes than those produced by Gradation A. However, for 5 percent asphalt equivalent, the rut depth is about the same for both gradations. It was expected that control mixes made with Gradation B should give higher rut depth than those made with A (as is the case with 4 and 6 percent asphalt equivalent), because A produced mixes having higher unit weight and lower air voids than those made with B. So, the behavior of mixes made with 5 percent asphalt equivalent could only be attributed to experimental error.

For a given asphalt equivalent, changing aggregate gradation from A to B resulted in an increase in rut depth for mixes containing coarse fly ash. This could be explained by both unit weight and air voids, because mixes containing Gradation A possess both lower air voids and higher unit weight than those containing Gradation B (*19*).

TABLE 9 ESTIMATED MAIN EFFECTS FOR ESTIMATED RUT DEPTH (mm)

| Parameter | Estimated Main Effects | Standard Deviation |
|---|---|---|
| Constant | 5.32 | 0.07 |
| Asphalt Equivalent | | |
| 6 Percent | 0.053 | 0.09 |
| 5 Percent | -0.046 | 0.09 |
| 4 Percent | -0.007 | 0.09 |
| Aggregate Gradation | | |
| A | -0.50 | 0.09 |
| B | 0.16 | 0.99 |
| C | -0.66 | 0.99 |
| Percent of Asphalt Replaced | | |
| 10 Percent | 0.35 | 0.12 |
| 20 Percent | 0.27 | 0.10 |
| 30 Percent | -0.20 | 0.10 |
| 40 Percent | -0.42 | 0.10 |
| Fly Ash Size | | |
| Fine | -0.53 | 0.09 |
| Medium | 0.15 | 0.09 |
| Coarse | 0.38 | 0.09 |

Table 9 shows the estimated main effects of various variables on the estimated rut depth. Also shown are the standard deviations of these effects. These effects are consistent with those mentioned earlier. A descriptive model of these effects was presented earlier.

## CONCLUSIONS

It was the purpose of this study to investigate the feasibility of using fly ash as an asphalt extender and to study the effect of fly ash particle size and other variables on the replacement process. The following is a summary of the main conclusions:

1. Fly ash having particle sizes between 1 and 44 μ is the best as an asphalt extender, because coarser particles tend to create more voids among aggregate particles and finer ones tend to stiffen mixes. In the latter case, a mix with low workability is produced that also possesses large amount of voids after compaction.
2. It was strongly indicated that increasing sand content increases the sensitivity of rutting potential of different mixes to changes in sizes of fly ash particles.
3. For a given asphalt equivalent and aggregate gradation, the three fly ash fractions are very similar in their effectiveness against moisture damage except for mixes having 40 percent replacement.
4. At 40 percent replacement, the fine fraction caused the least resistance to moisture damage.
5. As far as this study shows, it is reasonable to replace up to 40 percent of asphalt volume with medium fly ash (1 through 44 μ in size) for dry climates; however, for moist climates, the replacement should not exceed 30 percent.

## PRACTICAL APPLICATIONS

The results of various tests performed on different mixes clearly show that the replacement of up to 30 percent of the asphalt volume by medium-size fly ash (passing Sieve #325) proved to be not detrimental to the mixes' performance. Because 80 percent of most fly ash produced by power plants passes Sieve #325, fly ash should be quite satisfactory when used to replace up to 30 percent of the asphalt volume. It is also expected that these mixes should perform well if they are installed in the field. Furthermore, substituting fly ash for part of the asphalt can mean savings for the road builders, fewer disposal problems for the fly ash producers, and less damage to the environment.

## REFERENCES

1. *Summary on Use of Fly Ash in Construction.* GAI Consultant, Nov. 1983.
2. E. Tons et al. *Fly Ash as Asphalt Reducer in Bituminous Base Courses.* University of Michigan, Ann Arbor, June 1983.
3. W. L. Chilcote. Fly Ash: Its Possibilities as a Source of Fines in Portland Cement Concrete and Bituminous Concrete Pavement Mixtures. *U. S. Navy Civil Engineers Corps Bulletin*, Vol. 6, Oct. 1952, pp. 279–281.
4. S. Torrey. Coal Ash Utilization: Fly Ash, Bottom Ash, and Slag. *Pollution Technology Review*, No. 48, 1978.
5. J. H. Faber and A. M. DiGioia, Jr. Use of Ash in Embankment Construction. In *Transportation Research Record 593*, TRB, National Research Council, Washington, D.C., 1976, pp. 13–19.
6. J. P. Capp and J. D. Spencer. *Fly Ash Utilization: A Summary of Applications and Technology*. Information Circular 8483. Bureau of Mines, U.S. Department of the Interior, 1970.
7. C. M. Weinheimer. Evaluating Importance of the Physical and Chemical Properties of Fly Ash in Creating Commercial Outlets

for the Material. *Transaction of the American Society of Mechanical Engineers*, Vol. 66, No. 6, Aug. 1944, pp. 551–561.
8. L. J. Minnick. New Fly Ash and Boiler Slag Uses. *Technical Association of the Pulp and Paper Industry*, Vol. 2, No. 1, Jan. 1949, pp. 21–28.
9. F. V. Zimmer. *Fly Ash as a Bituminous Filler.* Information Circular 8488. Bureau of Mines, U.S. Department of the Interior, 1970, pp. 49–76.
10. C. A. Carpenter. A Cooperative Study of Fillers in Asphaltic Concrete. *Public Roads*, Vol. 27, No. 5, Dec. 1952, pp. 101–110.
11. J. C. Rosner et al. Fly Ash as a Mineral Filler and Anti-Strip Agent for Asphalt Concrete. *Proc., 6th International Ash Utilization Symposium*, Vol. 1, July 1982, pp. 57–78.
12. B. F. Kallas and V. P. Puzinauskas. A Study of Mineral Fillers in Asphalt Paving Mixtures. *Proc., Association of Asphalt Paving Technologists*, Vol. 30, 1961, pp. 493–528.
13. E. L. Dukatz, Jr. *The Effect of Mineral Fillers on Asphalt and Asphaltic Concrete.* M.S. thesis. Department of Civil Engineering, Pennsylvania State University, Aug. 1978.
14. E. L. Dukatz and D. A. Anderson. The Effect of Various Fillers on the Mechanical Behavior of Asphalt and Asphaltic Concrete. *Proc., Association of Asphalt Paving Technologists*, Vol. 49, 1980, pp. 530–549.
15. R. G. Ward and J. M. McGougal. *Bituminous Concrete Plant Dust Collection System: Effect of Using Recovered Dust in Paving Mix.* Final Report on Research Project 60. West Virginia Department of Highways, Charleston, Dec. 1979.
16. G. W. Maupin, Jr. *Effect of Baghouse Fines on Compaction of Bituminous Concrete.* Report VHTRC 81-R49. Virginia Transportation Research Council, Charlottesville, May 1981.
17. D. A. Anderson and J. P. Tarris. *NCHRP Report 252: Adding Dust Collector Fines to Asphalt Paving Mixtures.* TRB, National Research Council, Washington, D.C., Dec. 1982.
18. D. A. Anderson et al. Dust Collector Fines and Their Influence on Mixtures Design. *Proc., Association of Asphalt Paving Technologists*, Vol. 51, 1982, pp. 363–397.
19. A. S. Suhaibani. *The Use of Fly Ash as an Asphalt Extender in Asphalt Concrete Mixes.* Ph.D. dissertation. University of Michigan, Ann Arbor, 1986.
20. R. Hass and W. Hudson. *Pavement Management Systems*, reprinted. Robert E. Krieger Publishing Company, Malabar, Fla., 1982.
21. *Shell Pavement Design Manual—Asphalt Pavements and Overlays for Road Traffic.* Shell International Petroleum Company Ltd., London, England, 1978.
22. C. Van der Poel. A General System Describing the Visco-Elastic Properties of Bitumens and Its Relation to Routine Test Data. *Journal of Applied Chemistry*, Vol. 4, May 1954, pp. 221–236.
23. *Climatological Data, Michigan.* Vol. 89, No. 1–12, 1984.

*Publication of this paper sponsored by Committee on Nonbituminous Components of Bituminous Paving Mixtures.*

# Improving Adhesion Characteristics of Bituminous Mixes by Washing Dust-Contaminated Coarse Aggregates

FAHAD A. BALGHUNAIM

Whether the engineering characteristics of bituminous mixes (especially their resistance to moisture effects) can be improved by washing the coarse aggregates and mixing the coarse and fine aggregates separately has been investigated. Results indicated that the washing of the coarse aggregate was most effective with the weaker aggregate. Washing the coarse aggregates generally improves the strength characteristics and reduces the asphalt content required to attain a certain level of strength, density, and air voids.

Distresses in asphalt concrete pavements take different forms but are generally caused by a combination of load, environmental, and materials factors. Several distresses can be present at the same time. But it is common to find that each region is plagued by one or two distresses that receive most of the attention. In the city of Riyadh, Saudi Arabia, raveling and rutting are the two most predominant distresses found in the pavements.

Several studies (*1–3*) have been undertaken by the Ministry of Communications, Riyadh Municipality, and other agencies to investigate the causes and possible remedies of raveling. In a well-compacted mix, raveling is primarily caused by the loss of adhesion between the aggregate and the asphaltic binder coating the aggregate. The primary external factor causing this is moisture.

Several tests have been developed to simulate the effect of water on asphalt concrete mixes. These tests can be divided into three types (*4*):

1. Tests that estimate, visually, the degree of stripping of asphalt from the aggregates.
2. Tests that measure the time or number of cycles needed to cause a certain disruption in the stressed specimens.
3. Tests that measure the effect of some type of conditioning of mix specimens in water on the mechanical properties of the mix.

The shared objective of these tests is to predict the field performance of certain asphalt concrete mixes from the stripping point of view.

Stripping occurs when water gets between the asphalt film and the aggregate surface. Several mechanisms can initiate, or are responsible for, this stripping (*4*). The aggregate used in the asphalt concrete mix is usually the source of the problem. For this study, it was hypothesized that a major cause of stripping in pavements in Riyadh is the dust particles contaminating the surfaces of the coarse aggregates. This study investigated the prospects of improving the resistance to moisture effects that can be obtained by washing the coarse aggregates to eliminate, or at least minimize, the dust coating them.

Ministry of Agriculture and Water, Riyadh 11195, Saudi Arabia.

## MATERIALS USED

### Aggregates

Aggregates used in the Riyadh area for highway construction are produced by crushing limestone deposits. For this study, aggregates were selected from two crushers representing two of the most commonly used by contractors in highway construction: Al-Duhami and CERCON. In addition, a third aggregate was brought from western Saudi Arabia, where igneous rock formations are mostly used to produce aggregates. The aggregate selected was basalt and was provided by Al-Harbi, a contractor. The purpose was to compare the limestone aggregate of the Riyadh area with the basalt aggregate of the western region in its response to coarse aggregate washing. Table 1 summarizes the physical characteristics of the three aggregates used in this study. The coarse and fine portions of each aggregate came from the same location.

As the aggregate was brought from its source, it was sieved into the following size fractions: ¾ in.–½ in., ½ in.–⅜ in., ⅜ in.–#4, #4–#10, #10–#40, #40–#80, #80–#200, P. #200. These sieve sizes were selected to correspond to the aggregate gradation used in this study, which was that adopted by the Ministry of Communications, as shown in Table 2.

The next step was to wash part of the coarse aggregates to be used. Each size fraction, down to #10 sieve, was washed separately. The washing was performed by placing the aggregate size fraction in its lower-limit sieve size and letting tap water run over it until clean. The washed coarse aggregate sizes were placed, separately, in an oven at 50° to 60°C for 1 day to dry. The aggregates were then placed in separate, closed containers to protect them from dust in the laboratory.

### Asphalt

The asphalt cement used in this study was a 60 to 70 penetration grade obtained from PETROMIN Riyadh Refinery, the primary source of asphalt cement for contractors near Riyadh. Table 3 summarizes the results of characterization tests performed on the asphalt cement used in this study.

TABLE 1 SUMMARY OF PROPERTIES OF AGGREGATES

| Test No. | Property | Designation | Aggregate I AL-DUHAMI | Aggregate II CERCON | Aggregate III AL-HARBI |
|---|---|---|---|---|---|
| 1 | Bulk specific gravity of coarse aggregate | | 2.565 | 2.565 | 2.863 |
| 2 | Bulk specific gravity (saturated surface dry) of coarse aggregate | ASTM C-127-84 | - | 2.607 | 2.900 |
| 3 | Apparent specific gravity of coarse aggregate | AASHTO T-85-81 | 2.720 | 2.677 | 2.975 |
| 4 | Percent Absorption | | 2.230 | 1.627 | 1.316 |
| 5 | Bulk specific gravity of fine aggregate | | 2.387 | 2.403 | 2.773 |
| 6 | Bulk specific gravity (saturated surface dry) of fine aggregate | ASTM C-128-84 | - | 2.514 | 2.838 |
| 7 | Apparent specific gravity of fine aggregate | AASHTO T-84-81 | 2.701 | 2.703 | 2.973 |
| 8 | Percent Absorption | | 4.870 | 4.624 | 2.417 |
| 9 | Specific gravity of filler dust | ASTM D 854-83 AASHTO-T-100-70 | 2.731 | 2.710 | 2.954 |
| 10 | Percent loss by Los Angeles Abrasion | ASTM C-131-76 | | | |
| | Grading B | | 30.0 | 24.0 | 24.35 |
| | Grading C | AASHTO-T-96-77 | 32.3 | - | 26.70 |
| 11 | Soundness by Sodium Sulfate Solution | C-88-83 | | | |
| | Percent loss in coarse aggregate | | 10.18 | 3.2 | 5.37 |
| | Percent loss in fine aggregate | AASHTO-T-104-77 | 15.72 | 3.3 | 5.87 |
| 12 | Sand Equivalent | ASTM D2419-79 AASHTO-T-176-73 | 54.7 | 49.2 | 62.7 |

TABLE 2 AGGREGATE GRADATION USED

| Sieve Size | Percent Passing |
|---|---|
| 3/4" | 100 |
| 1/2" | 84.0 |
| 3/8" | 71.5 |
| No. 4 | 48.5 |
| No. 10 | 30.0 |
| No. 40 | 13.5 |
| No. 80 | 9.0 |
| No. 200 | 5.5 |

TABLE 3 RESULTS OF QUALITY TESTS ON ASPHALT CEMENT

| Test | ASTM Designation Method | Result |
|---|---|---|
| Penetration @ 25°C 100 grams, 5 seconds (0.1mm) | D5-83 | 64.0 |
| Softening Point degrees centigrade (°C) | D36-86 | 48.5 |
| Absolute Viscosity by Vacuum Capillary Viscometer @ 60°C (poises) | D2171-85 | 2627.0 |
| Kinematic Viscosity @ 135°C (centistokes) | D2170-85 | 453.0 |

## SPECIMEN PREPARATION

The study was aimed at evaluating the effect of washing the coarse aggregates in a bituminous mix on its characteristics, especially those associated with moisture susceptibility. For this reason, a mixing procedure had to be selected that incorporated the washed coarse aggregates. The coarse and fine aggregates could not be mixed together, with no binder; this would have defeated the purpose of washing the aggregates. After several laboratory attempts, the following procedure was selected to prepare mixes containing washed coarse aggregates:

1. The heated, washed coarse aggregate required to produce one Marshall specimen was introduced into the mixing bowl.
2. The asphalt cement required for the whole specimen was added to the washed coarse aggregate and mixed in a mechanical mixer until uniform coating was obtained. This normally required about 30 sec.
3. The fine aggregate was then added into the bowl and mixing was continued until a uniform mix was obtained.

The control mixes, with no washed coarse aggregates, were prepared using the normal Marshall mix design procedure and equipment. Seventy-five blows of the Marshall automatic compactor on each side were used to compact the specimens.

Because the moisture susceptibility of a mix is significantly affected by the binder content, mixes were prepared at various levels of asphalt cement content. Preliminary mix designs showed that the optimum binder content is about 3.5 percent by weight of total mix. For this reason, the asphalt contents selected for the study were 3.0, 3.5, and 4.0 percent by total weight of mix.

During the mixing process, it was observed that mixes containing washed aggregates exhibited a richer and more glossy look than mixes with the same asphalt content but containing unwashed aggregates.

In this paper, control mixes with unwashed aggregates will be labeled C-Mixes, whereas mixes with washed aggregates will be labeled S-Mixes.

## MIX CHARACTERIZATION

The following characterization tests were used to quantify the response of the mixes to the washing of the coarse aggregates:

1. Density-voids analysis,
2. Marshall stability,
3. Indirect tensile strength, and
4. Resilient modulus.

Table 4 summarizes the results obtained for the different mixes at the three asphalt contents used. Results shown represent the average for triplicate samples. Resilient modulus and indirect tensile strength tests were performed at 25°C. The test results are also shown graphically in Figures 1 and 2. Figure 1 shows the density-voids results; Figure 2 shows the strength tests' results with asphalt content for the three aggregates used in the C-Mixes and S-Mixes.

From Figure 1, it can be seen that mixes using Aggregate I (Al-Duhami) are the ones most affected by the washing of the coarse aggregates. S-Mixes have higher density and lower air voids and voids in mineral aggregates (VMA) than C-Mixes with the same asphalt content. Aggregate I is seen from Table 1 to have the highest loss in both the soundness and abrasion tests. It is anticipated that, for all mixes, washing the coarse aggregate improves the lubrication effect of the asphalt binder during compaction. This results in increased density and lower voids content.

Figure 2 shows the effect of washing the coarse aggregates on the Marshall stability, indirect tensile strength, and the resilient modulus. The general tendency, with few exceptions, especially for Aggregate III mixes, is for the washing process to improve the strength of the produced mixes. This is especially true for mixes produced from Aggregate I. There is no clear observation as to which test seems to be most affected by the washing process.

From this, it appears that the mixes that benefit most from the washing of the coarse aggregate are those produced from the "weakest" aggregate, namely Aggregate I. Nevertheless, the most significant measure of any improvement in this study is the improvement in moisture susceptibility.

## MOISTURE SUSCEPTIBILITY

This study was initiated primarily to evaluate the effect of washing the coarse aggregates on the adhesion and moisture susceptibility of bituminous mixes. The general approach was to test the two types of mixes (C-Mixes and S-Mixes) before subjecting them to any moisture conditioning. This is followed by subjecting the mixes to a moisture-conditioning procedure and testing them again using the same tests used before moisture conditioning. The results of the testing before and after moisture conditioning are then compared for the two mix types. The tests used to quantify the effect of water were Marshall stability, indirect tensile strength, and resilient modulus.

### Moisture Conditioning Procedure

Several procedures are described in the literature that have been used by different researchers to evaluate the effect of water on bituminous mixes (*5*). The procedure selected for this study to simulate the effect of water was to immerse the mix specimens in water maintained at 60°C for 24 hr. This moisture-conditioning procedure was selected because it is popular, simple, and fast. No freeze-thaw cycling procedure was selected because air temperature in Saudi Arabia rarely drops below 0°C.

### Strength Test Results

Table 5 summarizes the strength results for all mixes before and after moisture conditioning. It can be clearly seen that the strength values for specimens subjected to moisture conditioning are almost consistently higher for the S-Mixes than for the C-Mixes. In other words, washing the coarse aggregate

TABLE 4 SUMMARY OF MIXES CHARACTERIZATION TEST RESULTS

| | I | | II | | III | |
|---|---|---|---|---|---|---|
| | AL-DUHAMI | | CERCON | | AL-HARBI | |
| | C | S | C | S | C | S |
| **Asphalt Content = 3.0%** | | | | | | |
| Density $G_{mb}$ | 2.276 | 2.294 | 2.298 | 2.311 | 2.549 | 2.567 |
| Air Voids | 8.5 | 8.2 | 8.75 | 8.55 | 8.57 | 7.75 |
| VMA | 11.7 | 11.0 | 11.8 | 11.4 | 13.1 | 11.9 |
| Marshall Stability, lbs. | 4043 | 4294 | 4044 | 4006 | 3556 | 4193 |
| Indirect Tensile Strength, psi. | 124.2 | 165.4 | 134.0 | 135.3 | 143.5 | 150.4 |
| Resilient Modulus, $X10^6$ psi. | 0.80 | 1.10 | 0.61 | 0.80 | 0.67 | 0.63 |
| **Asphalt Content = 3.5%** | | | | | | |
| Density $G_{mb}$ | 2.281 | 2.333 | 2.341 | 2.337 | 2.582 | 2.583 |
| Air Voids | 7.6 | 6.3 | 6.36 | 6.82 | 6.58 | 6.41 |
| VMA | 11.9 | 9.9 | 10.7 | 10.9 | 12.40 | 12.4 |
| Marshall Stability, lbs. | 4413 | 5190 | 4088 | 3823 | 3888 | 4334 |
| Indirect Tensile Strength, psi. | 156.0 | 186.7 | 155.7 | 159.6 | 182.9 | 172.4 |
| Resilient Modulus, $X10^6$ psi. | 1.00 | 1.24 | 0.72 | 0.80 | 0.73 | 0.65 |
| **Asphalt Content = 4.0%** | | | | | | |
| Density $G_{mb}$ | 2.306 | 2.360 | 2.369 | 2.363 | 2.600 | 2.597 |
| Air Voids | 5.9 | 4.2 | 4.55 | 5.10 | 5.10 | 5.11 |
| VMA | 11.5 | 9.4 | 10.1 | 10.3 | 12.3 | 12.4 |
| Marshall Stability, lbs. | 4204 | 3799 | 3338 | 3192 | 4218 | 3745 |
| Indirect Tensile Strength, psi. | 177.7 | 201.8 | 157.2 | 163.5 | 173.6 | 164.2 |
| Resilient Modulus, $X10^6$ psi. | 0.99 | 1.24 | 0.64 | 0.65 | 0.61 | 0.72 |

also improves the strength characteristics for the moisture-conditioned mixes.

To quantify the retained strength in a mix after moisture conditioning, three indexes were defined.

Index of Retained Marshall Stability (IRMS)

$$IRMS = \frac{\text{Marshall stability after moisture conditioning}}{\text{Marshall stability before moisture conditioning}}$$

Index of Retained Tensile Strength (IRTS)

$$IRTS = \frac{\text{tensile strength after moisture conditioning}}{\text{tensile strength before moisture conditioning}}$$

Index of Retained Resilient Modulus (IRRM)

$$IRRM = \frac{\text{resilient modulus after moisture conditioning}}{\text{resilient modulus before moisture conditioning}}$$

Table 6 summarizes the retained strength indexes for the evaluated mixes. The results are also shown graphically in Figure 3. Several observations can be drawn from this figure. First, the general trend is for the indexes of the S-Mixes to be higher than those for the C-Mixes. Nevertheless, there are a few exceptions to this trend, especially for mixes with Aggregate III. Second, the indexes for Aggregate I mixes are consistently lower than the indexes of the other aggregate mixes at the same asphalt content. This means that mixes produced from Aggregate I have the highest susceptibility to the detrimental effects of water. Aggregate II mixes have the highest values for retained strength indexes, which implies that Aggregate II mixes are the least susceptible to the detrimental effects of water. Third, as expected, the indexes of retained strength increase with the addition of more asphalt binder.

### Extraction Test Results

At the end of the strength tests, specimens that were used for the dry indirect tensile strength test for mixes with 4.0 percent asphalt content were subjected to the reflux extraction test procedure, ASTM D2172. The purpose for the reflux extraction was twofold:

1. Determine if there is any difference in the effort, or extraction time, required to extract the asphalt binder from

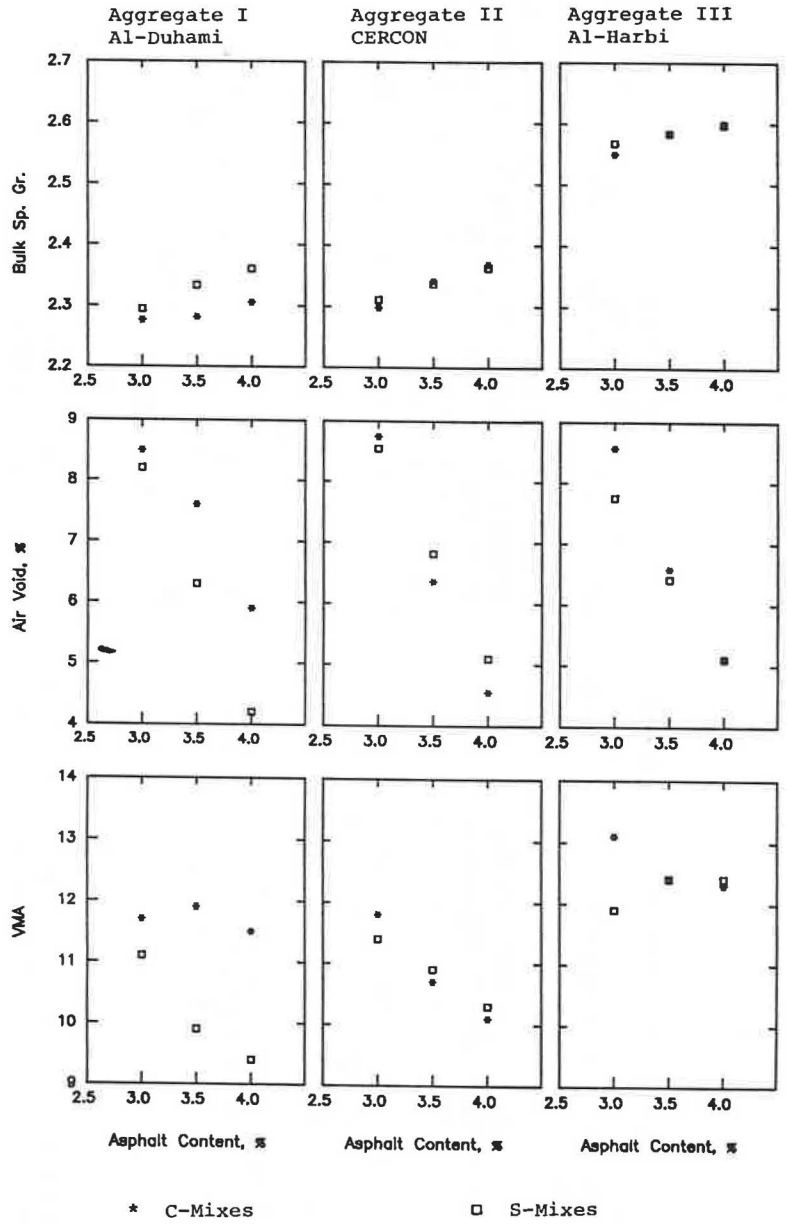


**FIGURE 1 Density and voids results.**

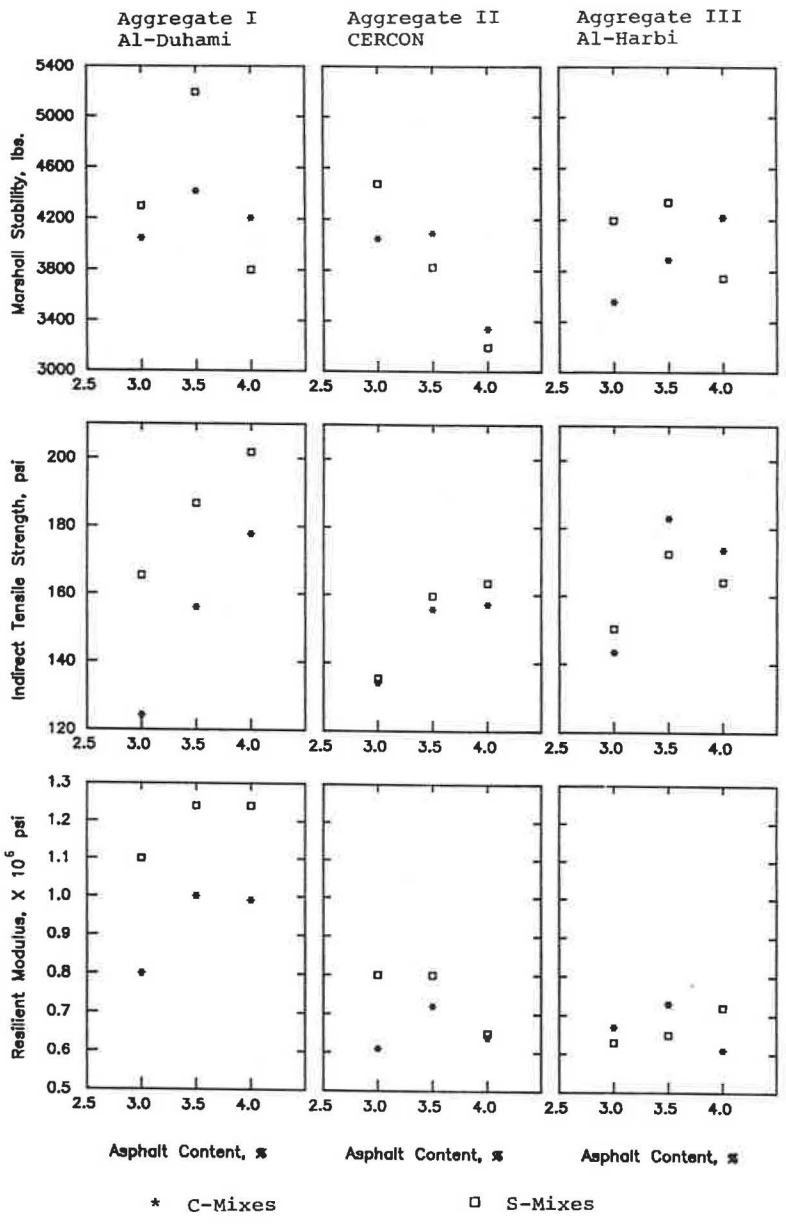


**FIGURE 2 Strength characteristics results.**

TABLE 5 SUMMARY OF STRENGTH RESULTS BEFORE AND AFTER MOISTURE CONDITIONING

| | MOISTURE CONDITIONING | I AL-DUHAMI C | I AL-DUHAMI S | II CERCON C | II CERCON S | III AL-HARBI C | III AL-HARBI S |
|---|---|---|---|---|---|---|---|
| **Asphalt Content = 3.0%** | | | | | | | |
| Marshall Stability, lbs. | Before | 4043 | 4294 | 4044 | 4473 | 3556 | 4193 |
| | After | 1749 | 1951 | 3108 | 3417 | 2537 | 2491 |
| Indirect Tensile Strength, psi. | Before | 124.2 | 165.4 | 134.0 | 135.3 | 143.5 | 150.4 |
| | After | 20.1 | 11.5 | 93.8 | 113.0 | 79.9 | 86.3 |
| Resilient Modulus, $X10^6$ psi. | Before | 0.80 | 1.10 | 0.61 | 0.80 | 0.67 | 0.63 |
| | After | 0.36 | 0.53 | 0.44 | 0.78 | 0.43 | 0.47 |
| **Asphalt Content = 3.5%** | | | | | | | |
| Marshall Stability, lbs. | Before | 4413 | 5190 | 4088 | 3823 | 3888 | 4334 |
| | After | 1236 | 2233 | 3116 | 3272 | 2863 | 2737 |
| Indirect Tensile Strength, psi. | Before | 156.0 | 186.7 | 155.7 | 159.6 | 182.9 | 172.4 |
| | After | 45.9 | 72.1 | 116.5 | 139.9 | 118.9 | 105.6 |
| Resilient Modulus, $X10^6$ psi. | Before | 1.00 | 1.24 | 0.72 | 0.80 | 0.73 | 0.65 |
| | After | 0.51 | 0.63 | 0.59 | 0.68 | 0.61 | 0.59 |
| **Asphalt Content = 4.0%** | | | | | | | |
| Marshall Stability, lbs. | Before | 4204 | 3799 | 3338 | 3192 | 4218 | 3745 |
| | After | 2195 | 2103 | 2937 | 3006 | 3177 | 3180 |
| Indirect Tensile Strength, psi. | Before | 177.7 | 201.8 | 157.2 | 163.5 | 173.6 | 164.2 |
| | After | 54.3 | 90.0 | 130.9 | 158.0 | 131.2 | 133.5 |
| Resilient Modulus, $X10^6$ psi. | Before | 0.99 | 1.24 | 0.64 | 0.65 | 0.61 | 0.72 |
| | After | 0.70 | 0.69 | 0.47 | 0.76 | 0.54 | 0.65 |

TABLE 6 RETAINED STRENGTH INDEXES AFTER MOISTURE CONDITIONING

| | I Al-Duhami C | I Al-Duhami S | II CERCON C | II CERCON S | III Al-Harbi C | III Al-Harbi S |
|---|---|---|---|---|---|---|
| **Asphalt Content = 3.0%** | | | | | | |
| Index of Retained Marshall Stability (IRMS) | 0.43 | 0.45 | 0.77 | 0.76 | 0.71 | 0.59 |
| Index of Retained Tensile Strength (IRTS) | 0.16 | 0.07 | 0.70 | 0.84 | 0.56 | 0.57 |
| Index of Retained Resilient Modulus (IRRM) | 0.45 | 0.48 | 0.72 | 0.97 | 0.64 | 0.75 |
| **Asphalt Content = 3.5** | | | | | | |
| Index of Retained Marshall Stability (IRMS) | 0.28 | 0.43 | 0.76 | 0.86 | 0.74 | 0.63 |
| Index of Retained Tensile Strength (IRTS) | 0.29 | 0.39 | 0.75 | 0.88 | 0.65 | 0.61 |
| Index of Retained Resilient Modulus (IRRM) | 0.51 | 0.51 | 0.82 | 0.85 | 0.84 | 0.91 |
| **Asphalt Content = 4.0%** | | | | | | |
| Index of Retained Marshall Stability (IRMS) | 0.52 | 0.55 | 0.88 | 0.94 | 0.75 | 0.85 |
| Index of Retained Tensile Strength (IRTS) | 0.31 | 0.45 | 0.83 | 0.97 | 0.76 | 0.81 |
| Index of Retained Resilient Modulus (IRRM) | 0.71 | 0.56 | 0.73 | 1.17 | 0.89 | 0.90 |

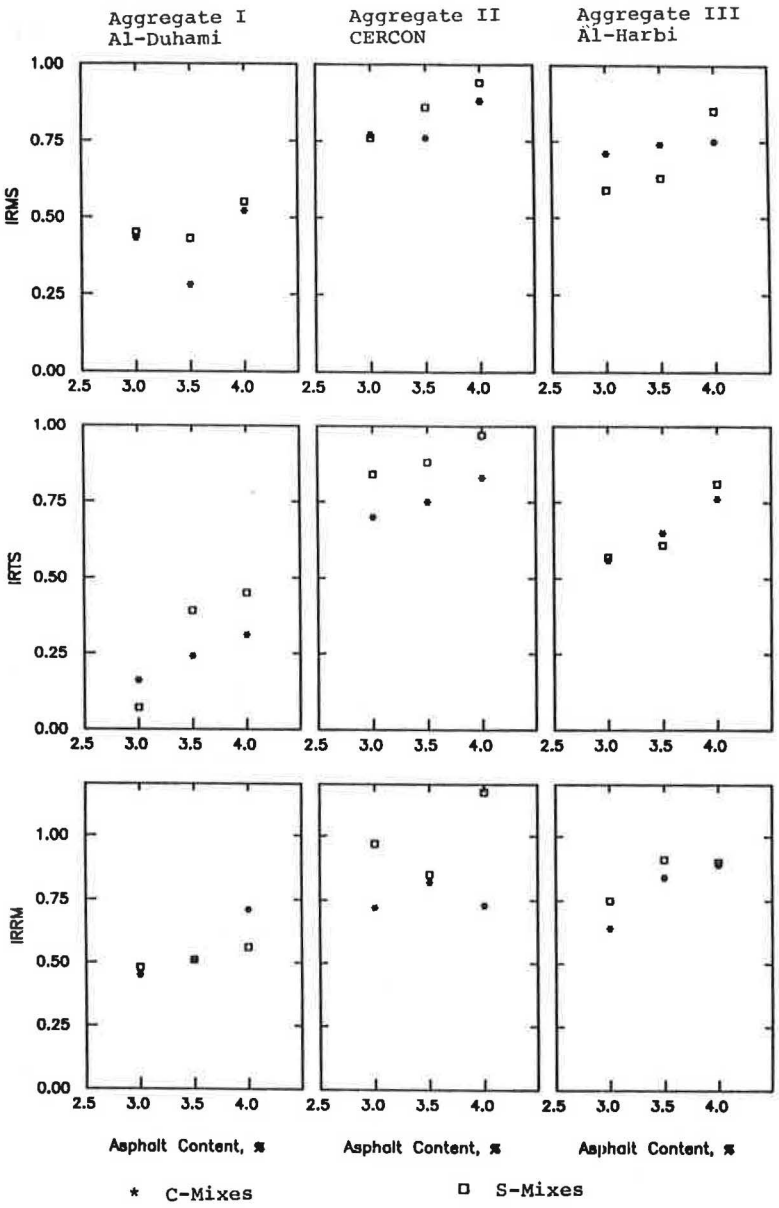


**FIGURE 3 Indexes of retained strength results.**

the mixes. If washing the coarse aggregate provides better adhesion with the asphalt binder, then it should be more difficult to extract the binder.

2. Determine the gradation of the aggregates. This is to determine the final fines content of the C-Mixes and S-Mixes after compaction.

The effect on the gradation of washing the coarse aggregates could have been determined by performing washed sieving analysis. But, because the extraction test was to be performed, it was decided to determine the gradation of the aggregates remaining after extracting the binder. This would give the true gradation of the aggregate after specimen preparation, compaction, and testing.

Table 7 shows the gradation of the aggregates recovered from the mixes as compared to the gradation at which specimens were prepared. The table also shows the differences, for each sieve, between the gradation after extraction and before compaction. It is expected that some level of degradation does occur during mixing and compaction. Resistance to this degradation depends primarily on the strength or toughness of the aggregate. It is seen from Table 7 that some fracture of the coarse portion of the aggregates does occur. This fracture is most noticeable in Aggregate I mixes. Aggregate III, the basalt aggregate, shows the highest resistance to degradation.

When observing the fine sieves, it can be seen that the percentages passing for the C-Mixes are consistently higher than those for the S-Mixes. If the fines produced from the fracture of the coarse aggregates are the same for the C-Mixes and S-Mixes, then the difference observed must come from the fines that are contaminating the coarse aggregates. This

TABLE 7 GRADATION OF AGGREGATES AS RECOVERED FROM MIXES

| Sieve | JMF % Pass | I DUHAMI Gradation C % Pass | I DUHAMI Gradation S % Pass | I DUHAMI Δ Grad. C % Diff. | I DUHAMI Δ Grad. S % Diff. | II CERCON Gradation C % Pass | II CERCON Gradation S % Pass | II CERCON Δ Grad. C % Diff. | II CERCON Δ Grad. S % Diff. | III AL-HARBI Gradation C % Pass | III AL-HARBI Gradation S % Pass | III AL-HARBI Δ Grad. C % Diff. | III AL-HARBI Δ Grad. S % Diff. |
|---|---|---|---|---|---|---|---|---|---|---|---|---|---|
| 3/4" | 100 | 100 | 100 | 0.32 | 0 | 100 | 100 | 0 | 0 | 100 | 100 | 0 | 0 |
| 1/2" | 84 | 89.79 | 88.84 | 5.79 | 4.84 | 91.25 | 90.88 | 7.25 | 6.88 | 86.50 | 88.47 | 2.50 | 4.47 |
| 3/8" | 71.5 | 75.59 | 76.29 | 4.09 | 4.79 | 70.07 | 71.66 | -1.43 | 0.16 | 71.51 | 74.29 | 0.01 | 2.79 |
| 4 | 48.5 | 56.00 | 53.24 | 7.50 | 4.74 | 50.09 | 50.35 | 1.59 | 1.85 | 51.91 | 51.18 | 3.41 | 2.68 |
| 10 | 30.0 | 38.12 | 36.42 | 8.12 | 6.42 | 32.19 | 32.36 | 2.19 | 2.36 | 34.09 | 33.97 | 4.09 | 3.97 |
| 40 | 13.5 | 22.78 | 19.82 | 9.28 | 6.32 | 16.78 | 16.08 | 3.28 | 2.58 | 17.76 | 17.59 | 4.26 | 4.09 |
| 80 | 9.0 | 18.44 | 15.92 | 10.44 | 6.92 | 12.99 | 11.95 | 3.95 | 2.95 | 13.30 | 13.14 | 4.30 | 4.14 |
| 200 | 5.5 | 15.12 | 12.91 | 9.62 | 7.41 | 10.34 | 9.48 | 4.84 | 3.98 | 9.30 | 9.18 | 3.80 | 3.68 |

difference is highest for Aggregate I mixes. In other words, Aggregate I has the highest amount of fines contaminating the coarse aggregate particles. It can also be seen that the difference between the gradation of the C-Mixes and the S-Mixes is negligible for the Aggregate III mixes. This clearly indicates that there are hardly any fines contaminating the coarse aggregates for Aggregate III.

A visual observation was also made of the time required for the reflux extractor to extract the asphalt binder. It was assumed that this provides an indirect way of assessing the adhesion of the binder to the aggregates. The better the adhesion between the aggregate and the binder, the longer the time required for extraction. It was observed that a much longer time was required for extraction of the S-Mixes than for the C-Mixes for Aggregates I and II. This may lead to the conclusion that, for Aggregates I and II, washing the coarse aggregates provides better adhesion of the asphalt binder to the aggregates. On the other hand, for Aggregate III, the opposite was observed. A longer time was required to extract the C-Mixes than the S-Mixes. This may indicate that washing the coarse portion of Aggregate III adversely affects the adhesion of the asphalt binder to the aggregate particles. This is consistent with the strength characteristics test results, which showed a reduction in strength for some of the S-Mixes of Aggregate III.

## SUMMARY AND CONCLUSIONS

A laboratory investigation examined the prospects of improving the engineering properties of bituminous mixes produced in the Riyadh area of Saudi Arabia by washing the coarse portion of the limestone aggregates used. A basalt aggregate from the western region of the country was also used in the study for comparison purposes. A two-cycle mixing sequence was used for the washed aggregate mixes in which the coarse aggregate was first mixed with the asphalt binder after which the fine aggregate was added and mixed. It was observed that washing the coarse aggregate does yield an improvement in the strength characteristics and moisture resistance of the limestone aggregate mixes. This was especially true for the limestone aggregate exhibiting the highest loss in the abrasion and soundness tests. Mixes produced from the basalt aggregate were generally less responsive to the beneficial effects of the washing process.

The results of the study also showed that the strength and density values for the C-Mixes can be obtained at a lower asphalt content using the S-Mixes. In other words, washing the coarse aggregate results in a reduction in the asphalt content required to attain certain levels of density and strength values.

It should be stated that a separate study is planned to evaluate the effect of incorporating a two-cycle mixing sequence without washing the aggregates. This should determine whether the improvement in mix characteristics was only due to the washing of the coarse aggregates or was contributed to by the use of a two-cycle mixing sequence.

In general, the following conclusions can be drawn from the results of this study:

1. Washing the coarse aggregate and using a two-cycle mixing sequence provides better coating of the asphalt and richer-looking mixes than conventional mixing with unwashed aggregate and at the same asphalt contents.
2. Washing the coarse aggregate improves the strength characteristics and moisture resistance of the limestone aggregate mixes. Mixes produced with basalt aggregate do not seem to benefit from the washing process.
3. The beneficial effects of washing the coarse aggregate is more pronounced with the weaker aggregates.
4. Washing the coarse aggregate appears to reduce the amount of asphalt required to attain certain levels of strength and density.

## REFERENCES

1. Municipality of Riyadh. *Moisture-Induced Damage to Asphaltic Concrete Pavements for Riyadh Roads.* Report 25018. Research Institute, King Fahd University of Petroleum and Minerals, Dhahran, Saudi Arabia, 1986.
2. K. W. Lee and M. I. Al-Jarallah. *Effect of Hydrated Lime, as an Antistripping Additive, on the Properties of Asphaltic Materials.* Research Report 21404. Research Center, College of Engineering, King Saud University, Riyadh, Saudi Arabia, 1986.
3. A. M. Mardini. *Bonding Failures of Asphalt Concrete Mixtures in Saudi Arabia.* Report CE 84-05-14. Civil Engineering Department, King Saud University, Riyadh, Saudi Arabia, 1984.
4. *Cause and Prevention of Stripping in Asphalt Pavements*, 2nd ed. Educational Series 10. Asphalt Institute, College Park, Md., 1981.
5. *Evaluation and Prevention of Water Damage to Asphalt Pavement.* ASTM STP 899, 1985.

*Publication of this paper sponsored by Committee on Nonbituminous Components of Bituminous Paving Mixtures.*